



**MONASH** University

**The role of acidic metabolites and their  
G protein-coupled receptors in the development  
of inflammatory diseases and allergies**

Craig McKenzie

BBiotech (Hons)

A thesis submitted for the degree of Doctor of Philosophy at

Monash University in 2017

Department of Biochemistry and Molecular Biology

School of Biomedical Sciences

## **Copyright Notice**

© Craig McKenzie (2017). Except as provided in the Copyright Act 1968, this thesis may not be reproduced in any form without the written permission of the author.

# **The role of acidic metabolites and their G protein-coupled receptors in the development of inflammatory diseases and allergies**

## **Contents**

Acknowledgments.....	6
Abstract.....	7
Publications arising from this thesis .....	9
Thesis including published works declaration .....	11
Abbreviations.....	18
<b>Chapter 1 – Introduction.....</b>	<b>21</b>
1. Diet, Hygiene and Disease.....	22
2. Dietary intake and metabolites.....	23
2.1 Short-chain fatty acids (SCFAs) .....	24
2.2 Medium-chain fatty acids (MCFAs) .....	25
3. Immunomodulatory mechanisms of acids, SCFAs and MCFAs via GPCRs .....	25
3.1 G protein-coupled receptors (GPCRs) .....	25
3.2 Proton-sensing receptor GPR65.....	26
3.3 SCFA receptors: GPR43, GPR109a.....	26
3.4 MCFA receptor: GPR84 .....	29
4. Immunomodulatory mechanisms of SCFAs via epigenetics .....	30
4.1 SCFA-mediated HDAC inhibition.....	30
4.2 Mechanism of HDAC inhibition.....	31



5. Asthma .....	32
5.1 Antigen presentation and T cell activation.....	33
5.2 Role of regulatory T cells (Treg) in asthma.....	34
5.3 Eosinophilic infiltration of the lung.....	36
6. Food Allergy .....	37
6.1 Th2 responses.....	37
6.2 Oral tolerance to antigens .....	38
7. Inflammatory Bowel Disease.....	39
7.1 Epithelial integrity.....	39
7.2 Neutrophils in IBD pathogenesis .....	40
7.3 Murine models of colitis .....	43
8. Rationale .....	43
<b>Chapter 2 – The Role of Dietary Fibre, SCFAs and GPR43 in Asthma and Infection .....</b>	<b>47</b>
1. Introduction.....	47
2. High fibre diet and acetate prevents allergic airways disease (AAD).....	47
3. Treatment with high fibre diet and acetate prevents AAD in offspring.....	50
4. High fibre and acetate protect against AAD independent of microbiota transfer at birth.....	53
5. Acetate protects against AAD via Tregs and epigenetic modification of the <i>Foxp3</i> promoter .....	56
6. The role of high fibre and SCFAs in asthma pathogenesis.....	58
7. Dietary fibre and SCFAs protect against <i>C. rodentium</i> infection .....	58
High acetate yielding diets protect mice from <i>Citrobacter rodentium</i> infection through enhanced mucosal immunity and control of bacterial growth .....	61
<b>Chapter 3 – The Role of GPR65 in Infection and Colitis .....</b>	<b>98</b>

1. Introduction.....	98
2. GPR65 protects against <i>C. rodentium</i> infection.....	98
3. <i>Gpr65</i> expression in haematopoietic and non-haematopoietic compartments limits <i>C. rodentium</i> infection.....	101
4. GPR65 regulates neutrophil chemotaxis and metabolism .....	104
Proton-sensing receptor GPR65 regulates colonic inflammation through effects on leukocyte migration and intracellular metabolic pathways .....	105
<b>Chapter 4 – The Role of Dietary MCFAs and GPR84 in Allergy and Inflammation.....</b>	<b>148</b>
1. Introduction.....	148
2. GPR84 signalling is not involved in food allergy .....	148
3. GPR84 enhances asthma pathogenesis .....	151
4. GPR84 protects against murine colitis.....	157
5. Discussion .....	161
<b>Chapter 5 – Conclusion .....</b>	<b>163</b>
References.....	165
Appendices.....	192

## **Acknowledgments**

I would first and foremost like to thank Charles Mackay, Laurence Macia and Remy Robert for the opportunities and tutelage they have provided. They have ensured that my doctoral studies have encompassed a wide variety of disciplines where I have learned many new skills and met fantastic people.

I would also like to thank all the members of the Mackay lab, past and present. They have been an amazing group of people who brought incredible character and variety to the lab. They have all helped me throughout countless experiments. In particular, I would like to thank Jian Tan and Keiran McLeod for their mateship and camaraderie both inside and outside the lab.

I would next like to thank my family. They have continually and selflessly provided me with an incredible amount of opportunity and support. They have always encouraged me in any endeavour and have genuinely ensured that I may pursue my dreams.

Finally, I would like to thank my partner Jess. She is the greatest companion, filling my life with continual laughter and happiness.

## Abstract

High incidences of allergic and inflammatory diseases can be attributed to a myriad of factors involving western lifestyle and host genetics. In particular, consumption of a western diet, low in dietary fibre and micronutrients while high in fat and sugar has been correlated with the development of obesity and non-communicable inflammatory diseases. Dietary fibre is fermented in the colon by the gut microbiota to short-chain fatty acids (SCFAs), metabolites that have been demonstrated to reduce inflammation and prevent disease in murine models of colitis and arthritis. SCFAs activate a number of G protein-coupled receptors (GPCRs) on immune or epithelial cells, which broadly regulate immune responses. The link between acidic metabolites, GPCRs and inflammation suggests that acid- or metabolite-sensing GPCRs may play an important role in preventing inflammatory diseases. However, our understanding of these GPCRs remains in its infancy. In particular, GPR43, GPR65 and GPR84 are three receptors whose function is not well understood. GPR43 is activated by acetate, the most abundant SCFA in the gut produced by bacterial fermentation. GPR65 is a proton-sensing receptor activated by low pH, a condition established under acidic extracellular conditions. GPR84 is activated by medium-chain fatty acids (MCFAs), the predominant component of coconut oil. Together, these three receptors and their agonists have a poorly understood role in immunology. To investigate their immunological function, we assessed the pathogenesis of allergic or inflammatory diseases in mice lacking GPR43, GPR65 or GPR84. All three displayed a regulatory function by preventing the pathogenesis of asthma, bacterial gut infection or colitis. Furthermore, we identified regulatory responses to ligands for GPR43 and GPR65 that were either dependent or independent of these receptors depending on the disease models and the immune cells involved. GPR43 agonist acetate enhanced regulatory T cell function in an epigenetic manner that prevented asthma independently of GPR43. However, dietary supplementation with high acetate-yielding diet enhanced protection against *Citrobacter rodentium* infection with partial dependence on GPR43. Furthermore, GPR65 regulated neutrophil chemotaxis and metabolism, reducing the severity of *C. rodentium* infection and colitis. In contrast, GPR84 exhibited both protective and detrimental functions by exacerbating asthma despite preventing colitis. Taken together, these studies have characterised a

novel role for GPR43, GPR65, GPR84 and their agonists, highlighting the potential for acid and acidic metabolites to modulate allergy and inflammatory disease.

## Publications arising from this thesis

### Refereed Journals (published)

- Alison N. Thorburn, **Craig I. McKenzie**, Sj Shen, Dragana Stanley, Laurence Macia, Linda J. Mason, Laura K. Roberts, Connie H. Y. Wong, Raymond Shim, Remy Robert, Nina Chevalier, Jian Tan, Eliana Mariño, Rob J. Moore, Lee Wong, Malcolm J. McConville, Dedreia L. Tull, Lisa G. Wood, Vanessa E. Murphy, Joerg Mattes, Peter G Gibson, Charles R. Mackay, Evidence that asthma is a developmental origin disease influenced by maternal diet and bacterial metabolites, *Nature Communications* (2015)
- Kara G. Lassen, **Craig I. McKenzie**, Muriel Mari, Tatsuro Murano, Jakob Begun, Leigh A. Baxt, Gautam Goel, Eduardo J. Villablanca, Szu-Yu Kuo, Hailiang Huang, Laurence Macia, Atul K. Bhan, Marcel Batten, Mark J. Daly, Fulvio Reggiori, Charles R. Mackay, Ramnik J. Xavier, Genetic coding variant in GPR65 alters lysosomal pH and links lysosomal dysfunction with colitis risk, *Immunity* (2016)

### Refereed Journals (submitted)

- Keiran H. McLeod\*, **Craig I. McKenzie\***, Yu Anne Yap, James L. Richards, Jian Tan, Jacinta Knight, Robert J. Moore, Trevor J. Lockett, Julie M. Clarke, Charles R. Mackay, Laurence Macia, Eliana Mariño, \* equal contribution, High acetate yielding diets protect mice from *Citrobacter rodentium* infection through enhanced mucosal immunity and control of bacterial growth, *Gastroenterology* (2017)

### Reviews

- **Craig I. McKenzie**, Charles R. Mackay, Laurence Macia, GPR43 – A prototypic metabolite receptor linking metabolic and inflammatory diseases, *Trends in Endocrinology and Metabolism* (2015)

- Jian Tan, **Craig I. McKenzie**, Maria Potamis, Alison N Thorburn, Charles Mackay, Laurence Macia, The role of short-chain fatty acids in health and disease, *Advances in Immunology* (2014)

#### Conference Posters

- **Craig McKenzie**, Jian Tan, Jot Hui Ooi, Laurence Macia, Charles Mackay, GPR65 regulates neutrophil chemotaxis, *International Congress of Immunology*, Melbourne, August (2016)
- **Craig McKenzie**, Laurence Macia, Alison N. Thorburn, Jian Tan, Sj Shen, Charles Mackay, The immunomodulatory effects of medium-chain fatty acids (MCFAs) on asthma and food allergy, *43<sup>rd</sup> Annual Scientific Meeting of the Australasian Society for Immunology*, Wellington, December (2013)
- **Craig McKenzie**, Charles Mackay, Alison N. Thorburn, Short-chain fatty acids differentially regulate the development of allergic airways disease, *42<sup>nd</sup> Annual Scientific Meeting of the Australasian Society for Immunology*, Melbourne, December (2012)

## Thesis including published works declaration

I hereby declare that this thesis contains no material which has been accepted for the award of any other degree or diploma at any university or equivalent institution and that, to the best of my knowledge and belief, this thesis contains no material previously published or written by another person, except where due reference is made in the text of the thesis.

This thesis includes 2 original papers published in peer reviewed journals and 1 unpublished publication. The core theme of the thesis involves G protein-coupled receptors with acid or fatty acid agonists and their role in allergy and inflammation. The ideas, development and writing up of all the papers in the thesis were the principal responsibility of myself, the student, working within the Department of Biochemistry and Molecular Biology under the supervision of Dr Laurence Macia.

The inclusion of co-authors reflects the fact that the work came from active collaboration between researchers and acknowledges input into team-based research.

In the case of chapters 1, 2 and 3 my contribution to the work involved the following:

Thesis Chapter	Publication Title	Status	Nature and % of student contribution
1	GPR43 – A prototypic metabolite receptor linking metabolic and inflammatory diseases	Accepted	85%. Conceptualised and wrote the majority of the manuscript
2	Evidence that asthma is a developmental origin disease influenced by maternal diet and bacterial metabolites	Accepted	30%. Large contribution to experimental work. Conceptual contribution to the epigenetic component
2	High acetate yielding diets protect mice from <i>Citrobacter rodentium</i> infection through enhanced mucosal immunity and control of bacterial growth	Submitted	40%. Majority of experimental work and contributed to study design



3	Genetic coding variant in GPR65 alters lysosomal pH and links lysosomal dysfunction with colitis risk	Accepted	10%. Experimental work, data analysis and study design for the infection component
3	Proton-sensing receptor GPR65 regulates colonic inflammation through effects on leukocyte migration and intracellular metabolic pathways	Pre-submission (awaiting collaborator review to determine data release date)	80%. Majority of experimental work, data analysis and study design

I have renumbered sections of submitted or published papers in order to generate a consistent presentation within the thesis.

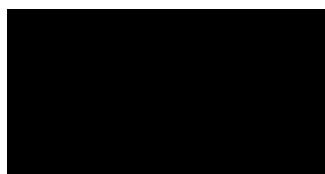
**Student signature:**



**Date:** 24/01/2017

The undersigned hereby certify that the above declaration correctly reflects the nature and extent of the student's and co-authors' contributions to this work. In instances where I am not the responsible author I have consulted with the responsible author to agree on the respective contributions of the authors.

**Main Supervisor signature:**



**Date:** 24/01/2017

## Declaration for thesis Chapter 1

In the case of Chapter 1, the nature and extent of my contribution to the work was the following:

Nature of contribution	Extent of contribution (%)
For text presented in Chapter 1 from McKenzie et al. 2015: Conceptualised and wrote the majority of the manuscript	95%
For text presented in Chapter 1 from Tan et al. 2014: Epigenetic component and editing manuscript	95%

The following co-authors contributed to the work. If co-authors are students at Monash University, the extent of their contribution in percentage terms must be stated:

Name	Nature of contribution	Extent of contribution (%)
Laurence Macia	For McKenzie et al 2015 and Tan et al. 2014: Gave advice for text composition	
Charles R. Mackay	For McKenzie et al 2015 and Tan et al. 2014: Gave advice for text composition	

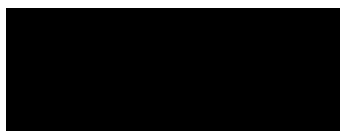
The undersigned hereby declare that the above declaration correctly reflects the nature and extent of the candidate's and co-authors' contributions to this work.

Student signature:



Date: 24/01/2017

Main Supervisor signature:



Date: 24/01/2017

## Declaration for thesis Chapter 2

In the case of Chapter 2, the nature and extent of my contribution to the work was the following:

Nature of contribution	Extent of contribution (%)
For data presented in Chapter 2 from Thorburn et al. 2015: Majority of experimental work and data analysis	90%
For McLeod and McKenzie et al. 2017 (full manuscript included): Study design, work on infection models and subsequent data analysis	40%

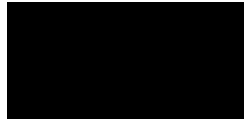
The following co-authors contributed to the work. If co-authors are students at Monash University, the extent of their contribution in percentage terms must be stated:

Name	Nature of contribution	Extent of contribution (%)
Alison Thorburn	For Thorburn et al. 2015: Graph layout and contributed to experimental design	
Linda Mason	For Thorburn et al. 2015: Assisted with time mating and caesarean section	
Keiran McLeod	For McLeod and McKenzie et al. 2017: Equal contribution to study design, work on infection models and data analysis	40%
Jian Tan	For McLeod and McKenzie et al. 2017: Assisted with organ processing of infected mice	2%
Yu Anne Yap	For McLeod and McKenzie et al. 2017: Assisted with organ processing of infected mice	2%
James L. Richards	For McLeod and McKenzie et al. 2017: Assisted with organ processing of infected mice	2%
Jacinta Knight	For McLeod and McKenzie et al. 2017: Assisted with organ processing of infected mice	
Robert J. Moore	For McLeod and McKenzie et al. 2017: Conducted sequencing and analysis	
Trevor J. Lockett	For McLeod and McKenzie et al. 2017: Assisted with design of the study	
Julie M. Clarke	For McLeod and McKenzie et al. 2017: Assisted with design of the study and the manuscript	
Charles R. Mackay	For McLeod and McKenzie et al. 2017: Assisted with design of the study and the manuscript	
Laurence Macia	For McLeod and McKenzie et al. 2017: Assisted with design of the study and the manuscript	

Eliana Mariño	For McLeod and McKenzie et al. 2017: Study design, data analysis, data presentation and writing the manuscript	
---------------	-------------------------------------------------------------------------------------------------------------------	--

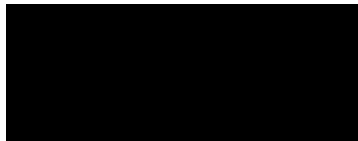
The undersigned hereby declare that the above declaration correctly reflects the nature and extent of the candidate's and co-authors' contributions to this work.

**Student signature:**



**Date:** 24/01/2017

**Main Supervisor signature:**



**Date:** 24/01/2017

## Declaration for thesis Chapter 3

In the case of Chapter 3, the nature and extent of my contribution to the work was the following:

Nature of contribution	Extent of contribution (%)
For data presented in Chapter 3 from Lassen et al. 2016: Majority of experimental work and data analysis	90%
For McKenzie et al. 2017 (full manuscript included, pre-submission): Majority of study design, experimental work and data analysis	80%

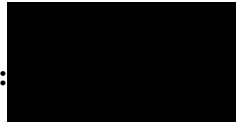
The following co-authors contributed to the work. If co-authors are students at Monash University, the extent of their contribution in percentage terms must be stated:

Name	Nature of contribution	Extent of contribution (%)
Laurence Macia	For Lassen et al. 2016: Sourced <i>C. rodentium</i> For McKenzie et al. 2017: Assisted with study design and manuscript	
Charles R. Mackay	For Lassen et al. 2016: Assisted with study design For McKenzie et al. 2017: Assisted with study design and manuscript	
Jian Tan	For McKenzie et al. 2017: Assisted with experiments on mice	5%
Jot Hui Ooi	For McKenzie et al. 2017: Conducting Fluidigm experiments	
Kara Lassen	For McKenzie et al. 2017: Assisted with study design	
Jaeyun Sung	For McKenzie et al. 2017: LC-MS analysis	
Isabel Latorre	For McKenzie et al. 2017: Conducting LC-MS experiments	
Nan Bing	For McKenzie et al. 2017: 23andMe liaison	
Padma Reddy	For McKenzie et al. 2017: Fluidigm analysis	

Ramnik Xavier	For McKenzie et al. 2017: Assisted with study design	
---------------	---------------------------------------------------------	--

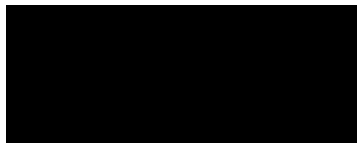
The undersigned hereby declare that the above declaration correctly reflects the nature and extent of the candidate's and co-authors' contributions to this work.

**Student signature:**



**Date:** 24/01/2017

**Main Supervisor signature:**



**Date:** 24/01/2017

## Abbreviations

AAD – allergic airways disease

AHR – airways hyperresponsiveness

APCs – antigen presenting cells

BALF – bronchiolar lavage fluid

cAMP – cyclic adenosine monophosphate

CCL – chemokine (C-C motif) ligand

CCR – chemokine (C-C motif) receptor

DC – dendritic cell

DNS – data not shown

Foxp3 – forkhead box P3

FMLP – N-formylmethionine-leucyl-phenylalanine

GDP – guanosine diphosphate

GIT – gastrointestinal tract

GPCR – G-protein coupled receptor

GWAS – genome-wide association study

HDAC – histone deacetylase

IBD – Inflammatory bowel disease

IFN- $\gamma$  – interferon- $\gamma$

IL – interleukin

KO – knockout

LPS – lipopolysaccharide

MCFA – medium-chain fatty acid

MCP-1 – monocyte chemotactic protein-1

MCP-1 $\alpha$  – macrophage inflammatory protein-1 $\alpha$

MCT – medium-chain triglyceride

NF $\kappa$ B – nuclear factor kappa-light-chain-enhancer of activated B cells

NKT cell – natural killer T cell

NO – nitric oxide

OVA – ovalbumin

PC – phosphatidylcholine

PE – phosphatidylethanolamine

PGE2 – prostaglandin E2

PIP<sub>3</sub> – Phosphatidylinositol (3,4,5)-trisphosphate

PMBC – peripheral blood mononuclear cells

RA – retinoic acid

SCFA – short-chain fatty acid

siRNA – small interfering ribonucleic acid

SNP – single nucleotide polymorphism

TGF- $\beta$  – transforming growth factor  $\beta$



TIM-4 – T cell immunoglobulin mucin-4

TLR-4 – toll-like receptor 4

TNF- $\alpha$  – tumour necrosis factor  $\alpha$

Treg – regulatory T cell

TSA – trichostatin A

VCAM-1 – vascular cell adhesion molecule-1

## Chapter 1 – Introduction

As the incidence of allergic and inflammatory diseases increases in the western world, the need to understand the underlying mechanisms of such diseases becomes paramount. Although excessive hygiene has been commonly attributed to rising disease incidence, some hygienic countries such as Japan have low disease incidence. Western diet that is high in energy and low in fibre has proven to be a predominant factor in predisposing to disease and may alter allergic and inflammatory disease incidence independently of hygiene. Differing diets yield a myriad of specific metabolites that can significantly influence the immune response. Understanding the immunological impact of these metabolites is crucial to establish healthy dietary guidelines to prevent disease. Furthermore, understanding the role of metabolite-receptors in immunity will also validate potential therapeutic agonists to these receptors.

A number of dietary acidic metabolites have been found to influence inflammation via G protein-coupled receptors (GPCRs) expressed on various immune cells. In particular, a host of GPCRs are activated by fatty acid metabolites. Fatty acid agonists of GPCRs vary in carbon chain length, ranging from short-chain (C2-5), medium-chain (C6-12) and long-chain (C13+) fatty acids. Furthermore, a number of GPCRs are activated independent of chain-length, and are instead activated by protons yielded from acids of any description. The immunological role of these receptors and acidic agonists is poorly understood.

Allergies and inflammatory diseases associated with western lifestyle are commonly located at mucosal sites, suggesting that mucosal immune responses are being altered by western diet<sup>1, 2, 3</sup>. The two predominant mucosal immune compartments encompass the respiratory and gastrointestinal tracts. Allergies and inflammatory diseases at these mucosal sites are typified by asthma, food allergy and inflammatory bowel disease (IBD), all of which have been associated in humans with the consumption a western diet low in fibre<sup>1, 4, 5</sup>. Asthma is characterised by pulmonary inflammation in response to the inhalation of a normally innocuous antigen that leads to airway remodelling and subsequent bronchoconstriction. Contrastingly, food allergy involves allergic inflammation in the gut,

triggered by the consumption of a normally innocuous dietary antigen that induces a multitude of different symptoms including nausea, abdominal pain and diarrhoea. Both asthma and food allergy involve chronic Th2 cell responses that drive allergic inflammation. Furthermore, both diseases can be fatal when allergic responses lead to anaphylaxis. Like food allergy, IBD is a severe inflammatory disease of the gut. However, IBD involves chronic Th1 and innate-driven inflammation that leads to a breakdown in epithelial integrity. Loss of epithelial integrity predisposes to bacterial translocation and exacerbated inflammation that ultimately manifests in clinical symptomology. Symptoms of IBD include abdominal pain, diarrhoea, fecal blood and weight loss.

This thesis investigates the immunological role of GPCRs activated by protons, short-chain fatty acids (SCFAs) or medium-chain fatty acids (MCFAs) in asthma, food allergy and colitis. It characterises their influence on the immune system of the respiratory and gastrointestinal tracts using a number of murine disease models of allergy and inflammation. In particular, SCFA receptor GPR43, proton-sensor GPR65 and MCFA receptor GPR84 have formed the predominant focus of this work, whereby knockout mice lacking these genes have been immunologically phenotyped. Taken together, these data provide a comprehensive analysis of how acids and acidic metabolites can influence allergic and inflammatory disease progression, yielding distinct implications for the prevention of human disease.

## **1. Diet, Hygiene and Disease**

The incidence of allergies and inflammatory disease is rapidly increasing in the western world and is commonly attributed to the hygiene hypothesis<sup>6</sup>. The hygiene hypothesis proposes that excess sanitation, antibiotic use and vaccinations has led to an under-developed and over-reactive immune system leading to an increase in allergies and inflammatory diseases<sup>7</sup>. Excessive hygiene causes our immune system to over-react to normally harmless substances (such as pollen) which induces allergic responses (such as hay fever). However, this does not explain rising incidences in non-allergic inflammatory diseases and does not always correlate with increased incidences in allergies. For example, the incidence of asthma in remarkably hygienic Japan is relatively low compared with Australia or the US, whereas poorer and less hygienic parts of America maintain higher incidences of

asthma<sup>8</sup>. As such, other environmental factors of western lifestyle may be involved in disease pathogenesis. Indeed, distinctions in diet amongst these countries correlate more closely with incidences of allergic and inflammatory diseases than other factors of western lifestyle such as hygiene, stress and pollution<sup>8</sup>. This suggests recent changes in western diet may be contributing to the increase in prevalence of such diseases.

Over the last two decades, global changes in diet have driven obesity to pandemic proportions, stemming from the consumption of foods high in energy and low in fibre<sup>9</sup>. The incidence of obesity-associated metabolic diseases is rapidly rising as a result<sup>10</sup>. Two broad clusters of inflammatory metabolic diseases have been induced by obesity: those associated with the direct impact of lipids on the immune system, and those that appear as indirect effects that are poorly understood<sup>11</sup>. Allergic and inflammatory diseases such as asthma, food allergy and IBD fall into this second category. Furthermore, protection from allergic and inflammatory diseases has been associated with diets high in non-digestible fibre in both human and murine studies<sup>12, 13, 14, 15, 16</sup>. This suggests that the lack of fibre in western diet might be contributing to the rising incidence of such diseases. Indeed, fibre intake has been associated with protection against mortality from cardiovascular disease, cancer, infectious and respiratory diseases<sup>17</sup>. Furthermore, fibre can alleviate symptoms of IBS<sup>18</sup>. As such, diet and its associated metabolites have the potential to play a major role in preventing or exacerbating allergic and inflammatory diseases. Moreover, the immunomodulatory mechanisms of these diets are becoming ever more relevant to global health as the diet of the developing world begins to mimic its western counterpart.

## **2. Dietary intake and metabolites**

Energy is harvested from our diet either by the direct metabolism of consumed foods or by the absorption of secondary metabolites produced from gut bacteria. Lipids, proteins and various carbohydrates can be metabolised directly. All aforementioned macromolecules are subject to enzymatic digestion and acidic pH to help expose them for absorption. In particular, medium chain fatty triglycerides (MCTs) are degraded by pancreatic lipases into medium-chain fatty acids (MCFAs;

6 – 12 carbons long) and subsequently absorbed directly across the gut epithelium<sup>19</sup>. In contrast, dietary fibre is not directly used as an energy source and is instead fermented by gut bacteria into rapidly absorbed SCFA metabolites. Dietary fibre consists of non-digestible carbohydrates sourced from plant polysaccharides and oligosaccharides that are resistant to enzymatic and chemical digestion until they reach the large intestine where they are fermented by gut bacteria<sup>20</sup>.

### *2.1 Short-chain fatty acids (SCFAs)*

Anaerobic bacteria ferment non-digestible carbohydrates (dietary fibre) to produce SCFAs that act as primary metabolites for the human host<sup>21</sup>. Dietary fibre is contained in grains, vegetables, fruit skins and nuts. Although SCFAs can also be formed from the metabolism of proteins and glycoproteins, the carbohydrate-sources of these metabolites are the most significant contributors<sup>22</sup>. Gut bacteria produce variable amounts and types of SCFAs depending on their access to carbon, accentuating the role that both microbial composition and diet can have on SCFA production in the human GIT<sup>22</sup>. The most abundant SCFAs are acetate (2 carbons), propionate (3 carbons) and butyrate (4 carbons) respectively<sup>23, 24</sup>. They are found at the highest concentrations in the proximal large intestine due to its large microbial population<sup>22</sup>.

SCFAs can pass across the gut epithelium and interact directly with cells in the gut-associated lymphoid tissue<sup>25</sup>. Immunohistochemical staining and mRNA quantification have identified the location of differing monocarboxylate transporter isoforms on the apical side and basolateral side of the colon that transport SCFAs through the gut epithelium. Whilst inside colonic epithelial cells, butyrate undergoes beta oxidation to acetyl-CoA and constitutes their primary energy source, highlighting the importance of SCFAs as a source of energy for the host<sup>24, 26, 27</sup>. From the gut, SCFAs are transported through the hepatic portal vein to the liver<sup>28</sup> – the primary site of SCFA metabolism<sup>23, 29</sup>. Acetate and propionate are the most common SCFAs to undergo this process and escape the gut into the periphery. Acetate can also be metabolised by muscle and brain tissue but is a minor energy source compared to blood glucose<sup>23, 29</sup>.

## *2.2 Medium-chain fatty acids (MCFAs)*

Medium-chain triglycerides (MCTs) are fatty acids of 6 - 12 carbons esterified to glycerol and are found predominantly in kernel and coconut oil as capric acid, a 10 carbon fatty acid<sup>30</sup>. MCTs are broken down to medium-chain fatty acids (MCFAs) by pancreatic lipases in the small intestine<sup>31</sup>. MCFAs can be absorbed either directly across the gut epithelium into the portal vein or via uptake alongside LCFAs via chylomicrons<sup>32</sup>. As such, MCFAs are metabolised rapidly in comparison to long-chain fatty acids that can only be absorbed via chylomicrons<sup>33</sup>. Indeed, this is supported by a study demonstrating that fat deposition in infants fed MCFAs increased compared to long-chain fatty acids<sup>34</sup>. Authors hypothesised that digestion of MCTs by pancreatic lipases is responsible for quicker breakdown and absorption of MCFAs.

## **3. Immunomodulatory mechanisms of acids, SCFAs and MCFAs via GPCRs**

A number of GPCRs have acid or acidic metabolite agonists that are increasingly being linked with the immune system. In particular, protons, SCFAs and MCFAs can act as agonists to a number of GPCRs on immune cells including GPR65, GPR43 and GPR84. However, our understanding of their immunological role is largely unknown.

### *3.1 G protein-coupled receptors (GPCRs)*

GPCRs are the largest family of membrane proteins and are integral to signal transduction pathways in vertebrates<sup>35</sup>. They are highly evolutionarily conserved due to extremely important control of cellular function, and can be found in plants and even in protozoa<sup>36</sup>. Ligand binding on the extracellular surface of GPCRs induces conformational changes through 7 transmembrane segments which result in further changes to the intracellular surface<sup>37</sup>. Upon agonist binding, the intracellular surface of the GPCR interacts with a GDP-bound G-protein heterotrimer made of the subunits  $\alpha\beta\gamma$ , inducing the exchange of GDP for GTP and releasing  $G\alpha$  subunits<sup>38</sup>. These  $G\alpha$  subunits include  $G_s$ ,  $G_{i/o}$ ,  $G_{q/11}$  and  $G_{12/13}$ <sup>39</sup>. Signalling cascades triggered by different  $G\alpha$  protein subunits can induce intracellular release

of  $\text{Ca}^{2+}$ , the production or reduction of cAMP,  $\text{PIP}_3$  production and the activation of  $\beta$ -arrestin, all of which induce transcriptional changes in gene expression<sup>38</sup>. Specificity of transcriptional change induced by different GPCRs includes: different G protein subunits, recruitment of signalling molecules by adaptor proteins anchored nearby GPCRs within the cell membrane, and cross-talk with other activated receptor signalling cascades<sup>39</sup>.

### 3.2 Proton-sensing receptor GPR65

GPR65 is activated by protons in extracellular acidic conditions<sup>40</sup>. This suggests that it may act as a surrogate receptor for concentrated acidic metabolites such as lactate from anaerobic glycolysis. This mechanism of GPR65 activation has been hypothesised to occur in the tumour microenvironment, as it is typically acidic from glycolysis and poor perfusion<sup>41</sup>. Northern blot analysis of human tissue revealed substantial GPR65 expression in blood leukocytes and spleen, alongside moderate expression in lymph nodes, thymus, lung and small intestine<sup>42</sup>. In particular, GPR65 is expressed on a variety of immune cells, including T and B lymphocytes, neutrophils, eosinophils and mast cells<sup>43, 44</sup>. Glucocorticoid treatment of T cells induces GPR65 expression, whereby GPR65 enhances glucocorticoid-induced T cell apoptosis<sup>45, 46</sup>. Activation of GPR65 under acidic conditions has been associated with increased viability of eosinophils and lymphomas<sup>43, 47</sup>. Indeed, the expression of GPR65 in chronic lymphocytic leukemia cells highly correlates with the expression of anti-apoptotic protein BCL-2<sup>48</sup>. Furthermore, multiple genome-wide association studies have associated single nucleotide polymorphisms (SNPs) in Gpr65 with increased susceptibility to IBD<sup>49, 50, 51</sup>. This suggests GPR65 may play an important role in preventing IBD pathogenesis.

### 3.3 SCFA receptors: GPR43, GPR109a

The two most abundant SCFAs in the gut, acetate and propionate, have an equal affinity for GPR43<sup>52</sup>.<sup>53</sup> GPR43 signals with a dual-coupling mechanism through  $G_{i/o}$  and  $G_q$  subunits<sup>54</sup>. Activation of GPR43 induces intracellular  $\text{Ca}^{2+}$  release and reduces cAMP, but can increase ATP production (the substrate for cAMP) in colonic epithelium *in vitro*<sup>53, 55, 56</sup>. GPR43 is found on neutrophils,

macrophages, dendritic cells (DCs), mast cells, and epithelial cells in rat intestine and human colon<sup>52, 53, 57, 58</sup>. Murine studies suggest signalling via GPR43 induces down-regulation of inflammatory responses<sup>8, 15</sup>. Indeed, GPR43 knockout (KO) mice have been demonstrated to exhibit exacerbated allergic airway disease, suggesting SCFA signalling plays a role in the prevention of asthma<sup>15</sup>. Furthermore, observations of impaired proliferation and increased susceptibility to apoptosis in colon cancer cells via GPR43 signalling suggest that SCFAs can regulate inflammatory responses via decreased survivability<sup>59</sup>. Indeed, direct contact with SCFAs also decreased production of a broad range of pro-inflammatory cytokines from monocytes and macrophages in a receptor-mediated manner<sup>60, 61</sup>, further suggesting an important role for GPR43 in regulating immune responses. Recently, we have shown that GPR43 activation from high fibre diet has been demonstrated to induce oral tolerance to peanut antigens in mice by enhancing tolerogenic CD103+ DC function via retinoic acid metabolism<sup>62</sup>. This mechanism protects against peanut allergy, highlighting the importance of metabolite GPCR signalling in the prevention of western lifestyle diseases. Furthermore, GPR43 function can have downstream effects on metabolism. A number of murine studies have demonstrated conflicting effects of GPR43 activation on insulin resistance and obesity<sup>63</sup>. However, these discrepancies may be accounted for by the activation of different G protein subunits. Downstream of GPR43 activation,  $G_{q/11}$  increases glucose-stimulated insulin secretion in murine islets whereas  $G_{i/o}$  decreases it<sup>64</sup>. This reveals the potential dichotomous role GPR43 may play in metabolism, though the details of such a role remain poorly understood.

Although niacin is the most investigated agonist of GPR109a, the SCFA butyrate also demonstrates agonistic activity when in millimolar concentrations<sup>65</sup>. Activation of GPR109a induces intracellular  $Ca^{2+}$  release, reduces cAMP, and activates kinases and  $\beta$ -arrestin 3 to internalise the receptor<sup>66</sup>. GPR109a is expressed on human adipocytes and immune cells including macrophages and neutrophils but not lymphocytes or eosinophils<sup>67, 68</sup>. Reporter mice reveal that GPR109a is broadly expressed in spleen and bone marrow<sup>69</sup>. In addition, transfected human cell lines also reveal GPR109a expression in the small intestine and colon<sup>65</sup>. GPR109a on adipose tissue is required for the inhibition of lipolysis by niacin which subsequently increases HDL in the blood<sup>70</sup>. Indeed, the increase in HDL



from niacin is not observed in mice lacking GPR109a, whilst subsequent increases in GPR109a in the liver can restore these effects<sup>71</sup>. This suggests an important role for the expression of GPR109a on adipocytes and hepatocytes for the control of blood cholesterol by niacin. However, immune cells are also altered by GPR109a. Activation of GPR109a on macrophages by niacin inhibited MCP-1-induced chemotaxis of macrophages to the peritoneum in mice and also increased lipid transporter expression associated with preventing the generation of atherosclerotic plaques<sup>67</sup>. This demonstrates that GPR109a activation on macrophages may protect against atherosclerosis. Secretion of pro-inflammatory cytokines by human monocytes was reduced by *in vitro* niacin treatment, an effect abrogated by knockdown of GPR109a by siRNA. This suggests activation of GPR109a provides an anti-inflammatory signal to macrophages<sup>72</sup>. Furthermore, pro-inflammatory cytokine release from retinal pigment epithelium (cells crucial for maintenance of retinal health) was also abrogated by GPR109a activation, accentuating another anti-inflammatory role for GPR109a<sup>73</sup>. In addition, niacin enhances human neutrophil apoptosis which may be induced by GPR109a due to the abrogation of this effect by pertussis toxin, a potent GPCR antagonist<sup>68</sup>. Neutrophil apoptosis is important in limiting excessive immune responses by depleting neutrophil numbers, again suggesting GPR109a can abrogate inflammation. However, niacin can induce regulatory responses independent of GPR109a. Migration of DCs to draining lymph nodes in response to contact sensitisation was impaired in mice fed niacin-supplemented diets, an effect unchanged in GPR109a KO mice<sup>74</sup>. Niacin may therefore alter DC migration independently of GPR109a to regulate inflammatory responses.

The study that identified butyrate as a novel GPR109a agonist investigated the role of GPR109a in colon cancer. It demonstrates GPR109a expression in both human and mouse colon cancer is reduced<sup>65</sup>. Furthermore, this study demonstrated that *in vitro* activation of GPR109a by butyrate induced apoptosis of colon cancer cells and also reduced NF- $\kappa$ B expression in a normal colon cell line<sup>65</sup>. Butyrate has also been demonstrated to induce colonic Treg differentiation via IL-10 release from macrophages and DCs or IL-18 from colonic epithelium, a mechanism dependent on GPR109a<sup>75</sup>. As a result, GPR109a KO mice develop severe inflammation in a model of dextran sulphate sodium (DSS) colitis, an effect dependent on hematopoietic cells demonstrated by bone

marrow chimeras<sup>75</sup>. This highlights another regulatory effect of GPR109a activation and identifies a significant role that immune cells can play in regulating inflammation in the gut when exposed to dietary metabolites. Therefore, metabolites from both dietary fibre and tryptophan can regulate immune responses by GPR109a agonists niacin and butyrate. Interestingly, GPR109a expression is reduced in the gut of germ free mice<sup>76</sup>, accentuating the role the gut microbiota may play in regulating immune responses not just from the activation of GPCR agonists, but also from the up-regulation of GPCR expression.

### *3.4 MCFA receptor: GPR84*

GPR84 is activated by MCFAs of 9-14 carbons long which induces the  $G_{i/o}$  signalling pathway, stimulating  $Ca^{2+}$  release whilst reducing cAMP production<sup>77</sup>. It is expressed in bone marrow, spleen and lymph nodes of both humans and mice<sup>77</sup>. More specifically, GPR84 is expressed on polymorphonuclear leukocytes, macrophages, DCs and lymphocytes<sup>78, 79, 80</sup>. Murine T cells lacking GPR84 produced more IL-4, IL-5 and IL-13, suggesting GPR84 regulates canonical Th2 cell cytokine production<sup>79</sup>. Contrastingly, another study found no difference in T cell cytokine production between GPR84 KO and WT controls<sup>78</sup>. In addition, this study demonstrated that LPS increases GPR84 expression on macrophages<sup>78</sup>. Furthermore, a potent agonist of GPR84, 6-n-octylaminouracil, increased LPS-induced release of IL-8 and TNF- $\alpha$  from a human macrophage cell line whereas knockdown of GPR84 decreased TNF- $\alpha$  release<sup>78</sup>. This suggests GPR84 enhances pro-inflammatory cytokine release from macrophages and may therefore exacerbate inflammation. Regardless, reports surrounding the role of GPR84 in immune responses are confounding.

Consumption of medium chain triglycerides can promote antigen intake from the gut and subsequently enhance Th2 responses in a murine model food allergy<sup>81</sup>. Therefore, absorption of MCFAs across the gut may promote allergen sensitisation, however the possible role of GPR84 in allergy remains unknown.

#### 4. Immunomodulatory mechanisms of SCFAs via epigenetics

SCFAs appear to modulate cellular function by altering the acetylation pattern of gene promoters, an epigenetic mechanism independent of GPCR activation. SCFAs inhibit histone deacetylases (HDACs)<sup>82</sup>, enzymes that remove acetyl groups from histones<sup>83</sup>. Inhibition of HDACs enhances the acetylation the lysine residues in histones. Acetylation of lysine residues induces gene activation by facilitating the access of transcription factors to promoter regions<sup>84</sup>. As such, inhibition of HDAC activity can increase gene transcription by increasing histone acetylation.

HeLa cells treated with sodium butyrate underwent dramatic increases in global histone acetylation correlating with reduced global HDAC activity<sup>85</sup>. Treatment of HeLa cells with propionate also reduced HDAC activity but to a lesser extent than butyrate, whereas acetate had no effect<sup>82</sup>. Hepatoma tissue culture cells exposed to butyrate, propionate or acetate exhibited increased global histone acetylation, whereby butyrate increased acetylation greater than propionate, and propionate greater than acetate<sup>86</sup>. Furthermore, numerous observations of colon cancer cells *in vitro* have demonstrated that propionate and butyrate increased histone acetylation by inhibiting global HDAC activity, whereas acetate had little to no effect<sup>82, 87, 88</sup>. Contrastingly, orally-administered acetate can specifically inhibit HDAC 2 activity and expression in the rodent brain *in vivo*, as determined by Western blot<sup>89</sup>. Taken together, these studies demonstrate a propensity for SCFAs to inhibit HDAC activity in a wide variety of cell types.

##### 4.1 SCFA-mediated HDAC inhibition

Where SCFA-mediated HDAC inhibition can be established or associated, the overwhelming result is an anti-inflammatory immune phenotype. Treatment of human macrophages with 1mM acetate *in vitro* significantly reduced global HDAC activity and increased global histone acetylation correlating with decreased production of inflammatory cytokines IL-6, IL-8 and TNF- $\alpha$ <sup>90</sup>. HDAC inhibition, in particular inhibition of HDAC9, increases expression of the forkhead box P3 (Foxp3) transcription factor *in vivo*, which subsequently increased proliferative and functional capabilities of Tregs<sup>91, 92</sup>.

Administration of butyrate moderately diminished human Treg proliferation but increased Treg CTLA-4-mediated suppression of T cell proliferation *in vitro* despite no change in Foxp3 expression<sup>93</sup>. Butyrate, propionate and acetate decreased LPS-induced TNF- $\alpha$  production *in vitro* from peripheral blood mononuclear cells (PMBCs) in a similar manner to the HDAC inhibitor trichostatin A (TSA)<sup>94</sup>. Furthermore, NF $\kappa$ B activity in PBMCs was also reduced *in vitro* by butyrate and propionate (but not acetate) in a similar manner to TSA<sup>94</sup>. Similar effects between SCFAs and TSA suggest HDAC inhibition as the mechanism responsible, though a direct effect of these SCFAs on histone acetylation in PMBCs is poorly understood. Global HDAC activity in rodent neutrophils was decreased *in vitro* by acetate, propionate and butyrate with increasing strength, respectively<sup>95</sup>. Correspondingly, butyrate and propionate but not acetate decreased LPS-induced TNF- $\alpha$  expression and NOS expression in rodent neutrophils<sup>95</sup>. Similarly, butyrate decreased LPS-induced release of pro-inflammatory mediators nitric oxide, IL-6 and IL-12 from bone marrow-derived macrophages in a manner dependent on HDAC inhibition<sup>96</sup>. In these instances where HDAC inhibition reduces pro-inflammatory gene expression independently of Tregs, it is likely inducing pro-apoptotic pathways or increasing expression of interferon regulatory factor that subsequently regulates pro-inflammatory pathways by inhibiting NF $\kappa$ B<sup>97</sup>. HDAC inhibition from SCFAs therefore regulates pro-inflammatory cytokine release from neutrophils and macrophages.

In addition to reducing pro-inflammatory mechanisms, SCFA-mediated HDAC inhibition can promote immune responses. HDAC inhibition by SCFAs enhances the acetylation of genes required for differentiation and IgA class-switching of B cells<sup>98</sup>. IgA production from B cells is required to protect the body from microbial gut infection<sup>99</sup>. Therefore, the inhibition of HDACs by SCFAs can promote humoral immunity to infection and maintain intestinal homeostasis despite anti-inflammatory effects on neutrophils and macrophages.

#### *4.2 Mechanism of HDAC inhibition*

Butyrate has been found to inhibit HDACs noncompetitively<sup>100</sup>, suggesting that it may not interfere with the associated binding between HDAC and substrate. However, it is hypothesised that 2 butyrate

molecules may occupy the hydrophobic cleft of the active site in a similar manner to the well-characterised HDAC inhibitor TSA<sup>101</sup>. The exact mechanism of how butyrate and other SCFAs can directly inhibit HDACs remains unknown.

SCFA transporters may be required for HDAC inhibition. The monocarboxylate transporter Slc5a8 transports SCFAs into DCs, and was required for butyrate- and propionate-induced blockade of murine DC development<sup>102</sup>. Global HDAC activity was reduced and global acetylation was increased in murine bone marrow cells (DC precursors) exposed to butyrate and propionate *in vitro*, accentuating the importance of Slc5a8 in HDAC-mediated effects of SCFAs in DCs<sup>102</sup>. Therefore, SCFAs do not necessarily require GPCRs to induce cellular signalling.

Having summarised the immunological role of specific acidic metabolite GPCRs, the following paragraphs will detail major diseases associated with deficiencies in these receptors or western diets deficient in their metabolite agonists. As described above, these are diseases of mucosal sites including asthma, food allergy and IBD.

## **5. Asthma**

Asthma is one of the most significant inflammatory diseases in the Western world, and has had a dramatic increase in incidence over the past 40 years<sup>25</sup>. Approximately 300 million people have asthma worldwide, with Australia having the highest incidence<sup>103</sup>. Asthma is an extremely diverse disease that encompasses a range of disease phenotypes. Common to almost all asthmatics is one or more exacerbation events that involve bronchoconstriction and difficulty breathing<sup>104</sup>. Allergic asthma is the most common phenotype<sup>104</sup> and is characterised by airway inflammation that leads to bronchoconstriction, whereby the smooth muscle of the airways contracts and makes breathing difficult, including breathlessness, cough and wheeze<sup>105</sup>. These symptoms correspond with airways hyperresponsiveness (AHR), a canonical diagnostic sign of asthma, whereby airways constrict in response to allergen or various chemical stimuli<sup>106</sup>. Ultimately, chronic inflammation leads to airway remodelling and irreversible changes in lung function<sup>105</sup>. Typically, asthma involves the inhalation of

a normally innocuous antigen such as pollen, which is recognised as an allergen and triggers an allergic response<sup>107</sup>. It remains unknown why some individuals develop asthma from exposure to usually non-innocuous substances, however, it is believed allergen sensitisation occurs at an early age<sup>108</sup>. Indeed, normal individuals do not elicit immune responses to inhaled antigens, termed respiratory tolerance, whereby Tregs and DCs can produce IL-10 to inhibit inflammation<sup>109, 110</sup>. Lung DCs expressing CD103 (an integrin that binds epithelium) can induce respiratory tolerance by increasing Treg differentiation<sup>111</sup>. Authors suggest this is mediated by retinoic acid (RA) production from CD103+ DCs due to observed increases in aldh1a2 expression, an enzyme responsible for RA production. Furthermore, TIM-4-expressing macrophages in the mediastinal LN also maintain respiratory tolerance by phagocytosing allergen-specific T cells that express PtdSer, the ligand for TIM-4<sup>112</sup>. Ultimately, deficiencies in respiratory tolerance may lead to complex immunological mechanisms that drive asthma pathogenesis, involving a multitude of immune cell responses discussed below.

### *5.1 Antigen presentation and T cell activation*

DCs coordinate allergic responses in asthma by migrating from the airways to mediastinal lymph nodes and subsequently activate Th2 and to some extent Th1 effector cells<sup>113</sup>. A murine model of AAD revealed that IL-33 is released from the lung epithelium upon exposure to allergen which up-regulates OX40L on DCs and subsequently stimulates Th2 activation<sup>114</sup>. Activation of Th2 cells induces IL-4, IL-5 and IL-13 production which stimulate IgE production from B cells and pro-inflammatory mediator release from eosinophils and mast cell which cause airway constriction and the symptoms of asthma (Figure 1.1). Furthermore, IL-4 can promote Th2 differentiation and proliferation<sup>115</sup>. IL-13 is critical for inducing AHR as blockade of IL-13 signalling with an anti-IL-13 antibody protects from OVA-induced AHR in mice<sup>116</sup>. DCs from asthmatics can promote the polarisation of Th2-inducing DCs via the release of PGE2 which subsequently increases CCL17 and CCL22 production from DCs, promoting Th2 cell differentiation and recruitment<sup>117</sup>. Antigen presentation therefore initiates the allergic response.

## 5.2 Role of regulatory T cells (Treg) in asthma

Tregs inhibit inflammation as indicated by the release of the immunosuppressive cytokines IL-10 and TGF- $\beta$ <sup>118, 119</sup>. Tregs may also express immunosuppressive molecules such as CTLA-4, which can bind B7 on DCs and down-regulate co-stimulation<sup>120</sup>, subsequently inhibiting differentiation and growth of CD4<sup>+</sup> T cells<sup>121</sup>. Subsequent deficiency in Treg function therefore exacerbates inflammation and can predispose to asthma. A study of Treg migration in a murine model of OVA-induced AAD revealed that Tregs accumulate in the lungs of allergic mice upon OVA challenge and fail to produce IL-10 or TGF $\beta$  and do not inhibit Th2 responses<sup>122</sup>. Indeed, pulmonary Tregs isolated from asthmatic children were lower in number, and exhibited reduced capability to suppress T cell proliferation and Th2 cytokine release<sup>123</sup>. Furthermore, Tregs isolated from asthmatics are more susceptible to cytotoxic effects of NKT cells than compared with healthy individuals, demonstrating how asthma could be linked to Treg deficiencies<sup>124</sup>. A study on Treg differentiation in the periphery via expression of the intronic Foxp3 enhancer CNS1 demonstrated how inducible Tregs (iTregs) can regulate Th2 mediated inflammation, as the lack of iTregs in CNS1-deficient mice induced dramatic Th2 responses<sup>125</sup>. These mice exhibited asthma-like symptoms including increased AHR, cellular infiltration of the lung, goblet cell numbers and mucus production. In addition, two studies of murine AAD demonstrate how Treg function appears crucial in preventing asthmatic responses. Firstly, in a murine OVA-induced model of AAD, transfer of OVA-specific CD4<sup>+</sup> CD25<sup>+</sup> Foxp3<sup>+</sup> cells to mice reduced AHR, eosinophilic infiltration and IL-5 and IL-13 in the lung in an IL-10-dependent mechanism (although IL-10 was not produced by Tregs directly)<sup>126</sup>. Secondly, depletion of Tregs via anti-CD25 administration in mice before HDM-induced AAD was established exacerbated features of AAD including increased cellular infiltration of the BALF, increased IgE, IL-4 and IL-5 in the blood<sup>127</sup>. Taken together, these studies demonstrate that asthma is strongly associated with Treg deficiency. As such, establishment of functional Treg responses in asthmatics may prove to be a strategy to alleviate disease.

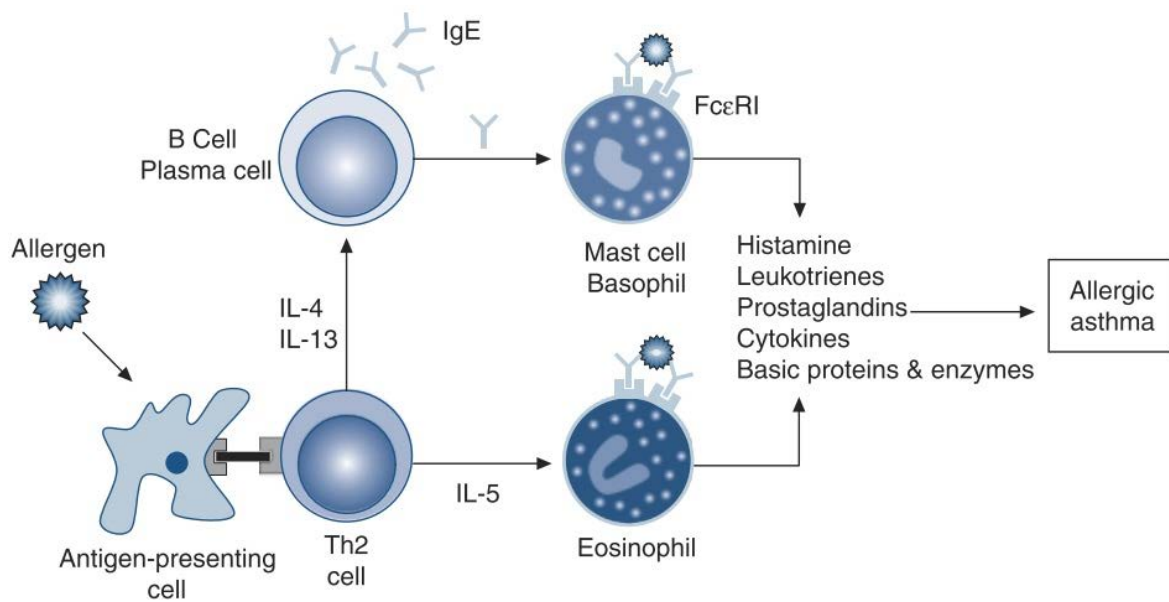


**Figure 1.1. Basic cellular mechanisms underlying asthma.** Allergen presentation by APCs activates Th2 cells inducing release of IL-4, 5 and 13<sup>98, 105, 106</sup>. IL-5 induces eosinophil recruitment, activation and development<sup>128</sup>. IL-4 and 13 induce IgE production from plasma cells, which when bound to allergen, induce activation of mast cells, basophils and eosinophils from IgE-bound FcεRI<sup>107</sup>. Subsequent release of pro-inflammatory mediators (histamine, leukotrienes, prostaglandins, cytokines and basic proteins) induce inflammation and airway remodelling that characterise asthma. Adapted from Holgate, S.T., 2008<sup>107</sup>.



### *5.3 Eosinophilic infiltration of the lung*

Amongst IL-4 and IL-5 production and increased responsiveness to IgE, the infiltration of eosinophils is a hallmark of both allergic and non-allergic asthma<sup>129</sup>. Eosinophils infiltrate the lung in asthmatic patients and subsequently degranulate, releasing a wide range of pro-inflammatory mediators including leukotrienes, metalloproteinases and growth factors that decrease epithelial integrity, induce tissue damage and promote mast cell-mediated responses<sup>130, 131</sup>.

Reports on the requirement of eosinophils in asthma are confounding. One study found that eosinophil-depleted C57BL/6 mice were protected from airway remodelling, but the depletion of eosinophils did not impact upon the asthma-associated loss of lung function described as airway hyper-responsiveness (AHR)<sup>132</sup>. Contrastingly, depletion of eosinophils in BALB/c mice can prevent the development of AHR in response to allergen challenge, despite no change in airway mucus production<sup>133</sup>. The discrepancies between these studies surrounding eosinophils and the development of AHR may be attributed to the use of different mouse strains. Indeed, eosinophils have been strongly associated with AHR in humans<sup>134</sup>. Eosinophils likely induce AHR by releasing eosinophil major basic protein which subsequently inhibits the function of neuronal M2 muscarinic receptors, reducing the capacity for parasympathetic nerves of the lung to maintain breathing<sup>135</sup>.

Recruitment of eosinophils in asthma is induced by the chemokines IL-5 and eotaxin that are released by airway epithelium and Th2 cells<sup>136, 137</sup>. IL-4 can up-regulate integrins required for eosinophil migration<sup>138</sup>, and through the actions of VCAM-1 expression on endothelial cells, can enhance eosinophil and macrophage migration to the lung<sup>139</sup>. Eotaxin, an eosinophil-specific chemoattractant, is produced in the lung of asthmatic individuals and is also increased by IL-4<sup>140</sup>, though not as potently as IL-13<sup>141</sup>. Furthermore, numbers of eosinophils in the lung are also significantly increased by the production of chemokines from mast cells in an IFN- $\gamma$ -dependent manner<sup>142</sup>. In particular, MIP-1 $\alpha$  is a chemokine crucial for eosinophil migration to the lung, as shown by the abrogation of eosinophil infiltration in allergic MIP-1 $\alpha$ -depleted mice<sup>143</sup>.

Ultimately, asthma is generated by an excessive allergic response in an environment that does not usually harbour excessive populations of such immune cells. Indeed, only a small number of eosinophils are present in normal lung tissue<sup>144</sup>. Contrastingly, food allergies to dietary antigens are characterised by excessive immune responses in the gut, a predominant location of basal inflammation.

## **6. Food Allergy**

Food allergy is defined as involving IgE-mediated responses and/or cell mediated mechanisms that develop skin, gastrointestinal, respiratory or circulatory symptoms<sup>145</sup>. Common symptoms of food allergy can be varied and include nausea, abdominal pain, diarrhoea, and in the most severe cases anaphylaxis<sup>146</sup>. The prevalence of food allergies in western countries is approximately 4% in adults and 5% in children<sup>147</sup> although it has been reported as high as 17% in both European children and adults<sup>145</sup>. Epidemiological evidence provides a number of risk factors, including obesity and dietary constituents<sup>148</sup>. Food allergy is diagnosed based upon a constellation of clinical and serological factors that consider medical history and possible serology or oral food challenge to identify an immune-mediated adverse reaction<sup>145</sup>.

### *6.1 Th2 responses*

Food allergy is generated from deficiencies in oral tolerance to dietary antigens that induce Th2-biased immune responses to normally innocuous antigens. Indeed, the most common presentation of food allergy involves IgE specific to a dietary allergen, although non-IgE mediated food allergy may still occur<sup>145</sup>. A murine model of food allergy revealed that the release of IL-33 by the gut epithelium induces OX40L expression on DCs in the mesenteric lymph node which subsequently activates Th2 cells, similar to sensitisation in AAD<sup>114</sup>. IL-4, IL-5 and IL-13 production from Th2 cells stimulates IgE production from B cells which activates eosinophils and mast cells that subsequently degranulate and release histamine<sup>149</sup>. However, in some cases IgE is not crucial for the development of allergy, as

is the case with enterocolitis and proctocolitis which are categorised more broadly with colonic cellular inflammation<sup>146</sup>.

## *6.2 Oral tolerance to antigens*

The breakdown in oral tolerance that induces food allergy is poorly understood. Although murine studies have extensively investigated oral tolerance, the particular disruption of these mechanisms that leads to food allergy in humans remains unclear. A study comparing two cohorts of Jewish children demonstrated that early exposure to peanuts during childhood may protect against development of peanut allergy independent of genetic factors<sup>150</sup>. This has been corroborated by the LEAP study, a large scale randomised trial that demonstrated that early peanut consumption in the first 11 months of life significantly protected against the onset of food allergy<sup>151</sup>. Changes in diet have also been linked to the increasing prevalence of food allergies, including a reduction in consumed vitamin A,  $\omega$ -3 fatty acids and antioxidants<sup>152</sup>. However, research into the mechanisms behind dietary causes of food allergy remains in its infancy.

Oral tolerance is the local and systemic unresponsiveness of the immune system to consumed antigens, inhibiting immune responses to commonly encountered antigens from our food. Enzymatic digestion of consumed foods and extremes in pH in the gut can render possible allergens unrecognisable to the immune system<sup>147</sup>. Furthermore, high doses of antigen can induce anergy (unresponsiveness to antigen) in T cells via DCs, whereas low doses can stimulate Treg responses to inhibit inflammation in the GIT to maintain tolerance<sup>153</sup>.

In a similar mechanism to tolerance in the lung, migration of CD103<sup>+</sup> DCs from the lamina propria to the mesenteric LN by via expression of CCR7 can induce Treg differentiation to maintain tolerance in the gut<sup>154, 155</sup>. CD103<sup>+</sup> DCs are common within the GIT of mice and are potent stimulators of Treg differentiation via the release of the cytokine TGF- $\beta$  and retinoic acid<sup>156</sup>. Indeed, retinoic acid production appears to be an imprinted phenotype of APCs in the GIT<sup>157</sup>. These CD103<sup>+</sup> DCs are

crucial in establishing oral tolerance by stimulating Treg responses and suppressing adaptive immune responses to innocuous antigens.

The mesenteric LN is the primary site for induction of oral tolerance to both dietary antigens and commensal bacteria<sup>158</sup>. Indeed, mice lacking mesenteric LNs do not generate oral tolerance to OVA<sup>159</sup>. Egg and peanut allergic infants display reduced circulating Treg numbers, suggesting that Treg impairment may lead to a break down in tolerance that leads to food allergy<sup>160</sup>. In addition, the microbiota appears crucial in maintaining oral tolerance as germ-free mice are more susceptible to developing allergies<sup>161</sup>. TLR-4 KO mice also develop severe allergies to dietary antigen, suggesting microbiota-induced stimulation of TLR-4 by bacterial LPS is important in maintaining oral tolerance and providing possible evidence of innate cell involvement<sup>162</sup>.

## **7. Inflammatory Bowel Disease**

IBD severely impacts upon the lifestyle and health of approximately 4 million people world-wide<sup>163, 164, 165</sup>. It broadly describes a group of disorders involving inflammation of the GIT that are typically diagnosed as either Crohn's disease or ulcerative colitis. Although Crohn's disease may affect any region of the GIT whereas ulcerative colitis is restricted to the colon<sup>166, 167</sup>. Symptoms of IBD include diarrhoea, fecal blood, abdominal pain and unintended weight loss. It involves a heterogeneous list of diagnostic factors that characterise the location and penetrance of inflammation throughout the gut. Like asthma and food allergy, the pathogenesis of IBD involves the interplay between genetics, the microbiome and a myriad of immunological processes<sup>168, 169, 170</sup>. This complex multifactorial network remains poorly understood.

### ***7.1 Epithelial integrity***

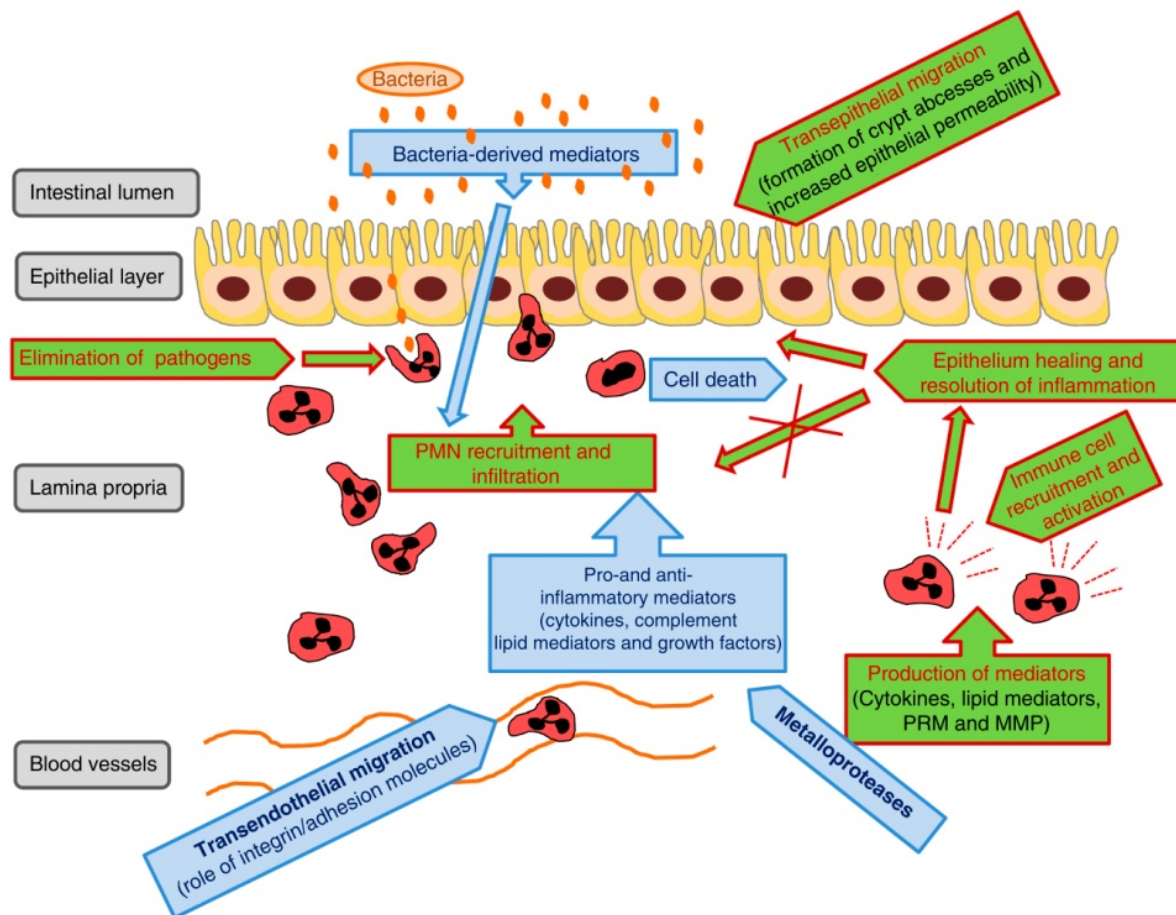
The first predominant primary event in IBD is the onset of epithelial permeability known as "leakiness"<sup>171</sup>. Permeability is derived from a breakdown in epithelial integrity, whereby bacteria and luminal antigens can cross the epithelium and establish inflammation characteristic of the disease. The cause of epithelial permeability is poorly understood given the complex aetiology of IBD. However, a

number of distinct mechanisms that determine epithelial integrity have been associated with IBD pathogenesis.

TLRs expressed on the epithelium are important in maintaining integrity. Mice deficient in TLR4 or TLR5 display enhanced susceptibility to experimental colitis and in the case of TLR5 can develop spontaneous colitis<sup>172</sup>. Indeed, a polymorphism in the *Tlr4* gene has associated impaired TLR4 function with IBD in humans<sup>173</sup>. This suggests TLR activation by the gut microbiota is required for maintaining gut integrity and preventing IBD. Furthermore, polymorphisms in CARD15/NOD2, a epithelial sensor of bacterial wall component MDP, have been associated with Crohn's disease and suggest bacterial sensing remains important in preventing IBD<sup>174</sup>. Tight junction proteins such as claudins and occludins maintain epithelial integrity by keeping epithelial cells connected. IBD has been associated with reduced expression and altered distribution of tight junction proteins, highlighting enhanced epithelial permeability as a hallmark of IBD<sup>175</sup>. Although the mechanisms that establish epithelial permeability are largely unknown and undoubtedly multifactorial, subsequent infiltration of the gut by immune cells constitutes the next stage in IBD pathogenesis.

## *7.2 Neutrophils in IBD pathogenesis*

A canonical indicator of inflammation in IBD is the accumulation and transepithelial migration of neutrophils in the gut<sup>176</sup>. Neutrophil chemotaxis to the gut is mediated by the release of canonical CXC chemokines from the epithelium, such as MIP-2 and IL-8<sup>177, 178</sup>. These chemokines are increased in the colon of IBD patients, facilitating subsequent neutrophil infiltration<sup>179, 180</sup>. The release of pro-inflammatory mediators from neutrophils in the gut can drive IBD pathogenesis by degrading epithelial junctions and reducing epithelial integrity<sup>181</sup>. Weakened integrity promotes bacterial translocation from the lumen to the mucosa, eliciting further inflammatory responses that exacerbate neutrophil migration and inflammation. Contrastingly, neutrophils also play an anti-inflammatory role in IBD by healing damaged epithelium and promoting epithelial integrity. Indeed, depleting neutrophils in rats exacerbated colitis, suggesting neutrophils are required for preventing disease<sup>182</sup>.



## Mucosal Immunology

**Figure 1.2. The interplay of neutrophils, epithelium and microbiota in IBD.** Involvement of neutrophils in disease indicated in green boxes. Factors affecting neutrophil contribution indicated in blue boxes. Infiltrating neutrophils demonstrate pro-inflammatory responses by eliminating bacteria that cross the epithelial layer when epithelial permeability is increased. Furthermore, neutrophils demonstrate anti-inflammatory function by helping to resolve inflammation. PMN, polymorphonuclear leukocytes (neutrophils); MMP, matrix metalloproteinase, PRM; pattern recognition molecule. Adapted from Fournier et al. 2012<sup>181</sup>.

As such, neutrophils play a complex role in the pathogenesis of IBD as a consequence of epithelial permeability and microbial translocation (Figure 1.2).

### 7.3 Murine models of colitis

In contrast to murine models of asthma or food allergy, murine models of colitis are extremely varied. Symptoms of the disease can be generated chemically, by cellular transfer or by bacterial infection. This thesis presents data using two different models of colitis – dextran sulphate sodium (DSS) administration and *Citrobacter rodentium* infection. The most common model of colitis involves the administration of DSS in the drinking water<sup>183</sup>. DSS chemically damages the colonic epithelium via an unknown mechanism that drives innate inflammation. Inflammation subsequently induces clinical symptoms of colitis including weight loss, diarrhoea and fecal blood. Adaptive immune responses are not required to induce disease in DSS colitis, as demonstrated by severe clinical symptoms in mice lacking T and B lymphocytes<sup>184</sup>. DSS colitis is therefore a robust model to interrogate innate immune responses in IBD. In contrast, bacterial-induced colitis by *C. rodentium* infection involves both innate and adaptive immune responses to resolve infection and prevent clinical symptomology<sup>185</sup>. Infection induces colitis-like symptoms such as weight loss and diarrhoea alongside pathological similarities involving inflammation of the colonic tissue<sup>186</sup>. Furthermore, *C. rodentium* is an attaching/effacing bacteria that causes epithelial lesions similar to enterohaemorrhagic and enteropathogenic *E. coli* infections in humans<sup>187</sup>. As such, assessing *C. rodentium* infection in mice provides insights into the pathogenesis of both IBD and bacterial gut infection.

## 8. Rationale

Rising incidences in inflammatory and allergic diseases demands the characterisation of their causes. Given the propensity for diet to associate with disease outcome, understanding the role of diet and dietary metabolites is becoming paramount in our pursuit to cure these diseases. Acidic metabolite-sensing GPCRs have been demonstrated to alter immune responses, suggesting that they may prove to



be valuable targets for dietary and pharmacological intervention. However, despite a flurry of recent publications on their function they remain immunologically dark.

This doctorate has focussed on the immunological role of three GPCRs and their agonists: GPR43, GPR65 and GPR84. Although three other major GPCRs with dietary fatty acid agonists GPR41, GPR109a and GPR120 have been associated with immunomodulatory function<sup>188</sup>, the investigation of these receptors was ongoing by other doctoral candidates of the Mackay laboratory. As such, my project focussing on GPR43, GPR65, GPR84 and their agonists fits within a broader scope of immunological GPCR research. Each of these receptors and their agonists have been separated into three main projects of my doctorate. The aim of my first project was to determine role of high fibre diet, SCFAs and GPR43 in the pathogenesis of asthma and *C. rodentium* infection. Secondly, I aimed to characterise GPR65 and its role in IBD and infection as a possible surrogate receptor for SCFAs. The aim of the third project was to determine the role of MCFAs and GPR84 in IBD, asthma and food allergy.

To achieve these aims, I have phenotyped *Gpr43*<sup>-/-</sup>, *Gpr65*<sup>-/-</sup> and *Gpr84*<sup>-/-</sup> mice using a number of inflammatory and allergic disease models to determine the immunological role of these receptors. Although some disease models have already been investigated in these knockout mice, a number have remained uncharacterised which form the core rationale of this thesis (Table 1.1). Mice deficient in GPR43, GPR65 and GPR84 were subject to murine disease models of asthma, food allergy and colitis to investigate the role of these GPCRs in disease pathogenesis. Moreover, cellular expression and function was assessed to determine specific immunological mechanisms controlled by GPR43, GPR65, GPR84 and their agonists. Furthermore, I administered dietary agonists to investigate the impact of GPCR activation through food, establishing novel links between diet and disease prevention.

This thesis presents these data in full. The following chapters combine a traditional thesis structure with that of a thesis by publication. As such, chapters 1, 2 and 3 present data from published and submitted papers, whilst chapter 4 is structured traditionally. Taken together, these three chapters

**Table 1.1. Summary of pre-doctorate murine studies of allergy (asthma and food allergy) and inflammatory disease (colitis, *Citrobacter rodentium* infection and arthritis) implicated with GPR43, 65, 84 and their agonists. (✓) Green boxes indicate known data already published. (X) Red boxes indicate unknown involvement of receptor/agonist with disease. (?) Yellow boxes indicate partial knowledge or possible implication.**

	<b>Mouse Models of Disease</b>			
<b>Receptor/Agonists:</b>	<b>Asthma</b>	<b>Food Allergy</b>	<b>Colitis</b>	<b>Citrobacter Infection</b>
GPR43/SCFAs	? Implicated by Maslowski et al. 2009	✓ published Tan et al. 2016	✓ published Macia et al. 2015	X
GPR65/H <sup>+</sup> ions	✓ published Kotyann et al. 2009	X	X	X
GPR84/MCFAs	X	? Agonist implicated by Li et al. 2013	X	X

communicate the experiments, data and scientific reasoning that constitute this doctorate of philosophy and present a novel role for GPR43, GPR65, GPR84 and their agonists in immunology and mouse models of human disease.

## **Chapter 2 – The Role of Dietary Fibre, SCFAs and GPR43 in Asthma and Infection**

### **1. Introduction**

The following chapter contains data included in two separate papers that investigate the preventative effects of SCFAs on asthma and gut infection, respectively. The first of these papers was published in *Nature Communications* in 2015, titled “Evidence that asthma is a developmental origin disease influenced by maternal diet and bacterial metabolites” (Appendix 1). The data from this doctorate included in this article is presented here as the first section of Chapter 2. All methods are included in the Appendix. The second paper is titled “High acetate yielding diets protect mice from *Citrobacter rodentium* infection through enhanced mucosal immunity and control of bacterial growth” and has been submitted to *Gastroenterology*. This manuscript is predominantly comprised of data from this PhD and has therefore been included in its entirety as the second half of this chapter. Taken together, these papers identify a new role for SCFA acetate in preventing asthma and gut infection via distinct mechanisms dependent or independent of GPR43. This establishes a novel link between fibre, allergies and infection by interrogating the immunomodulatory impact of SCFAs.

### **2. High fibre diet and acetate prevents allergic airways disease (AAD)**

Low intake of vegetables and therefore dietary fibre was associated with an increased incidence of asthma by a paediatric study of US children<sup>4</sup>. To investigate the immunomodulatory role of SCFAs on peripheral allergic responses such as asthma, we administered high fibre diet, zero fibre diet or acetate in the drinking water (200mM) to mice *ad libitum* for 3 weeks prior to and during the induction of AAD (Figure 2.1A). Briefly, AAD was established by intranasal injection of 50 µg/ml of house dust mite (HDM) that elicits allergic inflammation in the lung. Infiltration of eosinophils, macrophages and lymphocytes into the bronchiolar lavage fluid (BALF) was reduced in mice administered a high fibre

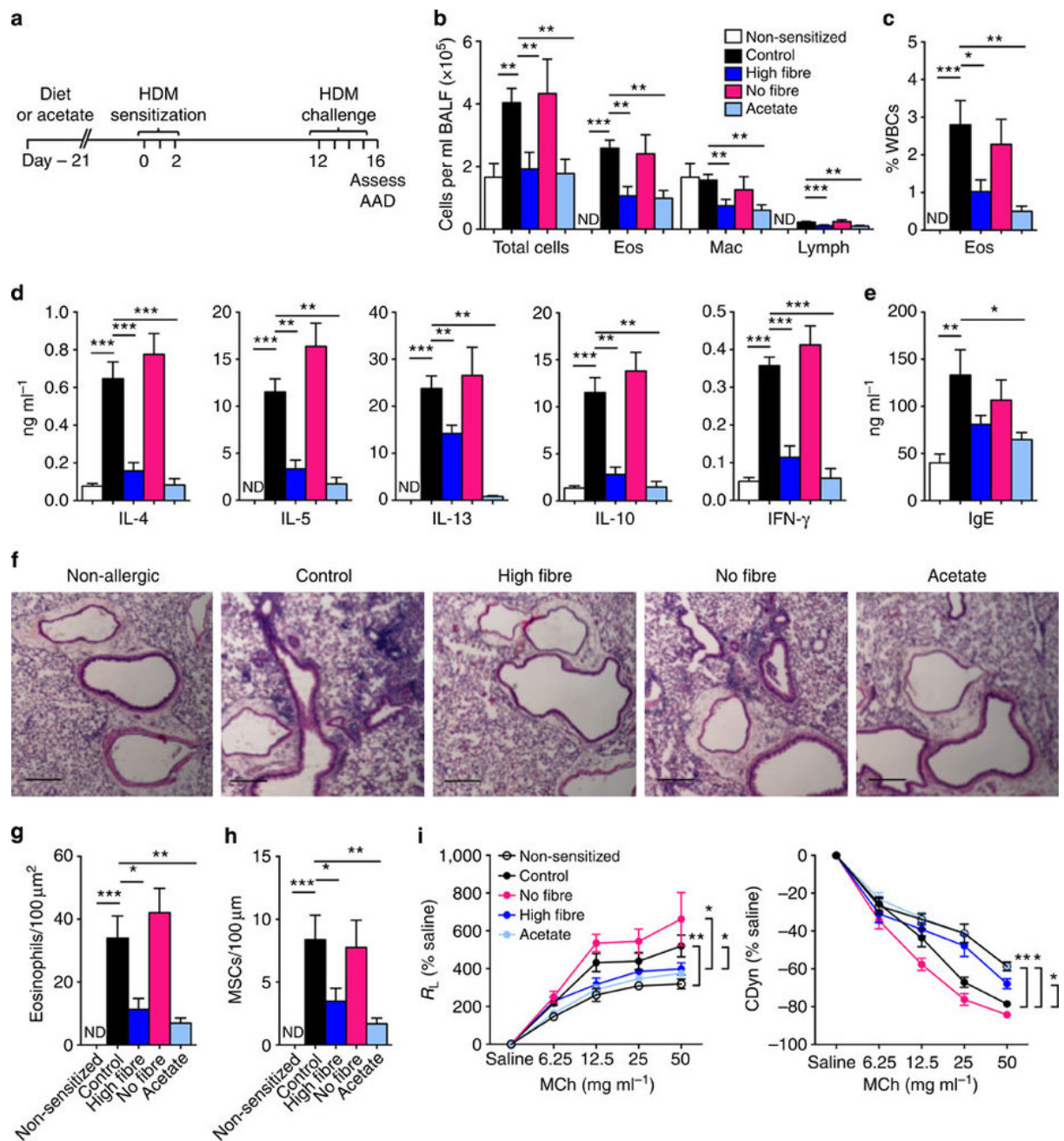


**Figure 2.1. The effect of high-fibre diet and acetate on the development of AAD in adult mice.**

(a) Mice (female C57Bl/6J) were weaned onto control, high-fibre diet, no-fibre diet, or acetate for 3 weeks and at 6 weeks old sensitized and challenged with HDM. The effect of high-fibre or no-fibre diet on (b) differential cell number in BALF, (c) eosinophils in blood, (d) IL-4, IL-5, IL-13, IL-10 and IFN $\gamma$  release from MLN T cells, (e) serum IgE, (f) lung histology (scale bar 200  $\mu$ m), (g) eosinophils in lung tissue, (h) mucous-secreting cells (MSCs) and (i) airway hyper-responsiveness in terms of airway resistance ( $R_L$ ) and dynamic compliance ( $C_{dyn}$ ). Data represent mean+SEM,  $n=8$ . Significance is represented by \* $P<0.05$ , \*\* $P<0.01$ , \*\*\* $P<0.001$ , Student's  $t$ -test. One representative experiment of three is shown. ND, not detected.

diet or acetate (Figure 2.1B). Both high fibre diet and acetate in the drinking water also reduced the quantity of eosinophils in the blood (Figure 2.1C). This suggests that high fibre feeding can prevent inflammation in the lung through fermentation to SCFAs that regulate cellular infiltration. Release of canonical Th2 cytokines IL-4, IL-5 and IL-13 from T lymphocytes was reduced by high fibre and acetate treatment (Figure 2.1D). In addition, total serum IgE was reduced by acetate (Figure 2.1E). These data demonstrate that adaptive responses to HDM are regulated by high fibre and acetate. Histological assessment of lungs in allergic mice revealed treatment with high fibre and acetate decreased eosinophil infiltration into the tissue and reduced the number of mucous-secreting cells (Figure 2.1F – H). Furthermore, high fibre and acetate improved lung function by preventing AAD-induced reduction in resistance and increase in dynamic compliance (Figure 2.1I). This suggests dietary fibre and SCFAs can prevent allergic airway inflammation and protect against clinical symptoms of asthma.

### **3. Treatment with high fibre diet and acetate prevents AAD in offspring**

There are two predominant mechanisms by which SCFAs can alter cellular function: GPCR activation and epigenetic alteration of histone acetylation. To investigate the role of GPR43 in acetate-induced prevention of AAD, we treated wild type (WT) or Gpr43<sup>-/-</sup> mice with acetate 3 weeks prior to and during AAD. Airway inflammation and lung function were unchanged between WT and Gpr43<sup>-/-</sup> mice (DNS). This suggests GPR43 is not involved in preventing AAD with dietary acetate.

Nutrition state of mothers alters the epigenetic profile of offspring<sup>189</sup> which prompted us to investigate the involvement of epigenetics in the prevention of AAD with SCFAs. To determine the role of epigenetics in the prevention of AAD we assessed the severity of AAD in pups of mothers treated with high fibre or acetate. Briefly, pregnant mice were administered high fibre diet or acetate from 13 days post fertilisation until pups were weaned at 3 weeks of age (Figure 2.2A). As such, pups never received diet or acetate directly as they were only exposed to either treatment through the mother's bloodstream during pregnancy or through milk after birth. As before, high fibre and acetate reduced

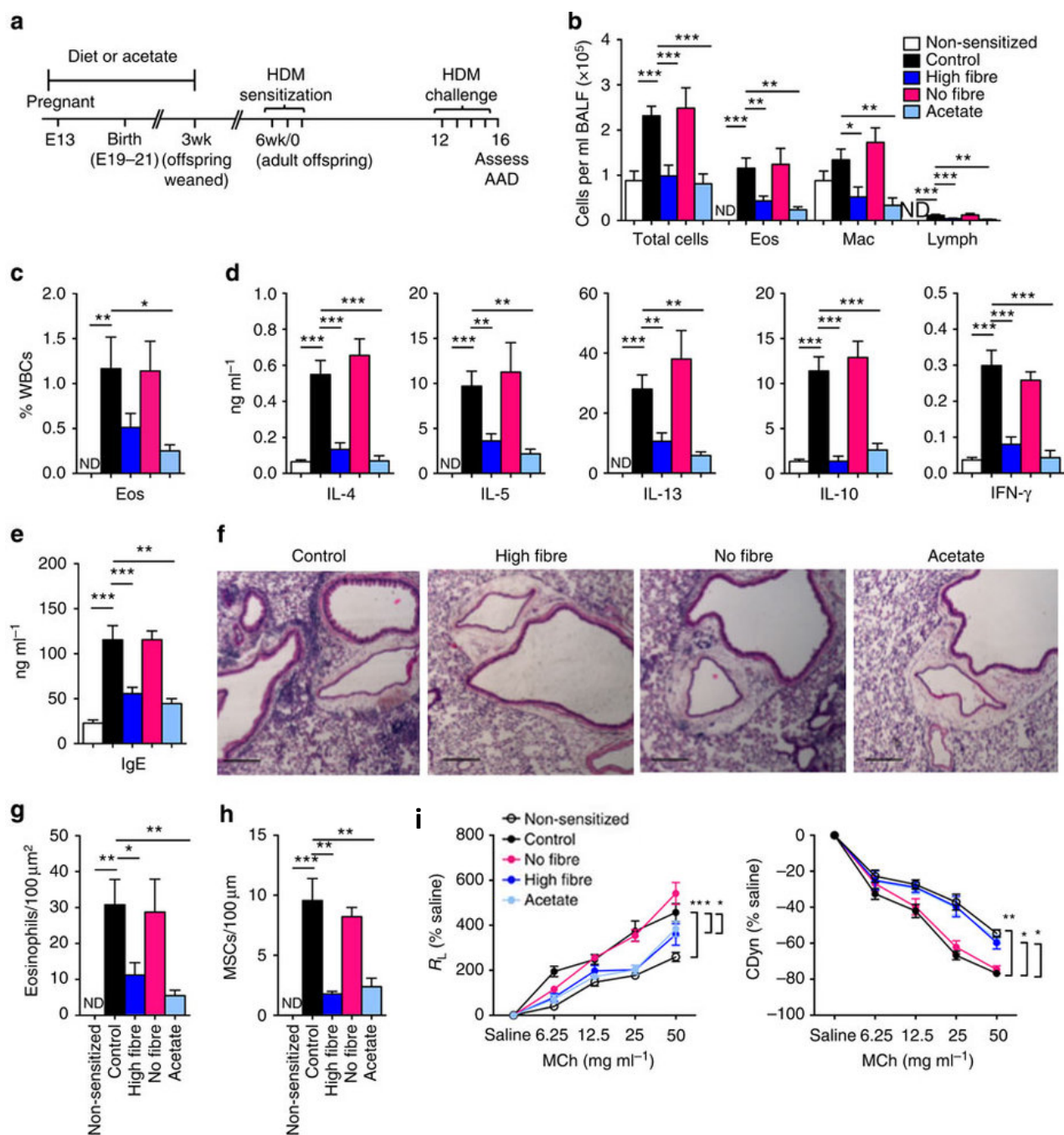




**Figure 2.2. The effect of maternal intake of high-fibre diet and acetate on the development of AAD in the offspring.** (a) Pregnant mice (E13, C57Bl/6J) were provided with control, high-fibre diet, no-fibre diet or acetate. Offspring (female C57Bl/6J) were weaned onto control diet and water at 3 weeks of age and at 6 weeks, sensitized and challenged with HDM. The effect of high-fibre diet or acetate on (b) differential cell number in BALF, (c) eosinophils in blood, (d) IL-4, IL-5, IL-13, IL-10 and IFN $\gamma$  release from MLN T cells, (e) serum IgE, (f) lung histology (scale bar, 200  $\mu$ m), (g) eosinophils in lung tissue, (h) mucous-secreting cells (MSCs), and (i) airway hyperresponsiveness in terms of airway resistance ( $R_L$ ) and dynamic compliance ( $C_{dyn}$ ). Data represent mean+SEM,  $n=8$ . Significance is represented by \* $P<0.05$ , \*\* $P<0.01$ , \*\*\* $P<0.001$ , Student's  $t$ -test. One representative experiment of three is shown. ND, not detected.

the eosinophil infiltration in the BALF and circulation in the blood (Figure 2.2B, C). Furthermore, high fibre and acetate reduced Th2 cytokine release and total serum IgE (Figure 2.2D, E). Presence of eosinophils and mucous-secreting cells in the lung were also reduced (Figure 2.2F – H). In addition, high fibre and acetate improved lung function in asthmatic mice (Figure 2.2I). Taken together, these data demonstrate that the offspring of mothers administered high fibre diet or acetate are protected from developing asthma.

#### **4. High fibre and acetate protect against AAD independent of microbiota transfer at birth**

Effects of high fibre and acetate in the offspring were mediated either *in utero* (E13 to birth) or throughout lactation (birth to weaning). To determine which phase required high fibre or acetate treatment to prevent AAD, we provided high fibre or acetate to mothers either during *in utero* or lactation only and assessed AAD in the offspring. When administered during the lactation phase between birth and weaning, high fibre and acetate had no effect on AAD in the offspring (DNS). However, high fibre and acetate administered only when pups were *in utero* reduced cellular infiltration of the BALF, Th2 cytokine release and serum IgE (Figure 2.3A – C). Furthermore, *in utero* administration protected against AAD-induced reduction of lung function (Figure 2.3D). This demonstrates that only maternal administration of SCFAs is required to maintain protection from asthma in offspring, whereas administration during lactation is too late to provide protection.

During birth, the gut microbiota of the mother is passed on to the offspring. However, caesarean section removes the exposure of the offspring to their mother's microbiota and prevents microbial transfer.<sup>190</sup>. Given the propensity for the gut microbiota to alter immune responses, we hypothesised that high fibre or acetate may establish a unique microbiota that can protect against AAD and be passed from mother to offspring. To investigate the involvement of the microbiota transfer at birth, we treated mothers from E13 to E18 before performing a caesarean section and transferring pups to a different mother on control diet and normal water. AAD was subsequently assessed in adult offspring. High fibre and acetate maintained protection against AAD even when offspring were raised by

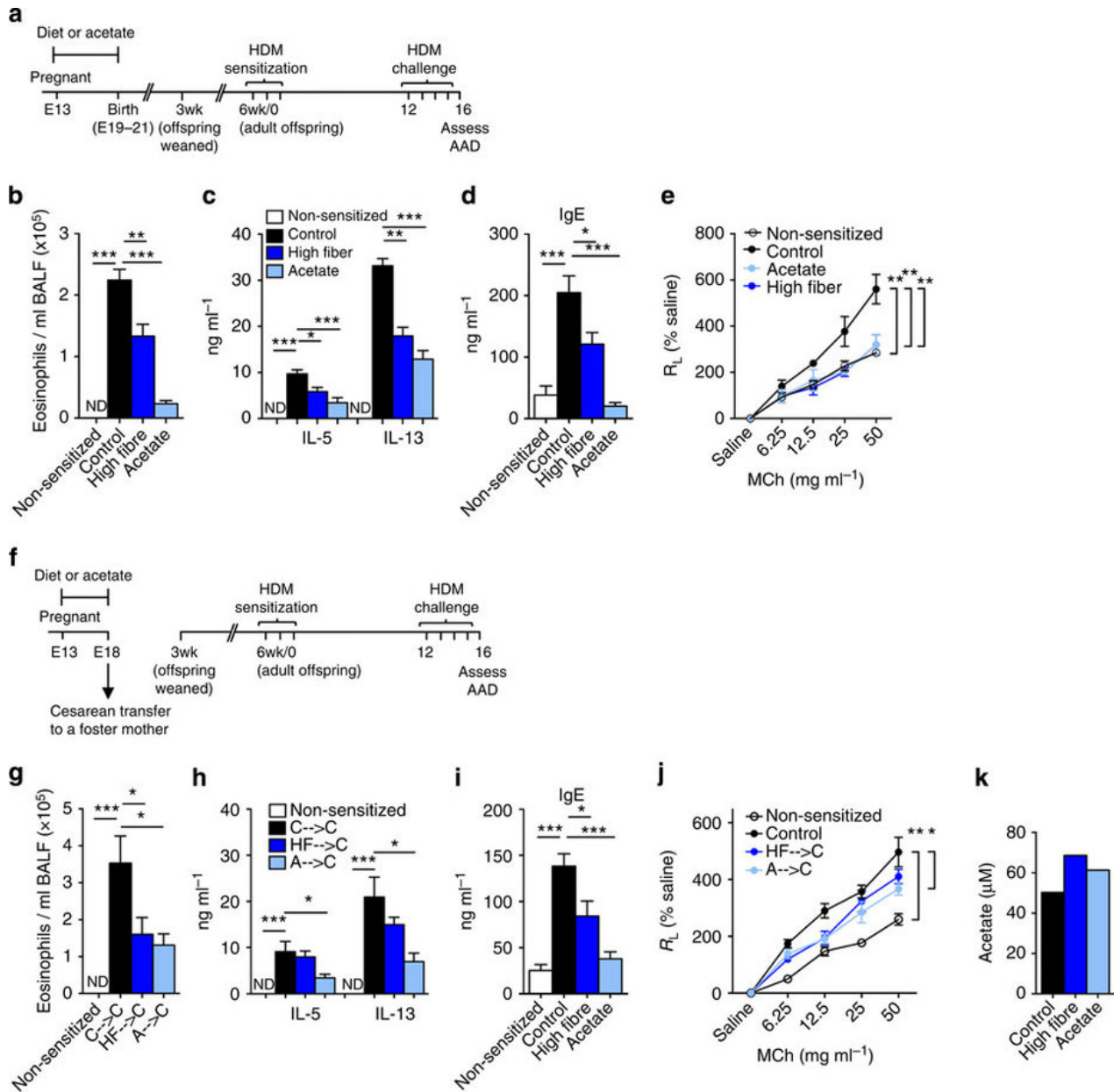


**Figure 2.3. Effects of maternal diet or acetate on AAD are mediated in utero independently of microbial transfer.** (a) Pregnant mice (E13, C57Bl/6J) were provided with control, high-fibre diet or acetate. At birth, the control diet or water was provided. Female offspring were also weaned onto control diet and water at 3 weeks of age and at 6 weeks, sensitized and challenged with HDM. The effect of high-fibre diet or acetate during pregnancy on (b) eosinophil cell number in BALF, (c) IL-5 and IL-13 release from MLN T cells, (d) serum IgE and (e) airway hyperresponsiveness in terms of airway resistance (RL). (f) Pregnant mice (E13) were provided with control, high-fibre diet or acetate. At E18, offspring were caesarean transferred to a foster mother (Balb/c) fed the control diet and water. Female offspring were weaned onto control diet and water at 3 weeks of age and at 6 weeks, sensitized and challenged with HDM. The effect of high-fibre diet or acetate during pregnancy after caesarean transfer on (g) eosinophil cell number in BALF, (h) IL-5 and IL-13 release from MLN T cells, (i) serum IgE and (j) airway hyper-responsiveness in terms of airway resistance (RL). Data represent mean+SEM, n=8. Significance is represented by \*P<0.05, \*\*P<0.01, \*\*\*P<0.001, Student's t-test. One representative experiment of three is shown. ND= not detected. (k) Serum was collected from offspring (n=35–40 per group) at E18 and acetate levels measured by 1H-NMR spectroscopy. Each measurement represents ~35–40 pooled individual blood collections.

mothers that were had not been exposed to either. Offspring exhibited reduced cellular infiltration of the BALF, Th2 cytokine release and serum IgE (Figure 2.3G – I). Furthermore, high fibre and particularly acetate reduced AHR and maintained lung function (Figure 2.3J). This demonstrates that altered microbiota in the mother and subsequent transfer of this microbiota to offspring is not involved in the prevention of AAD by high fibre and acetate. In addition, serum acetate in pups at E18 was slightly increased by high fibre and acetate (Figure 2.3J). However, significance could not be determined due to low sample numbers. This suggests that high fibre and acetate administered to pregnant mothers may enhance SCFA concentrations within the offspring *in utero* and subsequently alter immunological development to prevent AAD.

## **5. Acetate protects against AAD via Tregs and epigenetic modification of the *Foxp3* promoter**

Tregs are crucial in maintaining tolerance to antigens and preventing the pathogenesis of allergies such as asthma<sup>191</sup>. Histone acetylation of the *Foxp3* promoter has been demonstrated to enhance Treg differentiation and function<sup>93</sup>. To investigate the role of Tregs and epigenetics in the prevention of AAD, we assessed histone modification of *Foxp3* in T cells from the asthmatic offspring of mothers treated with acetate. H4 acetylation of the *Foxp3* promoter in T cells was increased by acetate, correlating with increased expression of *Foxp3* in Tregs (Figure 2.4A, B). This suggests that SCFAs enhance *Foxp3* expression by epigenetically priming the promoter with increased acetylation of H4 histones. Indeed, Treg number and function was increased by acetate (Figure 2.4C, D), suggesting that dietary SCFAs can regulate allergic responses by enhancing the involvement of Tregs.

To determine whether Tregs were required for prevention of AAD by acetate, we administered a Treg-depleting antibody specific for CD25 ( $\alpha$ -CD25) to mice treated with acetate prior to induction of AAD. Asthmatic mice treated with  $\alpha$ -CD25 exhibited increased cellular infiltration of the BALF, Th2 cytokine release, serum IgE and worsened lung function (Figure 2.4E – H). Furthermore, the protective effect of acetate was completely abrogated by  $\alpha$ -CD25 treatment. This demonstrates that dietary acetate enhances the involvement of Tregs in the prevention of AAD. Furthermore, Tregs were similarly required for the prevention of AAD in offspring of mothers receiving acetate as  $\alpha$ -

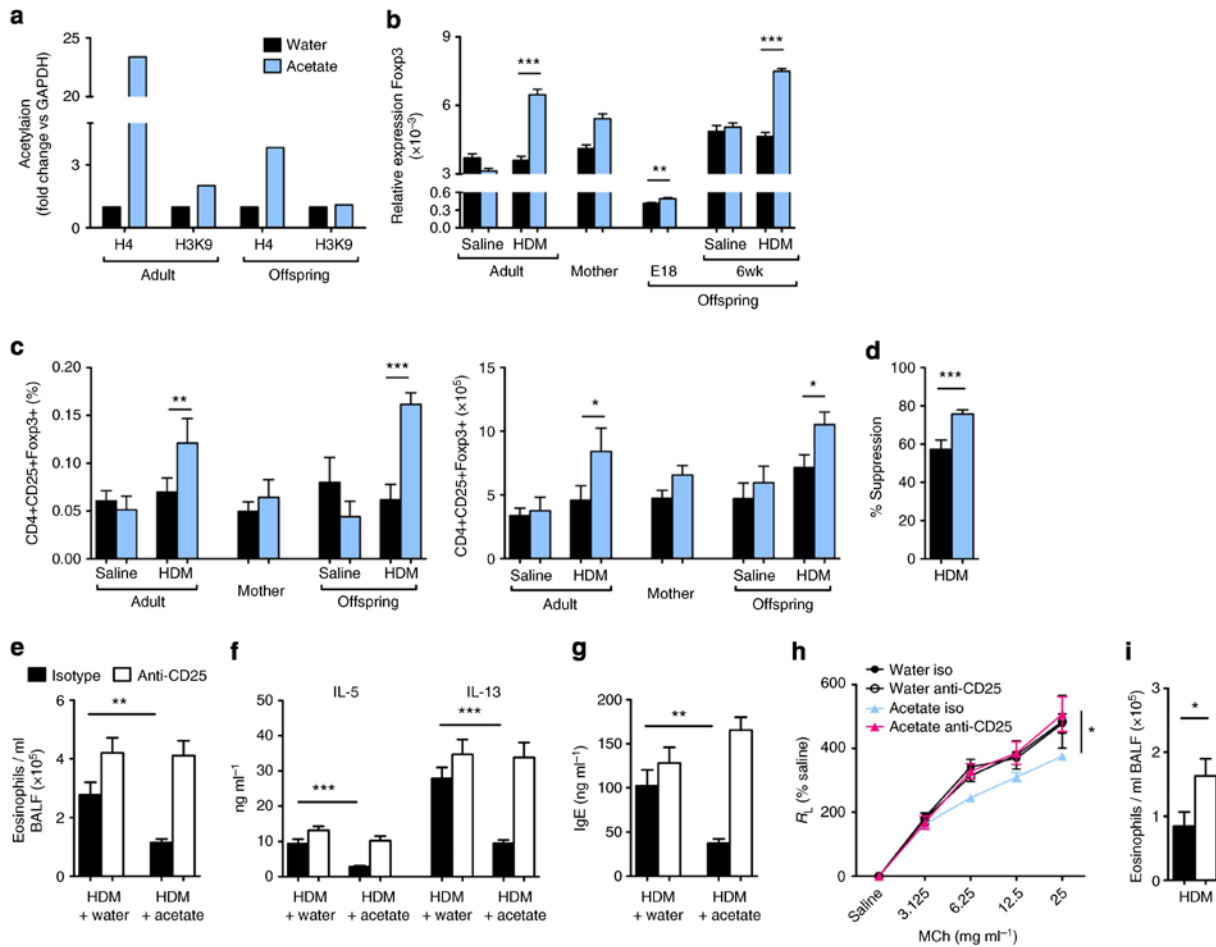


**Figure 2.4. Priming of Foxp3 expression and Tregs in acetate-mediated suppression of AAD.**

(a) Acetylation of histones at the Foxp3 promoter (adult=acetate from day -21 to end of model, offspring=acetate by mother D12-weaning). (b) Foxp3 expression in the lung. (c) Percentage and number of Treg cells in the lung. (d) Effect of acetate on Treg suppressive capacity (Tregs isolated from the spleen of mice receiving water or acetate). The effect of anti-CD25 mediated Treg depletion on acetate mediated suppression of AAD in terms of (e) eosinophil cell number in BALF, (f) IL-5 and IL-13 release from MLN T cells, (g) serum IgE and (h) airway hyperresponsiveness in terms of airway resistance ( $R_L$ ). (i) AAD and the effect of anti-CD25 mediated Treg depletion in 3-week-old female offspring from mothers (C57Bl/6J) fed acetate, in terms of eosinophil cell number in BALF. Data represent mean+SEM,  $n=8$ . Significance is represented by \* $P<0.05$ , \*\* $P<0.01$ , \*\*\* $P<0.001$ , Student's  $t$ -test. One representative experiment of three is shown.

CD25 treatment abrogated acetate-induced prevention of eosinophil infiltration of the BALF (Figure 2.4I). These data reveal that exposure to dietary acetate prevents asthma by potentially enhancing Treg function epigenetically. Furthermore, it demonstrates that enhancement of Treg function by acetate is inheritable by epigenetic means as it is transferred to offspring who are not exposed to acetate directly.

## **6. The role of high fibre and SCFAs in asthma pathogenesis**

We demonstrate that fermentation of fibre to acetate by gut bacteria can enhance Treg function and prevent Th2-driven inflammation in asthma (Figure 2.5). This is driven by inheritable epigenetic modification of the *Foxp3* promoter, whereby acetate enhances histone acetylation. Acetate inhibits HDAC function<sup>89</sup> and likely prevents deacetylation of histones at the *Foxp3* promoter which subsequently maintains histone acetylation. Furthermore, when mothers eat a fibrous diet they likely enhance foetal exposure to SCFAs *in utero* and similarly increase Treg function that can prevent asthma pathogenesis in their children. Taken together, these data establish a novel role for fibre diet and SCFAs to prevent allergies, highlighting the importance of diet in the prevention of Western lifestyle diseases.

## **7. Dietary fibre and SCFAs protect against *C. rodentium* infection**

The regulatory role of dietary fibre in preventing allergies suggests SCFAs have an anti-inflammatory role. However, in the setting of infection, anti-inflammatory responses may potentially hinder resolution of disease. We aimed to investigate the role of dietary fibre and SCFAs in *C. rodentium* infection to determine their impact on infectious diseases. The following section contains a submitted manuscript investigating the role of acetate in altering *C. rodentium* pathogenicity and infection.

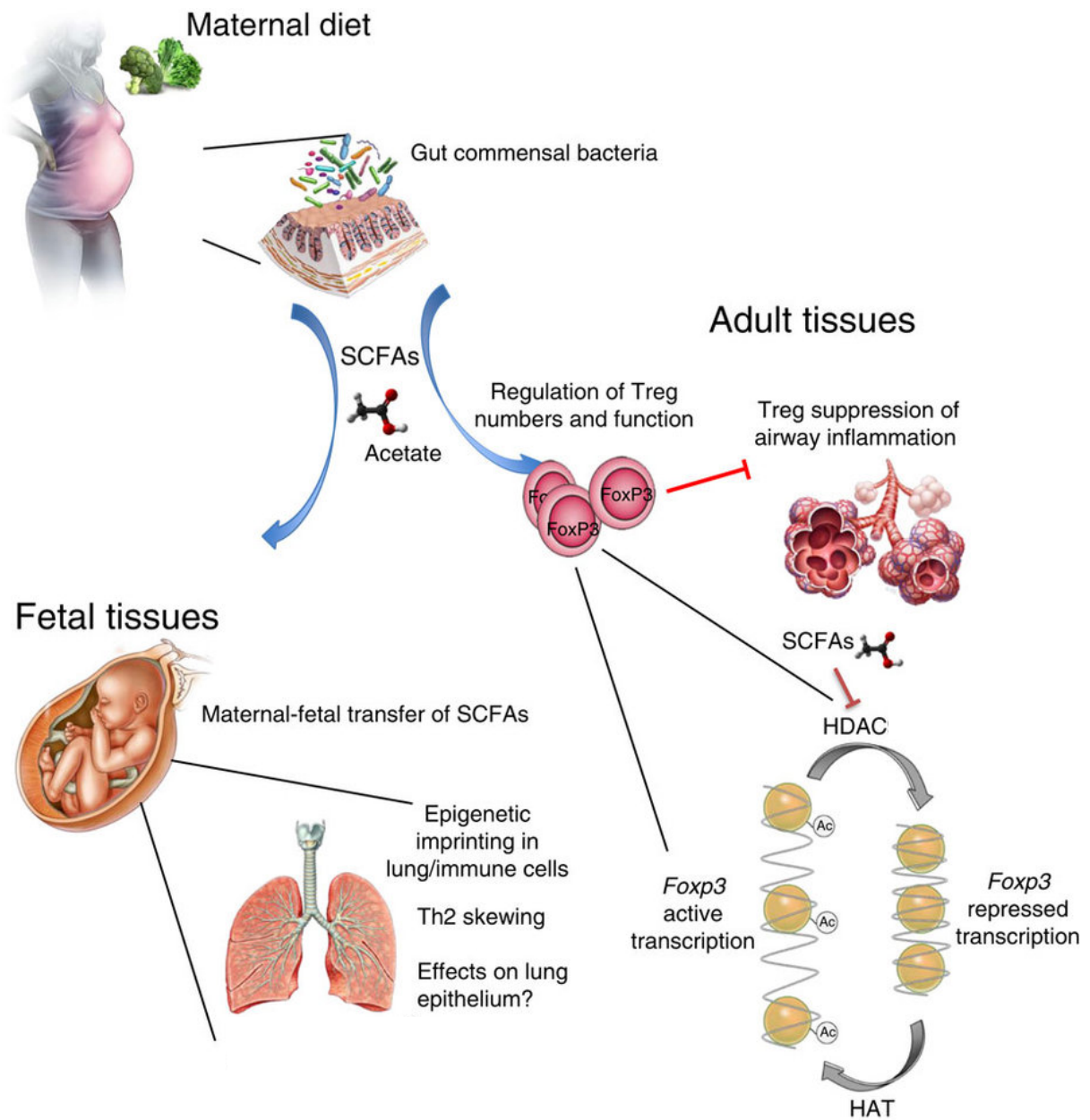




**Figure 2.5. Schematic representation of mechanism underlying the effect of maternal fibre intake on the development of asthma, both in the adult, and in offspring.** Fibre consumption leads to changes in the microbiota which results in increased SCFA production in the gut. Acetate enters the bloodstream and inhibits HDACs, leading to transcription of Foxp3. Foxp3 promotes Treg numbers and function, which suppress airway inflammation. During pregnancy, SCFAs such as acetate are capable of crossing the placenta and influencing gene expression in the fetal lung. It is also likely that maternally transferred acetate affects Treg biology in the fetus.

**High acetate yielding diets protect mice from *Citrobacter rodentium* infection through enhanced mucosal immunity and control of bacterial growth**

Keiran H. McLeod<sup>1</sup>, Craig McKenzie<sup>1</sup>, Yu Anne Yap<sup>1</sup>, James L. Richards<sup>1</sup>, Jian Tan<sup>1</sup>, Jacinta Knight<sup>1</sup>, Robert J. Moore<sup>2,3</sup>, Trevor J. Lockett<sup>4</sup>, Julie M. Clarke<sup>5</sup>, Charles R. Mackay<sup>1</sup>, Laurence Macia<sup>6,7</sup> and Eliana Mariño<sup>1</sup>

1. *School of Biomedical Sciences, Faculty of Medicine, Nursing and Health Sciences, Monash University, Wellington Road, Clayton, Victoria 3800, Australia.*
2. *Infection and Immunity Program, Biomedicine Discovery Institute, Department of Microbiology, Monash University, Clayton, Victoria 3800, Australia.*
3. *School of Science, RMIT University, Bundoora West Campus, Bundoora Vic. 3083 Australia.*
4. *CSIRO Health and Biosecurity, North Ryde, NSW 2113, Australia.*
5. *CSIRO Health and Biosecurity, Adelaide, SA, 5000 Australia.*
6. *Charles Perkins Centre, The University of Sydney, Camperdown NSW, 2006 Australia.*
7. *School of Medical Sciences, The University of Sydney, NSW, 2006 Australia*

## ABSTRACT

**Background and Aims:** Many inflammatory diseases are associated with microbial dysbiosis, which may considerably alter the production of short chain fatty acids (SCFAs). SCFAs are produced in the large bowel through bacterial fermentation of dietary fibre and play an important role in maintaining gut homeostasis. SCFAs, particularly acetate and butyrate, show beneficial immunomodulatory effects contributing to the prevention of inflammatory and allergic reactions. Thus, reduced production of SCFAs may impact on the mucosal immune responses critical to fight against pathogens. This study aims to determine the influence of SCFAs on a murine model of colonic bacterial infection.

**Methods:** We feed high acetate- or butyrate-yielding diets to mice prior to and during *C. rodentium* infection and assessed severity of disease in correlation with changes in fecal microbiota and the immunological profile.

**Results:** Here we show *in vitro* that acetate and butyrate directly inhibited growth of the attaching and effacing (A/E) pathogen *C. rodentium* in a bacteriostatic manner. This correlated with reduced expression of *Tir* by *C. rodentium*, a gene responsible for bacterial adherence and pathogenicity. Interestingly, only acetate reduced clinical scores during *C. rodentium* infection of mice when administered through a high acetate-yielding diet. This protection involved increased expression of *IL-17*, *IL-18* and *IL-22* in the colon and increased numbers of CD8 $\alpha\alpha^+$  TCR $\gamma\delta$  T cells in the colonic epithelium. These effects were dependent on GPR43, a metabolite-sensing GPCR that binds acetate.

**Conclusions:** Our findings unveil new mechanisms by which the dietary metabolite acetate impacts on colonic *C. rodentium* infection, demonstrating a novel role for acetate in reducing the severity of bacterial infection in the gut.

## INTRODUCTION

Bacterial infections of the gut are common and potentially lethal. In the US, the top 5 gut bacterial pathogens of children less than 5 years old are responsible for almost 300,000 illnesses a year<sup>192</sup>. This includes pathogenic strains of *E. coli* such as Enteropathogenic (EPEC) or Enterohaemorrhagic (EHEC) *E. coli*<sup>193</sup>.

Diet and its effects on the composition of the gut microbiota may underlie the increased incidence of many inflammatory and infectious diseases in western societies<sup>194, 195</sup>. High fat and high sugar diets have been associated with increased adherent-invasive *E. coli* infection in mice<sup>196</sup>. Furthermore, Western diet has been associated with dysbiosis and changes to the composition of the gut microbiota, with an increasing proportion of *E. coli*<sup>196</sup>.

A rapidly expanding body of knowledge has begun to highlight the potential role for diet in modulating gut infections. The health benefits of dietary fibre can in part be attributed to the production of short-chain fatty acids (SCFAs) and the alteration of the gut microbiota<sup>197, 198</sup>. SCFAs, mainly acetate, propionate and butyrate, are produced by bacterial fermentation of dietary carbohydrates in the large bowel. In particular, diet high in resistant starch enhances SCFA production in the human gut compared to a starch-free diet<sup>199</sup>. Furthermore, dietary fibre is also associated with changes to the gut microbiota. Indeed, Western diets low in fibre are associated with increased Bacteroidetes and reduced Firmicutes in American adults compared to African adults or South American Indians consuming a higher fibre diet<sup>200, 201</sup>.

SCFAs can alter immune responses by signalling through ‘metabolite-sensing’ G protein-coupled receptors (GPCRs). GPR43 is predominantly activated by acetate whereas GPR109a is activated by butyrate and niacin<sup>53, 75</sup>. Both GPR43 and GPR109a are expressed on the gut epithelium and a myriad of immune cell subsets<sup>198</sup>. Murine studies suggest signalling via GPR43 regulates inflammatory responses<sup>8, 15</sup>. GPR43 knockout (KO) mice show exacerbated colitis, arthritis and food allergy, demonstrating that SCFA signalling plays a role in the suppression of inflammation<sup>15, 62, 202</sup>. Butyrate induces colonic Treg differentiation via IL-10 release from macrophages and dendritic cells and IL-18

from colonic epithelium, a mechanism dependent on GPR109a<sup>75</sup>. As a result, GPR109a KO mice develop severe inflammation in the DSS-induced colitis model<sup>75, 202</sup>. These studies suggest that GPR43 and GPR109a play an important regulatory role in dampening inflammation and maintaining intestinal homeostasis.

Increasing prevalence of multiple antibiotic resistant strains of EHEC highlight the need for novel treatments to prevent the spread of these infections and reduce their severity<sup>203</sup>. *Citrobacter rodentium* is a mouse pathogen similar to EPEC, sharing approximately 67% of its genome including the pathogenicity islands necessary for causing A/E lesions<sup>204</sup>. It establishes an infection in the large intestine of rodents<sup>205</sup>. Infection of mice with *C. rodentium* provides a robust model for investigating the pathogenesis of EHEC and EPEC<sup>206</sup>. Both innate and adaptive arms of the immune response are required to resolve *C. rodentium* infection. Mice lacking T and B lymphocytes or impaired Myd88 signalling in innate immune cells suffer fatal *C. rodentium* infection<sup>207, 208</sup> and lethal translocation of gut bacteria during colonic damage<sup>209</sup>. Neutrophils are an important innate defence against *C. rodentium*, demonstrated by exacerbated infection in mice depleted of neutrophils<sup>210</sup>. In addition, a number of cytokines required for intestinal homeostasis including IL-1 $\beta$ , IL-17, IL-18 and IL-22 are important in clearing infection and preventing mortality<sup>211, 212, 213</sup>. Furthermore, *C. rodentium* is lethal to mice deficient in *Muc-2*<sup>214</sup>, a gene required for mucus production crucial in maintaining gastrointestinal barrier function.

Acetate delivered to the large bowel of mice fed acetylated high amylose maize starch (HAMSA) improved survival against EHEC O157:H7 infection<sup>215</sup>, but the mechanism is unknown. High amylose acetylated and butyrylated starches (HAMSA and HAMSB) deliver acetate and butyrate respectively to the large bowel of rodents<sup>216</sup> and humans<sup>217, 218</sup>, which is the main compartment of the gut infected by EHEC<sup>206</sup>. High-amylose maize starch (HAMS) is a resistant starch that passes largely undigested through the small intestine to the large bowel where it is fermented by the gut microbiota to SCFAs. When added to oral rehydration solution HAMS decreased diarrhea duration in both adults and children hospitalized for acute infectious diarrhea<sup>219</sup>. In an animal model of cholera-toxin induced diarrhoea, HAMSA promoted fluid and electrolyte uptake more effectively than HAMS or

HAMSB<sup>220</sup>. This suggests that SCFAs can reduce the clinical severity of gut bacterial infections. However, the role of individual SCFAs and their sensing GPCRs in preventing and containing bacterial infections remains poorly understood.

In the present study, we used diets containing HAMSA and HAMSB to deliver acetate and butyrate to the large bowel of mice infected with *C. rodentium* to assess the effects of these SCFAs on clinical burden and gut pathogenicity during this large bowel bacterial infection. We also investigated the role of the metabolite-sensing receptor GPR43 in the immune response to infection by assessing the severity of *C. rodentium* infection in *Gpr43*<sup>-/-</sup> mice. We demonstrate that acetate acting through GPR43 increases the number of CD8 $\alpha$ <sup>+</sup> TCR $\gamma$  $\delta$  T cells and the expression of anti-microbial cytokines in the colonic epithelium of infected mice. We establish a promising new approach to moderate bacterial gut infections by manipulating the gut microbiota and mucosal immune tolerance through the SCFA acetate.

## RESULTS

### Acetate and butyrate directly influence *C. rodentium* growth and virulence gene expression

We first investigated whether acetate and butyrate could directly impact *C. rodentium* growth by performing proliferation and viability assays *in vitro*. We found that both acetate and butyrate in culture medium significantly reduced *C. rodentium* growth up to 7 hrs in culture in a dose dependent manner (Figure 1A-C). At higher physiological doses in the feces of mice (60mM), both acetate and butyrate also showed a similarly potent effect (Figure 1D), which is likely to reflect what occurs *in vivo*. To understand if acetate and/or butyrate may have a bactericidal effect, we exposed *C. rodentium* to acetate or butyrate before growing the culture in a SCFA-free medium. *C. rodentium*, pre-cultured with 500mM acetate or butyrate for 2 hours was able to grow normally when returned to SCFA-free media (Figure 1E). As such, SCFAs acetate and butyrate exhibit a bacteriostatic rather than bacteriocidal effect on *C. rodentium* growth.

### Acetate-yielding diet protects from *C. rodentium* infection

We next evaluated whether acetate and butyrate delivered to the large bowel by HAMSA and HAMSB respectively could prevent or ameliorate disease in mice when fed prior to and during infection with *C. rodentium*. These diets contained 15% high-amylose maize starch (HAMS), 15% acetylated high amylose (HAMSA), or 15% butyrylated high amylose (HAMSB) (Supplementary Table 1). Acetylated and butyrylated starches are largely resistant to small intestinal amylolysis and pass to the colon where bacteria release their specific incorporated SCFAs<sup>216</sup>. Control HAMS diet was used to assess the individual role of acetylated high amylose (HAMSA) and butyrylated high amylose HAMSB diets, which have proven to be powerful tools for assessing the effects of specific SCFAs (i.e. acetate versus butyrate) on intestinal biology<sup>221, 222 215</sup>. The component of HAMS that passes into the large bowel is fermented to produce the normal range of SCFAs including acetate, propionate and butyrate. There were no differences in food intake between groups of mice fed the experimental diets (Supplementary Figure 1A).

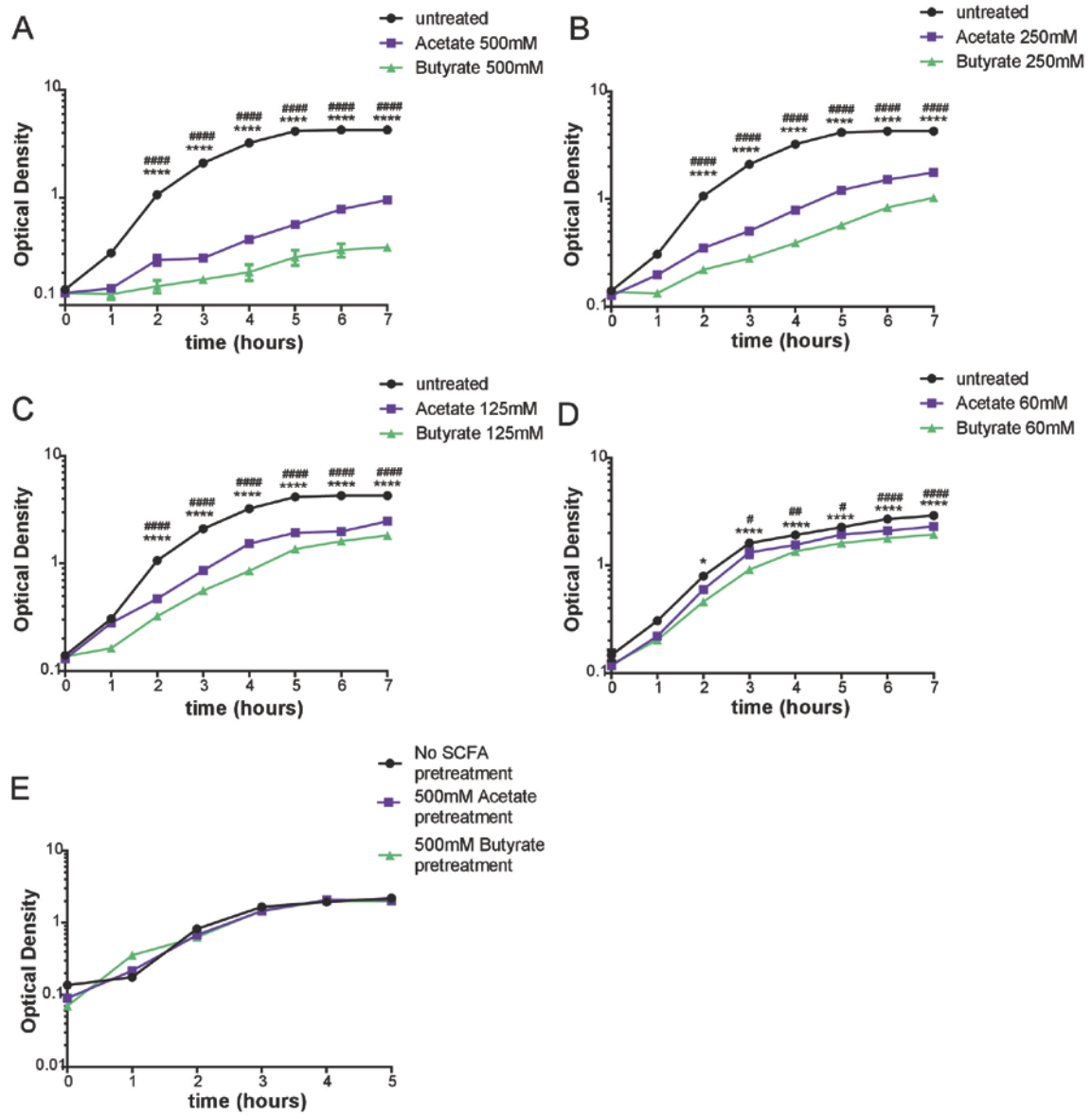




**Figure 1. Increased levels of SCFAs inhibit *C. rodentium* growth.**

Growth curve of *C. rodentium* in broth supplemented with acetate or butyrate. Concentrations of acetate and butyrate at **A**, 500mM, **B**, 250mM, **C**, 125mM and **D**, 60mM. p values calculated by two-way ANOVA with Bonferoni's correction (n = 3) Comparisons between acetate and untreated groups represented via \*, comparisons between butyrate and untreated groups represented by #. **E**, Growth curve of *C. rodentium* cultured for 2 hours in 500mM acetate or butyrate, washed, and cultured in untreated media. P values calculated by two-way ANOVA with Bonferoni's correction (n = 3) Comparisons between acetate and untreated groups represented via #, comparisons between butyrate and untreated groups represented by \*. # or \* p=<0.05, ## or \*\* p=<0.01, ### or \*\*\* p=<0.001, #### or \*\*\*\* p=<0.0001. All values are mean  $\pm$  S.E.M.

Feeding HAMSA to healthy uninfected mice increased fecal acetate from approximately 20 to 50mM and HAMSB increased fecal butyrate from 10mM to 30mM, when compared to HAMS diet (Figure 2A). We measured the concentration of acetate post *C. rodentium* infection and found a similar trend. In contrast, butyrate concentrations did not change significantly in infected HAMSB fed mice compared to infected HAMS-fed mice. Thus indicating *C. rodentium* infection did not affect the release of acetate but may affect butyrate release from modified starch substrates.

We assessed the clinical severity of *C. rodentium* infection by examining the severity of diarrhea in mice fed HAMS, HAMSA or HAMSB. Ingestion of HAMSA significantly reduced the clinical score over 10 to 14 days, compared to control HAMS-fed infected mice (Figure 2B). For HAMSB-fed mice, results were similar to those observed in control HAMS-fed mice on days 10-14 ( $P < 0.0001$ ) (Figure 2B). Although severe clinical score in infected HAMSB-fed mice correlated with a subtle trend in bacterial load in the colon, no significant differences were found in the *C. rodentium* numbers in the colon for any of the diets 14 days post-infection (Figure 2C). Similar to HAMSA supplement, non- or semi-purified diets containing 4.7% or 9.4% fibre provided resistance to *C. rodentium* infection compared to those receiving a diet containing no dietary fibre (Supplementary Figure 1B, C). This latter result suggests the level of dietary fibre plays a role in preventing *C. rodentium* infection.

To examine the effect of the diets on infection resolution, we monitored infected mice fed HAMS, HAMSA and HAMSB diets up until day 22. As expected, clinical symptoms of *C. rodentium* infection were resolved by day 22 regardless of diet (Figure 2D). Interestingly, both HAMSA and HAMSB diets completely depleted *C. rodentium* in the distal colon by day 22 (Figure 2E). As toxins and effector proteins produced by the pathogenic bacteria correlate with chronic infection<sup>223, 224, 225</sup>, we quantified the expression of the *Tir* gene, an intimin receptor responsible for *C. rodentium* *Tir* pathogenicity<sup>226</sup>. HAMSA- and HAMSB-fed mice exhibited decreased expression of *Tir* in their colon (Figure 2F). This suggests that acetate and butyrate can affect bacterial adhesion to the epithelium and directly reduce pathogenicity.

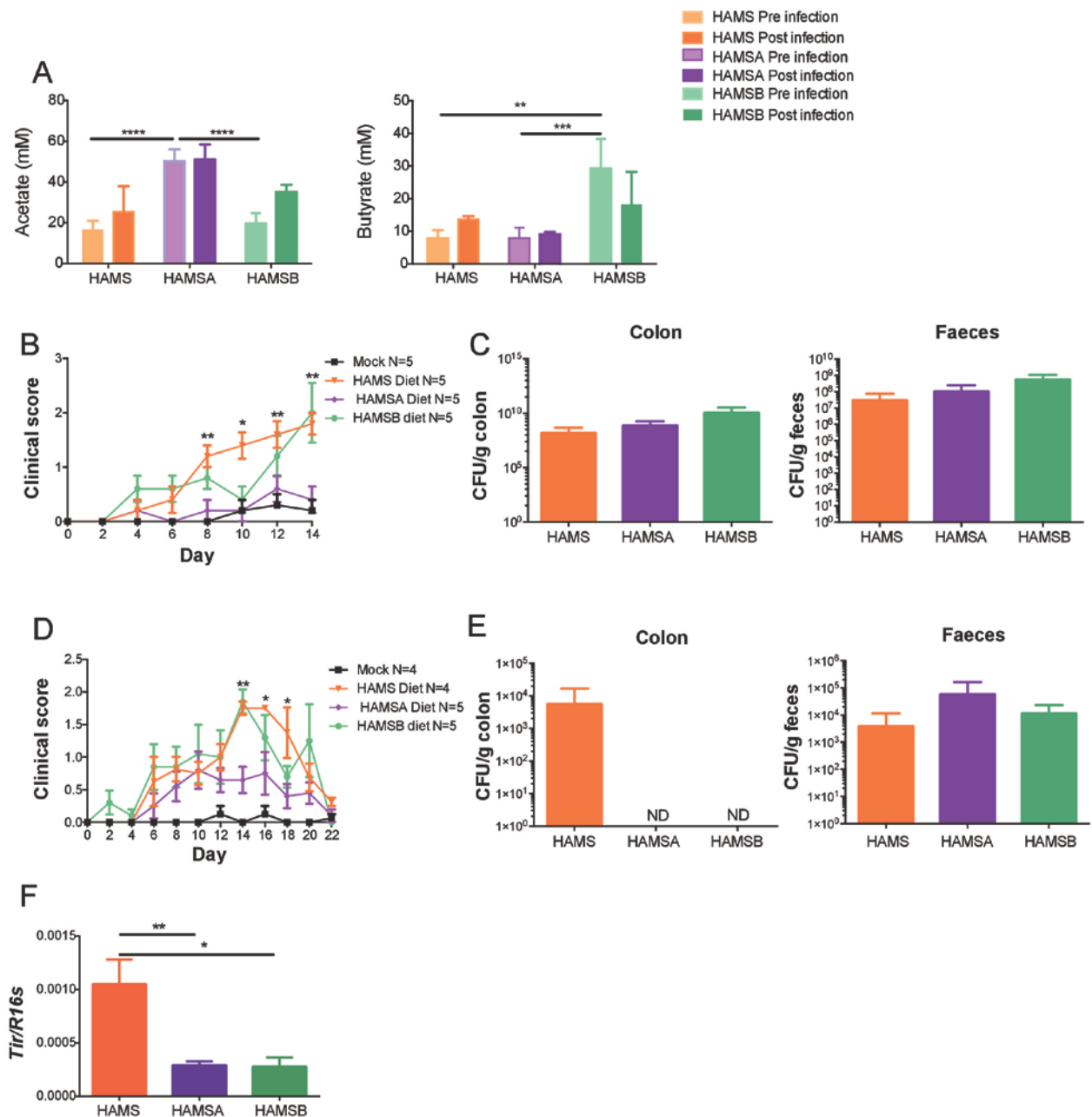


**Figure 2. Effects of experimental diets on clinical score, bacterial load and pathogenicity gene expression in mice infected with *C. rodentium*.**

**A**, Acetate and butyrate concentrations in the feces of C57Bl/6J mice fed high amylose starch (HAMS), acetylated HAMS (HAMSA) or a butyrylated HAMS (HAMSB) supplement *ad libitum* for 3 weeks, pre- and post-infection with *C. rodentium*. Pre-infection faecal SCFA concentrations determined at day 0 of *C. rodentium* infection model, and 14 days post-infection. **B**, Clinical burden of *C. rodentium* infection over 14 day on C57Bl/6J mice fed HAMS, HAMSA or HAMSB supplement *ad libitum* for 3 weeks prior to inoculation and for the length of the experiment. **C**, Bacterial load of *C. rodentium* in the colon and feces from mice in **B**. **D**, Clinical burden of *C. rodentium* infection for 21 days from C57Bl/6J mice fed HAMS, HAMSA or HAMSB *ad libitum* for 3 weeks prior to inoculation and for the length of the experiment. **E**, Bacterial load of *C. rodentium* in the colon and feces from mice in **D**. Expression of *C. rodentium* pathogenicity gene *Tir* relative to 16s in the colon of infected mice fed HAMS, HAMSA or HAMSB (n = 5) collected 14 days post infection. p values for **B**, and **D** calculated by two-way ANOVA with Bonferoni's correction.\* p = <0.05, \*\* p = <0.01. p values for **A**, **C**, **E** and **F** calculated by one-way ANOVA with Bonferoni's correction. \* p=<0.05, \*\* p=<0.01, \*\*\* p=<0.001, \*\*\*\* p=<0.0001. All values are mean ± S.E.M.

### **Acetylated starch supplement promotes the abundance of protective gut microbial communities that correlate with inhibition of *C. rodentium* growth**

Next we asked whether protection observed in mice fed with HAMSA supplement correlated with an altered gut microbiota that subsequently alters production of SCFAs. Indeed, only HAMSA supplement resulted in a significant change of the microbiota present in feces, as shown by principal component analysis (PCA) plot (Figure 3A). In contrast, the gut microbiota of HAMSB-fed mice was similar to control HAMS-fed mice, and did not show a strong separation from the non-purified (NP) diet. Further characterization of the fecal microbiota profile demonstrated that HAMSA supplement decreased the prevalence of the *Bacteroides* genus ( $P=0.0002$ ) and increased the population of an unknown genus of *Alphaproteobacteria* ( $P=0.0187$ ) compared to control HAMS supplement and the conventional NP diet (Figure 3B). Similarly, high concentrations of acetate in pigs fed resistant-starch diet have been positively correlated with increased *Alphaproteobacteria*<sup>227</sup>. This suggests acetate can selectively promote *Alphaproteobacteria*, however the physiological impact of this bacteria remains unknown.

Fecal acetate concentrations negatively correlated with the abundance of bacteria from the genera *Lactococcus*, *Anaeroplasma*, *Akkermansia*, *Allobaculum*, *Lactobacillus* and *Clostridium* (Figure 3C). Moreover, correlation between OTU and SCFA concentrations were different (Figure 3D), especially between acetate and butyrate where there was little overlap in highly correlated OTUs. Overall, high acetate-yielding diet shaped the makeup of the microbiota, which is integral for regulating acute antibacterial responses.

### **Acetylated starch supplement activates metabolite-sensor GPR43 which plays a crucial role in gut homeostasis and clearance of *C. rodentium* infection**

SCFAs can modulate gut homeostasis via GPCRs<sup>195, 197</sup>. We therefore examined the role of acetate and butyrate sensing receptors GPR43 and GPR109a in *C. rodentium* infection. We fed C57.*Gpr43*<sup>-/-</sup> and C57.*Gpr109*<sup>-/-</sup> mice with HAMS, HAMSA and HAMSB prior to and during infection. Similar to

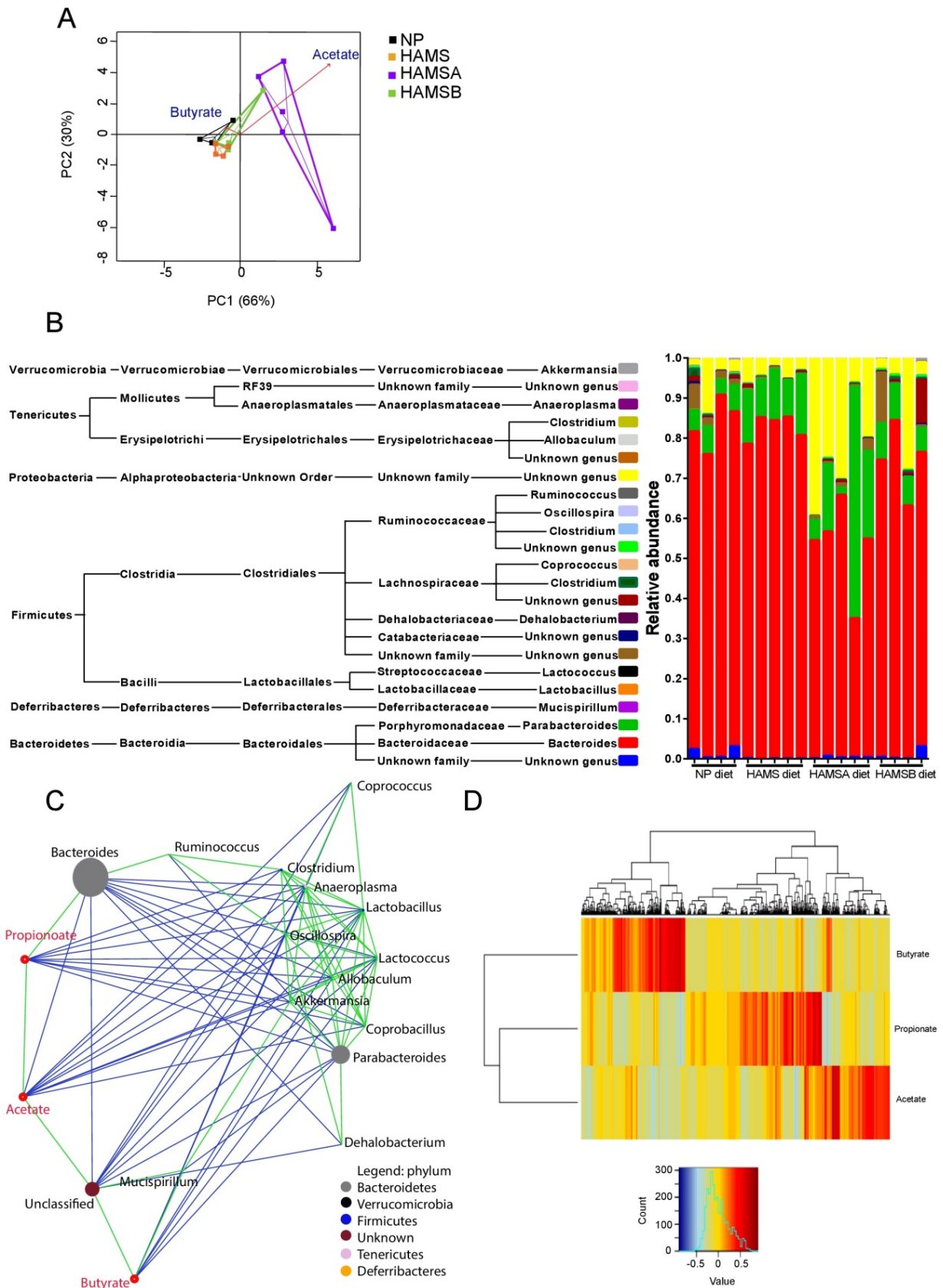


**Figure 3. Acetylated and butyrylated supplements alter gut microbiota.**

**A**, PCA plot showing variation between the faecal microbiota of mice fed NP diet, HAMS, HAMSA or HAMSB supplements. Vectors indicate influence of acetic and butyric acid, with length and direction of the arrows correlating with increased influence of the SCFA on the data points. PC1 axes accounted for 66% of total variation and strongly separated HAMSA supplement. **B**, Bar chart showing distribution of different genera detected in feces from C57Bl/6J wild type mice after being fed different supplements. Each genus, picked at 97% sequence identity (QIIME), is represented by a different colour and is proportional to the relative abundance in each sample. The key text provides QIIME blast taxonomy classification of the different genera in the samples. **C**, Pearson correlation-based network showing relationships between SCFAs acetate, butyrate and propionate and bacterial genera in C57Bl/6J wild type mice fed NP, HAMS, HAMSA or HAMSB supplements. Genera-depicting nodes are colored by phylum that genus belongs to. Size of each genus node is proportional to relative abundance of that genus; green lines connect positively and blue lines negatively correlated nodes. **D**, Heatmap showing Pearson correlations between OTUs (columns) and SCFA (rows).

what we found in our previous experiment (see Figure 2D), C57.*Gpr43*<sup>+/+</sup> littermates fed with HAMSA diet showed reduced clinical severity of infection as demonstrated by increased body weight, despite no changes in diarrhoea (Figure 4A). In contrast, C57.*Gpr43*<sup>-/-</sup> mice fed either HAMS or HAMSA supplements exhibited similar clinical severity compared to HAMS-fed C57.*Gpr43*<sup>+/+</sup> mice. We found that mice deficient in GPR43 displayed an enhanced severity of weight loss during *C. rodentium* infection. Thus, these data indicate that acetate plays an important role in limiting the clinical impact of infection through its primary receptor GPR43<sup>228</sup>. No significant changes were observed in the course of infection in C57.*Gpr109*<sup>-/-</sup> mice (Supplementary Figure 2), implying that GPR109A is unlikely to contribute to *C. rodentium* protection, also in accordance with the HAMSB results shown above. Neither HAMSA supplement nor a lack of GPR43 changed the bacterial load in colon and feces at 14 days post-infection (Figure 4B).

Enteropathogenic infections as well as many inflammatory diseases including colitis and celiac disease are associated with impaired gastrointestinal homeostasis in humans and mice. We found expression of *IL-22*, a gut homeostasis-related cytokine that maintains gut mucosal integrity and host-microbial balance<sup>229</sup>, was significantly elevated in HAMSA-fed infected C57.*Gpr43*<sup>+/+</sup> mice when compared to control HAMS-fed C57.*Gpr43*<sup>+/+</sup> mice (Figure 4C). In concordance with augmented *IL-22*, dietary acetate significantly increased the expression of *IL-18* and *IL-17* and in the colon, cytokines important for clearing bacterial infection<sup>230</sup>. Meanwhile, HAMSA supplement had no impact on the expression of any of these genes in the colon of infected C57.*Gpr43*<sup>-/-</sup> mice. Infected and non-infected C57.*Gpr109*<sup>-/-</sup> mice exhibited no differences in gene expression of colonic *IL-17*, *IL-18* and *IL-22* compared to WT mice (data not shown). HAMSA feeding increased *Muc-2* expression independently of GPR43, a gene essential for the production of mucus for the protection against colonic infection<sup>231,215, 232, 233</sup> (Figure 4D). We found infected HAMSA-fed C57.*Gpr43*<sup>+/+</sup> mice presented increased colon length compared to infected HAMS-fed C57.*Gpr43*<sup>+/+</sup> mice, similar to non-infected HAMS-fed C57.*Gpr43*<sup>+/+</sup> mice (Figure 4E, F). However, colon length, a measure of colitis severity<sup>202</sup>, was not reduced in C57.*Gpr43*<sup>-/-</sup> mice. Overall, these results suggest that GPR43 is



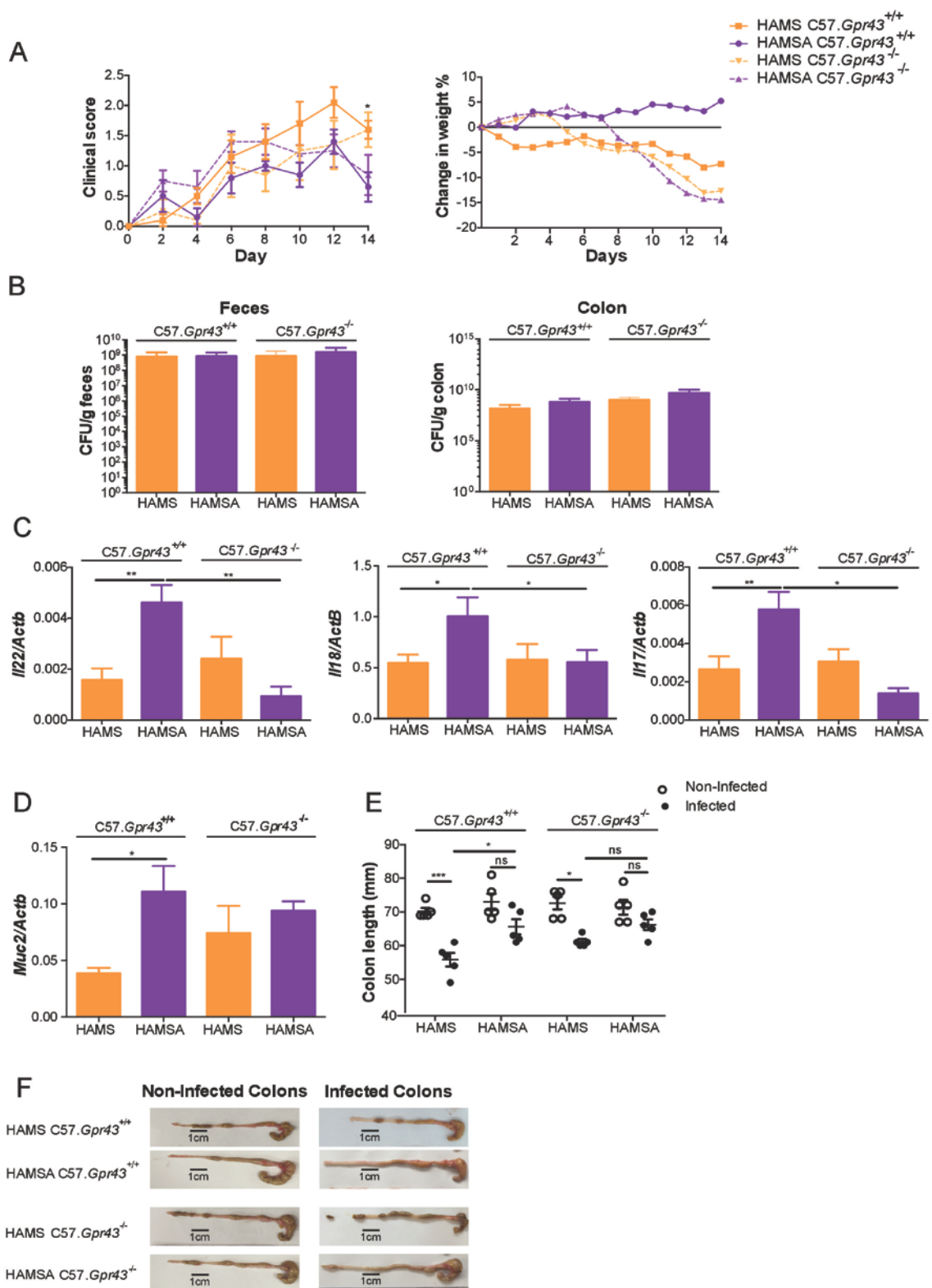


**Figure 4. Protection from *C. rodentium* infection by HAMSA displays dependence on GPR43.**

**A**, Clinical burden and percentage weight change in *C. rodentium* infected C57.*Gpr43*<sup>+/+</sup> or C57.*Gpr43*<sup>-/-</sup> mice fed HAMS or HAMSA supplement *ad libitum* 3 weeks prior to inoculation and for the length of the experiment. **B**, Bacterial load of *C. rodentium* in the colon and feces at the peak of disease, 14 days post-inoculation. **C**, Expression of *Il-22*, *Il-17* and *Il-18* in the colon of infected mice 14 days post infection determined by qPCR. **D**, Expression of *Muc-2* in the colon of infected mice 14 days post infection determined by qPCR. **E**, Colon length comparing infected and non-infected C57.*Gpr43*<sup>+/+</sup> or C57.*Gpr43*<sup>-/-</sup> mice fed HAMS or HAMSA supplement 14 days post infection. **F**, Photos representative of colons from each group. p values for **A** calculated by two-way ANOVAs with Bonferoni's correction. p values for **C**, **D** and **E** calculated by one-way ANOVAs with Bonferoni's correction. \* p<0.05, \*\* p<0.01, \*\*\* p<0.001. All values are shown as mean ± S.E.M. (n = 5).

essential for an effective barrier against *C. rodentium* infection by enhancing immune responses downstream of *IL-22*, *IL-18* and *IL-17* signalling.

### **Increased colonic CD8 $\alpha\alpha$ <sup>+</sup> TCR $\gamma\delta$ T cells correlates with reduced *C. rodentium* infection**

As IL-22 mediates early resistance to *C. rodentium* colonization<sup>210, 234, 235</sup>, we asked whether acetate can alter the mucosal immune response to infection. We investigated the role of the intraepithelial lymphocyte (IEL) compartment in the protection against pathogenic infection, as IELs are the first line of immunological defence to encounter bacteria and are equipped with fast responding effector T cells that can mount a strong immunity to a wide range of pathogens<sup>236</sup>. Furthermore, we investigated whether this response involved acetate-sensing receptor GPR43. We characterised colonic CD8 $\alpha\alpha$ <sup>+</sup> IELs in infected C57.*Gpr43*<sup>+/+</sup> and C57.*Gpr43*<sup>-/-</sup> mice by flow cytometry. The IEL compartment is 90% CD8<sup>+</sup> T cells<sup>237</sup> and of those we found HAMS diet significantly increased frequency and number of CD8 $\alpha\alpha$ <sup>+</sup> T cells in infected mice (Figure 5A and Supplementary Figure 3A, B). This effect was not observed in infected C57.*Gpr43*<sup>-/-</sup> mice. Similarly, HAMS supplement increased the frequency and number of CD103-expressing CD8 $\alpha\alpha$ <sup>+</sup> TCR $\gamma\delta$  T cells in infected C57.*Gpr43*<sup>+/+</sup> mice, but not C57.*Gpr43*<sup>-/-</sup> mice (Figure 5B, C). To examine the capacity for CD8 $\alpha\alpha$ <sup>+</sup> TCR $\gamma\delta$  T cells to be directly affected by acetate, we measured the expression of GPR43 on isolated CD8 $\alpha\alpha$ <sup>+</sup> TCR $\gamma\delta$  T cells from non-infected mice fed NP, HAMS or HAMS diet. We found that *Gpr43* was expressed on CD8 $\alpha\alpha$ <sup>+</sup> TCR $\gamma\delta$  T cells, though with no change induced by diet (Supplementary figure 3C). CD8 $\alpha\alpha$ <sup>+</sup> T cells are an unconventional or ‘natural’ subset of IELs, which have immune-regulatory properties thought to help maintain tolerance to bacteria and food antigens alongside anti-microbial responses to pathogenic bacteria<sup>238, 239</sup>. Mobilization of intraepithelial lymphocytes into or through the gut requires induction of CD103<sup>195</sup>, suggesting HAMS supplement may increase IEL recruitment to the gut alongside enhanced CD103 expression. GPR43 activation from acetylated starch therefore enhanced the population of CD8 $\alpha\alpha$ <sup>+</sup> TCR $\gamma\delta$  T cells in the colonic epithelium which was associated with increased expression of CD103 and protection against *C. rodentium* infection. Taken together, these data identify a novel mechanism of GPR43-dependent immunomodulation in the gut from HAMS supplement.

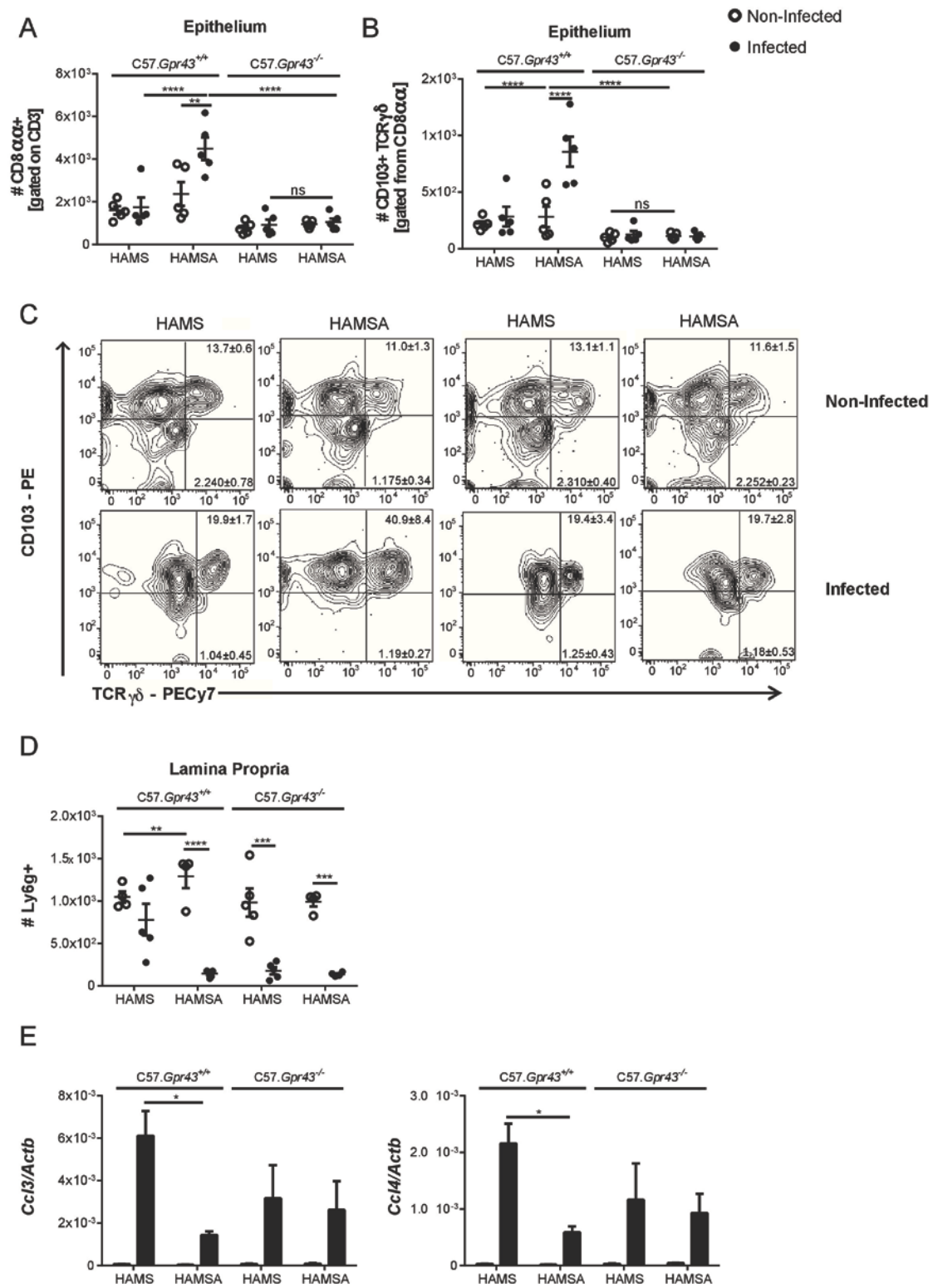


**Figure 5. CD8 $\alpha\alpha$ + TCR $\gamma\delta$  colonic intraepithelial T lymphocytes are increased by HAMSA supplement in a GPR43-dependent manner.**

**A**, Number of CD8 $\alpha\alpha$ + intraepithelial lymphocytes from the colonic epithelium from C57.*Gpr43*<sup>+/+</sup> or C57.*Gpr43*<sup>-/-</sup> mice fed HAMS or HAMSA supplement. **B**, Number of TCR $\gamma\delta$ + CD8 $\alpha\alpha$ + CD103+ intraepithelial lymphocytes from C57.*Gpr43*<sup>+/+</sup> or C57.*Gpr43*<sup>-/-</sup> mice fed HAMS or HAMSA supplement. **C**, Representative plots of TCR $\gamma\delta$ + and CD103+ IELs from C57.*Gpr43*<sup>+/+</sup> or C57.*Gpr43*<sup>-/-</sup> mice fed HAMS or HAMSA supplement shown in Figure **5B**. **D**, Number of neutrophils (Ly6g+ cells) in the colonic lamina propria from C57.*Gpr43*<sup>+/+</sup> or C57.*Gpr43*<sup>-/-</sup> mice fed HAMS or HAMSA supplement. **E**, Expression of *Ccl3* and *Ccl4* in colon tissue from C57.*Gpr43*<sup>+/+</sup> or C57.*Gpr43*<sup>-/-</sup> mice fed HAMS or HAMSA supplement, determined by qPCR. All cellular proportions determined by flow cytometry 14 days post infection. p values calculated by one-way ANOVAs with Bonferoni's correction. \* p<0.05, \*\* p<0.01, \*\*\* p<0.001, \*\*\*\* p<0.0001. All data is shown as mean  $\pm$  S.E.M (n = 5).

HAMSA feeding reduced colonic neutrophils in the lamina propria of C57.*Gpr43*<sup>+/+</sup> mice infected with *C. rodentium* (Figure 5D, Supplementary Figure 3D). This correlated with a reduction in neutrophil chemokines CCL3 and CCL4 (Figure 5E). These results were similar to what was observed by others in C57.*Gpr43*<sup>-/-</sup> mice, consistent with no leukocyte infiltration in the colonic lamina propria<sup>228</sup>. HAMSA or GPR43 deficiency did not change quantities of Th17 or Treg cells in the MLN of infected mice (Supplementary Figure 4). This suggests that acetate supplement can moderate the severity of *C. rodentium* infection without inducing an acute inflammatory response or by promoting the resolution of inflammation in a faster manner.

## DISCUSSION

In the current study we have identified a new mechanism by which colonic derived acetate modulates intestinal infection with the pathogen *C. rodentium* (Figure 6). We showed that acetate reduces bacterial growth and reduces expression of *Tir*, a gene responsible for *C. rodentium* pathogenicity. Acetate delivered to the large bowel by acetylated starch ameliorated the severity of infection. These effects were associated with increased production of anti-inflammatory cytokines in the gastrointestinal tract and increased numbers of immunoregulatory CD8 $\alpha\alpha^+$  TCR $\gamma\delta$  T cells. Thus, increasing concentrations of colonic SCFA acetate is likely to provide protection from intestinal bacterial pathogens by positively affecting the immune, mucosal and microbial responses.

SCFAs have an important role in immune and gut homeostasis by acting directly and indirectly on the immune system, epithelial gut barrier, gut microbiota and physiological responses<sup>195, 215, 240, 241</sup>. A healthy interaction between these elements in the gut is critical for combating intestinal infections. We found that butyrate and acetate have bacteriostatic effects by limiting bacterial growth *in vitro* and decreasing pathogenicity by reducing expression of protein effector genes such as *Tir* *in vivo*. However, we found that increased colonic concentrations of acetate, but not butyrate, delivered by acetylated starch ameliorated the severity of *C. rodentium* infection. In addition to being effective vehicles for increasing acetate in the human gut<sup>217, 218</sup>, acetylated starches promote fluid and electrolyte uptake to promote oral rehydration therapy in a rat model of cholera<sup>242</sup>. Given that HAMSA feeding reduced diarrhoeal severity in mice infected with *C. rodentium*, this suggests acetate from HAMSA promotes water retention in the large bowel which ameliorates diarrhoea induced by bacterial infections of the gut such as EHEC and EPEC. Furthermore, the composition of these acetylated starches can may also promote the adhesion of bacteria to starch in the gastrointestinal tract, as evidenced by other studies using similar corn-starches<sup>243</sup>. Indeed, *V. cholerae* has been shown to adhere to granular starch *in vitro*<sup>243</sup>. Thus the encapsulation of the pathogenic bacteria might explain the total clearance of the bacteria at 22 days post inoculation in the colon but not in the feces.

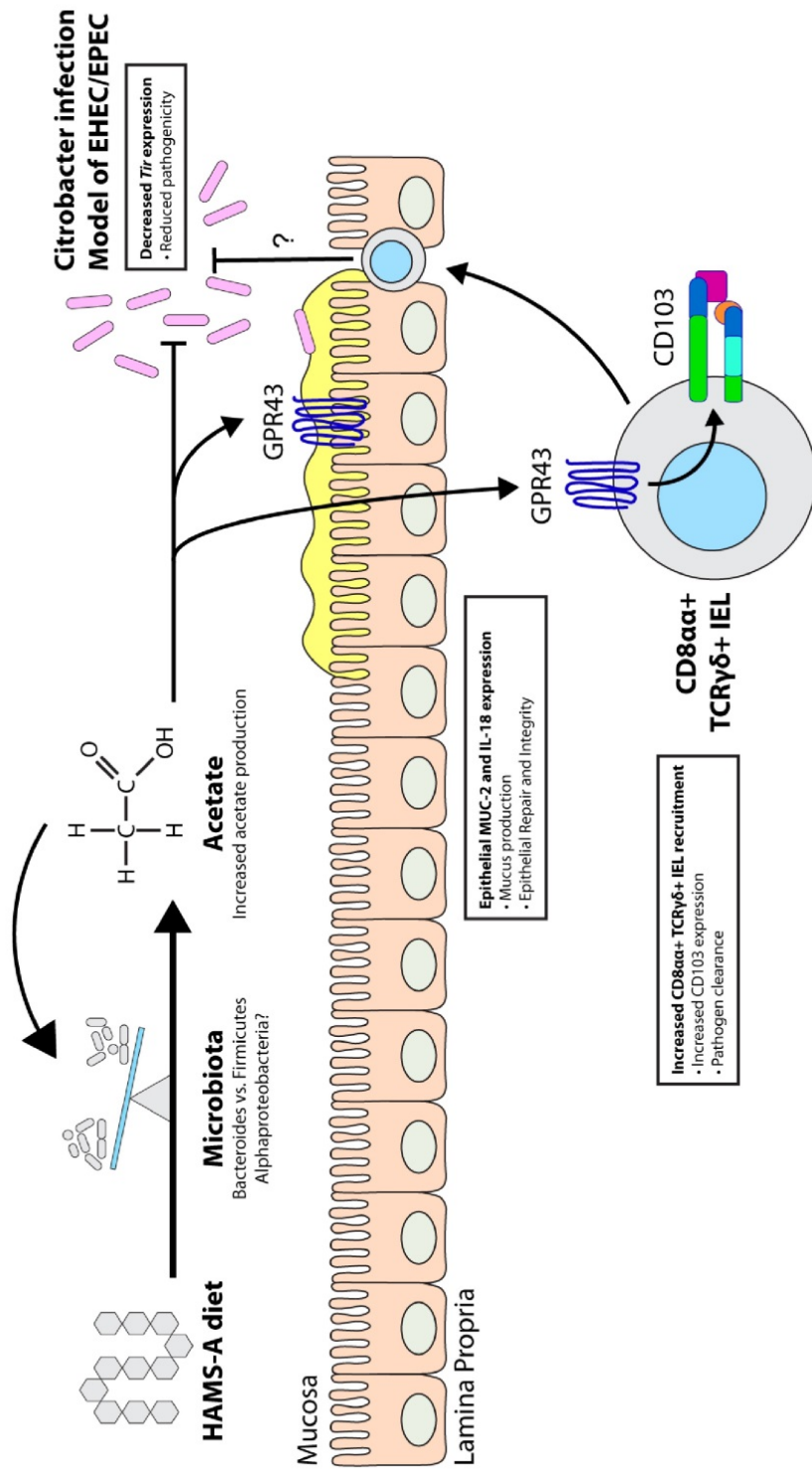




**Figure 6. Summary of study: increased acetate concentration in the large bowel promotes gut homeostasis and prevent *C. rodentium* infection.**

HAMSA increases acetate concentration in the large bowel which acts directly on *C. rodentium* to reduce growth and pathogenic *Tir* expression. Acetate acts indirectly to clear *C. rodentium* infection by activating GPR43 (and possibly other receptors such as GPR41) on epithelial cells and IELs promoting the migration of IELs to the large bowel. Increased acetate concentration is associated with increases in CD103 expression, an integrin that promotes immune cell residency in the gut. Acetate increases *Muc2* expression in epithelial cells, promoting mucus production to reduce severity of *C. rodentium* infection.

The profile of bacteria from the gut microbiota have been linked to increased severity of various infections<sup>244</sup>, suggesting that the microbiota promoted by a NP diet may exacerbate *C. rodentium* infection. In contrast, HAMSA feeding altered the fecal microbiota by decreasing proportions of the *Bacteroides* genus. Fibre supplements of inulin and pectin have been associated with increases in *Bacteroides* *in vitro*, with dependence on pH<sup>245</sup>. Increased acidity correlated with reduced *Bacteroides* abundance. Increased fecal acetate from HAMSA supplement may reduce pH to a level that suppresses *Bacteroides* growth. Furthermore, HAMSA feeding increased proportions of an unknown *Alphaproteobacteria* genus in the fecal microbiota, corresponding with similar increases observed in pigs fed resistant-starch diet<sup>227</sup>. However, little is known about the role of *Alphaproteobacteria* in immunity. Increased proportions of *Alphaproteobacteria* from colonic acetate may alter the microbial environment and subsequently prevent *C. rodentium* growth upon infection.

We found increased colonic CD8 $\alpha\alpha^+$  TCR $\gamma\delta$  T cells in infected mice fed HAMSA, suggesting CD8 $\alpha\alpha^+$  TCR $\gamma\delta$  T cells have an anti-bacterial response<sup>239, 246</sup>. This mechanism is also consistent with a decreased number of neutrophils and reduced expression of neutrophil chemokines CCL3 and CCL4, suggesting that IELs may be sufficient to mount an adequate immune response to clear infection. Indeed, IELs have been linked with a protective memory response against mycobacterial infection<sup>247</sup>, and TCR $\delta$ -deficient mice are fatally compromised in their resistance to lung infection by the bacterium *Nocardia asteroides*<sup>248</sup>. These studies suggest CD8 $\alpha\alpha^+$  TCR $\gamma\delta$  T cells are important in clearing infections at mucosal sites which may be a mechanism promoted by acetate to fight A/E lesion-forming pathogens like *C. rodentium* in mice or EHEC and EPEC in humans.

In addition to directly acting on the pathogenic bacteria, these studies demonstrate high concentrations of large bowel acetate has an important role in maintaining gut integrity during infection. HAMSA supplement prevented a reduction in colon length caused by infection, an important marker for damage caused by colitis<sup>249</sup>. Furthermore, dietary HAMSA also increased levels of *Muc-2* expression, a gene required for the production of mucus. Mice deficient in MUC-2 were lethally susceptible to *C. rodentium*, highlighting its essential role in gut health<sup>250</sup>. Increases in *Muc-2* expression from

HAMSA supplement suggests that acetate delivered by HAMSA can act directly on the epithelium to promote gut integrity and reduce *C. rodentium* infection. However, this mechanism was demonstrated to be independent of GPR43.

Our findings highlight how HAMSA supplement can protect against *C. rodentium* infection by inducing CD8 $\alpha$ <sup>+</sup> TCR $\gamma$  $\delta$  IELs that may control pathogenic bacteria or by altering the gut microbiota to reduce *C. rodentium* pathogenicity. Given acetate reduced pathogenic *Tir* gene expression *in vivo* and reduced *C. rodentium* growth in a dose dependent response *in vitro*, we also demonstrate how SCFAs such as acetate can act directly on pathogenic bacteria to reduce their pathogenicity.

## **ACKNOWLEDGEMENTS**

We thank Ben Scherer from CSIRO for making the AIN93-G based diets and undertaking SCFA analyses, Hoey Yein Goh, and Caroline Ang Kim Lian, for assistance.

## **METHODS**

### **Mice**

C57BL/6 mice were obtained from the Monash Animal Research Platform, Melbourne Australia. GPR43<sup>-/-</sup> and GPR109<sup>-/-</sup> mice were obtained from our own specific pathogen free breeding colony at Monash Animal Services. Mice were aged 6-10 weeks at the start point of experiments. Control mice for KO mice were conventional C57BL/6 mice, co-housed with the KO mice prior to the experiments beginning. See Supplementary table 1 for complete description of the diets. All experimental procedures involving mice were carried out according to protocols approved by the relevant Animal Ethics Committee of Monash University, Melbourne, Australia and complied with the NHMRC Australian code of practice for the care and use of animals for scientific purposes, as well as the ARRIVE guidelines for animal usage in research.

### **Administration of diets and infection with *C. rodentium***

Mice were fed on their respective diets for 3 weeks prior to *C. rodentium* infection, and continued until the endpoint of the experiment. Mice were orally gavaged with nalidixic acid resistant *C. rodentium* strain ICC169 with an infective dose of approximately  $3 \times 10^8$ . Over the 14 or 21 day monitoring periods mice were monitored daily for diarrhea and were weighed. Upon sacrifice, bacterial CFU levels in the feces and colon were determined by serial dilution and plating on LB agar plates supplemented with nalidixic acid.

### **SCFA analysis**

SCFAs in feces, blood and caecal content were analysed as previously described<sup>251</sup>.

### **Bacterial growth curve**

LB broth was supplemented with either Sodium Acetate or Sodium Butyrate (Sigma), and the pH adjusted to 7.4. *C. rodentium* was inoculated in 20ml of broth culture for a starting OD of 0.1, and incubated at 37°C with shaking. The sample's OD was checked every hour, and the growth recorded.

## **Sequencing and Bioinformatics**

Bacterial genomic DNA from feces was extracted using QIAamp DNA stool mini kit (QIAGEN). DNA samples were amplified targeting the V1-V3 region of bacterial 16S rRNA gene using forward primer 5' AGAGTTTGATCCTGG 3'; and a reverse primer, 5'TTACCGCGGCTGCT 3' and sequenced using Roche 454 GS FLX+ sequencer. Bioinformatics analysis was performed with Quantitative Insights into Microbial Ecology (QIIME) software. Chimeric sequences were detected and removed using the Pintail algorithm (Ashelford et al., 2005) and de-noised and error-corrected with Acacia (Bragg et al., 2012). OTUs were picked at 97% sequence identity using the uclust algorithm in QIIME. Taxonomies were assigned in QIIME using BLAST against the Greengenes database (DeSantis et al., 2006). The EzTaxon database was used to additionally compare representative OTU sequences with a database of culturable strains (Chun et al., 2007). Pearson correlation-based network showing relationships between SCFA acetate, butyrate and propionate and bacterial genera was visualized in Calypso (<http://cgenome.net/calypso/>).

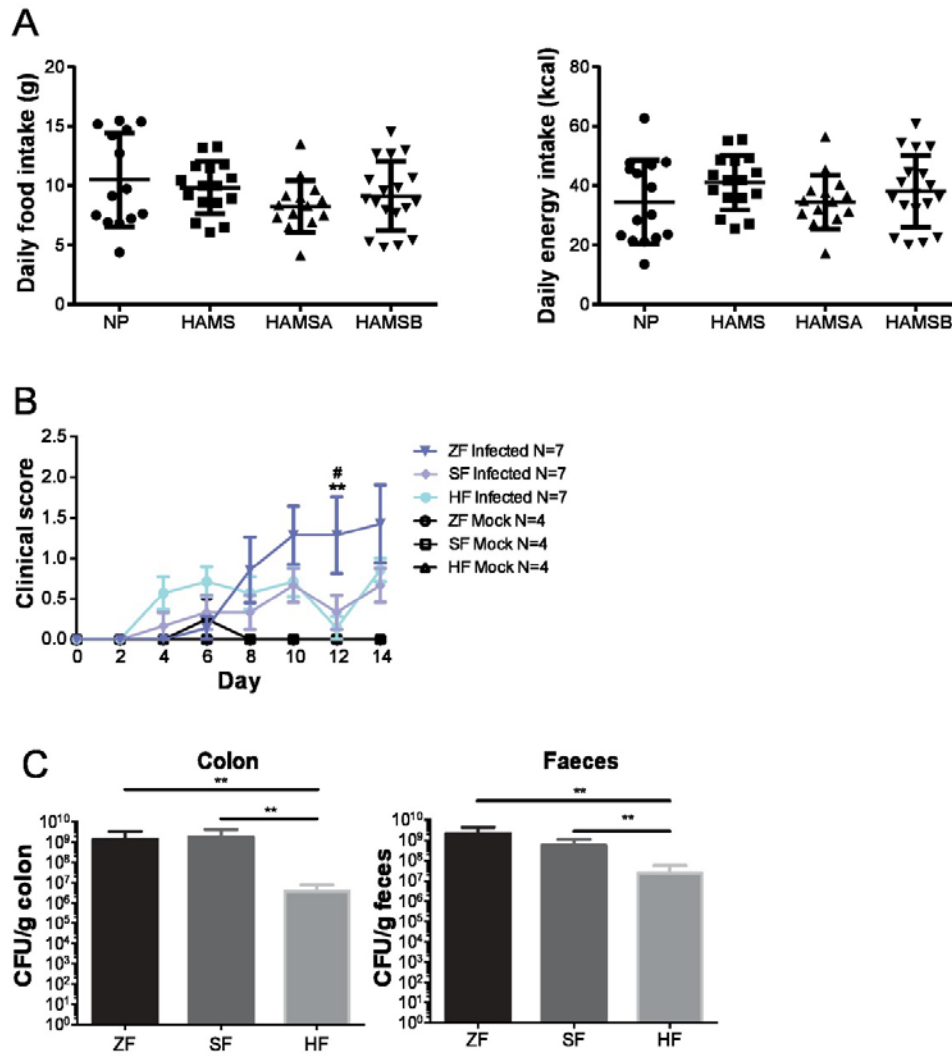
## **Real time quantitative PCR analysis**

RNA from the colon was extracted and converted to cDNA using Bioline's Tetro cDNA synthesis kit, using oligo (dT)18 primers to amplify mRNA. qPCR was performed using Bioneer's Accupower 2x Greenstar qPCR master mix on Biorad's Cfx384 real time system. All expression was standardized to the housekeeping gene  $\beta$ -actin. Primers used in the experiment are shown in Supplementary Table 2.

## **FACS analysis**

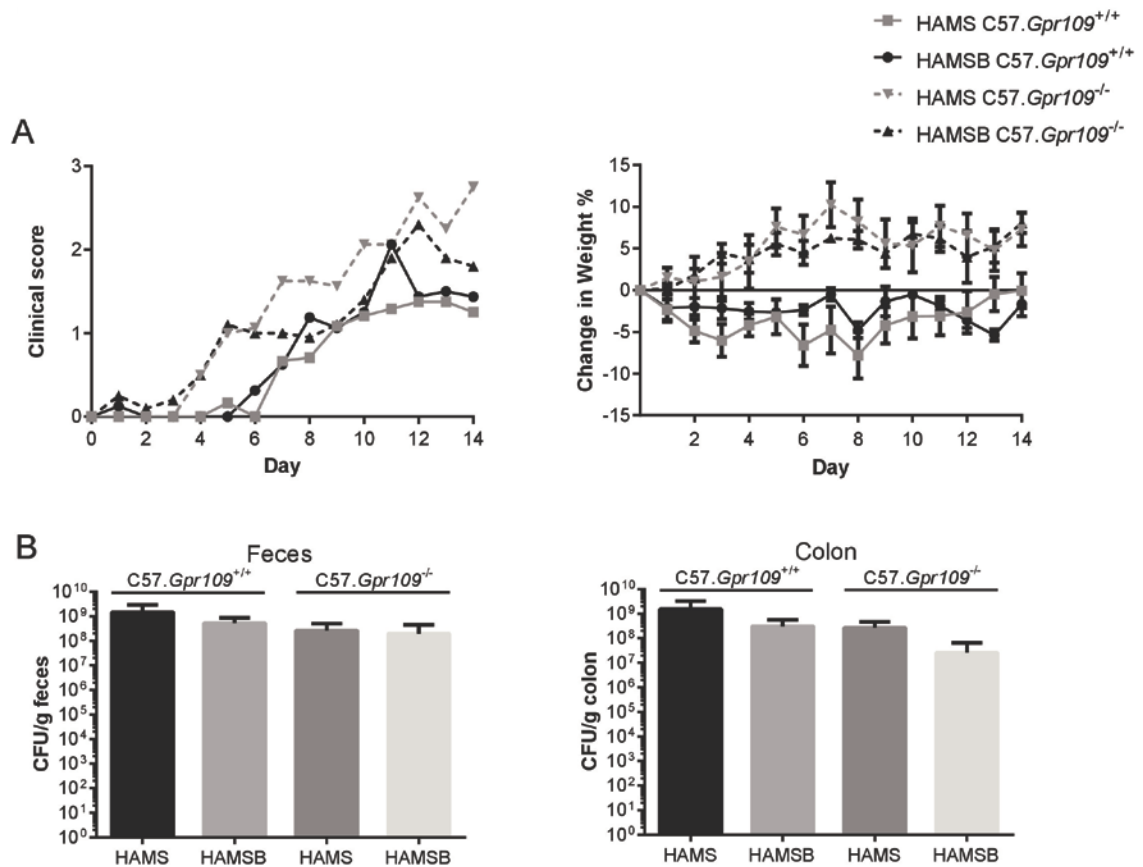
Immunophenotypic analysis of mononuclear cells used the mAbs listed in Supplementary Table 3. Intracellular staining of IL-17A and Foxp3 was performed using the Foxp3-staining kit (eBioscience). All Abs from BD Bioscience, eBioscience or Biolegend. Stained samples were analysed using BD LSRII flow cytometers with FACSDiva software (BD Biosciences) and FlowJo software version 9.3.2 (Tomy Digital Biology).

## SUPPLEMENTARY FIGURES



**Supplementary Figure 1. Non-HAMS fibre diet and *C. rodentium* infection, resistant starch supplement food intake and bacterial growth.**

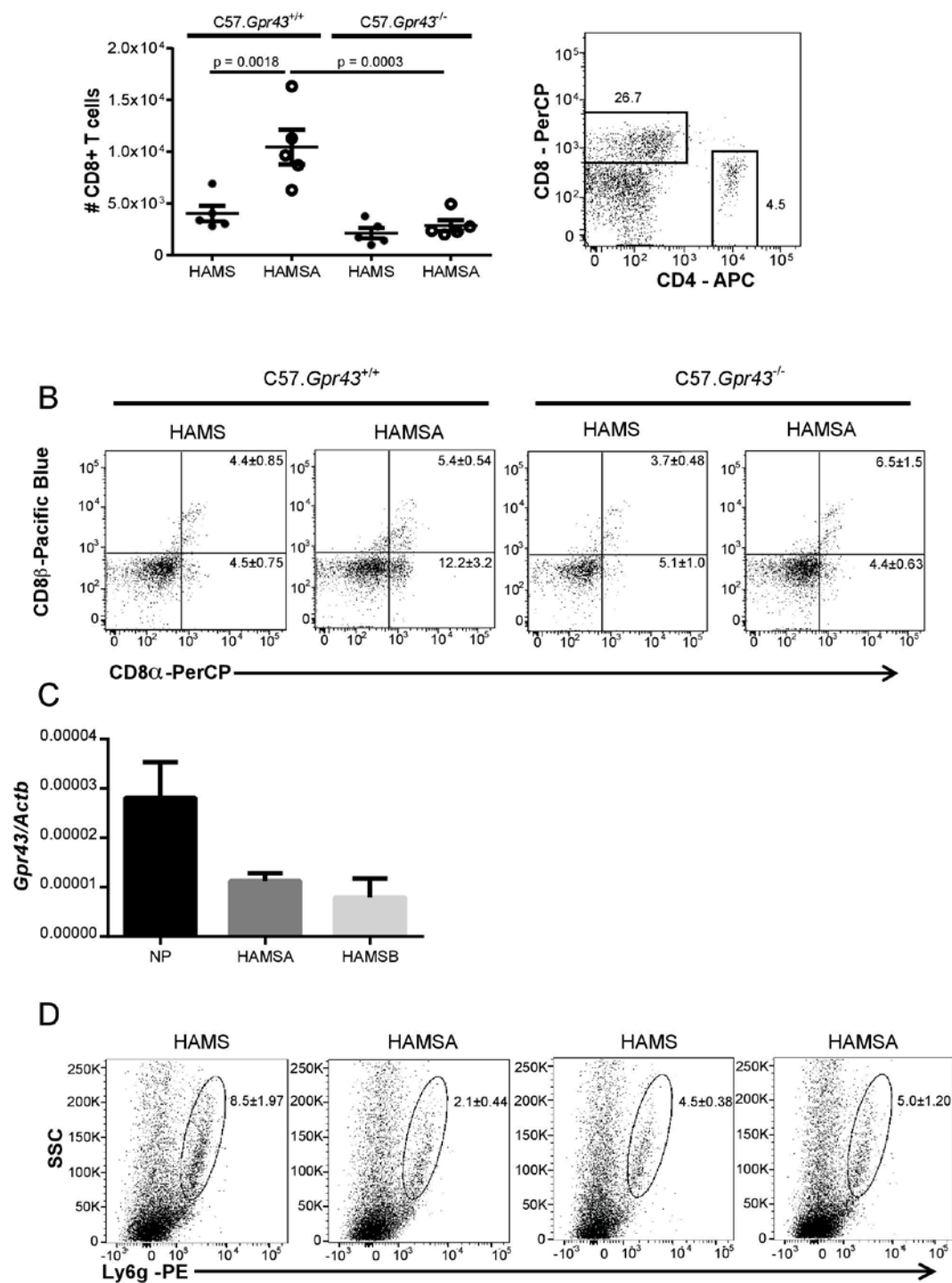
**A**, Comparison of food intake and energy intake between C57Bl6/J mice fed standard mouse chow, HAMS, HAMSA or HAMSB supplements (n = 16). **B**, Clinical burden of *C. rodentium* infection over 14 day on C57Bl/6J mice fed high fibre (HF), standard fibre (SF) or zero fibre (ZF) diet for 3 weeks *ad libitum* prior to inoculation and for the length of the experiment (n = 5). **C**, Bacterial load of *C. rodentium* in the colon and feces from mice in **B**. p values for **B** calculated by two-way ANOVAs with Bonferoni's correction. p values for **C** calculated by one-way ANOVAs with Bonferoni's correction. \* p=<0.05, \*\* p=<0.01. All data is shown as mean  $\pm$  S.E.M.



**Supplementary Figure 2. Protection from *C. rodentium* infection is not affected by GPR109 deficiency.**

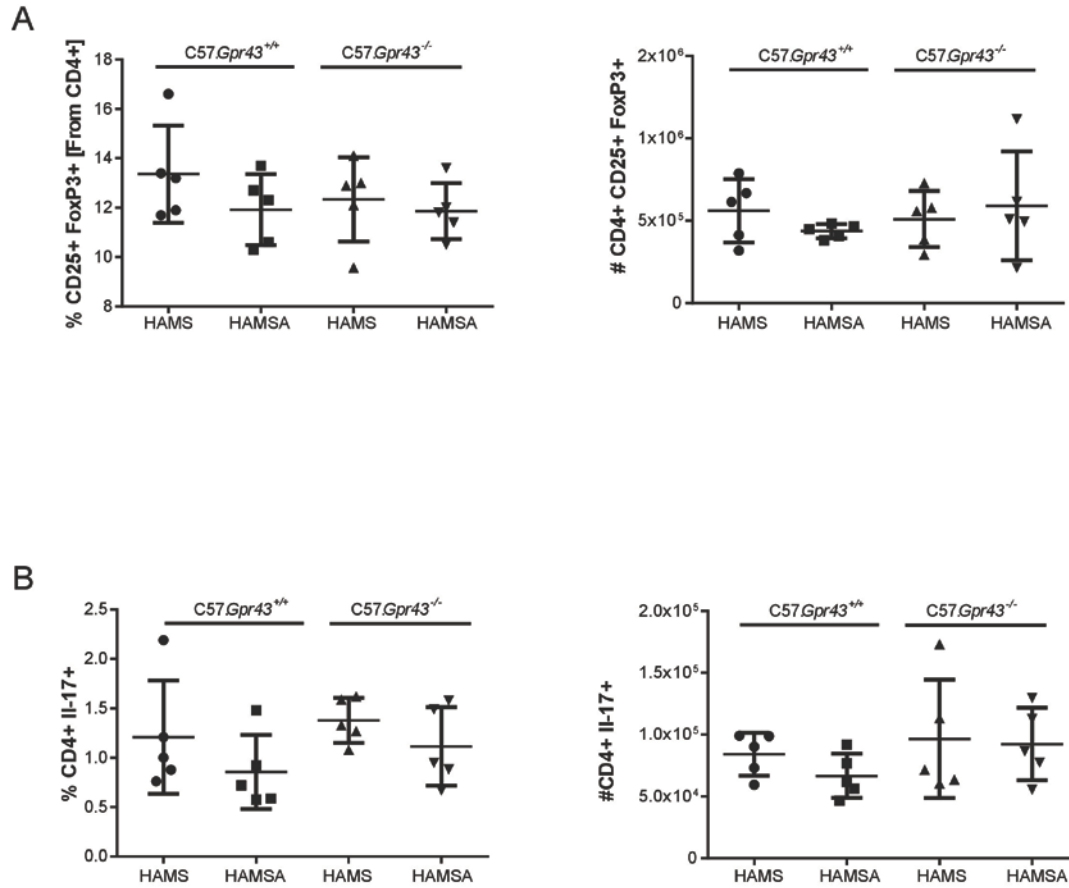
**A**, Clinical burden and percentage weight change in *C. rodentium* infected C57.Gpr109<sup>+/+</sup> or C57.Gpr109<sup>-/-</sup> mice fed HAMS or HAMSB supplement *ad libitum* 3 weeks prior to inoculation and for the length of the experiment. **B**, Bacterial load of *C. rodentium* in the colon and feces at the peak of disease, 14 days post-inoculation. All data are shown as mean  $\pm$  S.E.M. (n = 5).





**Supplementary Figure 3. IEL and neutrophil gating strategy.**

**A**, Number of CD8<sup>+</sup> T cells, and representative FACS plot demonstrating gating strategy for CD8<sup>+</sup> and CD4<sup>+</sup> IELs. **B**, Representative plots of CD8 $\alpha\alpha$  and CD8 $\alpha\beta$  T cells from C57.*Gpr43*<sup>+/+</sup> or C57.*Gpr43*<sup>-/-</sup> mice 14 days post infection fed HAMS or HAMSA supplement shown in Figure 4**A**. **C**, expression of *Gpr43* in isolated TCR $\gamma\delta$ <sup>+</sup> T cells from the spleens of non-infected C57Bl/6J mice fed NP, HAMS or HAMSA supplement. **D**, Representative plots of lamina propria neutrophils (Ly6g<sup>+</sup>) in the colon of C57.*Gpr43*<sup>+/+</sup> or C57.*Gpr43*<sup>-/-</sup> mice 14 days post infection fed HAMS or HAMSA supplement from 4**A**. All values are shown as mean  $\pm$  S.E.M. (n = 5).



**Supplementary Figure 4. T cell populations in the colonic epithelium and MLNs of infected *C57.Gpr43*<sup>+/+</sup> or *C57.Gpr43*<sup>-/-</sup> mice.**

**A**, Percentage and number of regulatory T cells (CD4+ CD25+ Foxp3+) in the colonic epithelium of mice from **4A**. **B**, Percentage and number of Th17 cells (CD4+ IL-17+) in the MLN of mice from Figure **4A**. All cellular proportions determined by flow cytometry. All data are shown as mean ± S.E.M. (n = 5).

**Supplementary Table 1.** Calculated nutritional parameters from diets used in this study.

Ingredient	15% HAMS	15% HAMSA	15% HAMSP	15% HAMSB	15% HAMSA/B
Maize starch - 3401C	379.5	379.5	379.5	379.5	229.5
<b>HAMS</b>	<b>150</b>	0	0	0	<b>150</b>
<b>HAMSA</b>	0	<b>150</b>	0	0	0
<b>HAMSP</b>	0	0	<b>150</b>	0	0
<b>HAMSB</b>	0	0	0	<b>150</b>	<b>150</b>
Casein	200	200	200	200	200
Sucrose	100	100	100	100	100
Sunflower Seed Oil	70	70	70	70	70
alpha cellulose	50	50	50	50	50
Mineral Mix AIN 93G	35	35	35	35	35
Vitamin Mix AIN 93VX	10	10	10	10	10
L-Cystine	3	3	3	3	3
Choline bitartrate	2.5	2.5	2.5	2.5	2.5
<b>Total</b>	<b>1000</b>	<b>1000</b>	<b>1000</b>	<b>1000</b>	<b>1000</b>

Control non-purified diet (SPECIALTY FEEDS)

MOUSE MAINTENANCE DIET

A nutritionally balanced diet to maintain good health for study of long term mice.

Ingredients pollard bran sorghum hominy bloodmeal meatmeal salt lime vitamin and mineral premix choline chloride

Proximate Analysis

Min. Crude Protein .....14%

Max. Crude Fat.....4%

Calculated Analysis Results:

Max. Crude Fibre .....6%

M.E. (Min.).....11mj/kg

Amino Acids

Lysine 4.6g/kg

Methionine & cystine 3.5g/kg

Threonine 4.0g/kg

Histidine 3.1g/kg

Leucine 10.0g/kg

Arginine 6.7g/kg

Valine 5.6g/kg

Isoleucine 3.8g/kg

Phenylalanine & Tyrosine 9.9g/kg

Tryptophan 2.0g/kg

Levels of free SCFAs content in control non-purified diet.

( $\mu$ mol/g)

Acetate 12.72

Propionate 1.8

Butyrate 1.2

**Supplementary Table 2.** Primers used in the study

Primer name	Forward primer	Reverse primer
Actb	5' ACC AGA GGC ATA CAG GGA CA 3'	5' CTA AGG CCA ACC GTG AAA AG 3'
Muc2	5' TCC TGA CCA AGA GCG AAC AC 3'	5' ACA GCA CGA CAG TCT TCA GG 3'
Il-22	5' GAT GGC TGT CCT GCA GAA AT 3'	5' GAA CAG TTT CTC CCC GAT GA 3'
Il-17	5' CAG GAC GCG CAA ACA TGA 3'	5' GCA ACA GCA TCA GAG ACA CAG AT 3'
Il-18	5' GAC AGC CTG TGT TCG AGG AT 3'	5' TGG ATC CAT TTC CTC AAA GG 3'
Ccl3	5' TCA TCG TTG ACT ATT TTG AAA 3',	5' GCC GGT TTC TCT TAG CAG GAA 3'
Ccl4	5' AGG GTT CTC AGC ACC AAT GG 3'	5' GCT GCC GGG AGG TGT AAG A 3'
Gpr43	5' CAG ACC AGC TGC AAA CTC G 3'	5' TTC TCC TCT GGT CCA GTG CT 3'

**Supplementary Table 3.** Antibodies used in the study

<b>Antibody target</b>	<b>Clone</b>
CD3	145-2C11
CD4	RM4-5
CD8a	53-6.7
CD8b.2	53-5.8
TCRgd	eBioGL3
CD103	M290
CD69	H1.2F3
CD25	PC61
IL-17A	TC11-18H10
FoxP3	FJK-16s

## Chapter 3 – The Role of GPR65 in Infection and Colitis

### 1. Introduction

The following chapter is comprised of data from 2 papers on the immunological role of GPR65. The first section presents data included in “Genetic Coding Variant in GPR65 Alters Lysosomal pH and Links Lysosomal Dysfunction with Colitis Risk” published in *Immunity* (Appendix 2). All methods for this data are included in the Appendix. The second section includes a paper titled “Proton-sensing receptor GPR65 regulates colonic inflammation through effects on leukocyte migration and intracellular metabolic pathways” soon to be submitted to *Gut*, comprised entirely of data from experiments completed in this PhD. Special mention must go to Jot Hui Ooi, Kara Lassen, Jaeyun Sung and Isabel Latorre for running fluidigm and mass spectrometry experiments on neutrophil samples that I prepared for analysis. These data demonstrate the regulatory role of GPR65 in lysosome formation and neutrophil chemotaxis that alter the outcome of bacterial gut infection and IBD. Furthermore, they demonstrate a novel impact of extracellular acidity on neutrophil chemotaxis and inflammation. Together, these papers display the discoveries made in this PhD that establish a novel role for GPR65 in inflammation and mucosal immunology.

### 2. GPR65 protects against *C. rodentium* infection

IBD has been associated with SNPs in a wide variety of genes responsible for bacterial sensing, metabolite sensing and autophagy<sup>252, 253</sup>. Specifically, polymorphisms in the *Gpr65* gene have been associated with ulcerative colitis and Crohn’s disease in three genome-wide association studies<sup>49, 50, 51</sup>. To investigate the role of GPR65 in bacterial infection and colitis, we assessed disease progression in *Gpr65*<sup>-/-</sup> mice infected with *Citrobacter rodentium*, a mouse-restricted pathogen that causes colitis-like symptoms<sup>205</sup>. *C. rodentium* is an attaching/effacing pathogen that predominantly infects the colon, causing diarrhoea and weight loss<sup>254</sup>. Disease progression was assessed at the peak of disease, 14 days post-infection. Infected *Gpr65*<sup>-/-</sup> mice exhibited increased epithelial damage and leukocyte

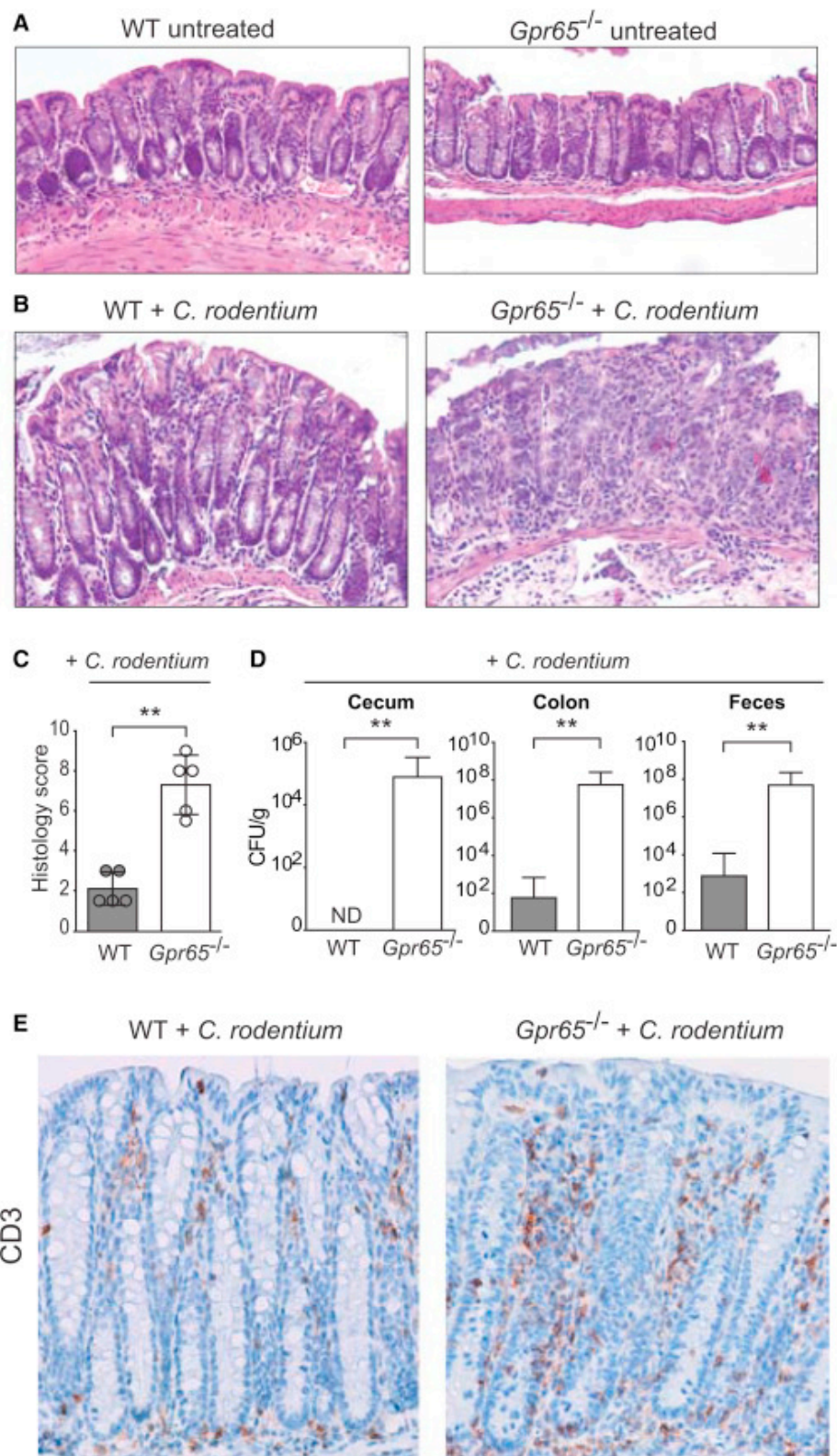




**Figure 3.1. *Gpr65*<sup>-/-</sup> Mice Are More Susceptible to Bacterial-Induced Colitis.** (A) Representative H&E-stained sections of distal colon tissue are shown from untreated WT and *Gpr65*<sup>-/-</sup> mice (20× magnification) (n = 4 mice per genotype). (B) Representative H&E-stained sections of distal colon tissue are shown from infected WT and *Gpr65*<sup>-/-</sup> mice (20× magnification) (n = 8 mice per genotype). (C) Histological score for inflammation in colon tissues 14 days after *C. rodentium* infection. Data shown as mean ± SD; n = 5/group. \*\*p < 0.01 (Mann-Whitney U test). (D) WT and *Gpr65*<sup>-/-</sup> mice were orally infected with *C. rodentium* and bacterial numbers (CFU) were measured in the cecum, colon, and feces 14 days after infection. Data are means + SEM (n = 10 [WT], 10 [*Gpr65*<sup>-/-</sup>]; 2 experiments). \*\*p < 0.01 (Mann-Whitney U test). (E) Immunohistochemistry image of CD3 staining on WT and *Gpr65*<sup>-/-</sup> colon tissue 14 days after infection with *C. rodentium*.

infiltration of the colon (Figure 3.1A – C). The bacterial load in the cecum, colon and feces was also increased in the colons of *Gpr65*<sup>-/-</sup> mice (Figure 3.1D). To confirm leukocyte migration, immunohistochemistry for CD3 also demonstrated enhanced *Gpr65*<sup>-/-</sup> leukocyte migration (Figure 3.1E). Taken together, these data demonstrate that GPR65 is required to protect mice from *C. rodentium* infection. Furthermore, enhanced leukocyte migration to the colon of *Gpr65*<sup>-/-</sup> mice suggests increased bacterial burden exacerbated the inflammatory response to infection.

### **3. *Gpr65* expression in haematopoietic and non-haematopoietic compartments limits *C. rodentium* infection**

Cells of the immune and epithelial compartments are required to clear *C. rodentium* infection. The haematopoietic lineage gives rise to the immune compartment, whilst the epithelium arises from non-haematopoietic progenitors. Although other non-haematopoietic cells may be involved in the response to infection, epithelial cells are the predominant non-immune cell type involved in clearing *C. rodentium* infection<sup>208, 255</sup>. To determine the role of GPR65 in either compartment during infection, we assessed disease progression in infected WT and *Gpr65*<sup>-/-</sup> bone marrow (BM) chimeras. Briefly, WT or *Gpr65*<sup>-/-</sup> recipient mice are irradiated and reconstituted with WT or *GPR65*<sup>-/-</sup> bone marrow. Chimeras develop a haematopoietic compartment of the opposite strain. As before, disease progression was assessed at the peak of disease, 14 days post-infection. The absence of GPR65 in both haematopoietic and non-haematopoietic compartments increased bacterial burden in the colon (Figure 3.2A). This demonstrates that expression of *Gpr65* in immune and epithelial cells is required to prevent infection. Colon length, a marker of colitic severity, was reduced in mice lacking GPR65 in the non-haematopoietic compartment (Figure 3.2B). *Gpr65*<sup>-/-</sup> bone marrow did not significantly alter colon length. This suggests that colitic dehydration and colon shortening caused by infection is reduced by *Gpr65* expression on epithelial cells. Significant differences in histopathology were not observed at this time point of infection (Figure 3.2C).

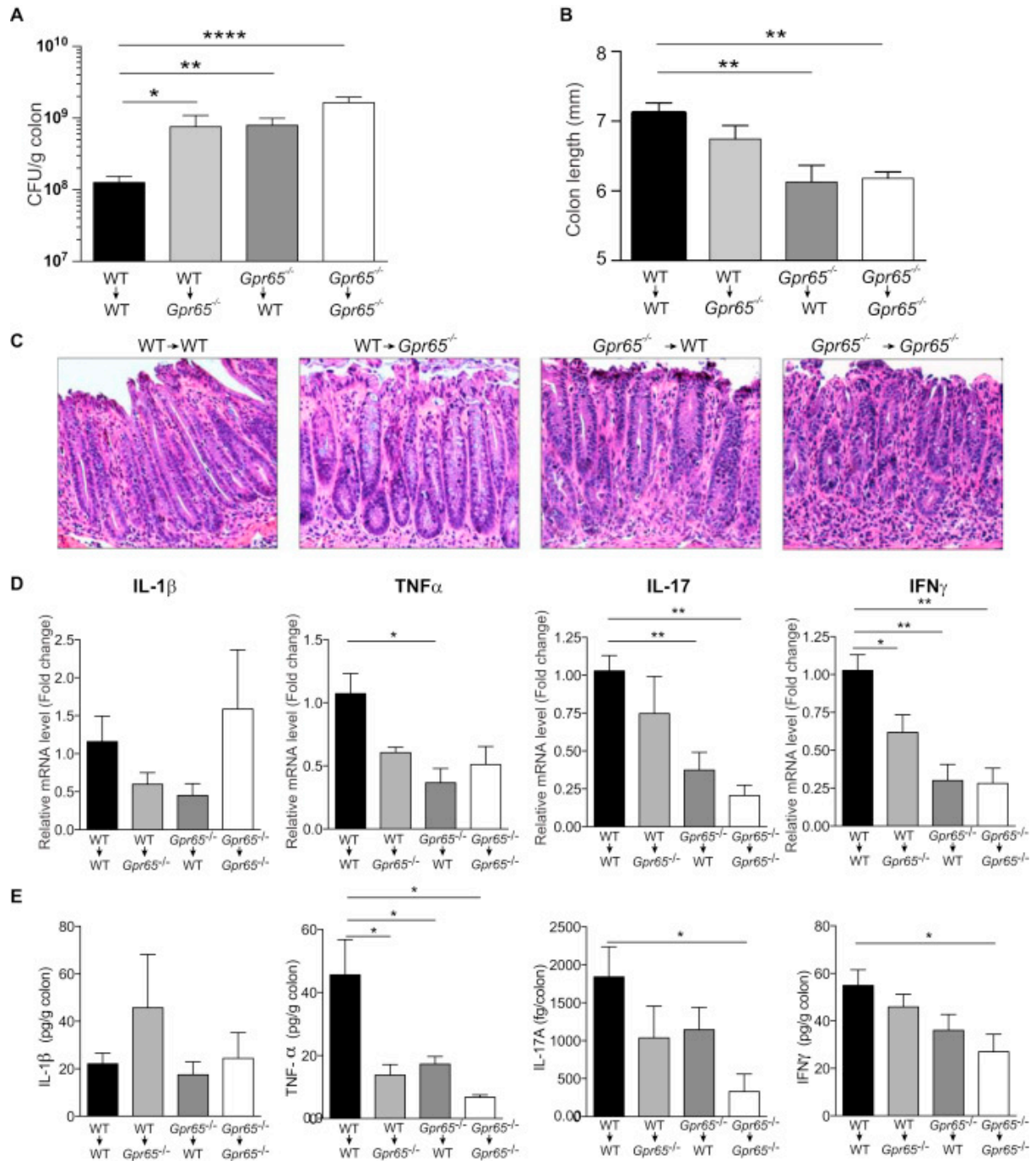


**Figure 3.2. *Gpr65* Expression in Non-hematopoietic and Hematopoietic Cells Limits *C. rodentium* Infection.** (A) Bone marrow chimeric mice were orally infected with *C. rodentium* and bacterial numbers (CFU) were measured in the colon at 11 days after infection. Data are means + SEM (n = 11 [WT→WT], n = 6 [WT→*Gpr65*<sup>-/-</sup>], n = 10 [*Gpr65*<sup>-/-</sup>→WT], n = 4 [*Gpr65*<sup>-/-</sup>→*Gpr65*<sup>-/-</sup>]). \*p < 0.05, \*\*p < 0.01, \*\*\*\*p < 0.0001 (unpaired t test). (B) Colon length from bone marrow chimeric mice infected with *C. rodentium* for 11 days. Data are means + SEM. \*\*p < 0.01 (unpaired t test). (C) Representative H&E-stained sections of distal colon tissue are shown from infected bone marrow chimeric mice at 11 days after infection (20× magnification). (D) Cytokine expression in *C. rodentium*-infected mice, as quantified by qRT-PCR. Relative mRNA levels of the indicated cytokine are shown. \*p < 0.05; \*\*p < 0.01 (unpaired t test). Data are means + SEM. (E) Secretion of cytokines from colon tissues 11 days after infection with *C. rodentium*. Data are means + SEM. \*p < 0.05 (unpaired t test).

To further characterise the inflammatory response to infection in bone marrow chimeras, we quantified the expression and protein of pro-inflammatory cytokines in the colon important for clearing *C. rodentium*, including IL-1 $\beta$ , TNF- $\alpha$ , IL-17 and IFN $\gamma$ . Levels of TNF- $\alpha$ , IL-17 and IFN $\gamma$  mRNA or protein were reduced in mice with *Gpr65*<sup>-/-</sup> haematopoietic and non-haematopoietic compartments (Figure 3.2D, E). In particular, mice with a combination of both *Gpr65*<sup>-/-</sup> compartments exhibited the lowest quantities of TNF- $\alpha$ , IL-17 and IFN $\gamma$  (Figure 3.2E). These data demonstrate that GPR65 signalling in immune and non-immune cells promotes pro-inflammatory cytokine production in response to *C. rodentium* infection in the colon. This pro-inflammatory response mediated by GPR65 was found to require efficient phagocytosis of bacteria to induce cytokine release, a process impaired in HeLa cells with a polymorphism in GPR65 (Appendix 2). As such, these data demonstrate that GPR65 signalling mediates efficient clearance of gut bacterial pathogens by enhancing the innate immune response to infection.

#### **4. GPR65 regulates neutrophil chemotaxis and metabolism**

Given that GPR65 enhances innate immunity to infection and that *Gpr65* polymorphisms are associated with IBD, we investigated the role of GPR65 in a murine model of DSS colitis. The following section includes a submitted manuscript demonstrating how GPR65 can regulate neutrophil chemotaxis in response to extracellular acidity. Furthermore, these alterations in neutrophil biology are associated with exacerbated ulcerative colitis, providing a novel explanation for the association between *Gpr65* SNPs and IBD.

# **Proton-sensing receptor GPR65 regulates colonic inflammation through effects on leukocyte migration and intracellular metabolic pathways**

## **Authors**

Craig McKenzie<sup>1</sup>, Laurence Macia<sup>2</sup>, Jian Tan<sup>1</sup>, Jot Hui Ooi<sup>3</sup>, Kara Lassen<sup>4</sup>, Jaeyun Sung<sup>4</sup>, Isabel Latorre<sup>4</sup>, Nan Bing<sup>5</sup>, Padma Reddy<sup>6</sup>, Ramnik Xavier<sup>4</sup>, Charles R. Mackay<sup>1</sup>

## **Affiliations**

1. Department of Biochemistry and Molecular Biology, Monash University, Clayton, VIC, Australia
2. Charles Perkins Centre, Sydney Medical School, University of Sydney, Sydney, NSW, Australia
3. Inflammation and Immunology Research Unit, Pfizer, Cambridge, MA, USA
4. The Broad Institute of MIT and Harvard, Cambridge, MA, USA
5. Human Genetics Research Unit, Pfizer, Cambridge, MA, USA
6. Clinical Research Unit, Pfizer, Cambridge, MA, USA

## ABSTRACT

GPR65 is a proton-sensing receptor expressed by immune cells and certain epithelia. This receptor is activated under acidic extracellular conditions, which suggests a role in locations such as the gastrointestinal tract, or in situations of acidosis. Interestingly, acidosis has long been known to regulate immune responses, including neutrophil chemotaxis. Single nucleotide polymorphisms (SNPs) in *Gpr65* in humans predispose to inflammatory bowel disease (IBD). In the present study, we assessed the severity of dextran sulphate sodium (DSS) colitis in *Gpr65*<sup>-/-</sup> mice, and found that they displayed exacerbated colitis, including enhanced infiltration of leukocytes into the mucosa of the colon. Bone marrow chimeras established that deficiency of GPR65 in bone marrow derived cells contributed to this phenotype. *Gpr65*<sup>-/-</sup> neutrophils migrated more readily to CXCL8 and were resistant to acid-induced inhibition of chemotaxis. To understand molecular changes in cells exposed to extracellular pH and GPR65 signalling, we assessed WT and *Gpr65*<sup>-/-</sup> neutrophils for their metabolic profiles under control and acidic conditions following stimulation with CXCL8. GPR65 signalling altered various lipid metabolites important for cell migration. We establish a novel role for GPR65 on neutrophils in the regulation of cell migration in response to acidic conditions.

## INTRODUCTION

Human IBD involves the interplay between genetics and environmental influences<sup>168, 169, 170</sup>. Among the environmental factors associating with IBD, poor gut homeostasis, and an altered microbiome composition are consistent features<sup>256</sup>. The mechanisms that drive tissue damage involve a myriad of immunological processes, involving various leukocyte cell types. These include effector T cells, dysregulated Treg cells, innate lymphoid cells, and neutrophils<sup>181, 257</sup>. Indeed a consistent feature of inflammation in IBD is the transepithelial migration of neutrophils to the gut and exacerbation of inflammation from the release of neutrophil products such as ROS and elastase<sup>176, 181</sup>. Neutrophil migration to the gut is initiated upon release of inflammatory chemokines such as CXCL2 (MIP-2) and CXCL8 by the epithelium<sup>177, 178</sup>. These chemokines are increased in the colon of IBD patients, facilitating subsequent neutrophil infiltration<sup>179, 180</sup>. The subsequent release of pro-inflammatory mediators from neutrophils in the gut can drive IBD pathogenesis by degrading epithelial junctions and reducing epithelial integrity<sup>181</sup>. Weakened integrity promotes bacterial translocation from the lumen to the mucosa, exposing neutrophils to LPS and other TLR ligands which elicit additional inflammatory responses that further exacerbate inflammation.

Interestingly, severe inflammation in IBD is associated with low luminal pH in the colon<sup>258</sup>. Indeed, localised acidification is a hallmark of inflammation. Acidosis is established in inflamed tissue by infiltrating neutrophils that induce hypoxia and produce lactate from glycolysis<sup>259</sup>. These pH changes may be integral to the regulation of responses, since extracellular acidity can be sensed by proton-sensing G protein-coupled receptors (GPCRs). Such receptors include GPR4, GPR68 and GPR65. GPR65 is activated by protons in low pH conditions<sup>40</sup>. The relevance of such receptors is highlighted by single nucleotide polymorphisms (SNPs) in Gpr65 that associate with susceptibility to IBD, including both ulcerative colitis and Crohn's disease<sup>49, 50, 51</sup>. Recently, we demonstrated that SNPs in human GPR65 impair lysosomal function in epithelial cells, and that *Gpr65*<sup>-/-</sup> mice were more susceptible to *Citrobacter rodentium* infection<sup>260</sup>.



GPR65-GFP reporter mice show that GPR65 is highly expressed on many immune cells, including T and B lymphocytes, eosinophils and neutrophils<sup>43</sup>. While a clear role for GPR65 has been established in epithelial cell autophagy<sup>260</sup>, knowledge of the receptor's function in other potentially pathogenic cell types remains unclear. GPR65 is upregulated in eosinophils under acidic conditions<sup>43</sup>, suggesting GPR65 gene expression is controlled by extracellular pH. Signalling through Gpr65 increased eosinophil viability and exacerbated allergic airway inflammation in mice<sup>43</sup>. This would suggest that Gpr65 can be activated under certain environmental conditions and affect disease development. A functional role for GPR65 is also suggested by enhanced survival of cancer cells *in vitro* due to GPR65-induced protection from localised acidosis<sup>261</sup>. Localised acidosis from excessive glycolysis can activate GPR65 and maintain cancer cell proliferation via up-regulation of anti-apoptotic proteins<sup>261</sup>. In addition, GPR65 regulates cell activation by decreasing the release of cytokines in dexamethasone-treated LPS-stimulated macrophages under acidic conditions<sup>262</sup>. Thus the acidic environment established during inflammation may activate GPR65 and alter immunological functions by modulating cell activity and survival, particularly in immune cells.

The neutrophil is an immune cell type that expresses high levels of GPR65 protein<sup>263</sup> and plays a pathogenic role in numerous inflammatory diseases, including IBD<sup>181</sup>. Neutrophil chemotaxis requires numerous alterations to intracellular metabolic pathways. These are required for many cellular processes such as cytoskeletal stabilisation, shape change and cell membrane synthesis. For instance, conversion of sphingomyelin to ceramide by the enzyme sphingomyelinase is required to maintain direction in chemotactic neutrophils<sup>264</sup>. Indeed, exogenous treatment of neutrophils with sphingomyelin decreases their chemotaxis to the chemoattractant FMLP<sup>264</sup>. Furthermore, dietary administration of long-chain fatty acid transporter carnitine, a molecule required for energy production from beta oxidation, restored neutrophil chemotaxis in aged rats to levels equivalent to their younger counterparts<sup>265</sup>. In contrast, oral gavage of phosphatidylcholine (PC), a class of lipids that constitute a major component of cell membranes, has been demonstrated to reduce neutrophil infiltration of the joint in a rat model of arthritis<sup>266</sup>. Indeed, i.p. injections with PC reduces neutrophil infiltration of the lung, liver and kidney in an LPS-induced rat model of multiple organ injury<sup>267</sup>.

Phosphatidylethanolamine (PE) is another class of lipid present in the cell membrane, involved in neutrophil chemotaxis. PE is important in membrane remodelling during cytokinesis and maintaining mitochondrial morphology<sup>268</sup>. The conversion of arachidonic acid to PE is increased in human neutrophils stimulated with TNF- $\alpha$ <sup>269</sup>. Furthermore, neutrophil chemotaxis requires GPCR-activated phospholipase C activity and events downstream of diacylglycerol (DAG) signalling<sup>270</sup>. Indeed, DAG is increased in human neutrophils activated by the chemoattractant FMLP<sup>271</sup>. The above findings aside, the myriad of changes to intracellular metabolism during neutrophil chemotaxis remains poorly understood.

Here we show that immune cell expression of GPR65 is important for the pathogenesis of dextran sulphate sodium (DSS) colitis in mice. Absence of GPR65 lead to exacerbated colitis and enhanced neutrophil infiltration to the colon. Altered cell migration was one consequence of low pH, and this was dependent on proton sensing by GPR65. Proton sensing by GPR65 also affected intracellular lipid metabolic pathways important for the directed migration of leukocytes. The genetic association of Gpr65 with human inflammatory disease (particularly IBD) may thus relate in part to GPR65 functions in immune cells, and the regulation of important intracellular lipid metabolites that control leukocyte function.

## RESULTS

### Severity of DSS-induced colitis is increased in *Gpr65*<sup>-/-</sup> mice

Because of the association between SNPs in *Gpr65* and IBD, and the high expression of GPR65 protein on inflammatory type immune cells, we investigated the role of GPR65 in colitis. In a DSS-induced model of colitis, mice deficient in GPR65 developed exacerbated disease with increased weight loss and diarrhoeal severity (Figure 1A, B). *Gpr65*<sup>-/-</sup> mice treated with DSS showed significantly shorter colons than WT mice (Figure 1C). Damage to the epithelial barrier in colitis has been associated with translocation of gut bacteria from the gut lumen to tissues, particularly in the liver and mesenteric lymph nodes<sup>272, 273</sup>. *Gpr65*<sup>-/-</sup> mice contained significantly more anaerobic bacteria in both organs (Figure 1D). In addition to reduced epithelial integrity, neutrophil infiltration is a hallmark of DSS colitis. We quantified neutrophils (Ly6g<sup>+</sup> cells) by flow cytometry, which revealed a significant increase in neutrophils in the colonic lamina propria in *Gpr65*<sup>-/-</sup> mice at day 4 (Figure 1E). Histological scoring of the colon of mice treated with DSS confirmed that immune cell infiltration is higher in *Gpr65*<sup>-/-</sup> mice compared to WT mice (Figure 1F, G). Taken together, these data suggest that GPR65 expression prevents exacerbation of symptoms in IBD by regulating leukocyte migration to the colon and enhancing epithelial integrity.

### Lack of GPR65 in both the hematopoietic and non-hematopoietic compartments exacerbate DSS colitis

We have previously shown that GPR65 expression in both haematopoietic and non-haematopoietic compartments is important in reducing the severity of *C. rodentium* infection in the gut<sup>260</sup>. To investigate the role of the haematopoietic and non-haematopoietic compartments in the exacerbation of colitis in *Gpr65*<sup>-/-</sup> mice, we conducted DSS colitis experiments on bone marrow chimeras. Briefly, irradiated WT or *Gpr65*<sup>-/-</sup> mice were reconstituted with bone marrow of the

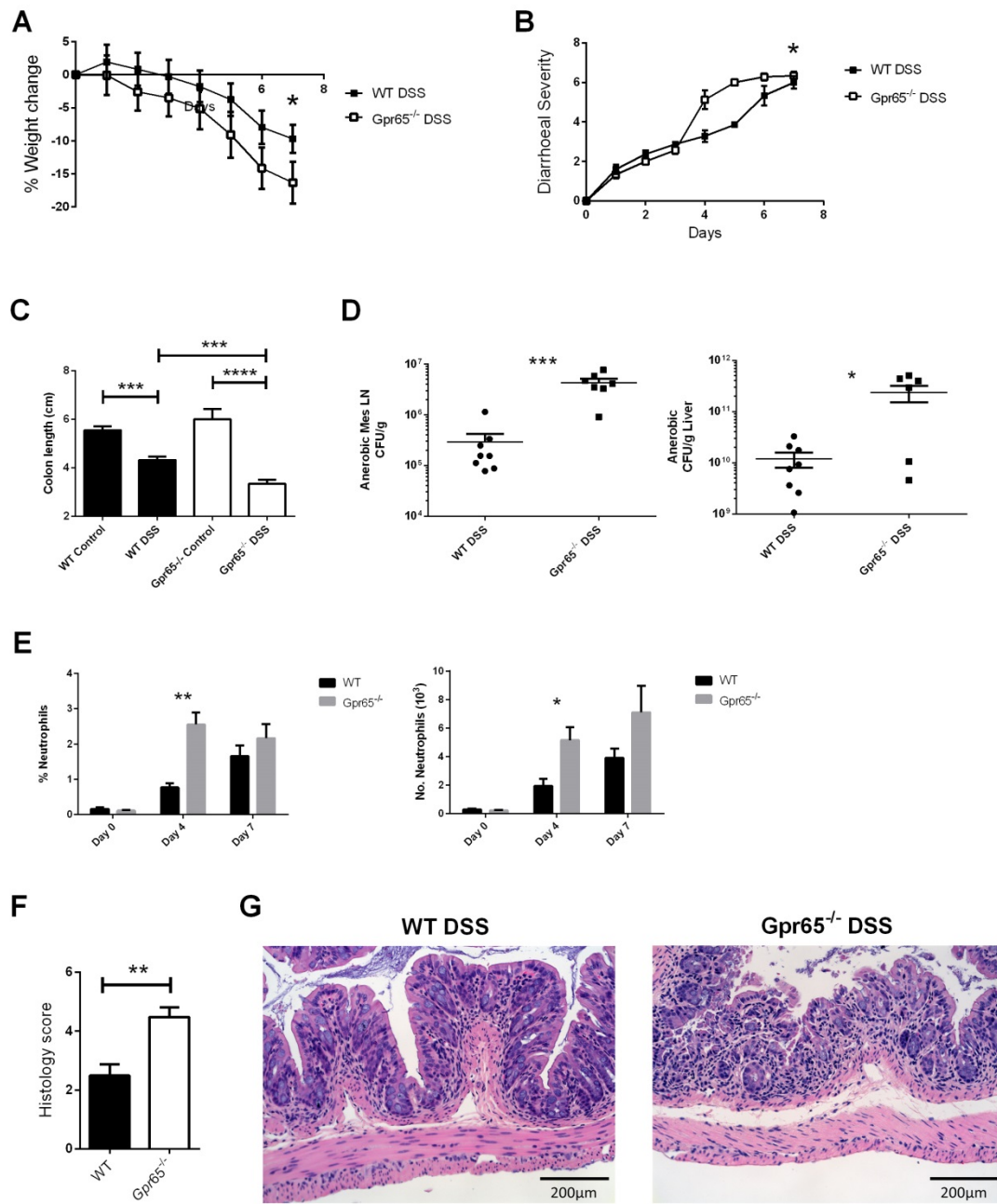


**Figure 1. *Gpr65*<sup>-/-</sup> mice are more susceptible to DSS colitis.**

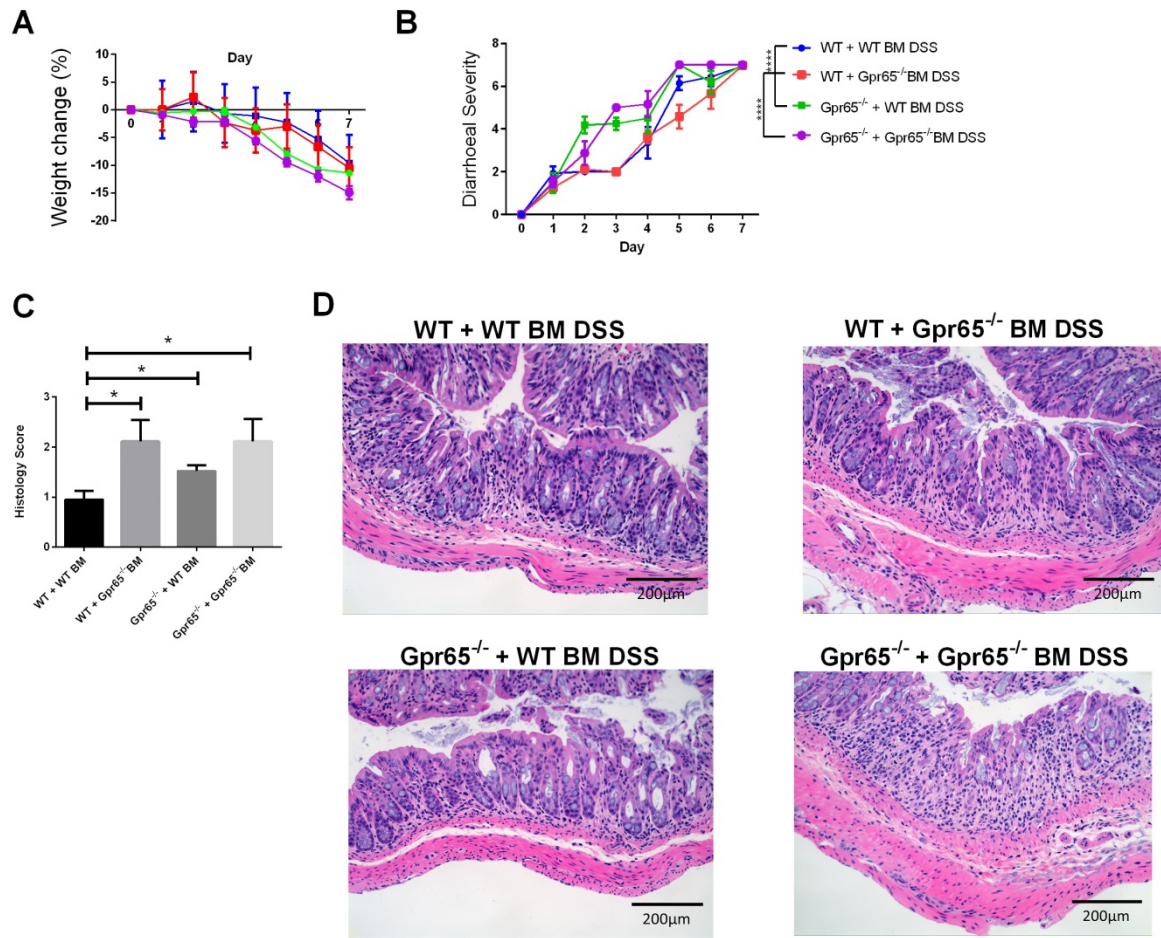
WT and *Gpr65*<sup>-/-</sup> mice were administered either normal drinking water (Control; n = 4/group) or 2% DSS in the drinking water (DSS; n = 8/group) for 7 days before being humanely culled. (A) Percentage weight change was measured daily. (B) Diarrhoeal severity scored from 0 – 8 representative of fecal consistency and blood as described in methods. (C) Colon length measured in millimetres. (D) Anaerobic growth of bacteria isolated from mesenteric LN and liver represented as log<sub>10</sub> colony forming units (cfu) per gram of organ. (E) Percentage and number of colonic neutrophils at day 0, 4 and 7 following DSS. (F) Histology score of H&E stained colon sections from 0 – 6 representing cellular infiltration and epithelial damage as described in methods. (G) Representative colon sections for scoring. Neutrophils identified as Ly6g+ cells by flow cytometry. \* p < 0.05, \*\* p < 0.005, \*\*\* p < 0.0005, \*\*\*\* p < 0.00005 (independent t test). All data represented as mean ± SEM.

opposing strain and subject to DSS colitis. The haematopoietic and non-haematopoietic compartments can be distinguished by comparing the strain of the donor with that of the recipient. WT recipients of *Gpr65*<sup>-/-</sup> bone marrow develop immune cells that are *Gpr65*<sup>-/-</sup> but maintain a *Gpr65*<sup>+/+</sup> non-haematopoietic compartment. Alternatively, *Gpr65*<sup>-/-</sup> recipients of WT bone marrow develop *Gpr65*<sup>+/+</sup> immune cells but maintain a *Gpr65*<sup>-/-</sup> non-haematopoietic compartment. The predominant non-haematopoietic cell-type involved in colitis is epithelial cells.

*Gpr65*<sup>-/-</sup> mice exhibited increased severity of diarrhoea and fecal blood at day 3, independent of the strain used for bone marrow reconstitution (Figure 2A, B). However, lack of GPR65 in the haematopoietic compartment had no impact on the severity of diarrhoea or fecal blood. Lack of GPR65 in the haematopoietic compartment led to increased leukocyte infiltration and epithelial damage in the colon after DSS treatment in both irradiated WT and *Gpr65*<sup>-/-</sup> mice (Figure 2D, E). *Gpr65*<sup>-/-</sup> mice showed increased leukocyte infiltration and epithelial damage of the colon when reconstituted with a WT or *Gpr65*<sup>-/-</sup> haematopoietic compartment (Figure 2D, E). These data suggest that GPR65 expression by epithelium and signalling in response to its agonists (i.e. protons) prevents clinical symptoms of diarrhoea and fecal blood. Furthermore, it demonstrates GPR65 expression in both immune and epithelial compartments can regulate inflammation in murine colitis.

### **SNPs in *Gpr65* are associated with IBD, asthma and eczema**

To understand the broad biological and disease impact of GPR65, we performed a phenome-wide association (PheWAS) for the *Gpr65* intronic SNP rs8005161. Rs8005161 has been reported as the top variant associated with IBD in multiple studies<sup>49, 50, 51</sup> and is in perfect linkage disequilibrium of the GPR65 missense variant I231L (rs3742704) based on the 1000 Genome Project European population data. The PheWAS was conducted on 1229 phenotypes collected from 647,776 genotyped subjects within 23andMe's data set. Rs8005161 showed significant association with inflammatory bowel disease ( $p=3.4\times 10^{-5}$ ) and asthma ( $p=3.6\times 10^{-5}$ ) after Bonferroni multiple test correction (Figure



**E**

Phenotype	Case(n)	Control(n)	OR (95% CI)	P value	FDR
Inflammatory Bowel Disease	12131	481868	1.1 [1.05-1.15]	$3.4 \times 10^{-5}$	0.02
Asthma	61035	318812	1.05 [1.02-1.07]	$3.6 \times 10^{-5}$	0.02
Eczema	56955	435504	1.04 [1.02-1.07]	$9.2 \times 10^{-5}$	0.04

**Figure 2. Both haematopoietic and non-haematopoietic compartments of *Gpr65*<sup>-/-</sup> mice contribute to DSS susceptibility.**

Irradiated WT or *Gpr65*<sup>-/-</sup> mice were reconstituted with bone marrow of the opposing strain and subject to DSS colitis (DSS; n = 8/group). (A) Percentage weight change was measured daily. (B) Diarrhoeal severity scored from 0 – 8 representative of fecal consistency and blood as described in methods. (C) Histology score of H&E stained colon sections from 0 – 6 representing cellular infiltration and epithelial damage as described in methods. (D) Representative colon sections for scoring. (E) Table summarising significant associated phenotypes for rs8005161 from PheWAS in 23andMe. \*\*\* p < 0.0005, \*\*\*\* p < 0.00005 (independent t test). All data represented as mean ± SEM.



2F). At the false discovery rate of 0.1, rs8005161 is also associated with eczema ( $p=9.2\times 10^{-5}$ ). This result confirms the predominant role of GPR65 in IBD. Furthermore, the association of asthma and eczema also suggests a broader biological impact of GPR65 on Th2-based allergic responses outside the gut, presumably not relating to epithelial cell autophagy. This is in accordance with exacerbated infiltration of eosinophils into the bronchioles of asthmatic mice deficient in GPR65<sup>263</sup>. To further investigate the role of GPR65 in allergy, we subject WT and *Gpr65*<sup>-/-</sup> mice to a murine model of peanut allergy. Despite no change in anaphylaxis or serum IgE, GPR65 reduced the number of cells in the mesenteric LN and decreased the production of Th2 cytokines IL-4, IL-5 and IL-13 from T cells stimulated with peanut allergen (Supplementary Figure 1). This demonstrates that GPR65 may regulate Th2 responses. However, this regulatory response was not sufficient to reduce the clinical outcome of anaphylaxis in food allergy, suggesting that allergic responses in the gut may not involve GPR65 signalling as much as those in the asthmatic lung. Indeed, polymorphisms in *Gpr65* assessed in our PheWas study were not significantly associated with food allergy (Supplementary Table 1).

#### ***Gpr65*<sup>-/-</sup> neutrophil chemotaxis *in vitro* is enhanced under basal and acidic extracellular pH**

Neutrophil chemotaxis is inhibited at low extracellular and intracellular pH<sup>274, 275</sup>. We hypothesised that enhanced colonic infiltration of neutrophils in *Gpr65*<sup>-/-</sup> mice undergoing DSS colitis may involve alterations to cell migration, and ultimately their recruitment to pathological sites. Indeed, *Gpr65*<sup>-/-</sup> neutrophils exhibited a strong GFP signal (Figure 3A), confirming maintain a highly activated *Gpr65* promoter. To determine whether GPR65 is involved in chemotaxis, we assessed the migratory properties of *Gpr65*<sup>-/-</sup> neutrophils towards CXCL8 using an *in vitro* chemotaxis assay. Furthermore, as GPR65 is a proton sensor we studied WT and *Gpr65*<sup>-/-</sup> neutrophil chemotaxis at physiological pH 7.4, or acidic pH 6.5.

Interestingly, the migration of *Gpr65*<sup>-/-</sup> neutrophils at either pH was increased compared to WT neutrophils (Figure 3B), indicating that lack of GPR65 signalling somehow altered the machinery

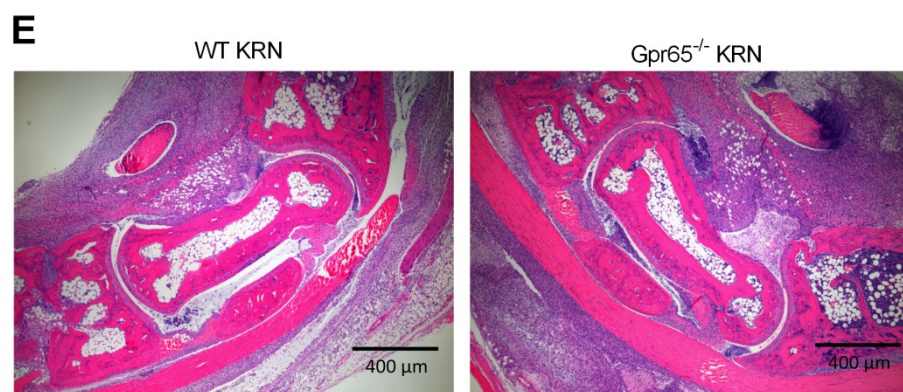
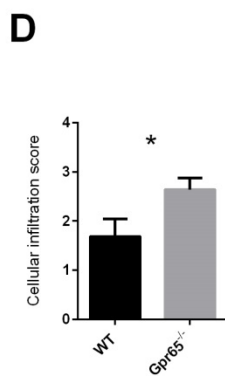
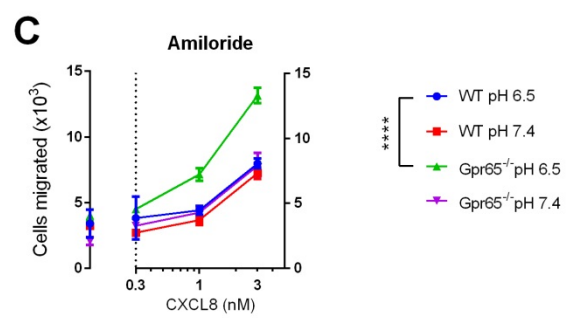
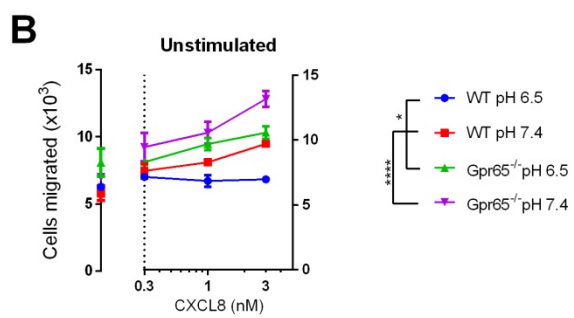
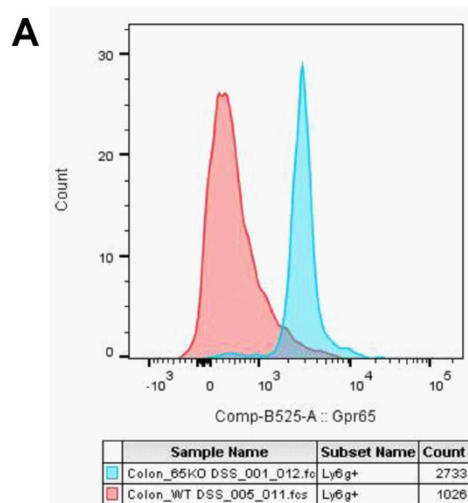


**Figure 3. *Gpr65*<sup>-/-</sup> neutrophil chemotaxis is enhanced *in vitro* and *in vivo*.**

(A) GFP signal of WT or *Gpr65*<sup>-/-</sup> neutrophils (Ly6g+) from the colon of mice administered DSS colitis. *Gpr65* is disrupted by insertion of GFP in *Gpr65*<sup>-/-</sup> mice. Neutrophil chemotaxis to CXCL8 was assessed (B) without or (C) with 5-amiloride hydrochloride. The number of neutrophils that migrated across a transwell membrane was determined by flow cytometry. (D) WT or *Gpr65*<sup>-/-</sup> mice were injected with KRN serum (KRN; n = 8/group). Histology score of H&E stained ankle sections from 0 – 3 representing cellular infiltration as described in methods. (E) Representative ankle sections stained with H&E. Purple cells are infiltrating neutrophils. \* p < 0.05 (independent t test). All data represented as mean ± SEM.

involved in cell migration. Of note, at pH 6.5, WT neutrophil migration was completely inhibited, whereas migration of *Gpr65*<sup>-/-</sup> neutrophils was only partially reduced (Figure 3B). Intracellular pH balance within neutrophils is maintained by sodium-hydrogen exchangers (NHE) that pump Na<sup>+</sup> ions into the cell and H<sup>+</sup> ions out. NHEs are crucial for neutrophil chemotaxis as they increase intracellular pH to provide a suitable environment for the cytoskeletal modifications required for rolling<sup>276</sup>. Indeed, such mechanisms of pH balance are crucial to migration, as inhibition of NHE function with amiloride can abrogate neutrophil chemotaxis<sup>277</sup>. To determine whether the function of NHE was altered in *Gpr65*<sup>-/-</sup> neutrophil migration, we conducted chemotaxis assays in the presence of an inhibitor of NHE, amiloride hydrochloride. Amiloride inhibited WT and *Gpr65*<sup>-/-</sup> neutrophil migration at pH 7.4 and inhibited WT but not *Gpr65*<sup>-/-</sup> neutrophil migration at pH 6.5 (Figure 3C). *Gpr65*<sup>-/-</sup> neutrophils treated with amiloride at pH 6.5 were inhibited at baseline (no CXCL8) but migrated more than untreated controls at higher CXCL8 concentrations. This suggests amiloride-sensitive ion channels such as NHE1 regulate neutrophil chemotaxis through GPR65 at neutral pH, whereas amiloride-independent mechanisms regulate chemotaxis at lower pH. Whilst signalling through GPR65 played a role in neutrophil migration, its absence did not affect the capacity of neutrophils to phagocytose *Escherichia coli*, or their viability in acidic conditions (data not shown).

To confirm an enhanced migratory phenotype of *Gpr65*<sup>-/-</sup> neutrophils *in vivo* we conducted a neutrophil-dependent model of arthritis. Briefly, serum from KRN mice containing autoantibodies was injected i.v. into WT or *Gpr65*<sup>-/-</sup> mice. Symptoms of arthritis develop within 2 -3 days independently of lymphocyte-mediated immune responses. While under arthritic conditions, WT and *Gpr65*<sup>-/-</sup> mice lost weight at the same rate and ankle thickness was significantly increased in *Gpr65*<sup>-/-</sup> mice compared to controls (Supplementary Figure 2A, B). Clinical scoring of swelling and redness was also significantly higher in *Gpr65*<sup>-/-</sup> mice (Supplementary 2C). Histological analysis shows neutrophil infiltration of the ankle was exacerbated in arthritic *Gpr65*<sup>-/-</sup> mice at day 7 (Figure 3D, E). This suggests GPR65 signalling regulates neutrophil infiltration of arthritic joints and delays the onset of clinical symptoms.

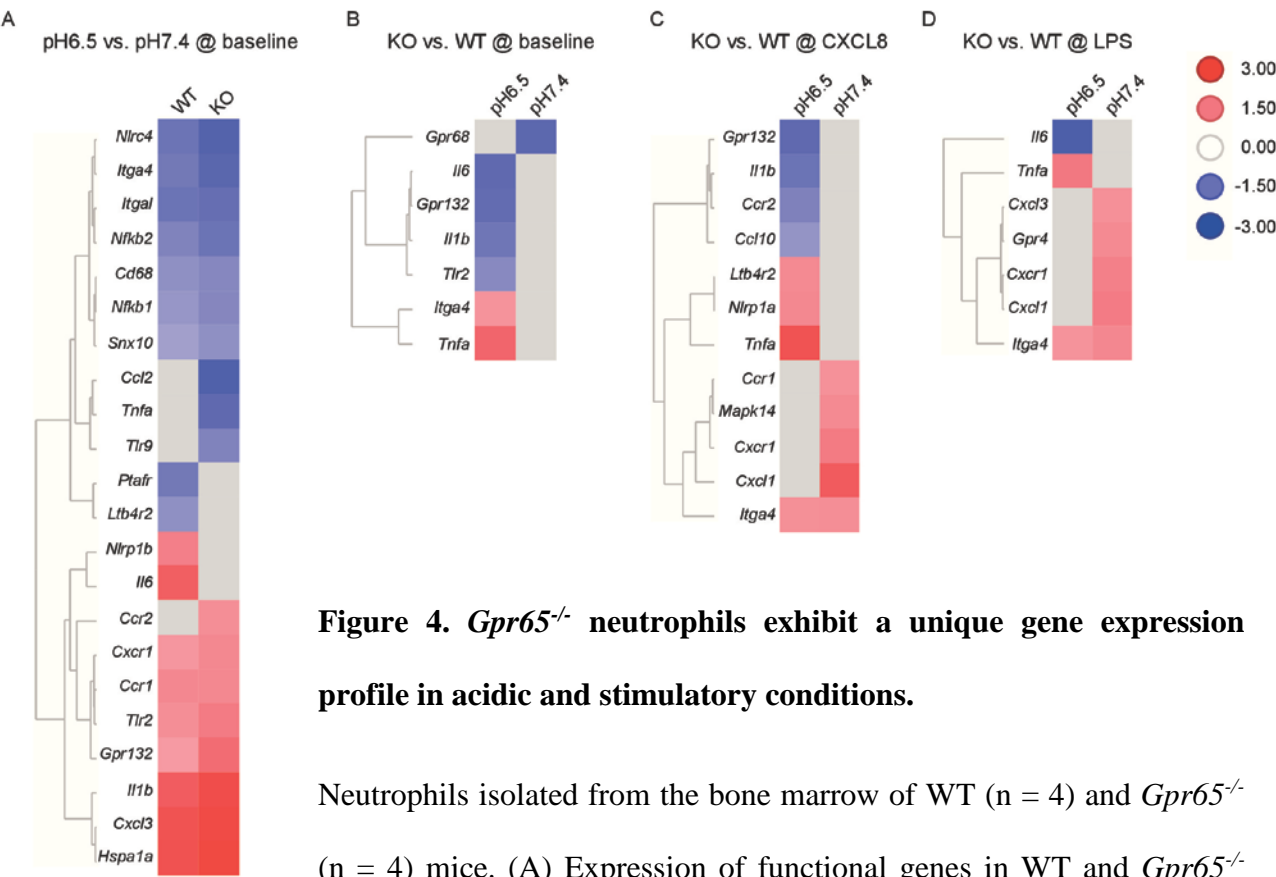
To determine whether the change in migration of GPR65-deficient neutrophils was associated with changes in gene expression, we quantified the expression of 86 genes crucial to chemotaxis, function and survival in WT and *Gpr65*<sup>-/-</sup> neutrophils (Figure 4 and Supplementary Figure 3). Neutrophils were exposed to an extracellular pH of 7.4 or 6.5 and stimulated with either CXCL8 or LPS. An acid-induced gene expression profile was concurrent in WT and *Gpr65*<sup>-/-</sup> neutrophils (Figure 4A). In the absence of CXCL8 and LPS, acidity increased expression of such genes as heat shock protein 1 in WT and *Gpr65*<sup>-/-</sup> neutrophils (Figure 4A). Contrastingly, acidity decreased expression of NLRC4 inflammasome, integrin  $\alpha 4$  and integrin  $\alpha L$ . Furthermore, *Gpr65*<sup>-/-</sup> neutrophils exhibited their own unique expression profile distinct from WT controls (Figure 4C – D). CXCL8 largely increased CXCL1 and CXCR1 expression in *Gpr65*<sup>-/-</sup> neutrophils, particularly at an extracellular pH of 7.4 (Figure 4C). Integrin  $\alpha 4$ , a component of multiple integrin receptors, was increased in *Gpr65*<sup>-/-</sup> neutrophils across all conditions. These data suggests GPR65 regulates chemokine receptor and integrin expression on neutrophils, reducing their capacity to migrate.

### **Extracellular pH and GPR65 signalling modify lipid metabolism in neutrophils stimulated with CXCL8**

Chemotaxis requires extensive changes to intracellular metabolism. To investigate changes in metabolism of chemotactic neutrophils in acidic extracellular environments, we quantified polar and lipid metabolites in WT neutrophils at baseline or stimulated with CXCL8 at pH 7.4 or 6.5. Metabolism was significantly altered by both acidic extracellular pH and stimulation with CXCL8. Broadly, lipid metabolites were increased in WT neutrophils upon stimulation with CXCL8 at pH 7.4 (Supplementary Figure 4). However, this increase in lipids was markedly decreased at pH 6.5, suggesting that a reduction in metabolic activity may lead to impaired neutrophil chemotaxis, which has been observed previously in acidic environments<sup>274, 275</sup>.

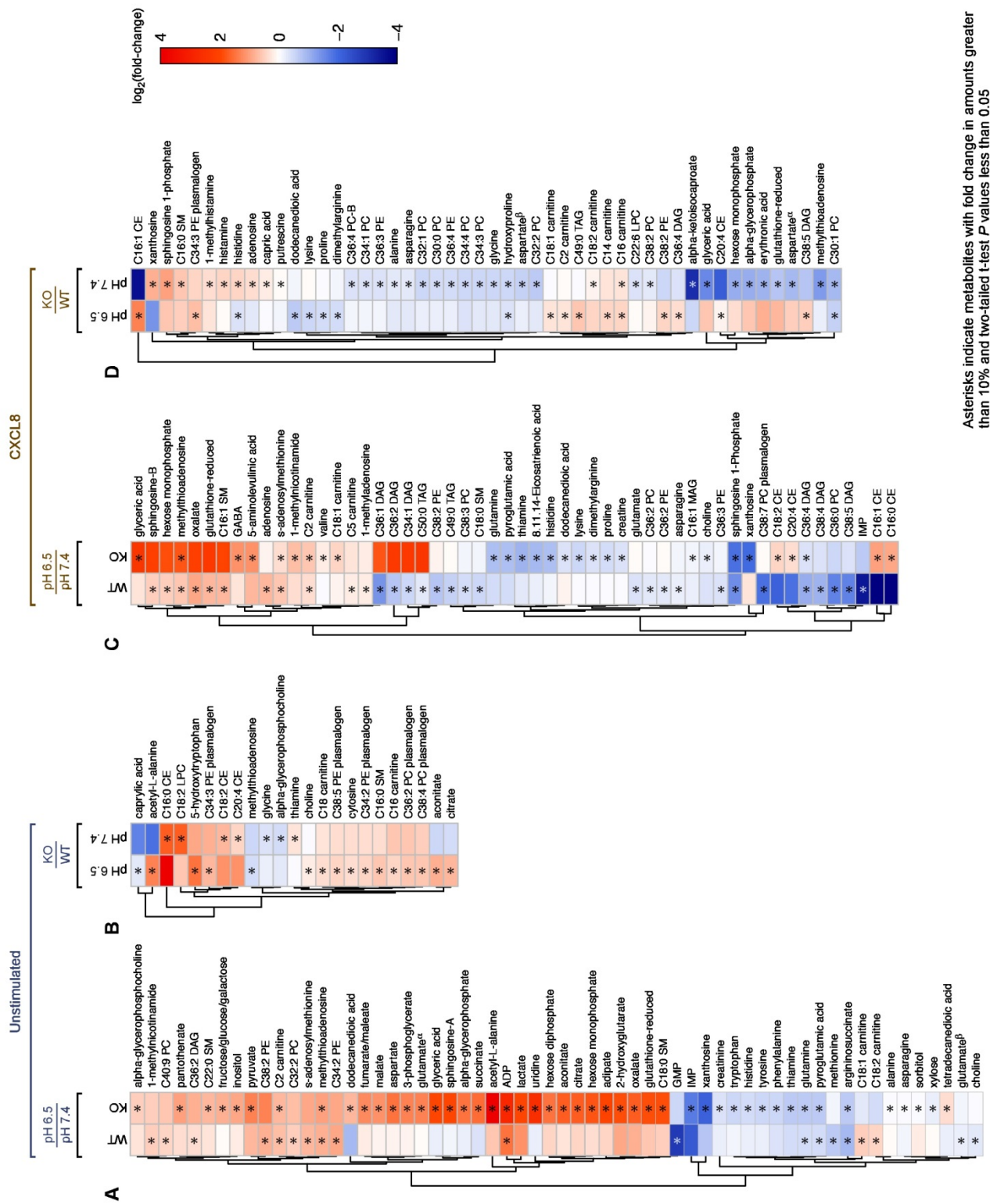
To investigate the role of GPR65 in this process we included *Gpr65*<sup>-/-</sup> neutrophils alongside WT controls. Quantities of numerous metabolites were altered in a GPR65-dependent manner (Figure 5).

Figure 4



**Figure 4. *Gpr65*<sup>-/-</sup> neutrophils exhibit a unique gene expression profile in acidic and stimulatory conditions.**

Neutrophils isolated from the bone marrow of WT (n = 4) and *Gpr65*<sup>-/-</sup> (n = 4) mice. (A) Expression of functional genes in WT and *Gpr65*<sup>-/-</sup> neutrophils at pH 6.5 compared to pH 7.4. Expression of functional genes at pH 6.5 or 7.4 in *Gpr65*<sup>-/-</sup> compared with WT when (B) unstimulated (baseline), (C) stimulated with CXCL8 or (D) stimulated with LPS. Benjamini-Hochberg q value < 0.05 for blue or red coloured data (independent t test). Grey indicates non-significance.



Asterisks indicate metabolites with fold change in amounts greater than 10% and two-tailed t-test *P* values less than 0.05

**Figure 5. WT and *Gpr65*<sup>-/-</sup> neutrophil lipid metabolism is differentially altered by extracellular acidity and CXCL8.**

WT or *Gpr65*<sup>-/-</sup> neutrophils were stimulated with CXCL8 at pH 6.5 or 7.4 and their polar and lipid metabolites were quantified by LC-MS. (A) Metabolite profile comparing fold change in unstimulated (no IL-8) WT or *Gpr65*<sup>-/-</sup> neutrophils between pH 6.5 or 7.4 . (B) Metabolite profile comparing fold change between unstimulated (no IL-8) WT and *Gpr65*<sup>-/-</sup> neutrophils at pH 6.5 or 7.4 . (C) Metabolite profile of CXCL8-stimulated WT or *Gpr65*<sup>-/-</sup> neutrophils comparing fold change between pH 6.5 or 7.4. (D) Metabolite profile comparing fold change between CXCL8-stimulated WT or *Gpr65*<sup>-/-</sup> neutrophils at pH 6.5 or 7.4. \*  $p < 0.05$  (independent t test).



These include a number of lipids associated with lipid remodelling and receptor signalling in neutrophil chemotaxis. Briefly, CXCL8-stimulated *Gpr65*<sup>-/-</sup> neutrophils exhibited decreased levels of PC (pH 7.4 and 6.5) and PE (pH 7.4) (Figure 5D). In contrast, CXCL8-stimulated *Gpr65*<sup>-/-</sup> neutrophils contained increased levels of sphingosine 1-phosphate (pH 7.4), fatty acyl carnitine (pH 7.4 and 6.5), PE (pH 6.5), DAG (pH 6.5) and triacylglycerol (TAG; pH 6.5) (Figure 5D). Taken together, these data demonstrate marked differences in lipid metabolism resulting from extracellular acidity and GPR65 activation in CXCL8 stimulated neutrophils. This suggests proton-sensing through GPR65 plays an important role in regulating intracellular metabolites, which thereby influences cell migration and inflammation.

## DISCUSSION

In the present study, we establish a role for GPR65 on leukocytes in colonic inflammation. GPR65 activation regulated neutrophil chemotaxis by altering chemokine receptor expression and lipid metabolism, which affected the recruitment of neutrophils into inflamed tissue in both colitis and arthritis. Furthermore, we showed that this process was partially dependent on NHE function and subsequent intracellular pH balance. This indicates that sensing of pH is an important mechanism for the regulation of leukocyte recruitment and inflammation.

NHE has been associated with G-protein subunits and GPCR agonists but has never been linked to activation of a specific GPCR<sup>233, 278</sup>. Here we identified a GPR65-dependent role for amiloride-sensitive ion channels in neutrophil chemotaxis. Interestingly, *Gpr65*<sup>-/-</sup> neutrophils at pH 6.5 but not 7.4 were resistant to an amiloride-related reduction in neutrophil chemotaxis. This suggests that secondary pH balancing mechanisms independent of NHE are at play. Such mechanisms could be induced by a plethora of other proton-activated GPCRs involved in regulating inflammation, including GPR4, GPR68 and GPR132<sup>279</sup>. Indeed, we observed a reduction in expression of GPR132 in *Gpr65*<sup>-/-</sup> neutrophils stimulated with CXCL8 at pH 6.5.

GPR65 regulated neutrophil chemotaxis in both acidic and neutral extracellular environments. Furthermore, we found that expression of CXCR1 and integrin  $\alpha 4$  were increased in *Gpr65*<sup>-/-</sup> neutrophils. Both molecules are important for neutrophil migration. Chemotaxis is induced by CXCL8 binding to its receptor CXCR1<sup>280</sup>. Similarly, adhesion molecules such as VLA-4 ( $\alpha 4\beta 1$  integrin) are expressed on murine neutrophils<sup>281</sup> and required for neutrophil chemotaxis and directed migration<sup>282</sup>. Inhibition of  $\alpha 4$  integrin with a small molecule antagonist reduces symptoms of DSS colitis in mice<sup>283</sup>. It is conceivable that some of this inhibition relates to  $\alpha 4$  integrin expression by neutrophils. It is also possible that the same phenomena we observed here for GPR65 function on neutrophils also holds for other GPR65-expressing leukocytes such as T cells. Moreover, the  $\alpha 4\beta 7$ -blocking antibody Vedolizumab shows promising efficacy for both ulcerative colitis and Crohn's disease in humans<sup>284</sup>. Our data suggests GPR65 regulates expression of CXCR1 and  $\alpha 4$  integrins on neutrophils and possibly other cells, which then reduces their migratory capacity and so serves to regulate inflammation.

Extracellular acidity markedly reduced the expression of NLRC4, integrin  $\alpha 4$  and integrin  $\alpha L$  in both WT and *Gpr65*<sup>-/-</sup> neutrophils. All of these molecules have been associated with neutrophil migration<sup>282, 285</sup>. NLRC4<sup>-/-</sup> mice infected with *Candida albicans* exhibit a marked reduction in neutrophil infiltration of the oral mucosa, suggesting NLRC4 is required for neutrophil chemotaxis to inflamed sites<sup>285</sup>. Similar to integrin  $\alpha 4$ , integrin  $\alpha L$  (CD11a; LFA-1) also plays an important role in neutrophil chemotaxis to CXCL8<sup>282</sup>. As such, extracellular acid-induced reduction in NLRC4, integrin  $\alpha 4$  and integrin  $\alpha L$  may abrogate neutrophil migration and provide new evidence as to why low extracellular pH can reduce chemotaxis. That  $\alpha L$  and  $\alpha 4$  integrins were down-regulated at low pH in a GPR65-independent manner suggests that other proton-sensing receptors such as GPR4, GPR68 and GPR132 may be involved. Indeed, GPR4 regulates tumour cell migration in murine melanoma and prostate cells<sup>286</sup>, suggesting GPR4 may play a similar role to GPR65 in chemotaxis.

PheWAS revealed a significant association between SNPs within the human *Gpr65* gene and IBD, as shown by others<sup>49, 50, 51</sup>. It may well be that the main proton sensing by GPR65 anywhere in the body is within the gut, as this is an environment that is normally acidic because of actions of the stomach,

or SCFA production from breakdown of fibre by commensal bacteria in the small and large intestine. Furthermore, *Gpr65* polymorphisms were associated with asthma and eczema, suggesting a role for GPR65 in pulmonary and cutaneous homeostasis. Indeed, the other animal model to date where GPR65 deficiency has shown a clear phenotype is in a murine OVA model of allergic airway inflammation<sup>263</sup>. As such, an acidic environment in the lung can enhance asthma pathogenesis. Thus the connection of both asthma and IBD to acidic conditions may explain why SNPs in human *Gpr65* associate with IBD and asthma, and why animal models for these conditions showed a clear phenotype in *Gpr65*<sup>-/-</sup> mice. Interestingly, acidic mammalian chitinase (AMCase) is induced via a Th2/ IL-13-mediated response in epithelial cells and macrophages and is expressed in large quantities in human asthma<sup>287</sup>. As such, GPR65 may play a role in AMCase regulation. Human *Gpr65* polymorphisms were not associated with arthritis although we identified exacerbation of inflammation and swelling in a murine model of arthritis. The KRN serum transfer model of arthritis skips the adaptive Th1 immune response required to cause arthritis, which may suggest GPR65 is not involved in this Th1 response. However, synovial biopsies from rheumatoid arthritis patients demonstrate distinct distribution of GPR4 and GPR68 expression throughout the tissue<sup>288</sup>. As such, other proton-sensing GPCRs may act redundantly in the absence of GPR65 to regulate inflammation during arthritis.

We show that GPR65 expression on both immune and epithelial cells is important for control of inflammation in the DSS colitis model. GPR65 agonists may therefore regulate inflammatory diseases by targeting multiple cell types, and thereby affect leukocyte chemotaxis, as shown here, as well as epithelial cell autophagy<sup>260</sup>. Allosteric agonists of GPR65 such as BTB09089<sup>289</sup> may be useful in regulating inflammation in environments of dysregulated pH.

The way in which extracellular pH alters neutrophil metabolism has been largely unknown. In the present study, we demonstrate a novel metabolic changes with both extracellular acidity, and GPR65 signalling, following stimulation with the chemokine CXCL8. Increased lipids following CXCL8 stimulation are likely required for membrane reorientation and increased energy expenditure during chemotaxis. Extracellular acidity dampened this increase in lipids, suggesting functional impedance of

neutrophils at low pH is accompanied by a catabolically weaker metabolism of lipids. GPR65 signalling reduced lipid metabolites at both acidic and neutral pH. Furthermore, the quantity of many specific lipids differed between WT and *Gpr65*<sup>-/-</sup> mice. Increased carnitine in *Gpr65*<sup>-/-</sup> neutrophils suggests GPR65 may reduce the reservoir of long-chain fatty acids for beta-oxidation and subsequent energy production. In addition, sphingomyelin and ceramide were increased in WT neutrophils when stimulated with CXCL8 at pH 7.4. Accumulation of sphingomyelin and ceramide upon CXCL8 stimulation suggests sphingomyelinase activity was enhanced to maintain orientation during chemotaxis. Increases in ceramide were not observed at pH 6.5, suggesting that acidity may inhibit CXCL8-induced enhancement of sphingomyelin metabolism. Compared to WT, *Gpr65*<sup>-/-</sup> neutrophils stimulated with CXCL8 at pH 7.4 exhibited increased levels of sphingomyelin but no change in ceramide. Exogenous treatment with sphingomyelin decreases the chemotaxis of neutrophils towards FMLP<sup>264</sup>. In contrast, we observed increased chemotactic indices in *Gpr65*<sup>-/-</sup> neutrophils at pH 7.4 despite increased levels of sphingomyelin. Confounding metabolic factors such as enhanced beta-oxidation may have enhanced *Gpr65*<sup>-/-</sup> neutrophil migration in spite of accumulated sphingomyelin. Furthermore, exogenous sphingomyelin may have different and as-yet unidentified effects on neutrophil chemotaxis than compared to when it is administered exogenously. *Gpr65*<sup>-/-</sup> neutrophils had decreased levels of PC compared to WT controls. This suggests that GPR65 enhances levels of PC, which may subsequently reduce neutrophil chemotaxis. However, human neutrophil chemotaxis is unaffected by PC (C24:0) *in vitro*<sup>264</sup>. In the present study, lipids of the PC class decreased in *Gpr65*<sup>-/-</sup> neutrophils were predominantly C30:1, which may alter chemotaxis differently to C24:0.

Metabolite profiling also demonstrated that PE in WT neutrophils was decreased by CXCL8 at pH 6.5 but increased at pH 7.4. Compared to WT controls, PE was higher in CXCL8-stimulated *Gpr65*<sup>-/-</sup> neutrophils at pH 6.5, but was lower at pH 7.4. Therefore, reduction in PE from stimulation with CXCL8 under acidic conditions was abrogated in *Gpr65*<sup>-/-</sup> neutrophils compared to WT controls. To our knowledge, this is the first time PE has been implicated in neutrophil chemotaxis. This data suggests that GPR65 activation at acidic pH reduces PE in response to CXCL8. Furthermore, an increase in PE following CXCL8 stimulation at pH 7.4 occurred in WT but not *Gpr65*<sup>-/-</sup> neutrophils.

We believe that PE metabolism is somehow involved in membrane remodelling during chemotaxis, a process which appears to be altered by extracellular acidity and regulated by GPR65. Particular species of PE differed across pH or stimulatory conditions, highlighting a complicated process for PE metabolism during neutrophil chemotaxis.

We observed that WT neutrophils stimulated with CXCL8 at pH 6.5 had decreased levels of DAG, compared to *Gpr65*<sup>-/-</sup> neutrophils. GPR65 signalling might somehow regulate DAG production, particularly in cells stimulated to migrate to chemoattractants. DAG has been observed to increase in activated neutrophils<sup>271</sup> and inhibition of DAG kinase enhances neutrophil chemotaxis<sup>290</sup>. GPR65 may regulate neutrophil chemotaxis at acidic pH by enhancing conversion of DAG to other metabolites such as phosphatidic acid via DAG kinase.

Furthermore, we observed that triacylglycerol (TAG, C49:0) was decreased by acidic pH 6.5 in WT neutrophils stimulated with CXCL8. However, TAG was increased in *Gpr65*<sup>-/-</sup> neutrophils compared to WT controls under the same conditions. This suggests that GPR65 activation reduces TAG in neutrophils, particularly those responding to a chemoattractant. The role of TAG in chemotaxis is unknown, though its quantity increases in neutrophils upon LPS stimulation<sup>291</sup>. Furthermore, human neutrophils stimulated with LPS convert palmitic acid, a common component of serum, into TAG<sup>292</sup>. We suggest that TAG production, like PC and PE, is involved in membrane re-modelling during chemotaxis under neutral pH, and this process is regulated by GPR65 when extracellular pH is reduced. The mechanism whereby GPR65 signalling regulates expression of PE, DAG or PC is unknown, though may be mediated downstream of G<sub>s</sub> mediated cAMP release from GPR65 activation<sup>293</sup>.

The data presented here demonstrates a novel role for proton-sensing receptor GPR65 in IBD and neutrophil chemotaxis. Furthermore, we show that acidity and GPR65 activation induce a plethora of gene expression and metabolic changes. This work highlights the role of proton-sensing in immune responses, and suggests that this pathway and possibly other proton-sensing GPCRs such as GPR4, GPR68 and GPR132 represent a means whereby pH can regulate inflammation.

## METHODS

### Mice

*Gpr65*<sup>-/-</sup> mice kindly gifted from Dr. Marcel Batten who previously purchased the strain from Jackson labs (stock number 008577). *Gpr65*<sup>-/-</sup> mice have 90% of an exon in GPR65 replaced with green fluorescent protein (GFP) to disrupt GPR65 function. GFP expression is driven by the *Gpr65* promoter. *Gpr65*<sup>+/+</sup> wild type controls were C57BL/6 mice obtained from the Monash Animal Research Platform, Monash University. All mice were maintained under specific pathogen free and controlled environmental conditions. Mice received AIN93G diet purchased from Specialty Feeds for at least 3 weeks prior to and during experiments. All mice were humanely culled by CO<sub>2</sub> asphyxiation. All procedures were approved by the Animal Ethics Committee of Monash University.

### DSS Colitis

Mice from 7 to 9 weeks old were provided with 2% DSS added to the drinking water for 7 days *ad libitum*. A minimum of *n*=6 mice per group were used. Mice were monitored daily. Diarrhoeal severity was determined by combining fecal consistency and fecal blood scores. Fecal consistency ranging from 0 to 4 was assessed as follows: 0, no sign of disease; 1, soft feces but intact shape 2, feces soft and shape deformed 3, feces somewhat liquid ; 4, entirely liquid feces, diarrhoea. The faecal blood score ranging from 0 to 4 was assessed as follows: 0, no sign of disease; 1, normal feces colour and faint positive haemoccult test; 2, feces turning dark and positive haemoccult test; 3, feces visibly red and positive haemoccult test; 4, visible liquid blood in feces and positive haemoccult test. Mice were humanely culled at day 7 following DSS treatment to harvest colon tissue. Assessment of colon histology scoring was conducted blindly on paraffin-embedded colon section stained with haematoxylin and eosin . Scores ranged from 0 to 6 by adding: 1. the tissue damage scoring (0, no mucosal damage; 1, lymphoepithelial lesions; 2, surface mucosal erosion and 3, extensive mucosal damage, extension into deeper structure) and 2. inflammatory cell infiltration scoring (0, occasional cell infiltrate; 1, increased number of infiltrating cells; 2, confluency of inflammatory cells extending

to the submucosa and 3, transmural extension of the inflammatory cells). Colon length was measured after 7 days of treatment with DSS.

### **Food Allergy**

Murine peanut allergy was induced as previously described<sup>62</sup>. Briefly, peanut allergen was extracted from raw peanuts by manual crushing and removal of lipids followed by dialysis and filtering. This provided a peanut extract (PE) to induce allergy. Mice were sensitized by intragastric gavage of 1 mg PE with 10 µg of cholera toxin (List Biologicals) in 200 µl of PBS on days 0 and 7. This was followed by a booster challenge with 10 mg PE on day 21, without cholera toxin. Mice were challenged with 1 mg PE intraperitoneally on day 28 and symptoms of clinical anaphylaxis monitored for 40–60 min: 0, no clinical symptoms; 1, repetitive mouth/ear scratching and ear canal digging with hind legs; 2, decreased activity, self-isolation, and puffiness around eyes and/or mouth; 3, periods of motionless for more than 1 min, lying prone on stomach, and decreased activity with increased respiratory rate; 4, no response to whisker stimuli and reduced or no response to prodding; 5, tremor, convulsion, and death.

### **Arthritis**

KRN serum was collected from 8w old KRN mice. Arthritis was induced by i.p. injection of 150µl KRN serum on days 0 and 2. Clinical severity of arthritis was scored every day for all 4 paws on a scale from 0 to 3 and assessed as follows: 0, normal; 1, erythema, swelling limited to individual digits or mild ankle swelling insufficient to reverse the normal V shape of the foot; 2, swelling sufficient to make the ankle and midfoot approximate in thickness to the forefoot; 3, reversal of the normal V shape of the foot, swelling of the entire paw including multiple digits. Score represented as accumulative of all 4 paws. Ankle and wrist thickness was recorded each day with a micrometer. Severity of inflammation in ankles sections stained with H&E were assessed by histology and scored as follows: 0, no infiltration; 1, mild infiltration on dorsal or plantar side, 2, mild inflammation on both sides; 3 severe inflammation on one side; 4 severe inflammation on both sides.

### **Bone Marrow (BM) chimeras**

To generate 50:50 BM chimeras, 6 week old female recipient WT or *Gpr65*<sup>-/-</sup> mice were subject to 2 doses of 450 rads to deplete bone marrow. Recipient mice were injected i.v with 10<sup>7</sup> donor WT and *Gpr65*<sup>-/-</sup> bone marrow cells in a 50:50 ratio 6 hours post-radiation. BM reconstitution for 8 weeks was followed by flow cytometry of blood leukocytes to verify success of reconstitution.

### **Cell isolation**

Cells were isolated from spleen and lymph nodes by mechanical disruption and washed through a 70µm filter. Cells isolated from spleen were subject to red blood cell lysis. Isolation of colonic leukocytes began by washing and incubating colon pieces with HBSS containing 5mM EDTA and 5% fetal calf serum (FCS) to remove epithelium. This was followed by digestion with Collagenase type IV (GIBCO), DNase I (Roche) and 10% FCS for 90min before being washed through a 70µm filter. Colonic leukocytes were enriched by 40% Percoll (GE Healthcare).

### **Flow cytometry**

10<sup>6</sup> cells per sample were stained with anti-mouse Ly6g PE (EL4J, 561104, BD Biosciences) in 2% FCS. Neutrophils identified as Ly6g<sup>+</sup>. All flow cytometry was conducted on an LSR II flow cytometer (BD), and flow cytometry data was analysed with FlowJo (FlowJo, LLC).

### **Chemotaxis**

Neutrophils were isolated from bone marrow as previously described<sup>294</sup>. Briefly, bone marrow was subject to red blood cell lysis and filtered. Neutrophils were purified by gradient density centrifugation. Neutrophils were resuspended in complete media with at pH 7.4 or 6.5. 3 x 10<sup>5</sup> neutrophils were added to the top wells of a transwell plate (Corning). The bottom wells contained complete media with 0, 0.3nM, 1nM or 3nM recombinant CXCL8 (574202, BioLegend). Cells were incubated at 37°C for 1.5 hours. Neutrophils in the bottom wells were quantified by flow cytometry (BD LSRII).

### **Genetic Profiling**



Neutrophils were isolated from the bone marrow as described above for neutrophil chemotaxis.  $3 \times 10^5$  neutrophils per sample were cultured in complete media at either pH 7.4 or pH 6.5. Neutrophils were either left unstimulated or stimulated with 3nM CXCL8 (574202, BioLegend) or 1 ng/ml LPS (Sigma Aldrich) for 1.5hr at 37°C. Following incubation, RNA was purified using RNeasy micro kit with DNase treatment (Qiagen) and reverse-transcribed to cDNA using Vilo cDNA master kit (Applied Biosystem). Pre-amplification was performed for 14 cycles with a pool of 96 TaqMan gene expression assays (final 0.2X of each) listed in Supplementary Table 1. Pre-amplified cDNA was then diluted 1:5 with dH<sub>2</sub>O and analysed in duplicate for RT-PCR using the 96x96 dynamic array (Fluidigm Corporation) according to the manufacturer's instructions. Data generated on the Fluidigm platform was imported into GeneData Expressionist software. The NormFinder algorithm, a method to identify good housekeeping gene(s) for RT-PCR experiments that ranks the set of candidate genes according to their expression stability in a given sample set and given experimental design was used<sup>232</sup>. Out of 10 endogenous genes, *B2M*, *GNB2L1*, *RPL13A* and *GAPDH* that met the stability criterion of  $< 0.25$  were selected as the normalizer genes for  $\Delta C_t$  calculations.  $\Delta C_t$ s were computed for all 96 genes using an average of the 4 normalizer genes. Relative fold changes were calculated using  $2^{(-\Delta\Delta C_t)}$ . T-Tests were performed for the relevant comparisons, and Benjamini-Hochberg q value of 0.05 was used as cut-off for significance.

### **Metabolite profiling by LC-MS**

Metabolite profiling was performed on lysed bone marrow derived-neutrophils (wild-type and *Gpr65*<sup>-/-</sup>), exposed to extracellular pH of 6.5 or 7.4, and stimulated with CXCL8 as described above. Four separate liquid chromatography tandem mass spectrometry (LC-MS) methods were used to measure polar metabolites and lipids in each sample. Specifically, two separate hydrophilic interaction liquid chromatography (HILIC) methods were used to measure polar small-molecule metabolites in positive and negative ionization modes; two reversed phase methods were used to profile lipids in positive and negative ion modes. Data for all methods were acquired using a Q Exactive hybrid quadrupole orbitrap mass spectrometer (Thermo Fisher Scientific; Waltham, MA). Conditions for the analysis

were set using a panel of routinely analyzed standards, in three separate replicates. Further details regarding each method can be found in Supplementary Text.

### **Identifying metabolites associated with GPR65 deletion**

Prior to feature comparisons across metabolome samples, all samples were set to have equal total intensity (total intensity normalization). Metabolites with mean fold change greater than 10% and t-test-based *P*-values less than 0.05 were considered to be different between two phenotypes.

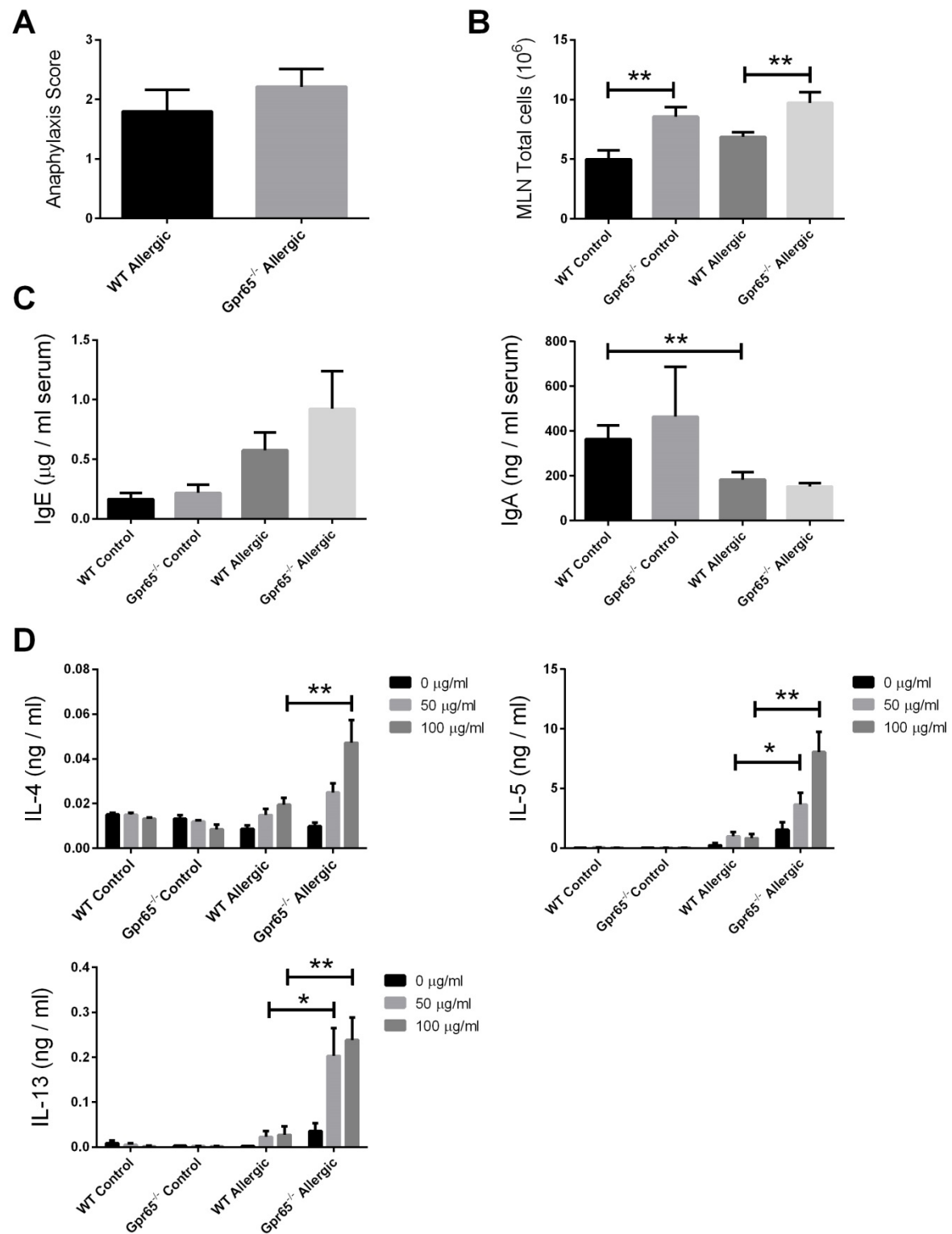
### **Statistics**

All graphical data are presented as mean  $\pm$  standard error of the mean (SEM). A two-tailed Student's independent t test was used to determine the statistical significance between groups. *p* values  $< 0.05$  were considered statistically significant.

### **Phenome-wide association studies of GPR65 SNP rs8005161**

Phenome-wide association study (PheWAS) was conducted in the 23andMe participant cohort from 647,776 subjects of European ancestry with link to genotyped arrays. A total of 1229 phenotypes collected within 23andMe's data were included for exploration (Supplementary Figure 5 and Table 1). Phenotype data are derived from responses to self-reported questionnaires. The association of rs8005161 with each phenotype was evaluated using a likelihood ratio test comparing the full model against null model with or without genotype adjusted for age, gender and PCs to correct for population stratification. Binary phenotypes were analyzed using logistic regression, quantitative phenotypes were analyzed using linear regression and survival phenotypes were analyzed using Cox proportional hazard regression. We assume additive allelic effects. False Discovery Rate (FDR) for each phenotype was calculated using the Benjamini-Hochberg procedure.

## SUPPLEMENTARY FIGURES

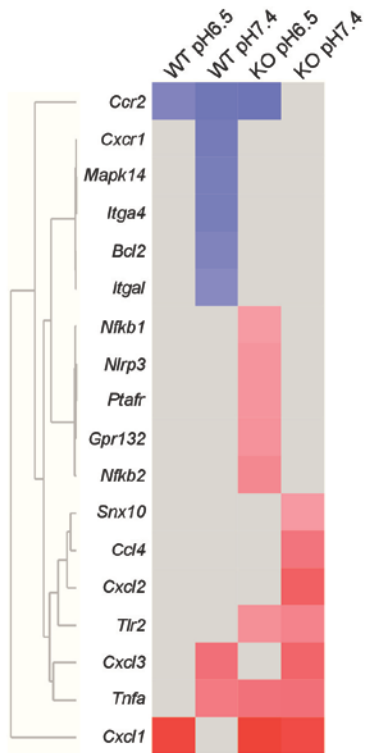


**Supplementary Figure 1. Anaphylaxis and serum IgE is unchanged in allergic Gpr65<sup>-/-</sup> mice despite increases Th2 cytokine release.**

WT and Gpr65<sup>-/-</sup> mice were subject to a murine model of peanut allergy and challenged with peanut allergen (n = 7). (A) Anaphylaxis scores indicate severity of anaphylaxis, including scratching, motionlessness and reduced whisker stimulus. (B) Total lymphocyte cell counts from the mesenteric lymph node. (C) Total serum IgE and IgA determined by ELISA. (D) Th2 cytokine release from lymphocytes of the mesenteric lymph node stimulated with peanut allergen. Data are mean + SEM (n = 7). Significance represented by \*p < 0.05, \*\*p < 0.01, Students t test.

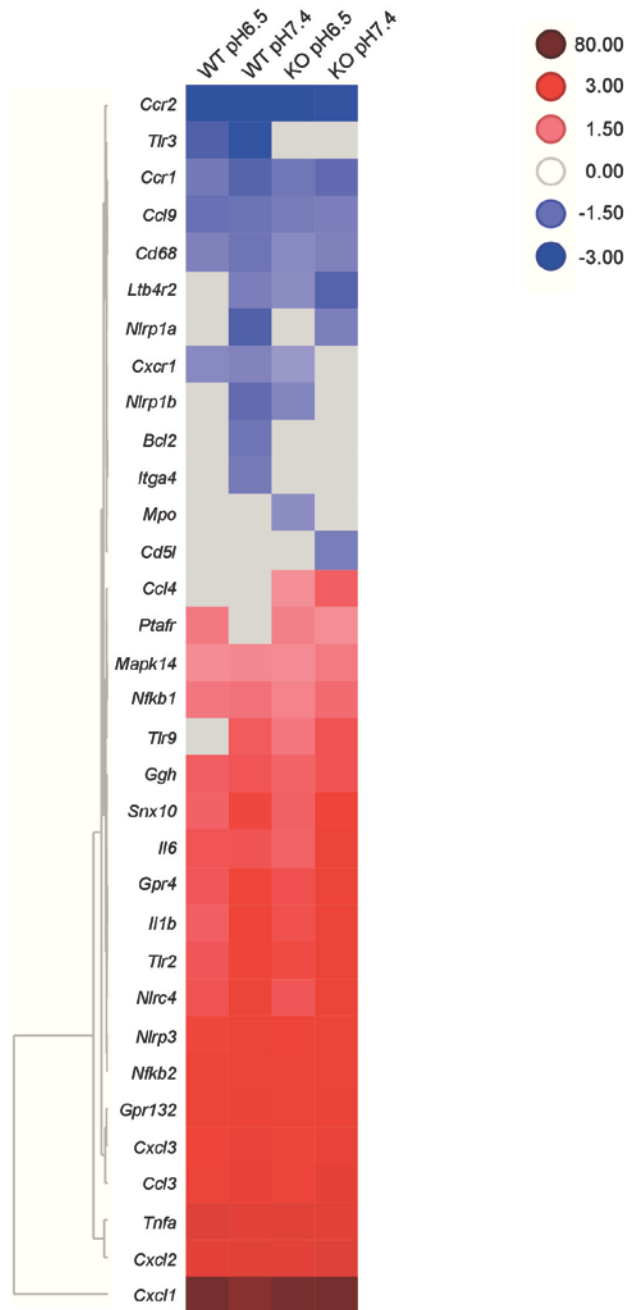
A

CXCL8 vs. baseline



B

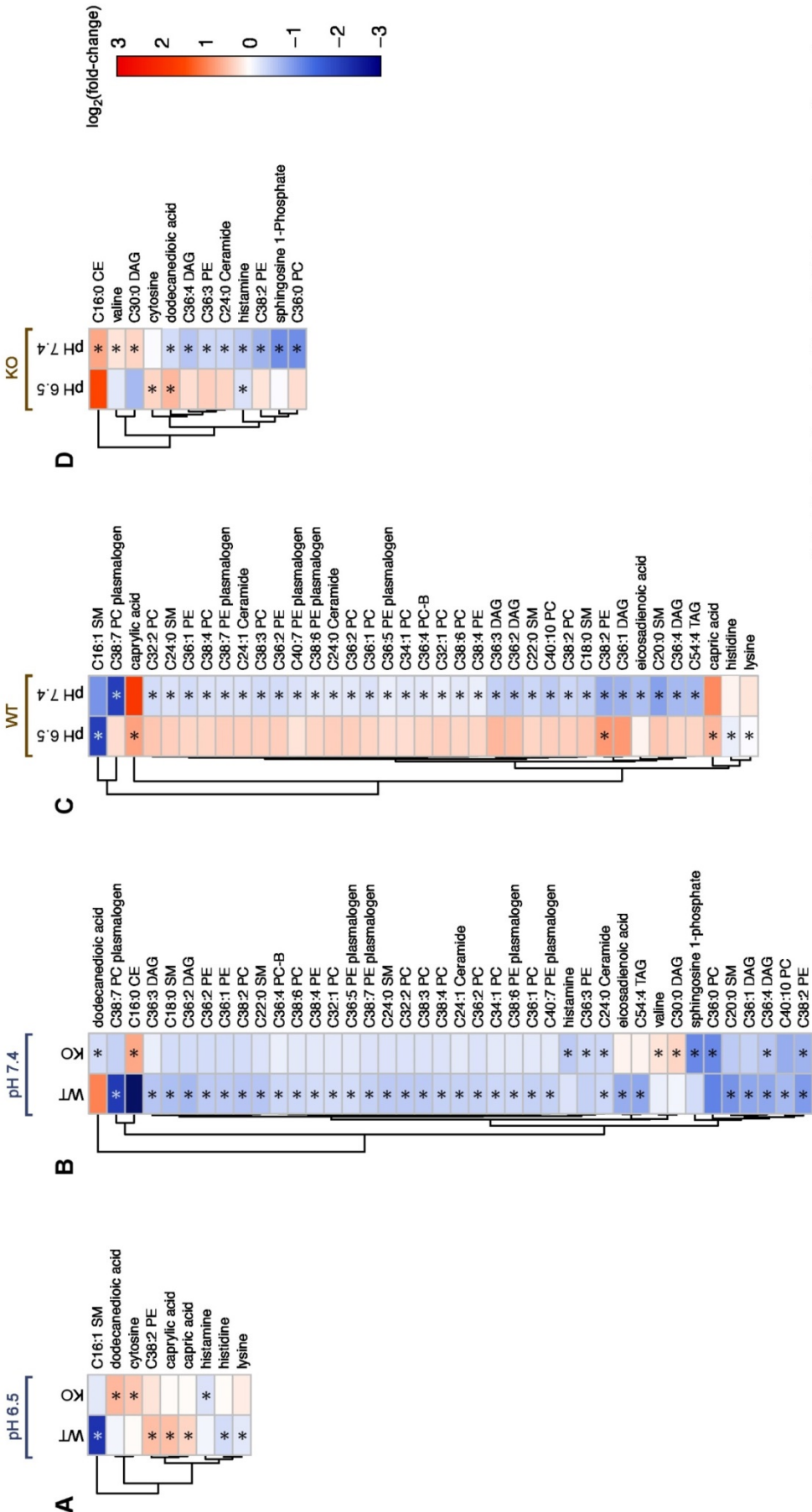
LPS vs. baseline



**Supplementary Figure 3. Gene expression profile of WT and *Gpr65*<sup>-/-</sup> neutrophils compared between unstimulated conditions and CXCL8 or LPS stimulation.**

Neutrophils isolated from the bone marrow of WT and *Gpr65*<sup>-/-</sup> (n = 4/group) mice. Expression of functional genes in WT and *Gpr65*<sup>-/-</sup> neutrophils at pH 6.5 or pH 7.4 comparing (A) CXCL8 stimulation vs. baseline unstimulated and (B) LPS vs. baseline unstimulated. Benjamini-Hochberg q value < 0.05 for blue or red coloured data (independent t test). For all coloured data p < 0.05 (independent t test). Grey indicates non-significance.

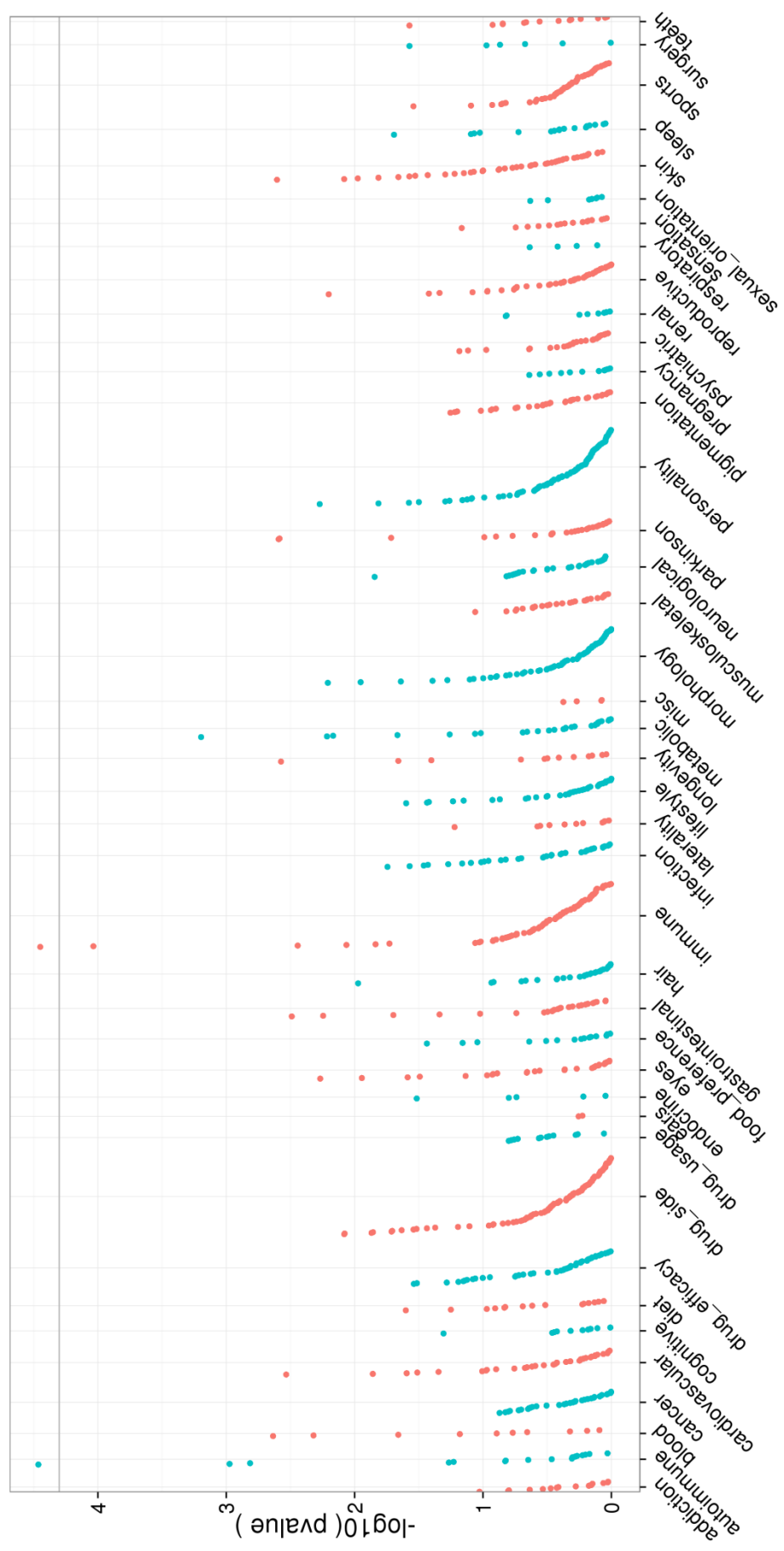
Comparisons of unstimulated vs. CXCL8 stimulation



**Supplementary Figure 4. Fold change of metabolites in WT or *Gpr65*<sup>-/-</sup> neutrophils comparing baseline with IL-8 stimulation.**

WT or *Gpr65*<sup>-/-</sup> neutrophils were stimulated with CXCL8 at pH 6.5 or 7.4 and their polar and lipid metabolites were quantified by LC-MS. All heat maps present fold change between unstimulated and CXCL8-stimulated neutrophils, displaying metabolite profile of WT or *Gpr65*<sup>-/-</sup> neutrophils at (A) pH 6.5 and (B) pH 7.4, or metabolite profile of (C) WT or (D) *Gpr65*<sup>-/-</sup> neutrophils at pH 6.5 or 7.4 . \* p < 0.05 (independent t test).





### **Supplementary Figure 5. PheWAS P value Plot**

Pvalue Plot depicting the distribution of association test statistics versus phenotypes arranged by their broad phenotypic categories along the X-axis. Y-axis represents log-scaled P values. Positions with  $P < 5e-5$  (a score of about 4.3) are shown in grey, which is a threshold for significance after controlling for the Family-Wise-Error-Rate (FWER) using Bonferroni correction. The vertical scale is adjusted nonlinearly (log scaled) to preserve detail for signals near the genome-wide threshold.

**Supplementary Table 1. Statistical associations between Gpr65 SNP rs8005161 and autoimmune or allergic diseases.**

Table indicating the p value of the associations between Gpr65 SNP rs8005161 and phenotypes of autoimmune and allergic diseases. P values determined using logistic regression.

Phenotype	p value	Phenotype	p value	Phenotype	p value
alopecia_areata	0.150369	dog_allergy	0.6657058	oats_allergy	0.15737
any_autoimmune	0.5952431	dog_allergy_clean	0.4211927	oats_allergy_clean	0.1193122
celiac	0.05903139	dust_mites_allergy	0.2953104	other_animal_allergy	0.8522349
crohns	0.00153317	dust_mites_allergy_clean	0.6803744	other_food_allergy	0.7580902
crohns_or_ulcerative_colitis	3.44E-05	dust_mites_allergy_metal	0.7115236	other_plant_allergy	0.09597478
iqb.celiac_w_biopsy	0.1487688	eczema	9.22E-05	peanut_allergy	0.2295837
iqb.gluten_intolerance	0.2250675	eggs_allergy	0.4545543	peanut_allergy_broad	0.2449947
iqb.psoriatic_arthritis	0.5397814	eggs_allergy_clean	0.2876964	peanut_allergy_clean	0.2088838
iqb.took_meds_anti_tnf_alpha	0.3427546	fish_allergy	0.8561484	penicillin_allergy	0.3264403
juvenile_t1d	0.523308	fish_allergy_clean	0.9045205	penicillin_allergy_clean	0.4786755
lupus	0.4976089	grasses_allergy	0.2912462	poison_oak	0.552843
multiple_sclerosis	0.05422546	grasses_allergy_clean	0.5641528	pollen_allergy	0.3142504
pediatric_ibd	0.6745161	hayfever_all	0.09354898	pollen_allergy_clean	0.745938

psoriasis	0.492895	hayfever_meta	0.27014 4	pollen_allergy_meta	0.735644
rheumatoid_arthritis	0.932782 5	honeybee_allergy	0.15081 98	red_ants_allergy	0.315536
t1d	0.627120 5	honeybee_allergy_clea n	0.24511 3	red_ants_allergy_clea n	0.397621 1
ulcerative_colitis	0.001060 553	insect_allergy	0.37884 1	rhinitis	0.991996 6
vitiligo	0.494308 2	iqb.allergic_to_jewelry	0.62432 27	rhinitis_eczema	0.003601 111
any_allergy	0.548480 9	iqb.mosquito_bite_size	0.17927 53	seasonal_allergies_br oad	0.513749 6
any_animal_allergy	0.758936 4	iqb.mosquito_bites_itch ing	0.75766	severe_asthma	0.400710 6
any_asthma	3.55E-05	iqb.peanut_allergy_chil d	0.74227 64	shellfish_allergy	0.584596 7
any_asthma_eczema	0.141239 7	iqb.poison_oak	0.29769 81	shellfish_allergy_clea n	0.382404 9
any_asthma_eczema_r hinitis	0.014545 68	iqb.sun_allergy	0.96085 42	soy_allergy	0.679724
any_asthma_rhinitis	0.566758 6	iqb.took_meds_asthma _or_lung	0.01866 666	soy_allergy_clean	0.706079 3
any_drug_allergy	0.167533 6	juvenile_asthma	0.00862 925	sulfa_drug_allergy	0.614536 9
any_food_allergy	0.330150 4	latex_allergy	0.53194 75	sulfa_drug_allergy_cl ean	0.366509 8
any_immune	0.120414 1	latex_allergy_clean	0.76293 33	tree_nuts_allergy	0.572901 3
any_plant_allergy	0.307857 2	metal_allergy	0.75787 63	tree_nuts_allergy_cle an	0.686416 1

aspirin_allergy	0.512424 4	milk_allergy	0.40122 17	trees_allergy	0.273232
aspirin_allergy_clean	0.441048	milk_allergy_clean	0.51291 98	trees_allergy_clean	0.485427
asthma_severity	0.710615 4	mold_allergy	0.42065 54	wasp_allergy	0.183047 5
cat_allergy	0.276096 1	mold_allergy_clean	0.58836 27	wasp_allergy_clean	0.309335 8
cat_allergy_clean	0.369423 5	mosquito_bit_more	0.12646 16	weeds_allergy	0.239661 3
cat_allergy_meta	0.414197 9	mosquito_combined	0.77414 11	weeds_allergy_clean	0.443651 8
chicken_allergy	0.285521	mosquito_severe	0.86778 86	wheat_allergy	0.859544 1
chicken_allergy_clean	0.235207 5	mycin_drug_allergy	0.08691 829	wheat_allergy_clean	0.685887 3
chronic_hives	0.595528 4	mycin_drug_allergy_clean	0.18308 31	yellow_jackets_allergy	0.250554
current_asthma	0.162813 3	no_allergies	0.14173 25	yellow_jackets_allergy_clean	0.364134 7

## SUPPLEMENTARY TEXT

### LC-MS metabolite profiling

*Method 1 – Positive ion mode MS analysis of polar metabolites.* Hydrophilic interaction liquid chromatography (HILIC) analysis of water-soluble metabolites in the positive ionization mode were carried out by extracting 10  $\mu$ l homogenate using 90  $\mu$ l of 74.9:24.9:0.2 vol/vol/vol acetonitrile/methanol/formic acid containing stable isotope-labeled internal standards (valine-d8, Isotec; and phenylalanine-d8, Cambridge Isotope Laboratories; Andover, MA). The samples were centrifuged (10 min, 9000 $\times$ g, 4°C), and the supernatants (10  $\mu$ l) were injected directly onto a 150  $\times$  2 mm Atlantis HILIC column (Waters; Milford, MA). The column was eluted isocratically at a flow rate of 250  $\mu$ l/min with 5% mobile phase A (10 mM ammonium formate and 0.1% formic acid in water) for 1 min followed by a linear gradient to 40% mobile phase B (acetonitrile with 0.1% formic acid) over 10 min. The electrospray ionization voltage was 3.5 kV and data were acquired using full scan analysis over m/z 70–800 at 70,000 resolution and a 3 Hz data acquisition rate.

*Method 2 – Negative ion mode MS analysis of polar metabolites.* Negative ionization mode analysis of polar metabolites was achieved using a HILIC method under basic conditions. Briefly, 30  $\mu$ l homogenate was extracted using 120  $\mu$ l of 80% methanol containing inosine-15N4, thymine-d4, and glycocholate-d4 internal standards (Cambridge Isotope Laboratories; Andover, MA). The samples were centrifuged (10 min, 9000 $\times$ g, 4°C) and the supernatants (10  $\mu$ l) were injected directly onto a 150  $\times$  2.0 mm Luna NH2 column (Phenomenex; Torrance, CA) that was eluted at a flow rate of 400  $\mu$ l/min with initial conditions of 10% mobile phase A (20 mM ammonium acetate and 20 mM ammonium hydroxide in water) and 90% mobile phase B (10 mM ammonium hydroxide in 75:25 vol/vol acetonitrile/methanol) followed by a 10 min linear gradient to 100% mobile phase A. MS full scan data were acquired over m/z 70–800. The ionization source voltage is –3.0 kV and the source temperature is 325°C.

*Method 3 – Negative ion mode analysis of metabolites of intermediate polarity (e.g. bile acids and free fatty acids).* Lipids were extracted from lysates (10 µl) using 90 µl of methanol containing PGE<sub>2</sub>-d<sub>4</sub> as an internal standard (Cayman Chemical Co., Ann Arbor, MI, USA) and centrifuged (10 min, 10,000 x g, 4°C). The supernatants (2µl) were injected onto a 150 x 2.1 mm ACQUITY UPLC BEH C18 column (Waters; Milford, MA, USA). The column was eluted isocratically at a flow rate: 450 µL/min with 20% mobile phase A (0.01% formic acid in water) for 3 min followed by a linear gradient to 100% mobile phase B (acetonitrile with 0.01% formic acid) over 12 min. MS analyses were carried out using electrospray ionization in the negative ion mode using full scan analysis over  $m/z$  70- 850 at 70,000 resolution and 3 Hz data acquisition rate. Additional MS settings were: ion spray voltage, 3.5 kV; capillary temperature, 320°C; probe heater temperature, 300°C; sheath gas, 45; auxiliary gas, 10; and S-lens RF level 60.

*Method 4 – Polar and nonpolar lipids.* Lipids were extracted from lysates (10 µl) using 190 µl of isopropanol containing 1-dodecanoyl-2-tridecanoyl-sn-glycero-3-phosphocholine as an internal standard (Avanti Polar Lipids; Alabaster, AL). After centrifugation (10 min, 9,000 x g, ambient temperature), supernatants (10 µl) were injected directly onto a 100 x 2.1 mm ACQUITY BEH C8 column (1.7 µm; Waters; Milford, MA). The column was eluted at a flow rate of 450 µL/min isocratically for 1 minute at 80% mobile phase A (95:5:0.1 vol/vol/vol 10 mM ammonium acetate/methanol/acetic acid), followed by a linear gradient to 80% mobile-phase B (99.9:0.1 vol/vol methanol/acetic acid) over 2 minutes, a linear gradient to 100% mobile phase B over 7 minutes, and then 3 minutes at 100% mobile-phase B. MS analyses were carried out using electrospray ionization in the positive ion mode using full scan analysis over  $m/z$  200-1100 at 70,000 resolution and 3 Hz data acquisition rate. Additional MS settings were: ion spray voltage, 3.0 kV; capillary temperature, 300°C; probe heater temperature, 300 °C; sheath gas, 50; auxiliary gas, 15; and S-lens RF level 60.

All raw data were processed using Progenesis CoMet software (version 2.0, NonLinear Dynamics) for feature alignment, signal detection, and signal integration. Targeted processing of a subset of known

metabolites metabolites was conducted using TraceFinder software (Thermo Fisher Scientific; Waltham, MA). Signal peak areas were converted into numerical intensity values and normalized to internal standards added to each sample, and to total signal of each sample.



## **Chapter 4 – The Role of Dietary MCFAs and GPR84 in Allergy and Inflammation**

### **1. Introduction**

Mice fed MCFA emulsions during the induction of peanut allergy developed an exacerbated allergic response associated with increased allergen absorption into Peyer's patches<sup>81</sup>. However, the involvement of GPR84 in such a process remains unknown. Furthermore, our broader understanding of MCFAs and GPR84 signalling in immune responses remains in its infancy despite clear patterns of *Gpr84* expression on immune cells<sup>78, 79, 80</sup>. The following chapter presents data investigating the influence of MCFA-enriched diets on disease outcomes in mice deficient in GPR84, establishing a novel role for both in asthma and inflammation. The methodology of murine disease models and experimental procedures in this chapter is identical to those displayed in Chapters 2 and 3 and Appendix 1 and 2.

### **2. GPR84 signalling is not involved in food allergy**

To investigate the role of GPR84 in food allergy, we fed WT or *Gpr84*<sup>-/-</sup> mice a MCFA-enriched diet containing 1.5% coconut oil prior to and during a model of peanut allergy. Coconut oil diet increased weight gain throughout the model in both WT and *Gpr84*<sup>-/-</sup> mice (Figure 4.1A). This is consistent with reports of increased weight gain in pre-term infants fed MCFAs<sup>295</sup> but contrasts with conflicting reports of weight loss in adults<sup>296</sup>. This may reflect the physiology of specific-pathogen free mice that have been shown to mimic the physiology of the human neonate more than the human adult<sup>297</sup>. Allergic *Gpr84*<sup>-/-</sup> mice exhibited no differences in anaphylaxis scores when challenged with peanut i.p (Figure 4.1B). Furthermore, GPR84 deficiency had no impact on the number of Tregs (CD4+ Foxp3+) or DCs (CD11c+ MHCII+) in the mesenteric lymph node (Figure 4.1B), the primary site of antigen presentation required to promote allergy or maintain oral tolerance<sup>159</sup>. Serum IgE trended

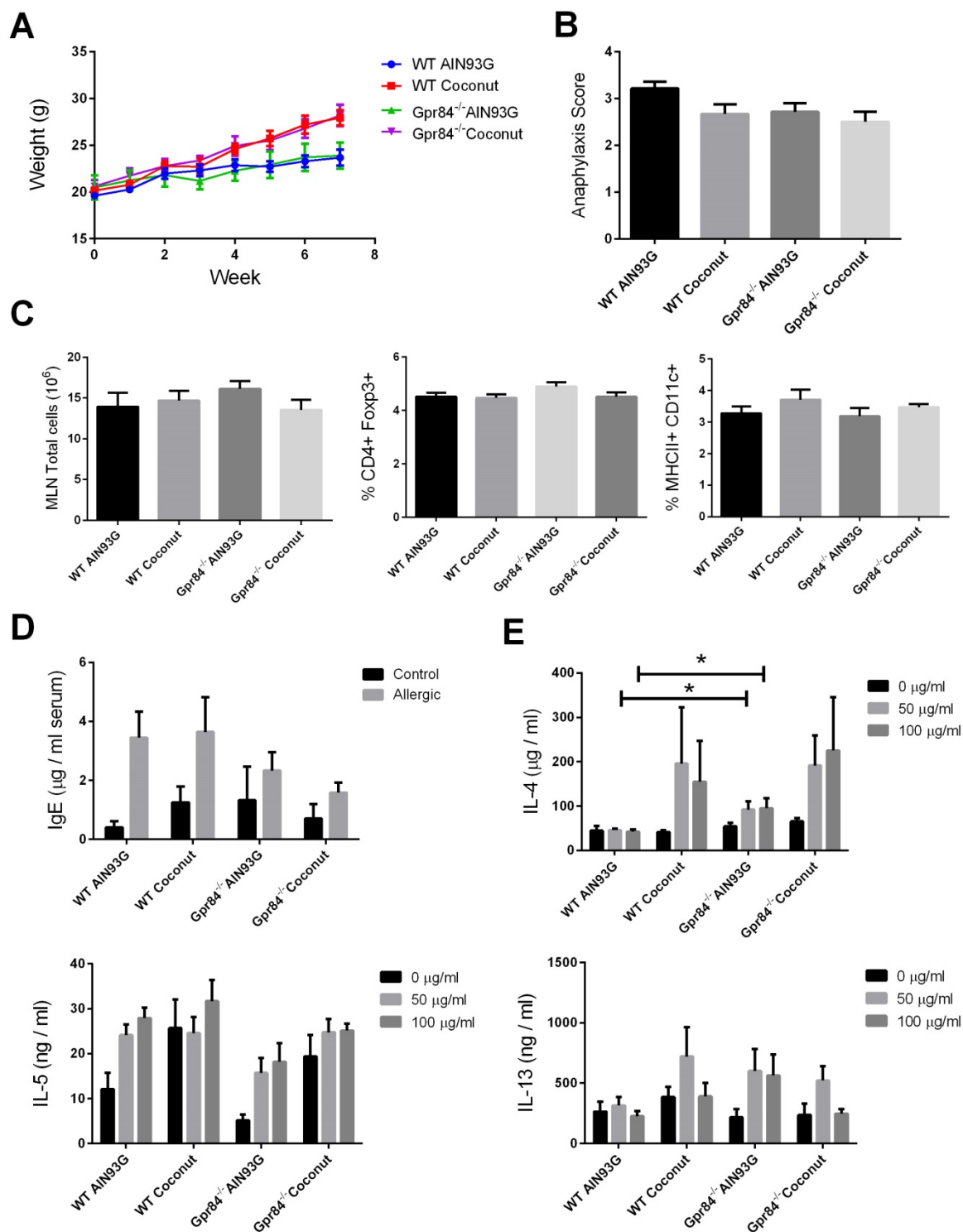
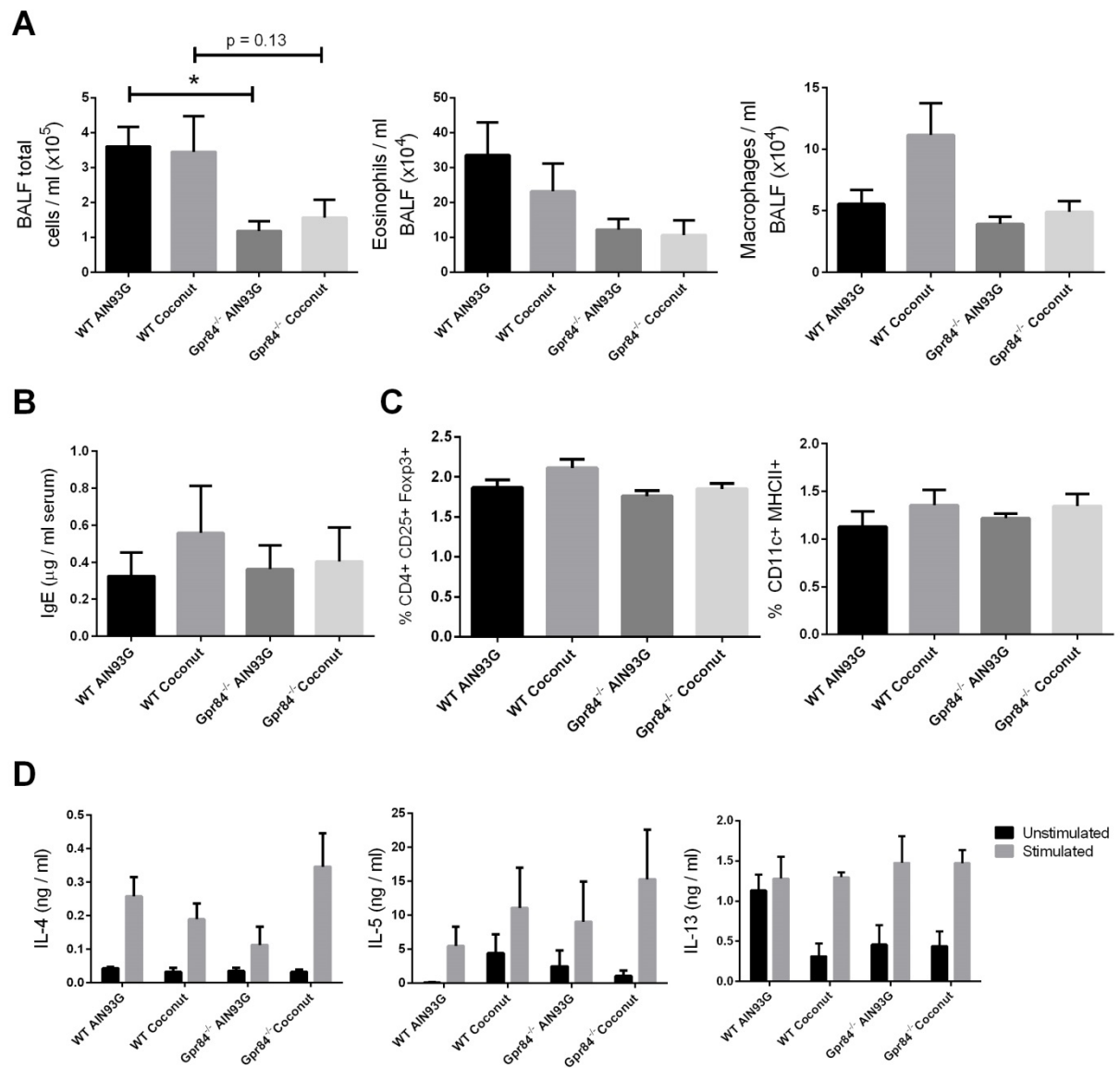


**Figure 4.1. A murine model of food allergy is not altered by MCFA-enriched diet or GPR84 deficiency.** (A) Weight of WT and *Gpr84*<sup>-/-</sup> mice fed control AIN93G or MCFA-enriched Coconut oil diet. (B) Anaphylaxis score of allergic WT or *Gpr84*<sup>-/-</sup> mice fed AIN93G or Coconut oil diet 3 weeks prior to and during a murine model of peanut allergy. (C) Percentage of Tregs (CD4<sup>+</sup> Foxp3<sup>+</sup>) and DCs (MHCII<sup>+</sup> CD11c<sup>+</sup>) from the mesenteric lymph node of allergic mice. (D) Total serum IgE of allergic mice. (E) Th2 cytokine production from lymphocytes of the mesenteric lymph node stimulated with peanut allergen. Data are means + SEM (n = 6). Significance represented by \*p < 0.05, Students t test.

lower in allergic *Gpr84*<sup>-/-</sup> mice but was not significant (Figure 4.1C). T cells from allergic *Gpr84*<sup>-/-</sup> mice fed AIN93G diet exhibited increased IL-4 release compared to WT controls (Figure 4.1D). However, IL-4 release was similar compared to WT when mice were fed coconut diet. Furthermore, coconut oil diet exhibited a trend towards increased IL-4 in WT and *Gpr84*<sup>-/-</sup> mice. This corresponds with the results of a prior study which demonstrates that dietary MCFAs increases IL-4 release from T cells in allergic mice<sup>81</sup>. Coconut oil diet and GPR84 deficiency did not impact upon IL-5 or IL-13 production. Despite minor changes in IL-4 release in *Gpr84*<sup>-/-</sup> T cells, GPR84 did not impact upon anaphylaxis or quantity of immune cells in the mesenteric lymph node which suggests that GPR84 is not involved in the pathogenesis of food allergy.

### **3. GPR84 enhances asthma pathogenesis**

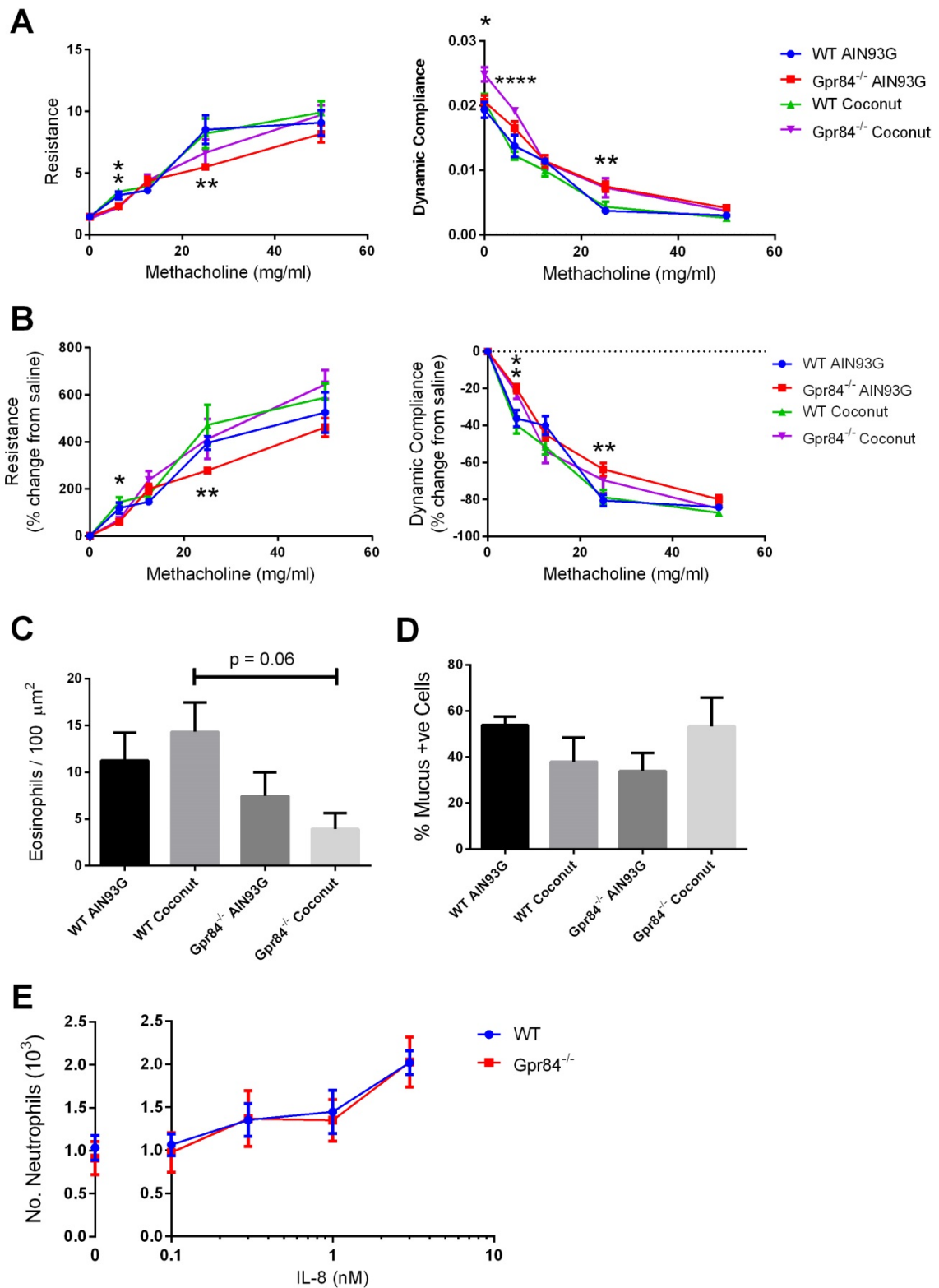
*Gpr84* is expressed in the lung but has no known role in its development or homeostasis<sup>77</sup>. Given the high expression of *Gpr84* on bone marrow, we aimed to investigate the role of GPR84 in an immunologically altered lung environment<sup>77</sup>. As such, we assessed asthma pathogenesis in WT and *Gpr84*<sup>-/-</sup> mice. Furthermore, to investigate the role of dietary MCFAs in this process, we fed mice AIN93G or Coconut oil diet for 3 weeks prior to and during a murine model of asthma. Infiltration of leukocytes into the bronchioles was decreased in *Gpr84*<sup>-/-</sup> mice (Figure 4.2A). This suggests that GPR84 signalling regulates the migration of inflammatory cells into the asthmatic lung, either by acting directly on leukocyte chemotaxis or by adaptive immune responses that drive recruitment. Although the lung epithelium is also important in recruiting inflammatory cells in asthma<sup>209</sup>, the lack of *Gpr84* expression in this compartment suggests it is not involved. The reduction in total BALF cells in *Gpr84*<sup>-/-</sup> mice was particularly associated with reduced infiltration of eosinophils, regardless of diet. Contrastingly, macrophage infiltration trended upwards in WT mice fed Coconut oil diet, but not in *Gpr84*<sup>-/-</sup> mice. As such, GPR84 signalling may play a role in the effect of dietary MCFAs on macrophage migration. However, we cannot be confident of such a result as it was not significant. During asthma pathogenesis, eosinophils infiltrate the lung by Th2-driven adaptive immune responses<sup>298</sup>.



**Figure 4.2. Cellular infiltration of the BALF is reduced in asthmatic *Gpr84*<sup>-/-</sup> mice without altering Th2 responses.** (A) Cellular infiltration of the BALF in asthmatic WT or *Gpr84*<sup>-/-</sup> mice fed control AIN93G or MCFA-enriched Coconut oil diet 3 weeks prior to and during the HDM model of murine asthma. (B) Total serum IgE in asthmatic mice. (C) Percentage of Tregs (CD4<sup>+</sup> CD25<sup>+</sup> Foxp3<sup>+</sup>) and DCs (CD11c<sup>+</sup> MHCII<sup>+</sup>) in the mediastinal lymph node of asthmatic mice. (D) Th2 cytokine production from lymphocytes of the mediastinal lymph node stimulated with HDM allergen. Data are means + SEM (n = 6).

To investigate the adaptive immune system in asthmatic *Gpr84*<sup>-/-</sup> mice, we quantified total IgE in the serum of asthmatic mice. IgE was unaffected by GPR84 deficiency or MCFA-enriched Coconut oil diet (Figure 4.2B). Furthermore, we quantified the adaptive immune cell subsets in the mediastinal lymph node, the primary location for allergen presentation<sup>299</sup>. Total cell numbers in the mediastinal lymph nodes were unchanged by diet or GPR84 deficiency (DNS). The percentage of Tregs (CD4+ CD25+ Foxp3+) and DCs (CD11c+ MHCII+) were unchanged by either strain or diet (Figure 4.2C). Moreover, the production of the canonical Th2 cytokines IL-4, IL-5 and IL-13 were also unchanged between *Gpr84*<sup>-/-</sup> mice and WT controls (Figure 4.2D). Taken together, these data suggest that the adaptive immune response is not altered by GPR84 signalling or by dietary MCFAs.

Despite no alteration to an adaptive immune response during asthma, reduced cellular infiltration of the BALF in asthmatic *Gpr84*<sup>-/-</sup> mice suggests that the clinical severity of asthma may still be reduced. To further investigate the impact of GPR84 deficiency on the clinical severity of asthma, we assessed the lung function of asthmatic WT or *Gpr84*<sup>-/-</sup> mice in response to increasing doses of methacholine. Coconut oil diet did not significantly alter lung function (Figure 4.3A). However, GPR84 deficiency protected against asthma-induced reduction in lung function as *Gpr84*<sup>-/-</sup> mice exhibited increased resistance and decreased dynamic compliance (Figure 4.3A, B). This suggests that GPR84 signalling contributes to reduced lung function in asthma, possibly through factors such as mucus production<sup>300</sup>. To determine the impact of GPR84 on the lung tissue of asthmatic mice, we quantified infiltrating eosinophils and mucus positive goblet cells by histology. Eosinophil infiltration exhibited a strong decreased trend in *Gpr84*<sup>-/-</sup> mice (Figure 4.3C). This corroborates our findings of decreased cellular infiltration of the BALF in *Gpr84*<sup>-/-</sup> mice, and further suggests that GPR84 signalling is involved in exacerbating this process. However, there was no difference in the percentage of mucus positive goblet cells in either strain or from either diet (Figure 4.3D). As such, the protective effect of GPR84 deficiency in maintaining lung function may involve reduced local inflammation from abrogated leukocyte chemotaxis to the lung, independent of mucus production in the airway. To investigate the chemotaxis of *Gpr84*<sup>-/-</sup> leukocytes, we conducted a chemotaxis assay on WT and *Gpr84*<sup>-/-</sup> neutrophils



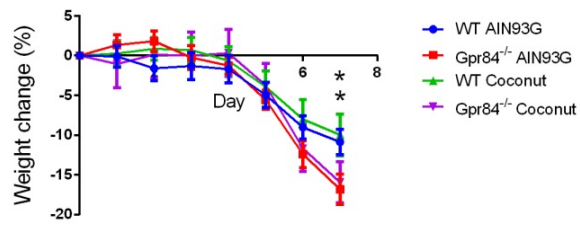
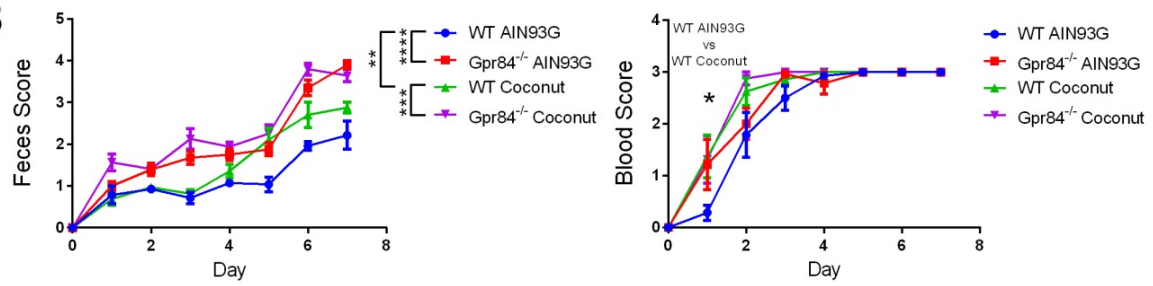
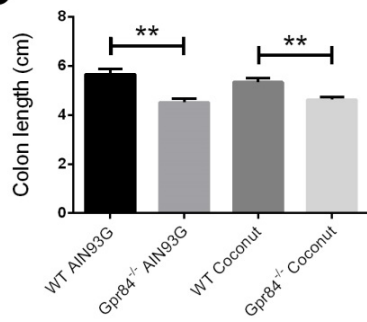
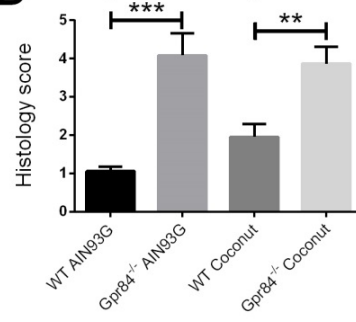
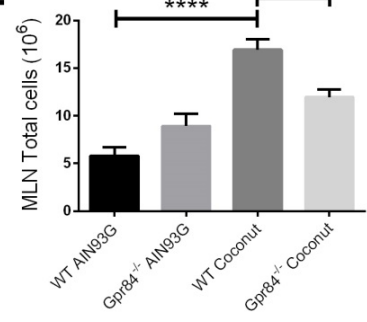
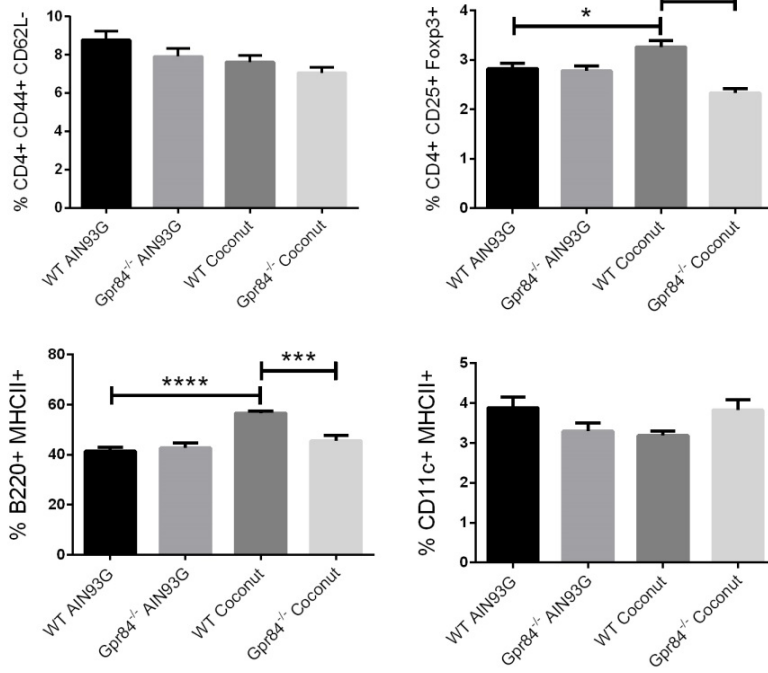


**Figure 4.3. *Gpr84*<sup>-/-</sup> mice are protected from asthmatic reductions in lung function.** Asthmatic WT or *Gpr84*<sup>-/-</sup> mice were fed control AIN93G or MCFA-enriched Coconut oil diet for 3 weeks prior to and during the HDM model of murine asthma (n = 5). (A) Raw and (B) percentage change in resistance and dynamic of asthmatic mice in response to increasing doses of methacholine. (C) Number of infiltrating eosinophils in asthmatic lung tissue determined by histology with H&E staining. (D) Percentage of mucus positive goblet cells in the lung tissue of asthmatic mice determined by histology with PAS staining. (E) WT or *Gpr84*<sup>-/-</sup> neutrophil chemotaxis assay to IL-8 (n = 4). Data are means ± SEM. Significance represented by \*p < 0.05, \*\*p < 0.01, \*\*\*\*p < 0.0001, Students t test.

exposed to the chemokine IL-8. We found that GPR84 deficiency had no impact on neutrophil chemotaxis (Figure 4.3E). Taken together, these data suggest that cellular infiltration into the asthmatic lung is increased by GPR84 signalling which correlates with an exacerbated deterioration in lung function. However, it remains unclear why cellular infiltration and lung function are altered by GPR84. We hypothesise that GPR84 signalling may enhance eosinophil chemotaxis without impacting upon neutrophil chemotaxis, or perhaps act as a metabolic sensor and maintain eosinophil viability like GPR65<sup>263</sup>. Indeed, a GPR84 antagonist GLPG1205 has been demonstrated to inhibit macrophage and neutrophil chemotaxis<sup>301</sup>, which suggests GPR84 signalling is involved in leukocyte migration. Furthermore, Coconut oil diet did not impact upon the allergic Th2 response in asthma. As such, MCFA-enriched diet may not impact upon peripheral allergic responses. However, perhaps a higher concentration of MCFAs may yield a stronger immunomodulatory effect, and in future experiments a worthwhile study would be to use higher amounts of coconut oil.

#### **4. GPR84 protects against murine colitis**

Recently, the potent GPR84 antagonist GLPG1205 was shown to protect against DSS colitis in mice and was determined to be tolerated in healthy human subjects<sup>301</sup>. This suggests GPR84 inhibition may play a potential role in treating IBD. We hypothesised that *Gpr84*<sup>-/-</sup> mice would be protected from DSS colitis in a similar manner to mice treated with GLPG1205. Furthermore, the impact of MCFA-enriched diet on colitis is unknown, and may activate GPR84 with opposite effects to GLPG1205. To investigate the role of GPR84 and MCFA-enriched diet in colitis, we treated WT or *Gpr84*<sup>-/-</sup> mice with AIN93G or Coconut oil diet for 3 weeks prior to and during the DSS colitis model. *Gpr84*<sup>-/-</sup> mice exhibited increased weight loss, exacerbated diarrhoea and bloodier feces compared to WT controls (Figure 4.4A, B). Moreover, the colons of colitic *Gpr84*<sup>-/-</sup> mice were shorter than WT controls (Figure 4.4C). This suggests that GPR84 protects against clinical symptoms of DSS colitis, delaying the onset of diarrhoea, fecal blood and the colonic dehydration responsible for reducing colon length.

**A****B****C****D****E****F**

**Figure 4.4. *Gpr84*<sup>-/-</sup> mice are susceptible to DSS colitis.** WT or *Gpr84*<sup>-/-</sup> mice were fed control AIN93G or MCFA-enriched coconut oil diet for 3 weeks prior to and during a DSS model of colitis. (A) Percentage weight change. (B) Feces score indicating diarrhoeal severity and blood score indicating quantity of blood in the feces. (C) Colon length of colitic mice. (D) Histological score of H&E stained colon sections indicating cellular infiltration and epithelial damage. (E) Total cell count in the mesenteric lymph. (F) Percentage of effector T cells (CD4<sup>+</sup> CD44<sup>+</sup> CD62L<sup>-</sup>), Tregs (CD4<sup>+</sup> CD25<sup>+</sup> Foxp3<sup>+</sup>), B cells (B220<sup>+</sup> MHCII<sup>+</sup>) and DCs (CD11c<sup>+</sup> MHCII<sup>+</sup>) in the mesenteric lymph node. Data are means  $\pm$  SEM (n = 8). Significance represented by \*p < 0.05, \*\*p < 0.01, \*\*\* p < 0.001, \*\*\*\* p < 0.0001, Students t test.

Paradoxically, Coconut oil diet increased diarrhoeal severity from day 5 and fecal blood at day 1 of the DSS colitis model (Figure 4.4B). MCFA-enriched diet may therefore exacerbate clinical severity of DSS colitis. Indeed, the method by which DSS can induce colitic inflammation has been demonstrated to involve binding to MCFAs and subsequently forming harmful nano-lipocomplexes that trigger inflammation<sup>302</sup>. As such, MCFA-enriched diet may exacerbate DSS colitis by increasing the formation of these nano-lipocomplexes and subsequently triggering more inflammation. This is of particular interest to experimental methodology surrounding diets and murine DSS colitis. One should seriously consider the presence of MCFAs in diets provided to colitic mice before interpreting the severity of disease as MCFAs may enhance the onset of disease.

To further investigate the impact of GPR84 deficiency on the inflammatory response in colitis, we assessed leukocyte infiltration and epithelial damage by histology of the colon. Leukocyte infiltration is a hallmark of inflammation and epithelial damage indicates a breakdown in epithelial integrity. Histological scoring was increased in *Gpr84*<sup>-/-</sup> mice regardless of diet (Figure 4.4D). Furthermore, Coconut oil diet also exacerbated histological scoring in WT mice. Leukocyte infiltration and epithelial damage therefore corresponded with clinical severity of disease, suggesting that GPR84 deficiency and MCFA-enriched diet can exacerbate inflammation and reduce epithelial integrity with distinct clinical outcomes.

To further assess the profile of immune cells in colitic *Gpr84*<sup>-/-</sup> mice, we characterised the immune cells of the mesenteric lymph node, the major compartment for presentation of translocating bacterial antigens during colitis<sup>303</sup>. Coconut diet exacerbated the total number of immune cells in the mesenteric lymph nodes of WT mice (Figure 4.4E). However, Coconut oil diet did not change these numbers in *Gpr84*<sup>-/-</sup> mice. This suggests MCFA-enriched diet enhances the proliferative or chemotactic response of lymphocytes during colitis with dependence on GPR84 signalling. Given that this effect was not seen during food allergy suggests that this may be an alteration of Th1 responses to bacterial antigen, rather than Th2 responses to food allergens. However, the percentage of effector T cells (CD4<sup>+</sup> CD44<sup>+</sup> CD62L<sup>-</sup>) or DCs (CD11c<sup>+</sup> MHCII<sup>+</sup>) were unchanged, whereas Coconut oil diet increased the proportion of Tregs (CD4<sup>+</sup> CD25<sup>+</sup> Foxp3<sup>+</sup>) and B cells (B220<sup>+</sup> MHCII<sup>+</sup>) in WT mice

only. This suggests MCFA-diets may increase Tregs and B cells in the mesenteric lymph node in a GPR84-dependent manner. However, the magnitude of the change is quite small when compared to the large increase in total immune cells of the mesenteric lymph node. As such, the predominant change to the immune cell profile of the mesenteric lymph node from MCFA-enriched diet and GPR84 activation appears to be broadly proliferative or migratory, rather than specifically enhancing one particular cell type over another. This increase in lymphocyte proliferation or migration may have been stimulated by nano-lipocomplexes generated from the contact of MCFAs and DSS. However, regardless of the effect of nano-lipocomplexes, GPR84 signalling increased the number of cells in the mesenteric lymph node despite protecting against the clinical severity of colitis. This suggests that lymphocytes may also require GPR84 signalling during migration in a similar manner to eosinophils observed in asthma.

## 5. Discussion

I have identified a role for GPR84 signalling in the migration of leukocytes into the lung mucosa during asthma, correlating with a reduction in lung function. GPR84 signalling therefore exacerbates asthma pathogenesis. GPR84 agonists enhance PMN chemotaxis<sup>78</sup>, suggesting that the deletion of GPR84 function in *Gpr84*<sup>-/-</sup> mice may similarly reduce the propensity for leukocyte chemotaxis to the lung during asthma. In contrast, GPR84 deficiency exacerbated the clinical severity of DSS colitis, including worsened weight loss, diarrhoea, faecal blood and shortened colon length. This suggests GPR84 signalling protects against colitis pathogenesis. The differences between exacerbation of asthma and protection from colitis highlight the complex role that GPR84 plays in immune and gut homeostasis. These differences may be explained by the separate mucosal compartments (lung vs. gut) and immune responses (innate and Th1 vs. Th2) involved in asthma and colitis. As yet unknown factors involved in the pathogenesis of either disease likely alter the severity of these diseases in *Gpr84*<sup>-/-</sup> mice.

The exacerbation of colitis in *Gpr84*<sup>-/-</sup> mice was unexpected due to the opposite result in WT mice treated with GLPG1205, a GPR84 inhibitor. However, recently GLPG1205 was found to be

ineffective at treating human patients with ulcerative colitis, which may suggest that investigating GPR84 function in the murine model of DSS colitis does not translate well to humans.

In mice, GPR84 deficiency alters lipid metabolism by increasing myocardial triglyceride accumulation and decreasing liver size<sup>304</sup>. GPR84 therefore plays a poorly understood role in metabolism. This altered metabolism via GPR84 signalling may favour a regulatory phenotype during colonic inflammation in WT mice, although no data has yet established such a link between myocardial triglyceride accumulation and colitis.

These results are particularly compounded by our finding that MCFA-enriched diet can exacerbate the clinical severity of colitis in WT mice, implicating the dietary agonists of GPR84 in the alteration of disease outcomes in this particular murine model of IBD. We therefore caution the use of diets that contain MCFAs when conducting DSS colitis. T cell transfer models of colitis that do not involve DSS would therefore be a preferable alternative when investigating dietary MCFAs and their impact on IBD.

## Chapter 5 – Conclusion

This thesis has defined novel roles for GPR43, GPR65, GPR84 and their agonists in murine models of inflammatory and allergic diseases. These receptors and their agonists enhance regulatory mechanisms or reduce inflammatory responses, which together prevent the clinical severity of immune-based diseases such as asthma and colitis. As such, I have characterised their importance in maintaining homeostasis at mucosal sites of the lung and gut.

SCFAs derived from fermented dietary fibre protected against asthma by enhancing Treg responses in an epigenetically inheritable manner. This process was independent of GPR43 signalling, which contrasts with the partial GPR43-dependence required for dietary acetate to protect against *C. rodentium* infection. Indeed, acetate and butyrate inhibited *C. rodentium* growth and *Tir* expression *in vitro*, independent of host responses to SCFAs. Furthermore, I have characterised the regulatory role of GPR65 in protecting against bacteria- and chemically-induced colitis. Neutrophil biology was significantly altered by extracellular pH and GPR65 activation. GPR65 regulated neutrophil migration, lipid metabolism and integrin expression. This provides a novel explanation for the increased incidence of IBD in humans with polymorphisms in *Gpr65*. In addition, I have demonstrated a novel role for GPR84 in asthma and colitis. GPR84 activation exacerbated cellular infiltration into the asthmatic lung and reduced lung function. Contrastingly, GPR84 protected against the clinical symptoms of DSS colitis which correlated with reduced leukocyte migration to the colon and enhanced epithelial integrity. Moreover, MCFA-enriched coconut oil diet enhanced the severity of DSS colitis, highlighting the need to consider MCFAs in the diets of mice subject to such a model of IBD.

Broadly, acid or acidic metabolite agonists of GPCRs appear to consistently play a role in regulating immune responses and maintaining homeostasis at mucosal sites. The regulation of immune responses exhibited by GPR43, GPR65 and GPR84 corresponds with similar responses from other acidic metabolite-sensors such as GPR41, GPR109a and GPR120. Many other acid- and metabolite-sensing GPCRs that have poorly characterised functions will likely play similar roles. Ultimately, my doctoral



studies have identified potential therapeutic consequences of dietary or pharmacological activation and inhibition of GPR43, GPR65 and GPR84, which provides new avenues for treating allergic or inflammatory diseases such as asthma and IBD.

## References

1. Julia V, Macia L, Dombrowicz D. The impact of diet on asthma and allergic diseases. *Nat Rev Immunol* 2015, **15**(5): 308-322.
2. Jacka FN, Cherbuin N, Anstey KJ, Sachdev P, Butterworth P. Western diet is associated with a smaller hippocampus: a longitudinal investigation. *BMC Medicine* 2015, **13**(1): 215.
3. Manzel A, Muller DN, Hafler DA, Erdman SE, Linker RA, Kleinewietfeld M. Role of "Western Diet" in Inflammatory Autoimmune Diseases. *Current allergy and asthma reports* 2013, **14**(1): 404.
4. Protudjer JLP, Sevenhuysen GP, Ramsey CD, Kozyrskyj AL, Becker AB. Low vegetable intake is associated with allergic asthma and moderate-to-severe airway hyperresponsiveness. *Pediatric pulmonology* 2012, **47**(12): 1159-1169.
5. Hou JK, Abraham B, El-Serag H. Dietary Intake and Risk of Developing Inflammatory Bowel Disease: A Systematic Review of the Literature. *Am J Gastroenterol* 2011, **106**(4): 563-573.
6. Okada H, Kuhn C, Feillet H, Bach JF. The 'hygiene hypothesis' for autoimmune and allergic diseases: an update. *Clinical and experimental immunology* 2010, **160**(1): 1-9.
7. Strachan DP. Family size, infection and atopy: the first decade of the "hygiene hypothesis". *Thorax* 2000, **55 Suppl 1**: S2-10.
8. Maslowski KM, Mackay CR. Diet, gut microbiota and immune responses. *Nat Immunol* 2011, **12**(1): 5-9.
9. Popkin BM, Adair LS, Ng SW. Global nutrition transition and the pandemic of obesity in developing countries. *Nutr Rev* 2012, **70**(1): 3-21.
10. Lumeng CN, Saltiel AR. Inflammatory links between obesity and metabolic disease. *The Journal of clinical investigation* 2011, **121**(6): 2111-2117.
11. Hotamisligil GS. Inflammation and metabolic disorders. *Nature* 2006, **444**(7121): 860-867.
12. Ellwood P, Asher MI, Björkstén B, Burr M, Pearce N, Robertson CF. Diet and asthma, allergic rhinoconjunctivitis and atopic eczema symptom prevalence: an ecological analysis of the International Study of Asthma and Allergies in Childhood (ISAAC) data. *European Respiratory Journal* 2001, **17**(3): 436-443.

13. Grimshaw KEC, Maskell J, Oliver EM, Morris RCG, Foote KD, Mills ENC, *et al.* Diet and food allergy development during infancy: Birth cohort study findings using prospective food diary data. *Journal of Allergy and Clinical Immunology* 2014, **133**(2): 511-519.
14. Frei R, Lauener RP, Cramer R, O'Mahony L. Microbiota and dietary interactions – an update to the hygiene hypothesis? *Allergy* 2012, **67**(4): 451-461.
15. Maslowski KM, Vieira AT, Ng A, Kranich J, Sierro F, Yu D, *et al.* Regulation of inflammatory responses by gut microbiota and chemoattractant receptor GPR43. *Nature* 2009, **461**(7268): 1282-1286.
16. Trompette A, Gollwitzer ES, Yadava K, Sichelstiel AK, Sprenger N, Ngom-Bru C, *et al.* Gut microbiota metabolism of dietary fiber influences allergic airway disease and hematopoiesis. *Nature medicine* 2014, **20**(2): 159-166.
17. Park Y, Subar AF, Hollenbeck A, Schatzkin A. Dietary fiber intake and mortality in the nih-aarp diet and health study. *Archives of internal medicine* 2011, **171**(12): 1061-1068.
18. Pituch-Zdanowska A, Banaszkiwicz A, Albrecht P. The role of dietary fibre in inflammatory bowel disease. *Przegląd Gastroenterologiczny* 2015, **10**(3): 135-141.
19. Bach AC, Babayan VK. Medium-chain triglycerides: an update. *The American Journal of Clinical Nutrition* 1982, **36**(5): 950-962.
20. Guillon F, Champ M. Structural and physical properties of dietary fibres, and consequences of processing on human physiology. *Food Research International* 2000, **33**(3–4): 233-245.
21. Wong JMW, de Souza RRD, Kendall CWCP, Emam AM, Jenkins DJAMD. Colonic Health: Fermentation and Short Chain Fatty Acids. *Journal of Clinical Gastroenterology* 2006, **40**(3): 235-243.
22. Macfarlane S, Macfarlane GT. Regulation of short-chain fatty acid production. *Proc Nutr Soc* 2003, **62**(1): 67-72.
23. Cummings JH, Macfarlane GT. Role of intestinal bacteria in nutrient metabolism. *JPEN J Parenter Enteral Nutr* 1997, **21**(6): 357-365.
24. Topping DL, Clifton PM. Short-chain fatty acids and human colonic function: roles of resistant starch and nonstarch polysaccharides. *Physiol Rev* 2001, **81**(3): 1031-1064.
25. Macia L, Thorburn AN, Binge LC, Marino E, Rogers KE, Maslowski KM, *et al.* Microbial influences on epithelial integrity and immune function as a basis for inflammatory diseases. *Immunological reviews* 2012, **245**(1): 164-176.

26. Roediger WE. Role of anaerobic bacteria in the metabolic welfare of the colonic mucosa in man. *Gut* 1980, **21**(9): 793-798.
27. Donohoe DR, Garge N, Zhang X, Sun W, O'Connell TM, Bunger MK, *et al.* The Microbiome and Butyrate Regulate Energy Metabolism and Autophagy in the Mammalian Colon. *Cell metabolism* 2011, **13**(5): 517-526.
28. Cummings JH, Pomare EW, Branch WJ, Naylor CP, Macfarlane GT. Short chain fatty acids in human large intestine, portal, hepatic and venous blood. *Gut* 1987, **28**(10): 1221-1227.
29. Hijova E, Chmelarova A. Short chain fatty acids and colonic health. *Bratislavské lekarske listy* 2007, **108**(8): 354-358.
30. Babayan VK. Medium-chain triglycerides—their composition, preparation, and application. *J Am Oil Chem Soc* 1968, **45**(1): 23-25.
31. Greenberger NJ, Rodgers JB, Isselbacher KJ. Absorption of medium and long chain triglycerides: factors influencing their hydrolysis and transport. *The Journal of clinical investigation* 1966, **45**(2): 217-227.
32. Swift LL, Hill JO, Peters JC, Greene HL. Medium-chain fatty acids: evidence for incorporation into chylomicron triglycerides in humans. *The American Journal of Clinical Nutrition* 1990, **52**(5): 834-836.
33. DeLany JP, Windhauser MM, Champagne CM, Bray GA. Differential oxidation of individual dietary fatty acids in humans. *Am J Clin Nutr* 2000, **72**(4): 905-911.
34. Jensen C, Buist NR, Wilson T. Absorption of individual fatty acids from long chain or medium chain triglycerides in very small infants. *The American Journal of Clinical Nutrition* 1986, **43**(5): 745-751.
35. Rosenbaum DM, Rasmussen SG, Kobilka BK. The structure and function of G-protein-coupled receptors. *Nature* 2009, **459**(7245): 356-363.
36. Bockaert J, Pin JP. Molecular tinkering of G protein-coupled receptors: an evolutionary success. *The EMBO journal* 1999, **18**(7): 1723-1729.
37. Venkatakrisnan AJ, Deupi X, Lebon G, Tate CG, Schertler GF, Babu MM. Molecular signatures of G-protein-coupled receptors. *Nature* 2013, **494**(7436): 185-194.
38. Musnier A, Blanchot B, Reiter E, Crepieux P. GPCR signalling to the translation machinery. *Cellular signalling* 2010, **22**(5): 707-716.

39. Hur EM, Kim KT. G protein-coupled receptor signalling and cross-talk: achieving rapidity and specificity. *Cellular signalling* 2002, **14**(5): 397-405.
40. Ishii S, Kihara Y, Shimizu T. Identification of T cell death-associated gene 8 (TDAG8) as a novel acid sensing G-protein-coupled receptor. *The Journal of biological chemistry* 2005, **280**(10): 9083-9087.
41. Justus CR, Dong L, Yang LV. Acidic tumor microenvironment and pH-sensing G protein-coupled receptors. *Frontiers in physiology* 2013, **4**: 354.
42. Kyaw H, Zeng Z, Su K, Fan P, Shell BK, Carter KC, *et al.* Cloning, characterization, and mapping of human homolog of mouse T-cell death-associated gene. *DNA and cell biology* 1998, **17**(6): 493-500.
43. Kottyan LC, Collier AR, Cao KH, Niese KA, Hedgebeth M, Radu CG, *et al.* Eosinophil viability is increased by acidic pH in a cAMP- and GPR65-dependent manner. *Blood* 2009, **114**(13): 2774-2782.
44. Zhu X, Mose E, Hogan SP, Zimmermann N. Differential eosinophil and mast cell regulation: Mast cell viability and accumulation in inflammatory tissue are independent of proton-sensing receptor GPR65. *American Journal of Physiology - Gastrointestinal and Liver Physiology* 2014, **306**(11): G974-G982.
45. Choi JW, Lee SY, Choi Y. Identification of a putative G protein-coupled receptor induced during activation-induced apoptosis of T cells. *Cellular immunology* 1996, **168**(1): 78-84.
46. Tosa N, Murakami M, Jia WY, Yokoyama M, Masunaga T, Iwabuchi C, *et al.* Critical function of T cell death-associated gene 8 in glucocorticoid-induced thymocyte apoptosis. *International immunology* 2003, **15**(6): 741-749.
47. Ryder C, McColl K, Zhong F, Distelhorst CW. Acidosis Promotes Bcl-2 Family-mediated Evasion of Apoptosis: INVOLVEMENT OF ACID-SENSING G PROTEIN-COUPLED RECEPTOR GPR65 SIGNALING TO MEK/ERK. *Journal of Biological Chemistry* 2012, **287**(33): 27863-27875.
48. Rosko AE, McColl KS, Zhong F, Ryder CB, Chang MJ, Sattar A, *et al.* Acidosis Sensing Receptor GPR65 Correlates with Anti-Apoptotic Bcl-2 Family Member Expression in CLL Cells: Potential Implications for the CLL Microenvironment. *J Leuk (Los Angel)* 2014, **2**(5).
49. Franke A, McGovern DPB, Barrett JC, Wang K, Radford-Smith GL, Ahmad T, *et al.* Genome-wide meta-analysis increases to 71 the number of confirmed Crohn's disease susceptibility loci. *Nature genetics* 2010, **42**(12): 1118-1125.

50. Ke X. Presence of Multiple Independent Effects in Risk Loci of Common Complex Human Diseases. *The American Journal of Human Genetics*, **91**(1): 185-192.
51. Ballester V, Guo X, Vendrell R, Haritunians T, Klomhaus AM, Li D, *et al.* Association of NOD2 and IL23R with inflammatory bowel disease in Puerto Rico. *PloS one* 2014, **9**(9): e108204.
52. Tazoe H, Otomo Y, Kaji I, Tanaka R, Karaki SI, Kuwahara A. Roles of short-chain fatty acids receptors, GPR41 and GPR43 on colonic functions. *Journal of physiology and pharmacology : an official journal of the Polish Physiological Society* 2008, **59 Suppl 2**: 251-262.
53. Brown AJ, Goldsworthy SM, Barnes AA, Eilert MM, Tcheang L, Daniels D, *et al.* The Orphan G protein-coupled receptors GPR41 and GPR43 are activated by propionate and other short chain carboxylic acids. *The Journal of biological chemistry* 2003, **278**(13): 11312-11319.
54. Le Poul E, Loison C, Struyf S, Springael J-Y, Lannoy V, Decobecq M-E, *et al.* Functional Characterization of Human Receptors for Short Chain Fatty Acids and Their Role in Polymorphonuclear Cell Activation. *Journal of Biological Chemistry* 2003, **278**(28): 25481-25489.
55. Wang A, Si H, Liu D, Jiang H. Butyrate Activates the cAMP-Protein Kinase A-cAMP Response Element-Binding Protein Signaling Pathway in Caco-2 Cells. *The Journal of Nutrition* 2012, **142**(1): 1-6.
56. Yonezawa T, Kobayashi Y, Obara Y. Short-chain fatty acids induce acute phosphorylation of the p38 mitogen-activated protein kinase/heat shock protein 27 pathway via GPR43 in the MCF-7 human breast cancer cell line. *Cellular signalling* 2007, **19**(1): 185-193.
57. Karaki S-i, Mitsui R, Hayashi H, Kato I, Sugiya H, Iwanaga T, *et al.* Short-chain fatty acid receptor, GPR43, is expressed by enteroendocrine cells and mucosal mast cells in rat intestine. *Cell and Tissue Research* 2006, **324**(3): 353-360.
58. Karaki S-i, Tazoe H, Hayashi H, Kashiwabara H, Tooyama K, Suzuki Y, *et al.* Expression of the short-chain fatty acid receptor, GPR43, in the human colon. *J Mol Hist* 2008, **39**(2): 135-142.
59. Tang Y, Chen Y, Jiang H, Robbins GT, Nie D. G-protein-coupled receptor for short-chain fatty acids suppresses colon cancer. *International journal of cancer Journal international du cancer* 2011, **128**(4): 847-856.
60. Vinolo MA, Rodrigues HG, Nachbar RT, Curi R. Regulation of inflammation by short chain fatty acids. *Nutrients* 2011, **3**(10): 858-876.

61. Cox MA, Jackson J, Stanton M, Rojas-Triana A, Bober L, Lavery M, *et al.* Short-chain fatty acids act as antiinflammatory mediators by regulating prostaglandin E(2) and cytokines. *World journal of gastroenterology : WJG* 2009, **15**(44): 5549-5557.
62. Tan J, McKenzie C, Vuillermin Peter J, Goverse G, Vinuesa Carola G, Mebius Reina E, *et al.* Dietary Fiber and Bacterial SCFA Enhance Oral Tolerance and Protect against Food Allergy through Diverse Cellular Pathways. *Cell Reports*, **15**(12): 2809-2824.
63. McKenzie CI, Mackay CR, Macia L. GPR43 &#x2013; A Prototypic Metabolite Sensor Linking Metabolic and Inflammatory Diseases. *Trends in Endocrinology & Metabolism*, **26**(10): 511-512.
64. Priyadarshini M, Villa SR, Fuller M, Wicksteed B, Mackay CR, Alquier T, *et al.* An Acetate-Specific GPCR, FFAR2, Regulates Insulin Secretion. *Molecular Endocrinology* 2015, **29**(7): 1055-1066.
65. Thangaraju M, Cresci GA, Liu K, Ananth S, Gnanaprakasam JP, Browning DD, *et al.* GPR109A Is a G-protein–Coupled Receptor for the Bacterial Fermentation Product Butyrate and Functions as a Tumor Suppressor in Colon. *Cancer research* 2009, **69**(7): 2826-2832.
66. Li G, Shi Y, Huang H, Zhang Y, Wu K, Luo J, *et al.* Internalization of the Human Nicotinic Acid Receptor GPR109A Is Regulated by Gi, GRK2, and Arrestin3. *Journal of Biological Chemistry* 2010, **285**(29): 22605-22618.
67. Lukasova M, Malaval C, Gille A, Kero J, Offermanns S. Nicotinic acid inhibits progression of atherosclerosis in mice through its receptor GPR109A expressed by immune cells. *The Journal of clinical investigation* 2011, **121**(3): 1163-1173.
68. Kostylina G, Simon D, Fey MF, Yousefi S, Simon HU. Neutrophil apoptosis mediated by nicotinic acid receptors (GPR109A). *Cell death and differentiation* 2008, **15**(1): 134-142.
69. Hanson J, Gille A, Zwykiel S, Lukasova M, Clausen BE, Ahmed K, *et al.* Nicotinic acid- and monomethyl fumarate-induced flushing involves GPR109A expressed by keratinocytes and COX-2-dependent prostanoid formation in mice. *The Journal of clinical investigation* 2010, **120**(8): 2910-2919.
70. Tunaru S, Kero J, Schaub A, Wufka C, Blaukat A, Pfeffer K, *et al.* PUMA-G and HM74 are receptors for nicotinic acid and mediate its anti-lipolytic effect. *Nature medicine* 2003, **9**(3): 352-355.
71. Li X, Millar JS, Brownell N, Briand F, Rader DJ. Modulation of HDL metabolism by the niacin receptor GPR109A in mouse hepatocytes. *Biochemical pharmacology* 2010, **80**(9): 1450-1457.

72. Digby JE, Martinez F, Jefferson A, Ruparelia N, Chai J, Wamil M, *et al.* Anti-inflammatory effects of nicotinic acid in human monocytes are mediated by GPR109A dependent mechanisms. *Arteriosclerosis, thrombosis, and vascular biology* 2012, **32**(3): 669-676.
73. Gambhir D, Ananth S, Veeranan-Karmegam R, Elangovan S, Hester S, Jennings E, *et al.* GPR109A as an Anti-Inflammatory Receptor in Retinal Pigment Epithelial Cells and Its Relevance to Diabetic Retinopathy. *Investigative ophthalmology & visual science* 2012, **53**(4): 2208-2217.
74. Ingersoll MA, Potteaux S, Alvarez D, Hutchison SB, van Rooijen N, Randolph GJ. Niacin inhibits skin dendritic cell mobilization in a GPR109A independent manner but has no impact on monocyte trafficking in atherosclerosis. *Immunobiology* 2012, **217**(5): 548-557.
75. Singh N, Gurav A, Sivaprakasam S, Brady E, Padia R, Shi H, *et al.* Activation of Gpr109a, Receptor for Niacin and the Commensal Metabolite Butyrate, Suppresses Colonic Inflammation and Carcinogenesis. *Immunity* 2014, **40**(1): 128-139.
76. Cresci GA, Thangaraju M, Mellinger JD, Liu K, Ganapathy V. Colonic gene expression in conventional and germ-free mice with a focus on the butyrate receptor GPR109A and the butyrate transporter SLC5A8. *Journal of gastrointestinal surgery : official journal of the Society for Surgery of the Alimentary Tract* 2010, **14**(3): 449-461.
77. Wang J, Wu X, Simonavicius N, Tian H, Ling L. Medium-chain Fatty Acids as Ligands for Orphan G Protein-coupled Receptor GPR84. *Journal of Biological Chemistry* 2006, **281**(45): 34457-34464.
78. Suzuki M, Takaishi S, Nagasaki M, Onozawa Y, Iino I, Maeda H, *et al.* Medium-chain fatty acid-sensing receptor, GPR84, is a proinflammatory receptor. *The Journal of biological chemistry* 2013, **288**(15): 10684-10691.
79. Venkataraman C, Kuo F. The G-protein coupled receptor, GPR84 regulates IL-4 production by T lymphocytes in response to CD3 crosslinking. *Immunology letters* 2005, **101**(2): 144-153.
80. Ishikawa F, Niino H, Iino T, Yoshida S, Saito N, Onohara S, *et al.* The developmental program of human dendritic cells is operated independently of conventional myeloid and lymphoid pathways. *Blood* 2007, **110**(10): 3591-3660.
81. Li J, Wang Y, Tang L, de Villiers WJ, Cohen D, Woodward J, *et al.* Dietary medium-chain triglycerides promote oral allergic sensitization and orally induced anaphylaxis to peanut protein in mice. *The Journal of allergy and clinical immunology* 2013, **131**(2): 442-450.



82. Waldecker M, Kautenburger T, Daumann H, Busch C, Schrenk D. Inhibition of histone-deacetylase activity by short-chain fatty acids and some polyphenol metabolites formed in the colon. *The Journal of Nutritional Biochemistry* 2008, **19**(9): 587-593.
83. Xu WS, Parmigiani RB, Marks PA. Histone deacetylase inhibitors: molecular mechanisms of action. *Oncogene* 0000, **26**(37): 5541-5552.
84. MacDonald VE, Howe LJ. Histone acetylation: where to go and how to get there. *Epigenetics : official journal of the DNA Methylation Society* 2009, **4**(3): 139-143.
85. Boffa LC, Vidali G, Mann RS, Allfrey VG. Suppression of histone deacetylation in vivo and in vitro by sodium butyrate. *Journal of Biological Chemistry* 1978, **253**(10): 3364-3366.
86. Sealy L, Chalkley R. The effect of sodium butyrate on histone modification. *Cell* 1978, **14**(1): 115-121.
87. Hinnebusch BF, Meng S, Wu JT, Archer SY, Hodin RA. The Effects of Short-Chain Fatty Acids on Human Colon Cancer Cell Phenotype Are Associated with Histone Hyperacetylation. *The Journal of Nutrition* 2002, **132**(5): 1012-1017.
88. Kiefer J, Beyer-Sehlmeyer G, Pool-Zobel BL. Mixtures of SCFA, composed according to physiologically available concentrations in the gut lumen, modulate histone acetylation in human HT29 colon cancer cells. *The British journal of nutrition* 2006, **96**(5): 803-810.
89. Soliman ML, Rosenberger TA. Acetate supplementation increases brain histone acetylation and inhibits histone deacetylase activity and expression. *Molecular and cellular biochemistry* 2011, **352**(1-2): 173-180.
90. Kendrick SFW, O'Boyle G, Mann J, Zeybel M, Palmer J, Jones DEJ, *et al.* Acetate, the key modulator of inflammatory responses in acute alcoholic hepatitis. *Hepatology* 2010, **51**(6): 1988-1997.
91. Lucas JL, Mirshahpanah P, Haas-Stapleton E, Asadullah K, Zollner TM, Numerof RP. Induction of Foxp3+ regulatory T cells with histone deacetylase inhibitors. *Cellular immunology* 2009, **257**(1-2): 97-104.
92. Tao R, de Zoeten EF, Ozkaynak E, Chen C, Wang L, Porrett PM, *et al.* Deacetylase inhibition promotes the generation and function of regulatory T cells. *Nature medicine* 2007, **13**(11): 1299-1307.
93. Akimova T, Ge G, Golovina T, Mikheeva T, Wang L, Riley JL, *et al.* Histone/protein deacetylase inhibitors increase suppressive functions of human FOXP3+ Tregs. *Clinical Immunology* 2010, **136**(3): 348-363.

94. Usami M, Kishimoto K, Ohata A, Miyoshi M, Aoyama M, Fueda Y, *et al.* Butyrate and trichostatin A attenuate nuclear factor kappaB activation and tumor necrosis factor alpha secretion and increase prostaglandin E2 secretion in human peripheral blood mononuclear cells. *Nutr Res* 2008, **28**(5): 321-328.
95. Vinolo MA, Rodrigues HG, Hatanaka E, Sato FT, Sampaio SC, Curi R. Suppressive effect of short-chain fatty acids on production of proinflammatory mediators by neutrophils. *J Nutr Biochem* 2011, **22**(9): 849-855.
96. Chang PV, Hao L, Offermanns S, Medzhitov R. The microbial metabolite butyrate regulates intestinal macrophage function via histone deacetylase inhibition. *Proceedings of the National Academy of Sciences* 2014, **111**(6): 2247-2252.
97. Licciardi PV, Karagiannis TC. Regulation of immune responses by histone deacetylase inhibitors. *ISRN hematology* 2012, **2012**: 690901.
98. Kim M, Qie Y, Park J, Kim Chang H. Gut Microbial Metabolites Fuel Host Antibody Responses. *Cell host & microbe* 2016, **20**(2): 202-214.
99. Corthésy B. Role of secretory IgA in infection and maintenance of homeostasis. *Autoimmunity Reviews* 2013, **12**(6): 661-665.
100. Cousens LS, Gallwitz D, Alberts BM. Different accessibilities in chromatin to histone acetylase. *The Journal of biological chemistry* 1979, **254**(5): 1716-1723.
101. Davie JR. Inhibition of histone deacetylase activity by butyrate. *J Nutr* 2003, **133**(7 Suppl): 2485S-2493S.
102. Singh N, Thangaraju M, Prasad PD, Martin PM, Lambert NA, Boettger T, *et al.* Blockade of dendritic cell development by bacterial fermentation products butyrate and propionate through a transporter (Slc5a8)-dependent inhibition of histone deacetylases. *The Journal of biological chemistry* 2010, **285**(36): 27601-27608.
103. To T, Stanojevic S, Moores G, Gershon AS, Bateman ED, Cruz AA, *et al.* Global asthma prevalence in adults: findings from the cross-sectional world health survey. *BMC public health* 2012, **12**: 204.
104. Wenzel SE. Asthma: defining of the persistent adult phenotypes. *The Lancet*, **368**(9537): 804-813.

105. Boxall C, Holgate ST, Davies DE. The contribution of transforming growth factor- $\beta$  and epidermal growth factor signalling to airway remodelling in chronic asthma. *European Respiratory Journal* 2006, **27**(1): 208-229.
106. Berend N, Salome CM, King GG. Mechanisms of airway hyperresponsiveness in asthma. *Respirology* 2008, **13**(5): 624-631.
107. Holgate ST. Pathogenesis of Asthma. *Clinical & Experimental Allergy* 2008, **38**(6): 872-897.
108. Holgate ST, Davies DE. Rethinking the Pathogenesis of Asthma. *Immunity* 2009, **31**(3): 362-367.
109. Umetsu DT, McIntire JJ, Akbari O, Macaubas C, DeKruyff RH. Asthma: an epidemic of dysregulated immunity. *Nat Immunol* 2002, **3**(8): 715-720.
110. Umetsu DT, Akbari O, DeKruyff RH. Regulatory T cells control the development of allergic disease and asthma. *The Journal of allergy and clinical immunology* 2003, **112**(3): 480-487; quiz 488.
111. Khare A, Krishnamoorthy N, Oriss TB, Fei M, Ray P, Ray A. Cutting Edge: Inhaled Antigen Upregulates Retinaldehyde Dehydrogenase in Lung CD103+ but Not Plasmacytoid Dendritic Cells To Induce Foxp3 De Novo in CD4+ T Cells and Promote Airway Tolerance. *The Journal of Immunology* 2013, **191**(1): 25-29.
112. Albacker LA, Yu S, Bedoret D, Lee WL, Umetsu SE, Monahan S, *et al.* TIM-4, expressed by medullary macrophages, regulates respiratory tolerance by mediating phagocytosis of antigen-specific T cells. *Mucosal Immunol* 2013, **6**(3): 580-590.
113. Kuipers H, Lambrecht BN. The interplay of dendritic cells, Th2 cells and regulatory T cells in asthma. *Current Opinion in Immunology* 2004, **16**(6): 702-708.
114. Chu DK, Llop-Guevara A, Walker TD, Flader K, Goncharova S, Boudreau JE, *et al.* IL-33, but not thymic stromal lymphopoietin or IL-25, is central to mite and peanut allergic sensitization. *The Journal of allergy and clinical immunology* 2013, **131**(1): 187-200.e188.
115. Zhu J, Guo L, Min B, Watson CJ, Hu-Li J, Young HA, *et al.* Growth Factor Independent-1 Induced by IL-4 Regulates Th2 Cell Proliferation. *Immunity* 2002, **16**(5): 733-744.
116. Wills-Karp M, Luyimbazi J, Xu X, Schofield B, Neben TY, Karp CL, *et al.* Interleukin-13: Central Mediator of Allergic Asthma. *Science* 1998, **282**(5397): 2258-2261.
117. Bosnjak B, Stelzmueller B, Erb KJ, Epstein MM. Treatment of allergic asthma: modulation of Th2 cells and their responses. *Respiratory research* 2011, **12**: 114.

118. Bettelli E, Korn T, Oukka M, Kuchroo VK. Induction and effector functions of TH17 cells. *Nature* 2008, **453**(7198): 1051-1057.
119. Forchielli ML, Walker WA. The role of gut-associated lymphoid tissues and mucosal defence. *The British journal of nutrition* 2005, **93 Suppl 1**: S41-48.
120. Wing K, Onishi Y, Prieto-Martin P, Yamaguchi T, Miyara M, Fehervari Z, *et al.* CTLA-4 Control over Foxp3+ Regulatory T Cell Function. *Science* 2008, **322**(5899): 271-275.
121. Sojka DK, Hughson A, Fowell DJ. CTLA-4 is required by CD4+CD25+ Treg to control CD4+ T-cell lymphopenia-induced proliferation. *Eur J Immunol* 2009, **39**(6): 1544-1551.
122. Faustino L, Mucida D, Keller AC, Demengeot J, Bortoluci K, Sardinha LR, *et al.* Regulatory T cells accumulate in the lung allergic inflammation and efficiently suppress T-cell proliferation but not Th2 cytokine production. *Clinical & developmental immunology* 2012, **2012**: 721817.
123. Hartl D, Koller B, Mehlhorn AT, Reinhardt D, Nicolai T, Schendel DJ, *et al.* Quantitative and functional impairment of pulmonary CD4+CD25hi regulatory T cells in pediatric asthma. *The Journal of allergy and clinical immunology* 2007, **119**(5): 1258-1266.
124. Thorburn AN, Hansbro PM. Harnessing regulatory T cells to suppress asthma: from potential to therapy. *American journal of respiratory cell and molecular biology* 2010, **43**(5): 511-519.
125. Josefowicz SZ, Niec RE, Kim HY, Treuting P, Chinen T, Zheng Y, *et al.* Extrathymically generated regulatory T cells control mucosal TH2 inflammation. *Nature* 2012, **482**(7385): 395-399.
126. Kearley J, Barker JE, Robinson DS, Lloyd CM. Resolution of airway inflammation and hyperreactivity after in vivo transfer of CD4+CD25+ regulatory T cells is interleukin 10 dependent. *The Journal of Experimental Medicine* 2005, **202**(11): 1539-1547.
127. Lewkowich IP, Herman NS, Schleifer KW, Dance MP, Chen BL, Dienger KM, *et al.* CD4+CD25+ T cells protect against experimentally induced asthma and alter pulmonary dendritic cell phenotype and function. *The Journal of Experimental Medicine* 2005, **202**(11): 1549-1561.
128. O'Byrne PM, Inman MD, Parameswaran K. The trials and tribulations of IL-5, eosinophils, and allergic asthma. *The Journal of allergy and clinical immunology* 2001, **108**(4): 503-508.
129. Humbert M, Menz G, Ying S, Corrigan CJ, Robinson DS, Durham SR, *et al.* The immunopathology of extrinsic (atopic) and intrinsic (non-atopic) asthma: more similarities than differences. *Immunology today* 1999, **20**(11): 528-533.

130. Foster PS, Rosenberg HF, Asquith KL, Kumar RK. Targeting eosinophils in asthma. *Current molecular medicine* 2008, **8**(6): 585-590.
131. Rothenberg ME, Hogan SP. The eosinophil. *Annual review of immunology* 2006, **24**: 147-174.
132. Humbles AA, Lloyd CM, McMillan SJ, Friend DS, Xanthou G, McKenna EE, *et al.* A critical role for eosinophils in allergic airways remodeling. *Science* 2004, **305**(5691): 1776-1779.
133. Lee JJ, Dimina D, Macias MP, Ochkur SI, McGarry MP, O'Neill KR, *et al.* Defining a link with asthma in mice congenitally deficient in eosinophils. *Science* 2004, **305**(5691): 1773-1776.
134. Obase Y, Shimoda T, Mitsuta K, Matsuo N, Matsuse H, Kohno S. Correlation between airway hyperresponsiveness and airway inflammation in a young adult population: eosinophil, ECP, and cytokine levels in induced sputum. *Annals of Allergy, Asthma & Immunology*, **86**(3): 304-310.
135. Evans CM, Fryer AD, Jacoby DB, Gleich GJ, Costello RW. Pretreatment with antibody to eosinophil major basic protein prevents hyperresponsiveness by protecting neuronal M2 muscarinic receptors in antigen-challenged guinea pigs. *Journal of Clinical Investigation* 1997, **100**(9): 2254-2262.
136. Possa SS, Leick EA, Prado CM, Martins MA, Tibério IFLC. Eosinophilic Inflammation in Allergic Asthma. *Frontiers in Pharmacology* 2013, **4**: 46.
137. Pease JE, Williams TJ. Eotaxin and asthma. *Current Opinion in Pharmacology* 2001, **1**(3): 248-253.
138. Moser R, Fehr J, Bruijnzeel PL. IL-4 controls the selective endothelium-driven transmigration of eosinophils from allergic individuals. *J Immunol* 1992, **149**(4): 1432-1438.
139. Steinke JW, Borish L. Th2 cytokines and asthma. Interleukin-4: its role in the pathogenesis of asthma, and targeting it for asthma treatment with interleukin-4 receptor antagonists. *Respiratory research* 2001, **2**(2): 66-70.
140. Gleich GJ. Mechanisms of eosinophil-associated inflammation. *The Journal of allergy and clinical immunology* 2000, **105**(4): 651-663.
141. Li L, Xia Y, Nguyen A, Lai YH, Feng L, Mosmann TR, *et al.* Effects of Th2 cytokines on chemokine expression in the lung: IL-13 potently induces eotaxin expression by airway epithelial cells. *J Immunol* 1999, **162**(5): 2477-2487.

142. Yu M, Eckart MR, Morgan AA, Mukai K, Butte AJ, Tsai M, *et al.* Identification of an IFN-gamma/mast cell axis in a mouse model of chronic asthma. *The Journal of clinical investigation* 2011, **121**(8): 3133-3143.
143. Lukacs NW, Standiford TJ, Chensue SW, Kunkel RG, Strieter RM, Kunkel SL. C-C chemokine-induced eosinophil chemotaxis during allergic airway inflammation. *Journal of Leukocyte Biology* 1996, **60**(5): 573-578.
144. Foster PS, Mould AW, Yang M, Mackenzie J, Mattes J, Hogan SP, *et al.* Elemental signals regulating eosinophil accumulation in the lung. *Immunological reviews* 2001, **179**(1): 173-181.
145. Sicherer SH, Sampson HA. Food allergy: Epidemiology, pathogenesis, diagnosis, and treatment. *Journal of Allergy and Clinical Immunology* 2014, **133**(2): 291-307.e295.
146. Wang J, Sampson HA. Food allergy: recent advances in pathophysiology and treatment. *Allergy, asthma & immunology research* 2009, **1**(1): 19-29.
147. Sicherer SH, Sampson HA. Food allergy. *Journal of Allergy and Clinical Immunology* 2010, **125**(2, Supplement 2): S116-S125.
148. Sicherer SH. Epidemiology of food allergy. *Journal of Allergy and Clinical Immunology* 2011, **127**(3): 594-602.
149. Eigenmann PA. Mechanisms of food allergy. *Pediatric Allergy and Immunology* 2009, **20**(1): 5-11.
150. Du Toit G, Katz Y, Sasieni P, Mesher D, Maleki SJ, Fisher HR, *et al.* Early consumption of peanuts in infancy is associated with a low prevalence of peanut allergy. *The Journal of allergy and clinical immunology* 2008, **122**(5): 984-991.
151. Du Toit G, Roberts G, Sayre PH, Bahnson HT, Radulovic S, Santos AF, *et al.* Randomized Trial of Peanut Consumption in Infants at Risk for Peanut Allergy. *New England Journal of Medicine* 2015, **372**(9): 803-813.
152. Lack G. Update on risk factors for food allergy. *The Journal of allergy and clinical immunology* 2012, **129**(5): 1187-1197.
153. Chehade M, Mayer L. Oral tolerance and its relation to food hypersensitivities. *The Journal of allergy and clinical immunology* 2005, **115**(1): 3-12.
154. Scott CL, Aumeunier AM, Mowat AM. Intestinal CD103+ dendritic cells: master regulators of tolerance? *Trends in immunology* 2011, **32**(9): 412-419.

155. Strobel S, Mowat AM. Oral tolerance and allergic responses to food proteins. *Current opinion in allergy and clinical immunology* 2006, **6**(3): 207-213.
156. Del Rio M-L, Bernhardt G, Rodriguez-Barbosa J-I, Förster R. Development and functional specialization of CD103+ dendritic cells. *Immunological reviews* 2010, **234**(1): 268-281.
157. Brandtzaeg P. Mucosal Immunity: Induction, Dissemination, and Effector Functions. *Scandinavian Journal of Immunology* 2009, **70**(6): 505-515.
158. Macpherson AJ, Smith K. Mesenteric lymph nodes at the center of immune anatomy. *The Journal of Experimental Medicine* 2006, **203**(3): 497-500.
159. Spahn TW, Weiner HL, Rennert PD, Lugering N, Fontana A, Domschke W, *et al.* Mesenteric lymph nodes are critical for the induction of high-dose oral tolerance in the absence of Peyer's patches. *Eur J Immunol* 2002, **32**(4): 1109-1113.
160. Dang TD, Allen KJ, J. Martino D, Koplin JJ, Licciardi PV, Tang MLK. Food-allergic infants have impaired regulatory T-cell responses following in vivo allergen exposure. *Pediatric Allergy and Immunology* 2016, **27**(1): 35-43.
161. Sudo N, Sawamura S, Tanaka K, Aiba Y, Kubo C, Koga Y. The requirement of intestinal bacterial flora for the development of an IgE production system fully susceptible to oral tolerance induction. *The Journal of Immunology* 1997, **159**(4): 1739-1745.
162. Bashir MEH, Louie S, Shi HN, Nagler-Anderson C. Toll-Like Receptor 4 Signaling by Intestinal Microbes Influences Susceptibility to Food Allergy. *The Journal of Immunology* 2004, **172**(11): 6978-6987.
163. Ananthakrishnan AN. Epidemiology and risk factors for IBD. *Nat Rev Gastroenterol Hepatol* 2015, **12**(4): 205-217.
164. Johnson MW, Lithgo K, Prouse T, Price T. PTH-155 The Hospital Admission Burden of Inflammatory Bowel Disease: A 10 Year Review from a District General Hospital. *Gut* 2013, **62**(Suppl 1): A274.
165. Høivik ML, Moum B, Solberg IC, Henriksen M, Cvancarova M, Bernklev T, *et al.* Work disability in inflammatory bowel disease patients 10 years after disease onset: results from the IBSEN Study. *Gut* 2013, **62**(3): 368-375.
166. Laass MW, Roggenbuck D, Conrad K. Diagnosis and classification of Crohn's disease. *Autoimmunity Reviews* 2014, **13**(4–5): 467-471.

167. Conrad K, Roggenbuck D, Laass MW. Diagnosis and classification of ulcerative colitis. *Autoimmunity Reviews* 2014, **13**(4–5): 463-466.
168. Roberts-Thomson IC, Fon J, Uylaki W, Cummins AG, Barry S. Cells, cytokines and inflammatory bowel disease: a clinical perspective. *Expert review of gastroenterology & hepatology* 2011, **5**(6): 703-716.
169. Knights D, Lassen KG, Xavier RJ. Advances in inflammatory bowel disease pathogenesis: linking host genetics and the microbiome. *Gut* 2013, **62**(10): 1505-1510.
170. Khor B, Gardet A, Xavier RJ. Genetics and pathogenesis of inflammatory bowel disease. *Nature* 2011, **474**(7351): 307-317.
171. Baumgart DC, Carding SR. Inflammatory bowel disease: cause and immunobiology. *Lancet* 2007, **369**(9573): 1627-1640.
172. Pastorelli L, De Salvo C, Mercado J, Vecchi M, Pizarro T. Central Role of the Gut Epithelial Barrier in the Pathogenesis of Chronic Intestinal Inflammation: Lessons Learned from Animal Models and Human Genetics. *Frontiers in immunology* 2013, **4**(280).
173. Franchimont D, Vermeire S, El Housni H, Pierik M, Van Steen K, Gustot T, *et al.* Deficient host-bacteria interactions in inflammatory bowel disease? The toll-like receptor (TLR)-4 Asp299gly polymorphism is associated with Crohn's disease and ulcerative colitis. *Gut* 2004, **53**(7): 987-992.
174. Hugot J-P, Chamaillard M, Zouali H, Lesage S, Cezard J-P, Belaiche J, *et al.* Association of NOD2 leucine-rich repeat variants with susceptibility to Crohn's disease. *Nature* 2001, **411**(6837): 599-603.
175. Suzuki T. Regulation of intestinal epithelial permeability by tight junctions. *Cellular and Molecular Life Sciences* 2013, **70**(4): 631-659.
176. Chin AC, Parkos CA. Neutrophil transepithelial migration and epithelial barrier function in IBD: potential targets for inhibiting neutrophil trafficking. *Annals of the New York Academy of Sciences* 2006, **1072**: 276-287.
177. Ohtsuka Y, Lee J, Stamm DS, Sanderson IR. MIP-2 secreted by epithelial cells increases neutrophil and lymphocyte recruitment in the mouse intestine. *Gut* 2001, **49**(4): 526-533.
178. Kucharzik T, Hudson JT, Lügering A, Abbas JA, Bettini M, Lake JG, *et al.* Acute induction of human IL-8 production by intestinal epithelium triggers neutrophil infiltration without mucosal injury. *Gut* 2005, **54**(11): 1565-1572.



179. Banks C, Bateman A, Payne R, Johnson P, Sheron N. Chemokine expression in IBD. Mucosal chemokine expression is unselectively increased in both ulcerative colitis and Crohn's disease. *The Journal of Pathology* 2003, **199**(1): 28-35.
180. Neurath MF. Cytokines in inflammatory bowel disease. *Nat Rev Immunol* 2014, **14**(5): 329-342.
181. Fournier BM, Parkos CA. The role of neutrophils during intestinal inflammation. *Mucosal Immunol* 2012, **5**(4): 354-366.
182. Kühl AA, Kakirman H, Janotta M, Dreher S, Cremer P, Pawlowski NN, *et al.* Aggravation of Different Types of Experimental Colitis by Depletion or Adhesion Blockade of Neutrophils. *Gastroenterology*, **133**(6): 1882-1892.
183. Chassaing B, Aitken JD, Malleshappa M, Vijay-Kumar M. Dextran Sulfate Sodium (DSS)-Induced Colitis in Mice. *Current protocols in immunology / edited by John E Coligan [et al]* 2014, **104**: Unit-15.25.
184. Kim TW, Seo JN, Suh YH, Park HJ, Kim JH, Kim JY, *et al.* Involvement of lymphocytes in dextran sulfate sodium-induced experimental colitis. *World journal of gastroenterology : WJG* 2006, **12**(2): 302-305.
185. Borenshtein D, McBee ME, Schauer DB. Utility of the *Citrobacter rodentium* infection model in laboratory mice. *Current Opinion in Gastroenterology* 2008, **24**(1): 32-37 10.1097/MOG.1090b1013e3282f1092b1090fb.
186. Koroleva EP, Halperin S, Gubernatorova EO, Macho-Fernandez E, Spencer CM, Tumanov AV. *Citrobacter rodentium*-induced colitis: A robust model to study mucosal immune responses in the gut. *Journal of immunological methods* 2015, **421**: 61-72.
187. Deng W, Li Y, Vallance BA, Finlay BB. Locus of Enterocyte Effacement from *Citrobacter rodentium*: Sequence Analysis and Evidence for Horizontal Transfer among Attaching and Effacing Pathogens. *Infection and immunity* 2001, **69**(10): 6323-6335.
188. Tan JK, McKenzie C, Mariño E, Macia L, Mackay CR. Metabolite-Sensing G Protein–Coupled Receptors—Facilitators of Diet-Related Immune Regulation. *Annual review of immunology* 2017, **35**(1): 371-402.
189. Geraghty AA, Lindsay KL, Alberdi G, McAuliffe FM, Gibney ER. Nutrition During Pregnancy Impacts Offspring's Epigenetic Status—Evidence from Human and Animal Studies. *Nutrition and Metabolic Insights* 2015, **8**(Suppl 1): 41-47.

190. Grönlund M-M, Lehtonen O-P, Eerola E, Kero P. Fecal Microflora in Healthy Infants Born by Different Methods of Delivery: Permanent Changes in Intestinal Flora After Cesarean Delivery. *Journal of pediatric gastroenterology and nutrition* 1999, **28**(1): 19-25.
191. Robinson DS. Regulatory T cells and asthma. *Clinical & Experimental Allergy* 2009, **39**(9): 1314-1323.
192. Scallan E, Mahon BE, Hoekstra RM, Griffin PM. Estimates of Illnesses, Hospitalizations and Deaths Caused by Major Bacterial Enteric Pathogens in Young Children in the United States. *The Pediatric Infectious Disease Journal* 2013, **32**(3): 217-221.
193. Nataro JP, Kaper JB. Diarrheagenic Escherichia coli. *Clin Microbiol Rev* 1998, **11**(1): 142-201.
194. Thorburn Alison N, Macia L, Mackay Charles R. Diet, Metabolites, and “Western-Lifestyle” Inflammatory Diseases. *Immunity*, **40**(6): 833-842.
195. Ericsson A, Svensson M, Arya A, Agace WW. CCL25/CCR9 promotes the induction and function of CD103 on intestinal intraepithelial lymphocytes. *European Journal of Immunology* 2004, **34**(10): 2720-2729.
196. Martinez-Medina M, Denizot J, Dreux N, Robin F, Billard E, Bonnet R, *et al.* Western diet induces dysbiosis with increased E coli in CEABAC10 mice, alters host barrier function favouring AIEC colonisation. *Gut* 2014, **63**(1): 116-124.
197. Tan J, McKenzie C, Potamitis M, Thorburn AN, Mackay CR, Macia L. The role of short-chain fatty acids in health and disease. *Advances in immunology* 2014, **121**: 91-119.
198. Richards JL, Yap YA, McLeod KH, Mackay CR, Marino E. Dietary metabolites and the gut microbiota: an alternative approach to control inflammatory and autoimmune diseases. *Clin Trans Immunol* 2016, **5**: e82.
199. Cummings JH, Beatty ER, Kingman SM, Bingham SA, Englyst HN. Digestion and physiological properties of resistant starch in the human large bowel. *British Journal of Nutrition* 1996, **75**(5): 733-747.
200. De Filippo C, Cavalieri D, Di Paola M, Ramazzotti M, Poullet JB, Massart S, *et al.* Impact of diet in shaping gut microbiota revealed by a comparative study in children from Europe and rural Africa. *Proc Natl Acad Sci U S A* 2010, **107**(33): 14691-14696.
201. Blaser MJ, Dominguez-Bello MG, Contreras M, Magris M, Hidalgo G, Estrada I, *et al.* Distinct cutaneous bacterial assemblages in a sampling of South American Amerindians and US residents. *ISME j* 2013, **7**(1): 85-95.

202. Macia L, Tan J, Vieira AT, Leach K, Stanley D, Luong S, *et al.* Metabolite-sensing receptors GPR43 and GPR109A facilitate dietary fibre-induced gut homeostasis through regulation of the inflammasome. *Nature communications* 2015, **6**.
203. Venturini C, Beatson SA, Djordjevic SP, Walker MJ. Multiple antibiotic resistance gene recruitment onto the enterohemorrhagic *Escherichia coli* virulence plasmid. *FASEB J* 2010, **24**(4): 1160-1166.
204. Petty NK, Bulgin R, Crepin VF, Cerdeno-Tarraga AM, Schroeder GN, Quail MA, *et al.* The *Citrobacter rodentium* genome sequence reveals convergent evolution with human pathogenic *Escherichia coli*. *J Bacteriol* 2010, **192**(2): 525-538.
205. Bhinder G, Sham HP, Chan JM, Morampudi V, Jacobson K, Vallance BA. The *Citrobacter rodentium* mouse model: studying pathogen and host contributions to infectious colitis. *Journal of visualized experiments : JoVE* 2013(72): e50222.
206. Mohawk KL, O'Brien AD. Mouse Models of *Escherichia coli* O157:H7 Infection and Shiga Toxin Injection. *Journal of Biomedicine and Biotechnology* 2011, **2011**: 258185.
207. Mundy R, MacDonald TT, Dougan G, Frankel G, Wiles S. *Citrobacter rodentium* of mice and man. *Cellular microbiology* 2005, **7**(12): 1697-1706.
208. Lebeis SL, Bommarius B, Parkos CA, Sherman MA, Kalman D. TLR Signaling Mediated by MyD88 Is Required for a Protective Innate Immune Response by Neutrophils to *Citrobacter rodentium*. *The Journal of Immunology* 2007, **179**(1): 566-577.
209. Schleimer RP, Kato A, Kern R, Kuperman D, Avila PC. Epithelium: At the interface of innate and adaptive immune responses. *Journal of Allergy and Clinical Immunology* 2007, **120**(6): 1279-1284.
210. Wang Y, Koroleva EP, Kruglov AA, Kuprash DV, Nedospasov SA, Fu Y-X, *et al.* Lymphotoxin Beta Receptor Signaling in Intestinal Epithelial Cells Orchestrates Innate Immune Responses against Mucosal Bacterial Infection. *Immunity*, **32**(3): 403-413.
211. Liu Z, Zaki MH, Vogel P, Gurung P, Finlay BB, Deng W, *et al.* Role of inflammasomes in host defense against *Citrobacter rodentium* infection. *The Journal of biological chemistry* 2012, **287**(20): 16955-16964.
212. Song X, Zhu S, Shi P, Liu Y, Shi Y, Levin SD, *et al.* IL-17RE is the functional receptor for IL-17C and mediates mucosal immunity to infection with intestinal pathogens. *Nat Immunol* 2011, **12**(12): 1151-1158.

213. Zheng Y, Valdez PA, Danilenko DM, Hu Y, Sa SM, Gong Q, *et al.* Interleukin-22 mediates early host defense against attaching and effacing bacterial pathogens. *Nature medicine* 2008, **14**(3): 282-289.
214. Bergstrom KSB, Kisooson-Singh V, Gibson DL, Ma C, Montero M, Sham HP, *et al.* Muc2 Protects against Lethal Infectious Colitis by Disassociating Pathogenic and Commensal Bacteria from the Colonic Mucosa. *PLoS pathogens* 2010, **6**(5): e1000902.
215. Fukuda S, Toh H, Hase K, Oshima K, Nakanishi Y, Yoshimura K, *et al.* Bifidobacteria can protect from enteropathogenic infection through production of acetate. *Nature* 2011, **469**(7331): 543-547.
216. Raqib R, Sarker P, Mily A, Alam NH, Arifuzzaman AS, Rekha RS. Efficacy of sodium butyrate adjunct therapy in shigellosis: a randomized, double-blind, placebo -controlled clinical trial. *BMC Infect Dis* 2012, **12**.
217. Clarke JM, Bird AR, Topping DL, Cobiac L. Excretion of starch and esterified short-chain fatty acids by ileostomy subjects after the ingestion of acylated starches. *The American Journal of Clinical Nutrition* 2007, **86**(4): 1146-1151.
218. Gaboriau-Routhiau V, Rakotobe S, Lécuyer E, Mulder I, Lan A, Bridonneau C. The key role of segmented filamentous bacteria in the coordinated maturation of gut helper T cell responses. *Immunity* 2009, **31**.
219. Binder HJ, Brown I, Ramakrishna BS, Young GP. Oral Rehydration Therapy in the Second Decade of the Twenty-first Century. *Current gastroenterology reports* 2014, **16**(3): 376.
220. Clarke JM, Dharmalingam T, Srinivasan P, Young GP, Lockett T, Ramakrishna BS. Acetylated High Amylose Maize Starch Improves the Efficacy of Oral Rehydration Solution in a Rat Model of Cholera. *Gastroenterology* 2011, **140**(5): S-134.
221. Peng LY, Li Z, Green RS, Holzman IR, Lin J. Butyrate enhances the intestinal barrier by facilitating tight junction assembly via activation of AMP-activated protein kinase in Caco-2 cell monolayers. *J Nutr* 2009, **139**.
222. Bajka BH, Clarke JM, Topping DL, Cobiac L, Abeywardena MY, Patten GS. Butyrylated starch increases large bowel butyrate levels and lowers colonic smooth muscle contractility in rats. *Nutr Res* 2010, **30**(6): 427-434.
223. Eaton KA, Friedman DI, Francis GJ, Tyler JS, Young VB, Haeger J, *et al.* Pathogenesis of renal disease due to enterohemorrhagic *Escherichia coli* in germ-free mice. *Infection and immunity* 2008, **76**(7): 3054-3063.

224. Mundy R, Petrovska L, Smollett K, Simpson N, Wilson RK, Yu J, *et al.* Identification of a novel *Citrobacter rodentium* type III secreted protein, EspI, and roles of this and other secreted proteins in infection. *Infection and immunity* 2004, **72**(4): 2288-2302.
225. Arbeloa A, Blanco M, Moreira FC, Bulgin R, Lopez C, Dahbi G, *et al.* Distribution of espM and espT among enteropathogenic and enterohaemorrhagic *Escherichia coli*. *Journal of medical microbiology* 2009, **58**(Pt 8): 988-995.
226. Frankel G, Phillips AD. Attaching effacing *Escherichia coli* and paradigms of Tir-triggered actin polymerization: getting off the pedestal. *Cell Microbiol* 2008, **10**(3): 549-556.
227. Haenen D, Zhang J, Souza da Silva C, Bosch G, van der Meer IM, van Arkel J, *et al.* A Diet High in Resistant Starch Modulates Microbiota Composition, SCFA Concentrations, and Gene Expression in Pig Intestine. *The Journal of Nutrition* 2013, **143**(3): 274-283.
228. Kim MH, Kang SG, Park JH, Yanagisawa M, Kim CH. Short-Chain Fatty Acids Activate GPR41 and GPR43 on Intestinal Epithelial Cells to Promote Inflammatory Responses in Mice. *Gastroenterology*, **145**(2): 396-406.e310.
229. Stamm I, Lottspeich F, Plaga W. The pyruvate kinase of *Stigmatella aurantiaca* is an indole binding protein and essential for development. *Molecular microbiology* 2005, **56**.
230. Munoz M, Eidenschenk C, Ota N, Wong K, Lohmann U, Kuhl AA, *et al.* Interleukin-22 induces interleukin-18 expression from epithelial cells during intestinal infection. *Immunity* 2015, **42**(2): 321-331.
231. Johansson MEV, Larsson JMH, Hansson GC. The two mucus layers of colon are organized by the MUC2 mucin, whereas the outer layer is a legislator of host–microbial interactions. *Proceedings of the National Academy of Sciences* 2011, **108**(Supplement 1): 4659-4665.
232. Andersen CL, Jensen JL, Orntoft TF. Normalization of real-time quantitative reverse transcription-PCR data: a model-based variance estimation approach to identify genes suited for normalization, applied to bladder and colon cancer data sets. *Cancer research* 2004, **64**(15): 5245-5250.
233. Kandasamy RA, Yu FH, Harris R, Boucher A, Hanrahan JW, Orłowski J. Plasma membrane Na<sup>+</sup>/H<sup>+</sup> exchanger isoforms (NHE-1, -2, and -3) are differentially responsive to second messenger agonists of the protein kinase A and C pathways. *The Journal of biological chemistry* 1995, **270**(49): 29209-29216.
234. Guo X, Liang Y, Zhang Y, Lasorella A, Kee BL, Fu YX. Innate Lymphoid Cells Control Early Colonization Resistance against Intestinal Pathogens through IL2-Dependent Regulation of the Microbiota. *Immunity* 2015, **42**(4): 731-743.

235. Lee K, Kim S-H, Yoon HJ, Paik DJ, Kim JM, Youn J. Bacillus-derived poly- $\gamma$ -glutamic acid attenuates allergic airway inflammation through a Toll-like receptor-4-dependent pathway in a murine model of asthma. *Clinical and experimental allergy : journal of the British Society for Allergy and Clinical Immunology* 2011, **41**.
236. Cheroutre H, Lambolez F, Mucida D. The light and dark sides of intestinal intraepithelial lymphocytes. *Nature reviews Immunology* 2011, **11**(7): 445-456.
237. Guy-Grand D, Vassalli P. Gut intraepithelial T lymphocytes. *Current Opinion in Immunology* 1993, **5**(2): 247-252.
238. Cheroutre H, Lambolez F. Doubting the TCR Coreceptor Function of CD8 $\alpha\alpha$ . *Immunity* 2008, **28**(2): 149-159.
239. Ismail AS, Severson KM, Vaishnava S, Behrendt CL, Yu X, Benjamin JL, *et al.*  $\gamma\delta$  intraepithelial lymphocytes are essential mediators of host–microbial homeostasis at the intestinal mucosal surface. *Proc Natl Acad Sci U S A* 2011, **108**(21): 8743-8748.
240. Smith PM, Howitt MR, Panikov N, Michaud M, Gallini CA, Bohlooly-Y M, *et al.* The Microbial Metabolites, Short-Chain Fatty Acids, Regulate Colonic Treg Cell Homeostasis. *Science* 2013, **341**(6145): 569-573.
241. Furusawa Y, Obata Y, Fukuda S, Endo TA, Nakato G, Takahashi D, *et al.* Commensal microbe-derived butyrate induces the differentiation of colonic regulatory T cells. *Nature* 2013, **advance online publication**.
242. Clarke JM, Dharmalingam T, Srinivasan P, Young GP, Lockett T, Ramakrishna BS. Acetylated High Amylose Maize Starch Improves the Efficacy of Oral Rehydration Solution in a Rat Model of Cholera. *Gastroenterology* 2011, **140**(5): S134-S134.
243. Gancz H, Niderman-Meyer O, Broza M, Kashi Y, Shimon E. Adhesion of *Vibrio cholerae* to granular starches. *Applied and environmental microbiology* 2005, **71**(8): 4850-4855.
244. Shen S, Wong CHY. Bugging inflammation: role of the gut microbiota. *Clin Trans Immunol* 2016, **5**: e72.
245. Chung WSF, Walker AW, Louis P, Parkhill J, Vermeiren J, Bosscher D, *et al.* Modulation of the human gut microbiota by dietary fibres occurs at the species level. *BMC Biology* 2016, **14**(1): 1-13.

246. Ismail AS, Behrendt CL, Hooper LV. Reciprocal interactions between commensal bacteria and gamma delta intraepithelial lymphocytes during mucosal injury. *J Immunol* 2009, **182**(5): 3047-3054.
247. Shen Y, Zhou D, Qiu L, Lai X, Simon M, Shen L, *et al.* Adaptive Immune Response of V $\gamma$ 2V $\delta$ 2(+) T Cells During Mycobacterial Infections. *Science (New York, NY)* 2002, **295**(5563): 2255-2258.
248. King DP, Hyde DM, Jackson KA, Novosad DM, Ellis TN, Putney L, *et al.* Cutting Edge: Protective Response to Pulmonary Injury Requires  $\gamma\delta$  T Lymphocytes. *The Journal of Immunology* 1999, **162**(9): 5033-5036.
249. Okayasu I, Hatakeyama S, Yamada M, Ohkusa T, Inagaki Y, Nakaya R. A novel method in the induction of reliable experimental acute and chronic ulcerative colitis in mice. *Gastroenterology* 1990, **98**(3): 694-702.
250. Bergstrom KS, Kisson-Singh V, Gibson DL, Ma C, Montero M, Sham HP, *et al.* Muc2 protects against lethal infectious colitis by disassociating pathogenic and commensal bacteria from the colonic mucosa. *PLoS Pathog* 2010, **6**(5): e1000902.
251. Bajka BH, Topping DL, Cobiac L, Clarke JM. Butyrylated starch is less susceptible to enzymic hydrolysis and increases large-bowel butyrate more than high-amylose maize starch in the rat. *The British journal of nutrition* 2006, **96**(2): 276-282.
252. Kaser A, Blumberg RS. Autophagy, Microbial Sensing, Endoplasmic Reticulum Stress, and Epithelial Function in Inflammatory Bowel Disease. *Gastroenterology* 2011, **140**(6): 1738-1747.e1732.
253. Knights D, Lassen KG, Xavier RJ. Advances in inflammatory bowel disease pathogenesis: linking host genetics and the microbiome. *Gut* 2013, **62**(10): 1505-1510.
254. Higgins LM, Frankel G, Douce G, Dougan G, MacDonald TT. *Citrobacter rodentium* infection in mice elicits a mucosal Th1 cytokine response and lesions similar to those in murine inflammatory bowel disease. *Infection and immunity* 1999, **67**(6): 3031-3039.
255. Ma C, Wickham ME, Guttman JA, Deng W, Walker J, Madsen KL, *et al.* *Citrobacter rodentium* infection causes both mitochondrial dysfunction and intestinal epithelial barrier disruption in vivo: role of mitochondrial associated protein (Map). *Cellular microbiology* 2006, **8**(10): 1669-1686.
256. Maloy KJ, Powrie F. Intestinal homeostasis and its breakdown in inflammatory bowel disease. *Nature* 2011, **474**(7351): 298-306.

257. Cader MZ, Kaser A. Recent advances in inflammatory bowel disease: mucosal immune cells in intestinal inflammation. *Gut* 2013, **62**(11): 1653-1664.
258. NUGENT SG, KUMAR D, RAMPTON DS, EVANS DF. Intestinal luminal pH in inflammatory bowel disease: possible determinants and implications for therapy with aminosalicylates and other drugs. *Gut* 2001, **48**(4): 571-577.
259. Colgan SP. Targeting hypoxia in inflammatory bowel disease. *Journal of investigative medicine : the official publication of the American Federation for Clinical Research* 2016, **64**(2): 364-368.
260. Lassen Kara G, McKenzie Craig I, Mari M, Murano T, Begun J, Baxt Leigh A, *et al.* Genetic Coding Variant in GPR65 Alters Lysosomal pH and Links Lysosomal Dysfunction with Colitis Risk. *Immunity*.
261. Ryder C, McColl K, Zhong F, Distelhorst CW. Acidosis promotes Bcl-2 family-mediated evasion of apoptosis: involvement of acid-sensing G protein-coupled receptor Gpr65 signaling to Mek/Erk. *The Journal of biological chemistry* 2012, **287**(33): 27863-27875.
262. He XD, Tobo M, Mogi C, Nakakura T, Komachi M, Murata N, *et al.* Involvement of proton-sensing receptor TDAG8 in the anti-inflammatory actions of dexamethasone in peritoneal macrophages. *Biochemical and biophysical research communications* 2011, **415**(4): 627-631.
263. Kottyan LC, Collier AR, Cao KH, Niese KA, Hedgebeth M, Radu CG, *et al.* Eosinophil viability is increased by acidic pH in a cAMP- and GPR65-dependent manner. *Blood* 2009, **114**(13): 2774-2782.
264. Sitrin RG, Sassanella TM, Petty HR. An Obligate Role for Membrane-Associated Neutral Sphingomyelinase Activity in Orienting Chemotactic Migration of Human Neutrophils. *American journal of respiratory cell and molecular biology* 2011, **44**(2): 205-212.
265. Izgut-Uysal VN, Agac A, Karadogan I, Derin N. Effects of L-carnitine on neutrophil functions in aged rats. *Mechanisms of ageing and development* 2003, **124**(3): 341-347.
266. Hartmann P, Szabó A, Erős G, Gurabi D, Horváth G, Németh I, *et al.* Anti-inflammatory effects of phosphatidylcholine in neutrophil leukocyte-dependent acute arthritis in rats. *European journal of pharmacology* 2009, **622**(1–3): 58-64.
267. Jung YY, Nam Y, Park YS, Lee HS, Hong SA, Kim BK, *et al.* Protective Effect of Phosphatidylcholine on Lipopolysaccharide-Induced Acute Inflammation in Multiple Organ Injury. *The Korean Journal of Physiology & Pharmacology : Official Journal of the Korean Physiological Society and the Korean Society of Pharmacology* 2013, **17**(3): 209-216.



268. Vance JE, Tasseva G. Formation and function of phosphatidylserine and phosphatidylethanolamine in mammalian cells. *Biochimica et Biophysica Acta (BBA) - Molecular and Cell Biology of Lipids* 2013, **1831**(3): 543-554.
269. Robinson BS, Hii CS, Poulos A, Ferrante A. Effect of tumor necrosis factor- $\alpha$  on the metabolism of arachidonic acid in human neutrophils. *Journal of lipid research* 1996, **37**(6): 1234-1245.
270. Xu X, Jin T. The Novel Functions of the PLC/PKC/PKD Signaling Axis in G Protein-Coupled Receptor-Mediated Chemotaxis of Neutrophils. *Journal of Immunology Research* 2015, **2015**: 817604.
271. Dougherty RW, Dubay GR, Nidel JE. Dynamics of the diacylglycerol responses of stimulated phagocytes. *The Journal of biological chemistry* 1989, **264**(19): 11263-11269.
272. Andrade MER, Santos RdGCd, Soares ADN, Costa KA, Fernandes SOA, de Souza CM, *et al.* Pretreatment and Treatment With L-Arginine Attenuate Weight Loss and Bacterial Translocation in Dextran Sulfate Sodium Colitis. *Journal of Parenteral and Enteral Nutrition* 2015.
273. Porras M, Martín MT, Yang P-C, Jury J, Perdue MH, Vergara P. Correlation between cyclical epithelial barrier dysfunction and bacterial translocation in the relapses of intestinal inflammation. *Inflammatory Bowel Diseases* 2006, **12**(9): 843-852.
274. Rotstein OD, Fiegel VD, Simmons RL, Knighton DR. The deleterious effect of reduced pH and hypoxia on neutrophil migration in vitro. *Journal of Surgical Research* 1988, **45**(3): 298-303.
275. Simchowicz L, Cragoe EJ, Jr. Regulation of human neutrophil chemotaxis by intracellular pH. *The Journal of biological chemistry* 1986, **261**(14): 6492-6500.
276. Stock C, Schwab A. Role of the Na/H exchanger NHE1 in cell migration. *Acta Physiol (Oxf)* 2006, **187**(1-2): 149-157.
277. Simchowicz L. Chemotactic factor-induced activation of Na<sup>+</sup>/H<sup>+</sup> exchange in human neutrophils. II. Intracellular pH changes. *The Journal of biological chemistry* 1985, **260**(24): 13248-13255.
278. Wallert MA, Thronson HL, Korpi NL, Olmschenk SM, McCoy AC, Funfar MR, *et al.* Two G protein-coupled receptors activate Na<sup>+</sup>/H<sup>+</sup> exchanger isoform 1 in Chinese hamster lung fibroblasts through an ERK-dependent pathway. *Cellular signalling* 2005, **17**(2): 231-242.
279. Okajima F. Regulation of inflammation by extracellular acidification and proton-sensing GPCRs. *Cellular signalling* 2013, **25**(11): 2263-2271.

280. Fan X, Patera AC, Pong-Kennedy A, Deno G, Gonsiorek W, Manfra DJ, *et al.* Murine CXCR1 Is a Functional Receptor for GCP-2/CXCL6 and Interleukin-8/CXCL8. *Journal of Biological Chemistry* 2007, **282**(16): 11658-11666.
281. Pereira S, Zhou M, Mócsai A, Lowell C. Resting Murine Neutrophils Express Functional  $\alpha 4$  Integrins that Signal Through Src Family Kinases. *The Journal of Immunology* 2001, **166**(6): 4115-4123.
282. Heit B, Colarusso P, Kubes P. Fundamentally different roles for LFA-1, Mac-1 and  $\alpha 4$ -integrin in neutrophil chemotaxis. *Journal of Cell Science* 2005, **118**(22): 5205-5220.
283. Sugiura T, Kageyama S, Andou A, Miyazawa T, Ejima C, Nakayama A, *et al.* Oral treatment with a novel small molecule alpha 4 integrin antagonist, AJM300, prevents the development of experimental colitis in mice. *Journal of Crohn's and Colitis* 2013, **7**(11): e533-e542.
284. Cherry LN, Yunker NS, Lambert ER, Vaughan D, Lowe DK. Vedolizumab: an  $\alpha 4\beta 7$  integrin antagonist for ulcerative colitis and Crohn's disease. *Therapeutic Advances in Chronic Disease* 2015.
285. Tomalka J, Ganesan S, Azodi E, Patel K, Majmudar P, Hall BA, *et al.* A Novel Role for the NLR4 Inflammasome in Mucosal Defenses against the Fungal Pathogen *Candida albicans*. *PLoS pathogens* 2011, **7**(12): e1002379.
286. Castellone RD, Leffler NR, Dong L, Yang LV. Inhibition of tumor cell migration and metastasis by the proton-sensing GPR4 receptor. *Cancer Letters* 2011, **312**(2): 197-208.
287. Zhu Z, Zheng T, Homer RJ, Kim Y-K, Chen NY, Cohn L, *et al.* Acidic Mammalian Chitinase in Asthmatic Th2 Inflammation and IL-13 Pathway Activation. *Science* 2004, **304**(5677): 1678.
288. Albloui FS, Muthana M, Wilson AG, Grabowski PS. AB0087 Tissue localisation of acid sensing proteins in synovial biopsies from patients with rheumatoid arthritis. *Annals of the rheumatic diseases* 2013, **72**(Suppl 3): A812.
289. Huang XP, Karpiak J, Kroeze WK, Zhu H, Chen X, Moy SS, *et al.* Allosteric ligands for the pharmacologically dark receptors GPR68 and GPR65. *Nature* 2015, **527**(7579): 477-483.
290. Boonen GJJ, de Koster BM, VanSteveninck J, Elferink JGR. Neutrophil chemotaxis induced by the diacylglycerol kinase inhibitor R59022. *Biochimica et Biophysica Acta (BBA) - Molecular Cell Research* 1993, **1178**(1): 97-102.

291. May GL, Wright LC, Obbink KG, Byleveld PM, Garg ML, Ahmad ZI, *et al.* Increased saturated triacylglycerol levels in plasma membranes of human neutrophils stimulated by lipopolysaccharide. *Journal of lipid research* 1997, **38**(8): 1562-1570.
292. Wright LC, Obbink KL, Delikatny EJ, Santangelo RT, Sorrell TC. The origin of <sup>1</sup>H NMR-visible triacylglycerol in human neutrophils. Highfatty acid environments result in preferential sequestration of palmitic acid into plasma membrane triacylglycerol. *European journal of biochemistry / FEBS* 2000, **267**(1): 68-78.
293. Wang J-Q, Kon J, Mogi C, Tobo M, Damirin A, Sato K, *et al.* TDAG8 Is a Proton-sensing and Psychosine-sensitive G-protein-coupled Receptor. *Journal of Biological Chemistry* 2004, **279**(44): 45626-45633.
294. Swamydas M, Lionakis MS. Isolation, Purification and Labeling of Mouse Bone Marrow Neutrophils for Functional Studies and Adoptive Transfer Experiments. *Journal of visualized experiments : JoVE* 2013(77): 50586.
295. Roy CC, Ste-Marie M, Chartrand L, Weber A, Bard H, Doray B. Correction of the malabsorption of the preterm infant with a medium-chain triglyceride formula. *The Journal of pediatrics* 1975, **86**(3): 446-450.
296. Nagao K, Yanagita T. Medium-chain fatty acids: functional lipids for the prevention and treatment of the metabolic syndrome. *Pharmacological research : the official journal of the Italian Pharmacological Society* 2010, **61**(3): 208-212.
297. Beura LK, Hamilton SE, Bi K, Schenkel JM, Odumade OA, Casey KA, *et al.* Recapitulating adult human immune traits in laboratory mice by normalizing environment. *Nature* 2016, **532**(7600): 512-516.
298. Gonzalo JA, Lloyd CM, Kremer L, Finger E, Martinez-A C, Siegelman MH, *et al.* Eosinophil recruitment to the lung in a murine model of allergic inflammation. The role of T cells, chemokines, and adhesion receptors. *Journal of Clinical Investigation* 1996, **98**(10): 2332-2345.
299. Vermaelen KY, Carro-Muino I, Lambrecht BN, Pauwels RA. Specific Migratory Dendritic Cells Rapidly Transport Antigen from the Airways to the Thoracic Lymph Nodes. *The Journal of Experimental Medicine* 2001, **193**(1): 51-60.
300. Wills-Karp M. IMMUNOLOGIC BASIS OF ANTIGEN-INDUCED AIRWAY HYPERRESPONSIVENESS. *Annual review of immunology* 1999, **17**(1): 255-281.
301. F. Vanhoutte SD, T. Van Kaem, M-H. Gouy, R. Blanqué, R. Brys, N. Vandeghinste, L. Gheyle, W. Haazen, G. van't Klooster, J. Beetens. Human safety, pharmacokinetics and

pharmacodynamics of the GPR84 antagonist GLPG1205, a potential new approach to treat IBD. *10th Congress of ECCO*. Barcelona: European Crohn's and Colitis Organisation 2015.

302. Laroui H, Ingersoll SA, Liu HC, Baker MT, Ayyadurai S, Charania MA, *et al.* Dextran Sodium Sulfate (DSS) Induces Colitis in Mice by Forming Nano-Lipocomplexes with Medium-Chain-Length Fatty Acids in the Colon. *PloS one* 2012, **7**(3): e32084.
303. Stagg AJ, Hart AL, Knight SC, Kamm MA. The dendritic cell: its role in intestinal inflammation and relationship with gut bacteria. *Gut* 2003, **52**(10): 1522-1529.
304. Du Toit E, Browne L, Irving-Rodgers H, Massa HM, Fozzard N, Jennings MP, *et al.* Effect of GPR84 deletion on obesity and diabetes development in mice fed long chain or medium chain fatty acid rich diets. *European Journal of Nutrition* 2017: 1-10.

## Appendices

### Appendix 1

Alison N. Thorburn, **Craig I. McKenzie**, Sj Shen, Dragana Stanley, Laurence Macia, Linda J. Mason, Laura K. Roberts, Connie H. Y. Wong, Raymond Shim, Remy Robert, Nina Chevalier, Jian Tan, Eliana Mariño, Rob J. Moore, Lee Wong, Malcolm J. McConville, Dedreia L. Tull, Lisa G. Wood, Vanessa E. Murphy, Joerg Mattes, Peter G Gibson, Charles R. Mackay, Evidence that asthma is a developmental origin disease influenced by maternal diet and bacterial metabolites, *Nature Communications* (2015)

## ARTICLE

Received 5 Mar 2015 | Accepted 27 Apr 2015 | Published 23 Jun 2015

DOI: 10.1038/ncomms8320

# Evidence that asthma is a developmental origin disease influenced by maternal diet and bacterial metabolites

Alison N. Thorburn<sup>1</sup>, Craig I. McKenzie<sup>1</sup>, Sj Shen<sup>1</sup>, Dragana Stanley<sup>2</sup>, Laurence Macia<sup>1</sup>, Linda J. Mason<sup>1</sup>, Laura K. Roberts<sup>1</sup>, Connie H.Y. Wong<sup>1</sup>, Raymond Shim<sup>1</sup>, Remy Robert<sup>1</sup>, Nina Chevalier<sup>1,3</sup>, Jian K. Tan<sup>1</sup>, Eliana Mariño<sup>1</sup>, Rob J. Moore<sup>4,5</sup>, Lee Wong<sup>6</sup>, Malcolm J. McConville<sup>7,8</sup>, Dedreia L. Tull<sup>8</sup>, Lisa G. Wood<sup>9</sup>, Vanessa E. Murphy<sup>9</sup>, Joerg Mattes<sup>9</sup>, Peter G. Gibson<sup>9</sup> & Charles R. Mackay<sup>1,10</sup>

Asthma is prevalent in Western countries, and recent explanations have evoked the actions of the gut microbiota. Here we show that feeding mice a high-fibre diet yields a distinctive gut microbiota, which increases the levels of the short-chain fatty acid, acetate. High-fibre or acetate-feeding led to marked suppression of allergic airways disease (AAD, a model for human asthma), by enhancing T-regulatory cell numbers and function. Acetate increases acetylation at the Foxp3 promoter, likely through HDAC9 inhibition. Epigenetic effects of fibre/acetate in adult mice led us to examine the influence of maternal intake of fibre/acetate. High-fibre/acetate feeding of pregnant mice imparts on their adult offspring an inability to develop robust AAD. High fibre/acetate suppresses expression of certain genes in the mouse fetal lung linked to both human asthma and mouse AAD. Thus, diet acting on the gut microbiota profoundly influences airway responses, and may represent an approach to prevent asthma, including during pregnancy.

<sup>1</sup> Department of Immunology, Monash University, Clayton, Victoria 3800, Australia. <sup>2</sup> School of Medical and Applied Sciences, Central Queensland University, Rockhampton, Queensland 4702, Australia. <sup>3</sup> Department of Rheumatology and Clinical Immunology, University Medical Center, 79106 Freiburg, Germany. <sup>4</sup> CSIRO Animal, Food, and Health Sciences, Geelong, Victoria 3220, Australia. <sup>5</sup> Department of Microbiology, Monash University, Clayton, Victoria 3800, Australia. <sup>6</sup> Department of Biochemistry and Molecular Biology, Monash University, Clayton, Victoria 3800, Australia. <sup>7</sup> Department of Biochemistry and Molecular Biology, Bio21 Institute of Molecular Science and Biotechnology, University of Melbourne, Melbourne, Victoria 3010, Australia. <sup>8</sup> Metabolomics Australia, Bio21 Institute of Molecular Sciences and Biotechnology, University of Melbourne, Melbourne, Victoria 3010, Australia. <sup>9</sup> Centre for Asthma and Respiratory Disease, Hunter Medical Research Institute, University of Newcastle, Newcastle, New South Wales 2300, Australia. <sup>10</sup> Charles Perkins Centre, Sydney University Medical School, University of Sydney, Sydney, New South Wales 2006, Australia. Correspondence and requests for materials should be addressed to C.M. (email: Charles.Mackay@monash.edu).

The prevailing explanation for the increase in certain inflammatory conditions such as asthma and allergies has been the hygiene hypothesis<sup>1,2</sup>, which proposes that declining family size and improvements in personal hygiene reduce the opportunities for cross-infections in young families. This lack of exposure to infectious agents is thought to result in inappropriate immune regulation, resulting in polarization to Th2 responses. Recently, however, much more attention has focused on diet<sup>3–6</sup>, or the gut microbiota<sup>7–9</sup>, to explain prevalence of inflammatory diseases particularly in Western countries. Numerous studies have noted a correlation between asthma incidence and obesity<sup>10–13</sup>. High fat<sup>14</sup> and low fruit and vegetable<sup>15</sup> consumption is correlated with worse asthma outcomes. Furthermore, Western-style fast food increases asthma risk<sup>16–18</sup>, while a Mediterranean diet (high in fish, fruits, nuts and vegetables) protects against wheeze and asthma in childhood<sup>19</sup>. Consumption of fibre is often reduced in severe asthmatics, and associated with increased eosinophilic airway inflammation<sup>20</sup>.

Although the above studies suggest that diet or the gut microbiota may influence asthma in humans, the cellular mechanisms that have been evoked to date involve either inadequate immune regulation<sup>21</sup>, or a compromised airway epithelium<sup>22</sup>. It is well documented that asthmatics have fewer T regulatory cells (Tregs), and these are also less functional<sup>21,23</sup>. Another view is that asthma is primarily an epithelial disorder<sup>22</sup>, and, in certain susceptible individuals, impaired epithelial barrier function renders the airways vulnerable to various insults, which predispose to asthma. Recently, several groups including our own have outlined mechanisms whereby diet or gut microbial products might affect inflammatory diseases<sup>6,24</sup>, Treg biology<sup>25–28</sup>, dendritic cell (DC) biology<sup>6</sup> or epithelial integrity<sup>29</sup>. Dietary fibre is fermented by colonic commensal bacteria to short-chain fatty acids (SCFAs). SCFAs are anti-inflammatory<sup>24</sup>, promote gut homeostasis<sup>30</sup> and epithelial integrity<sup>4,29</sup>, and regulate the size and function of the colonic Treg pool<sup>25–27</sup>. A recent study reported that dietary fibre and the SCFA propionate protected against allergic airway disease (AAD) in mice<sup>6</sup>. This study found that propionate altered DC biology, which affected their ability to promote Th2 responses. SCFAs are known to act via two principal mechanisms: signalling through ‘metabolite-sensing’ G-protein coupled receptors (GPCRs) such as GPR43, GPR41 and GPR109A, and inhibition of histone deacetylases (HDACs) and consequent effects on gene transcription<sup>4</sup>. In one study<sup>31</sup>, HDAC9 proved particularly important in regulating Foxp3-dependent suppression, and optimal Treg function required acetylation of several lysines in the forkhead domain of Foxp3, and this suppressed IL-2 production. Although Foxp3 and its target genes have been implicated mostly in Treg biology<sup>32</sup>, FoxP3 might also be expressed by non-immune cells such as certain epithelia<sup>33</sup> although this topic remains controversial.

The important role of Tregs in asthma<sup>21</sup>, coupled with profound effects of SCFAs on Treg biology, prompted us to examine diet and metabolites as a basis for the development of asthma. Here we report that a high-fibre diet promotes a microbiota that produces high levels of SCFAs, particularly acetate, which suppressed the development of AAD in mice. This was dependent on Treg cells, and HDAC9 inhibition by SCFAs was a likely molecular mechanism whereby dietary fibre suppressed AAD, since *Hdac9*<sup>−/−</sup> mice were highly resistant to the development of AAD. Our findings emphasize the importance of diet and bacterial metabolites, over hygiene, to explain asthma. Moreover, in addition to our studies in adult mice, we show that maternal diet and metabolites had profound effects on the developing fetus, by affecting transcription of certain Foxp3 target genes in the lung that have been linked to asthma development.

## Results

**A high-fibre diet shapes gut microbial ecology.** First, we investigated whether a high-fibre diet alters gut microbial ecology, or produces higher levels of SCFAs in faeces or blood. Faecal pellets were collected after 3 weeks and microbiota composition assessed by 16S sequencing. The diets had marked effects on the composition of the microbiota by both unweighted and weighted UniFrac ( $P = 2 \times 10^{-5}$ , Fig. 1a). Alpha diversity metrics available in Qiime were compared between the three diets. While there were no significant differences between control and high-fibre, differences were observed between control and no-fibre diet. No-fibre diet had lower Shannon index ( $P = 0.009$ ), observed species ( $P = 0.012$ ) and chao1 ( $P = 0.027$ ) than control. All of the significant metrics with corresponding  $P$  values are given in Supplementary Fig. 1. The diets caused significant perturbations at the phylum level (Fig. 1b). Firmicutes dominated with the control diet ( $P = 8.22 \times 10^{-6}$ ; Qiime calculated ANOVA at a phylum level), Bacteroidetes with a high-fibre diet ( $P = 0.0017$ ) and Proteobacteria with a no-fibre diet ( $P = 7.49 \times 10^{-9}$ ). Interestingly, the high-fibre diet increased ( $P = 1.53 \times 10^{-5}$  and  $8.01 \times 10^{-4}$ , 58- and 215-fold) two operational taxonomical units (OTUs) of the Bacteroidetes phylum, with 95.0 and 98.5% identity to high-acetate-producing *Bacteroides acidifaciens* A40(T) strain (EzTaxon database). Differences in abundance were also observed on the family level (Fig. 1c). The most representative genera were *Clostridium*, *Bacteroides*, *Pandoraea* and unknown genus of *Alphaproteobacteria* (Fig. 1d). An unknown genus of *Alphaproteobacteria* appeared only with the high-fibre diet. A massive blooming of Proteobacteria with the no-fibre diet related to the genus *Pandoraea*, a member of family *Burkholderiaceae* (Fig. 1c,d) with most abundant OTUs from this genera aligning with *Pandoraea norimbergensis* CCUG 39188(T) strain (97.55 to 99.6% sequence similarity, EzTaxon database). Changes in the microbiota composition prompted us to assess SCFA levels in faeces and serum by NMR spectroscopy. The high-fibre diet increased total SCFA levels in both faeces and serum (Fig. 1e). Of the SCFAs, acetate was the most abundant and the high-fibre diet increased acetate in the faeces and serum, whereas the no-fibre diet decreased acetate levels in the serum. In addition, the high-fibre diet increased propionate in the serum, although levels were still very low. Therefore, a high-fibre diet alters the composition of the gut microbiota to produce high levels of SCFAs, leading in particular to high levels of acetate in serum.

**High-fibre diet protects against the development of AAD.** To investigate the immune regulatory effects of diet, and the changes to the microbiota, on AAD, we used the house-dust mite (HDM) model of AAD, which replicates many of the features of human asthma. We fed mice with a control diet, a high-fibre diet (in which the carbohydrates were replaced with high amylose maize resistant starch) or a diet with no-fibre (Supplementary Table 1). All diets contained similar levels of protein, fat and digestible energy, and there were no differences in weight gain over the course of any of the experiments. Mice were provided with the different diets and three weeks later sensitized to HDM intranasally (i.n. day 0, 1 and 2) and challenged i.n. on days 12–15 to induce AAD, which was assessed on day 16 (Fig. 2a). In addition, we also administered acetate (200 mM) in the drinking water and assessed the development of AAD. As expected, HDM induced all the characteristic features of AAD: increased total cells and eosinophils in bronchoalveolar lavage fluid (BALF), eosinophils in blood, Th2 cytokine levels and IFN- $\gamma$  release from mediastinal lymph node (MLN) T cells, IgE levels, lung inflammation, tissue eosinophils, mucous-secreting cells (MSCs) and airway



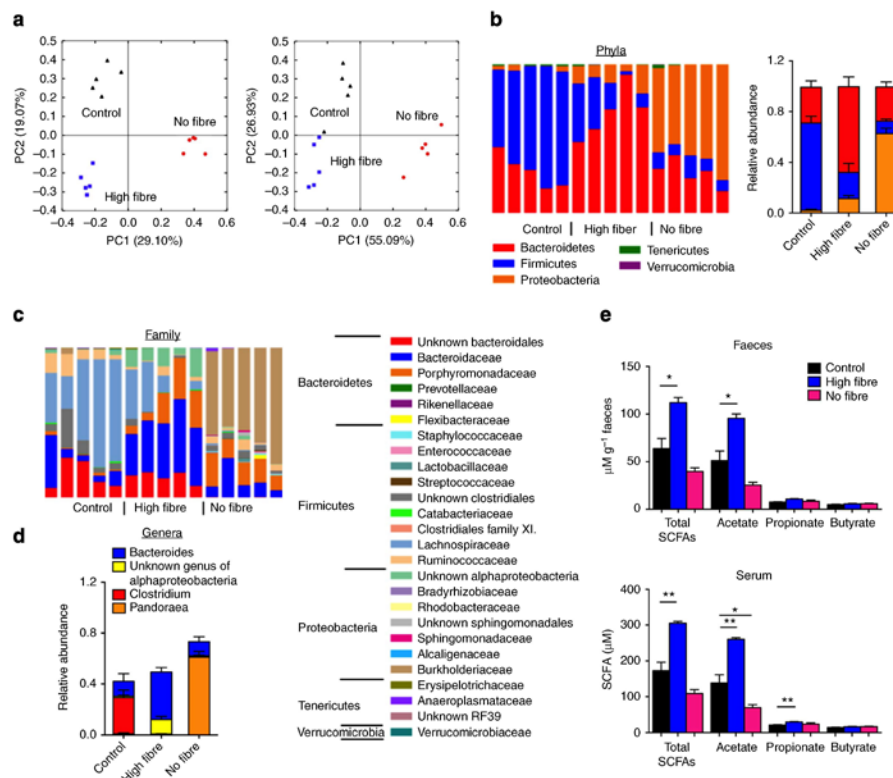


**Figure 1 | High-fibre diet alters the composition of the gut microbiota to produce high levels of acetate.** Adult (6 week old female C57Bl6) mice (obtained from the same facility and cohoused for 3 weeks) were provided different diets for 3 weeks then faeces and blood were collected. The composition of the microbiota was significantly different (Anosim,  $10^6$  permutations) between diets using (a) unweighted ( $P = 2 \times 10^{-5}$ ) and weighted UniFrac ( $P = 2 \times 10^{-5}$ ) analysis. Control diet (black triangles), high-fibre diet (blue squares), no-fibre diet (red circles). Relative abundance and significantly (ANOVA) different (b) phyla, (c) family and (d) genera. (e) SCFA levels in faeces and serum measured by  $^1\text{H}$ -NMR spectroscopy. Data represent mean  $\pm$  s.e.m.,  $n = 5$ . Significance is represented by \* $P < 0.05$ , \*\* $P < 0.01$ , Student's  $t$ -test.

hyper-reactivity (AHR) in terms of airway resistance and dynamic compliance (Fig. 2b–i). When the mice consumed the high-fibre diet or acetate in the drinking water, features of AAD failed to develop (Fig. 2b–i). Acetate had to be given for at least 3 weeks to reduce the development of AAD and acetate still suppressed AAD when administered 3 weeks before sensitization only (Supplementary Fig. 2). Of note, the results were not explained by pH of the acetate solution (Supplementary Fig. 3) and extended to other models of AAD such as ovalbumin (OVA) sensitization (Supplementary Fig. 4). However, acetate did not suppress established AAD (Supplementary Fig. 5), at least using the protocols used here. We also added propionate to the drinking water (200 mM) and found a trend towards lower eosinophil numbers in BALF, decreased IL-13 release from MLN T cells and decreased IgE levels (Supplementary Fig. 6), although these differences did not reach significance. Propionate did result in a small but significant decrease in IL-5 release from MLN T cells. Together these data show that a high-fibre diet and the consumption of acetate, in particular, protects against the development of AAD.

**Maternal diet suppresses AAD responses in adult offspring.** High levels of SCFAs could be expected to induce epigenetic modifications, since SCFAs are natural inhibitors of HDACs. We therefore determined whether the protective effect of high fibre diet, or acetate, could extend to the developing fetus. Indeed previous studies have established that maternal exposures may influence asthma symptoms in offspring<sup>34</sup>. Pregnant mice (embryonic age (E)13) were provided with control, high-fibre or no-fibre diet, or acetate in the drinking water (Fig. 3a). The offspring were weaned at 3 weeks of age onto the control diet. When the offspring were 6 weeks old, AAD was induced. Strikingly, when the mother consumed the high-fibre diet or acetate, features of AAD failed to develop in the adult (6–8 wk old) offspring, as evidenced by a reduction of total cells and eosinophils in BALF, eosinophils in blood, Th2 cytokine and IFN- $\gamma$  release from MLN T cells, IgE, lung inflammation, tissue eosinophils, MSCs and AHR (Fig. 3b–i). Maternal intake of a high-fibre diet or acetate also protected against the development of AAD when the offspring were younger (3 weeks old) or older (16 weeks old) (Supplementary Fig. 7).



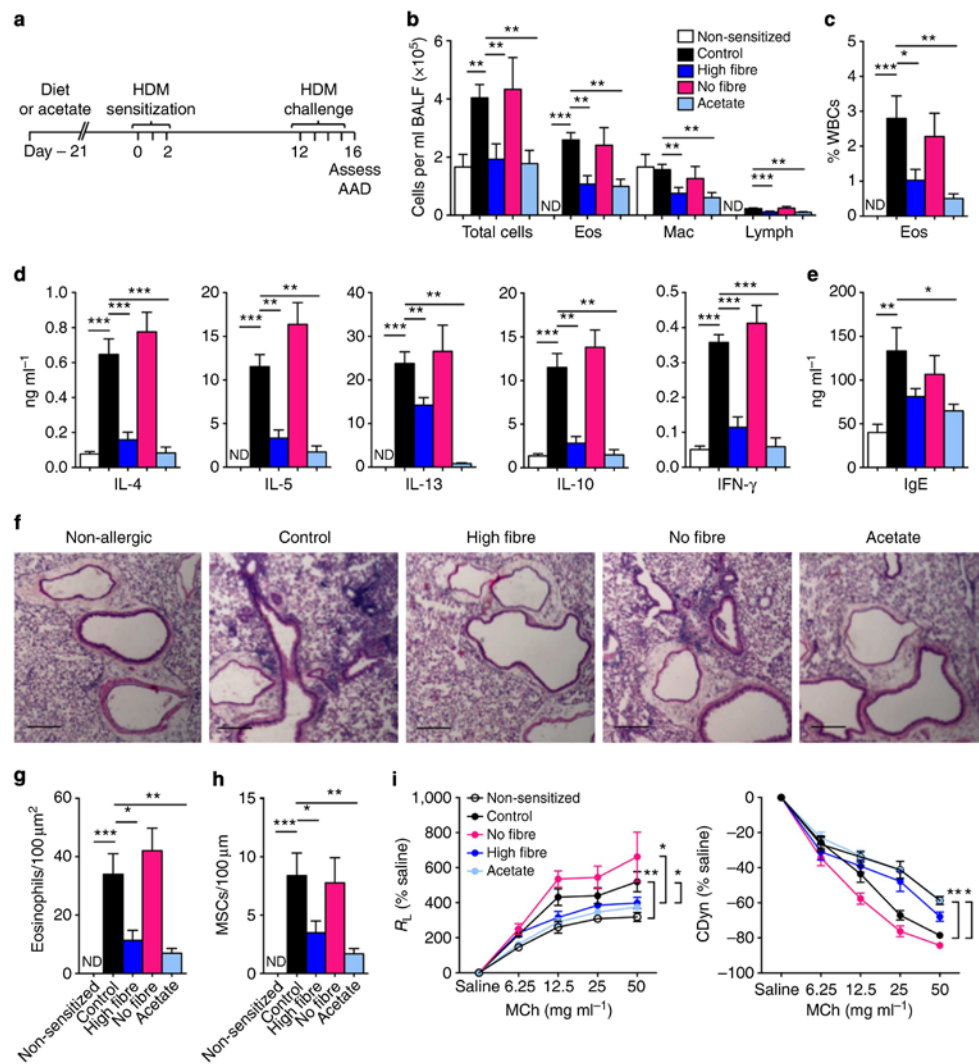


**Figure 2 | The effect of high-fibre diet and acetate on the development of AAD in adult mice.** (a) Mice (female C57Bl6) were weaned onto control, high-fibre diet, no-fibre diet, or acetate for 3 weeks and at 6 weeks old sensitized and challenged with HDM. The effect of high-fibre or no-fibre diet on (b) differential cell number in BALF, (c) eosinophils in blood, (d) IL-4, IL-5, IL-13, IL-10 and IFNγ release from MLN T cells, (e) serum IgE, (f) lung histology (scale bar 200 μm), (g) eosinophils in lung tissue, (h) mucous-secreting cells (MSCs) and (i) airway hyper-responsiveness in terms of airway resistance ( $R_L$ ) and dynamic compliance (Cdyn). Data represent mean ± s.e.m.,  $n = 8$ . Significance is represented by \* $P < 0.05$ , \*\* $P < 0.01$ , \*\*\* $P < 0.001$ , Student's  $t$ -test. One representative experiment of three is shown. ND, not detected.

**Effects of maternal diet are mediated *in utero*.** Interestingly, we found that consumption of the high-fibre diet or acetate after birth and throughout lactation (birth–3wks) had no effect on the development of AAD in the offspring later in life (Supplementary Fig. 8). In contrast, when mice received high-fibre diet or acetate from E13 until birth only, AAD failed to develop in the offspring (Fig. 4a–e). The effect of high-fibre diet and/or acetate may be due to maternal transfer of a specific microbiota to the offspring at

birth. We next caesarean-transferred offspring from mice receiving high-fibre diet or acetate to mothers receiving control diet or water (Fig. 4f) and found that features of AAD were still markedly reduced in the offspring (Fig. 4g–j). Similarly, the same result was seen when the offspring were transferred immediately after birth (Supplementary Fig. 9). However, when offspring were transferred from mothers receiving the control diet or water to mothers that had received high-fibre or acetate, they continued to

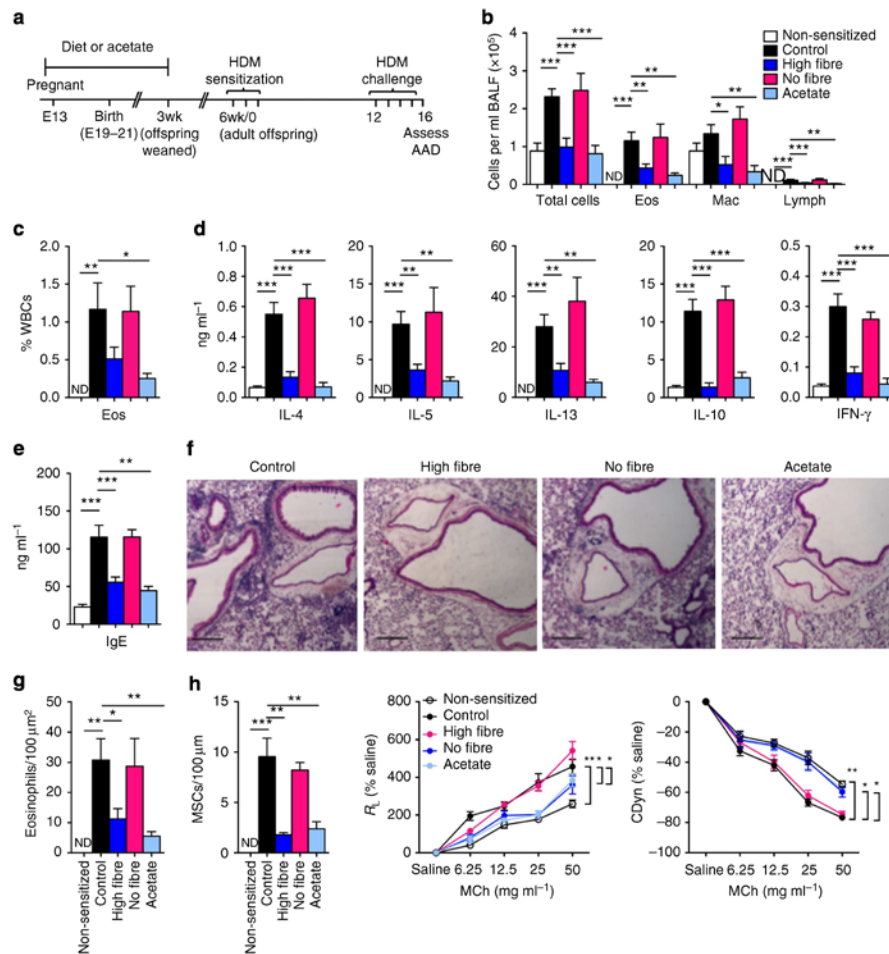


**Figure 3 | The effect of maternal intake of high-fibre diet and acetate on the development of AAD in the offspring.** (a) Pregnant mice (E13, C57Bl6) were provided with control, high-fibre diet, no-fibre diet or acetate. Offspring (female C57Bl6) were weaned onto control diet and water at 3 weeks of age and at 6 weeks, sensitized and challenged with HDM. The effect of high-fibre diet or acetate on (b) differential cell number in BALF, (c) eosinophils in blood, (d) IL-4, IL-5, IL-13, IL-10 and IFN-γ release from MLN T cells, (e) serum IgE, (f) lung histology (scale bar, 200 μm), (g) eosinophils in lung tissue, (h) mucous-secreting cells (MSCs), and airway hyperresponsiveness in terms of airway resistance ( $R_L$ ) and dynamic compliance (Cdyn). Data represent mean ± s.e.m.,  $n = 8$ . Significance is represented by \* $P < 0.05$ , \*\* $P < 0.01$ , \*\*\* $P < 0.001$ , Student's  $t$ -test. One representative experiment of three is shown. ND, not detected.

develop AAD (Supplementary Fig. 10), despite adopting a microbiota more similar to their foster mother (Supplementary Fig. 11). To investigate whether the effect was transferable between mice, we cohoused the offspring from different mothers. Only the mice whose mother received high-fibre diet or acetate failed to develop AAD (Supplementary Fig. 12). Since the microbial transfer was not a key factor in mediating suppression of AAD in the offspring, we investigated whether acetate was being transferred across the placenta to the fetus. It is likely that, levels of acetate in the fetal blood were increased when the mother was on a high-fibre diet or acetate (Fig. 4k). Together this data shows that the effects of maternal intake of a high-fibre diet

or acetate on AAD are mediated *in utero* and are independent of transfer of a specific microbiota.

#### Evidence that human asthma may associate with maternal diet.

To investigate the relationship between dietary fibre intake during human pregnancy and SCFA levels, we obtained sera from pregnant women and dietary fibre intake was calculated by a 24 h food recall (Supplementary Table 2). Consistent with previous studies on the relationship between fibre intake and serum acetate levels<sup>35</sup>, we found that high dietary fibre intake during late pregnancy was associated with higher acetate (but not propionate

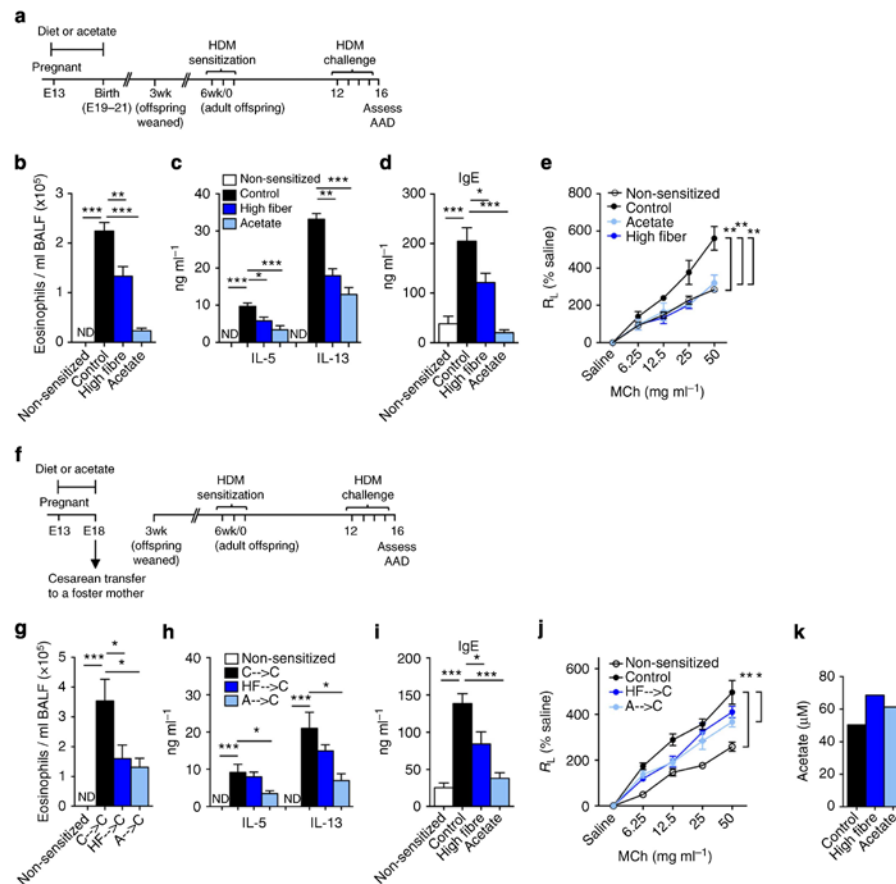


**Figure 4 | Effects of maternal diet or acetate on AAD are mediated *in utero* independently of microbial transfer.** (a) Pregnant mice (E13, C57Bl/6) were provided with control, high-fibre diet or acetate. At birth, the control diet or water was provided. Female offsprings were also weaned onto control diet and water at 3 weeks of age and at 6 weeks, sensitized and challenged with HDM. The effect of high-fibre diet or acetate during pregnancy on (b) eosinophil cell number in BALF, (c) IL-5 and IL-13 release from MLN T cells, (d) serum IgE and (e) airway hyperresponsiveness in terms of airway resistance ( $R_s$ ). (f) Pregnant mice (E13) were provided with control, high-fibre diet or acetate. At E18, offspring were caesarean transferred to a foster mother (Balb/c) fed the control diet and water. Female offspring were weaned onto control diet and water at 3 weeks of age and at 6 weeks, sensitized and challenged with HDM. The effect of high-fibre diet or acetate during pregnancy after caesarean transfer on (g) eosinophil cell number in BALF, (h) IL-5 and IL-13 release from MLN T cells, (i) serum IgE and (j) airway hyper-responsiveness in terms of airway resistance ( $R_s$ ). Data represent mean  $\pm$  s.e.m.,  $n = 8$ . Significance is represented by \* $P < 0.05$ , \*\* $P < 0.01$ , \*\*\* $P < 0.001$ , Student's  $t$ -test. One representative experiment of three is shown. ND = not detected. (k) Serum was collected from offspring ( $n = 35$ – $40$  per group) at E18 and acetate levels measured by  $^1\text{H-NMR}$  spectroscopy. Each measurement represents  $\sim 35$ – $40$  pooled individual blood collections.

or butyrate) levels in serum (Fig. 5a). We next obtained serum from pregnant women and data on the development of respiratory symptoms in their infants, in the first year of life (Supplementary Table 3). Strikingly, maternal acetate (but not propionate or butyrate) levels equal to or above the median were associated with a significant decrease in percentage of infants requiring two or more general practitioner (GP) visits for cough or wheeze and a trend toward reduced parent-reported wheeze (Fig. 5b). Furthermore, this association was not observed if the mothers were asthmatic (Supplementary Fig. 13, Supplementary Table 4). Taken together, these results provide initial evidence for

a role of a high-fibre diet and production of acetate in protecting against the development of airway disease in the offspring.

**Hdac9<sup>-/-</sup> mice are protected against AAD.** We next sought to understand mechanisms whereby diet and metabolites affected AAD, in both adults, and in offspring exposed to high-fibre/acetate *in utero*. We have demonstrated previously that the metabolite-sensing receptor GPR43 plays a role in the regulation of inflammatory responses, including OVA-induced AAD<sup>24</sup>. Trompette *et al.*<sup>6</sup> likewise established a role for another

SCFA-sensing receptor, GPR41, in the regulation of AAD. Both GPR43 and GPR41 bind acetate, as well as other SCFAs with various affinities. High-fibre diet and acetate still suppressed AAD in *Gpr43*-deficient mice (Supplementary Fig. 14), suggesting that signalling via GPR43 was not required for suppression of AAD. This result was a deviation from our previous study<sup>24</sup> and presumably relates to animal house differences or different AAD models. Regardless, this prompted us to explore a role for HDACs, as SCFAs are known inhibitors of HDAC activity. Indeed, cells from whole-lung of acetate-treated adult mice had reduced HDAC activity (Fig. 6a). However, acetate had no effect on HDAC activity in the offspring (Fig. 6a). It is unknown which HDAC class acetate affects specifically, although HDAC9 has

been strongly implicated in the control of Treg biology<sup>31</sup>. In support of this, we found that *Hdac9*<sup>-/-</sup> mice were highly resistant to the development of AAD (Fig. 6b–e). Furthermore, when *Hdac9*<sup>-/-</sup> females were crossed with WT males, the *Hdac9*<sup>+/-</sup> offspring were protected against the development of AAD (Fig. 6f). Although indirect, this highlights the possibility that acetate may inhibit HDAC9, as there are similar effects of acetate-feeding, and HDAC9 deficiency, on AAD.

**Acetate promotes Treg suppression of AAD.** HDAC inhibition is known to induce Treg cells<sup>31</sup>. We assessed acetylation at the *Foxp3* promoter region and found that acetate increased

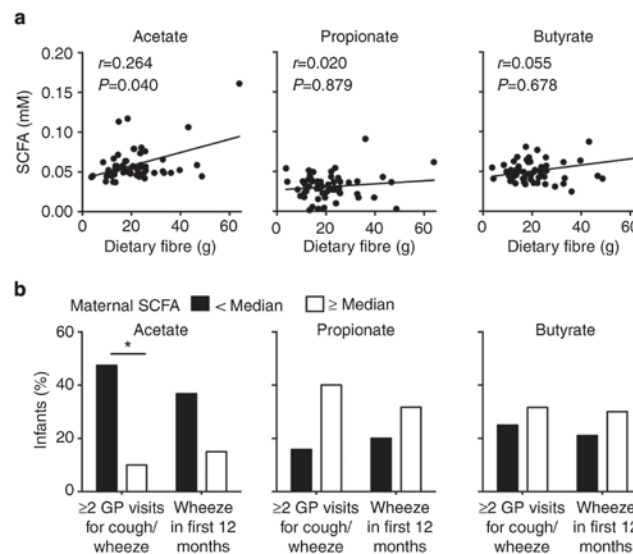


**Figure 5 | SCFA levels and dietary fibre intake in pregnant women, and respiratory symptoms in their offspring.** (a) Serum was collected from pregnant women (during late phase pregnancy) and SCFA levels determined by <sup>1</sup>H-NMR spectroscopy. Dietary fibre was calculated from a 24 h food recall at the same time as serum collection; *n* = 61, Spearman rank correlation. (b) Serum was collected from pregnant women (during late phase pregnancy) and SCFA levels determined by <sup>1</sup>H-NMR spectroscopy. Percentage of offspring (infants) with ≥2 general practitioner (GP) visits for cough/wheeze and with parent-reported wheeze in the first 12 months was recorded. Solid bars represent mothers with SCFA < median (acetate = 0.05315 mM, propionate = 0.03083 mM, butyrate = 0.03385 mM) open bars represent mothers with SCFA ≥ median, *n* = 40, \**P* < 0.05,  $\chi^2$ -test.

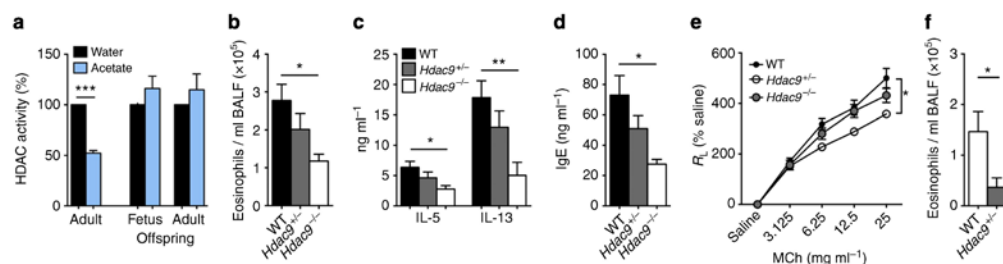


**Figure 6 | The effect of acetate on HDAC activity in the lung, and the development of AAD in *Hdac9*<sup>-/-</sup> versus WT (C57Bl6, female) mice.** (a) HDAC activity in the whole lung (*n* = 6). Development of AAD in *Hdac9*<sup>-/-</sup> versus WT mice in terms of (b) eosinophil cell number in BALF, (c) IL-5 and IL-13 release from MLN T cells, (d) serum IgE and (e) airway hyperresponsiveness in terms of airway resistance (R<sub>t</sub>). (f) Eosinophils in BALF in *Hdac9*<sup>+/-</sup> offspring from *Hdac9*<sup>-/-</sup> females crossed with WT males, in the HDM AAD model. Data represent mean ± s.e.m., *n* = 8. Significance is represented by \**P* < 0.05, \*\**P* < 0.01, \*\*\**P* < 0.001, Student's *t*-test. One representative experiment of three is shown.



acetylation at H4 in both the adult and the offspring (Fig. 7a), which depicts a 'primed' Foxp3 state. Indeed, Foxp3 was expressed at higher levels in whole-lung of acetate-treated mice, both adults and offspring, but only when AAD was induced (Fig. 7b). This extended to an increase in the percentage and number of Tregs in peripheral lymph nodes in adult and offspring, when AAD was induced (Fig. 7c). Furthermore, the Tregs from mice receiving acetate were more suppressive on a per cell basis (Fig. 7d). To confirm the importance of Tregs, we next employed anti-CD25 to deplete Tregs, and showed that Tregs were required for acetate-mediated suppression of AAD in adult mice (Fig. 7e–h). Furthermore, to address whether the inheritable suppression of AAD induced by acetate involves Tregs and can be recapitulated in young mice, we administered anti-CD25 to 3-week-old offspring from mothers given acetate during pregnancy and induced AAD. Acetate administered to pregnant mothers suppressed AAD in young offspring, and this was at least partially dependent on Treg cells (Fig. 7i). Therefore, acetate promotes acetylation at Foxp3, which promotes Tregs that are highly suppressive and required for suppression of AAD in both young and adult mice.

**High-fibre/acetate promote gene regulation in fetal lung.** Foxp3 is expressed by certain epithelia in the lung<sup>33</sup>. As acetylation at the Foxp3 promoter was altered in the offspring when the mother received acetate in the drinking water, we speculated that gene expression in the lung may be affected by metabolites *in utero*. Using microarray, we identified 23 genes, some of which were highly differentially expressed in the lung of E21 fetuses from high-fibre fed mothers versus control groups, and 20 differentially expressed genes between acetate and control groups (Supplementary Fig. 15, Supplementary Table 5). The majority of genes identified were downregulated, which included the genes with the highest fold-change. Molecular network analysis indicated that putative targets for the effects of both high-fibre and acetate were principally involved in embryonic and organ development, cardiovascular disease, developmental disorders and others (Supplementary Tables 6–8).

As both high-fibre and acetate suppressed the development of AAD, we focused on genes that associated with both groups (Fig. 8a, Supplementary Table 5). Three genes *Nppa*, *Ankrd1* and *Pln* were markedly downregulated in the lungs of both the high-fibre and acetate-fed groups, versus control-fed mice, and

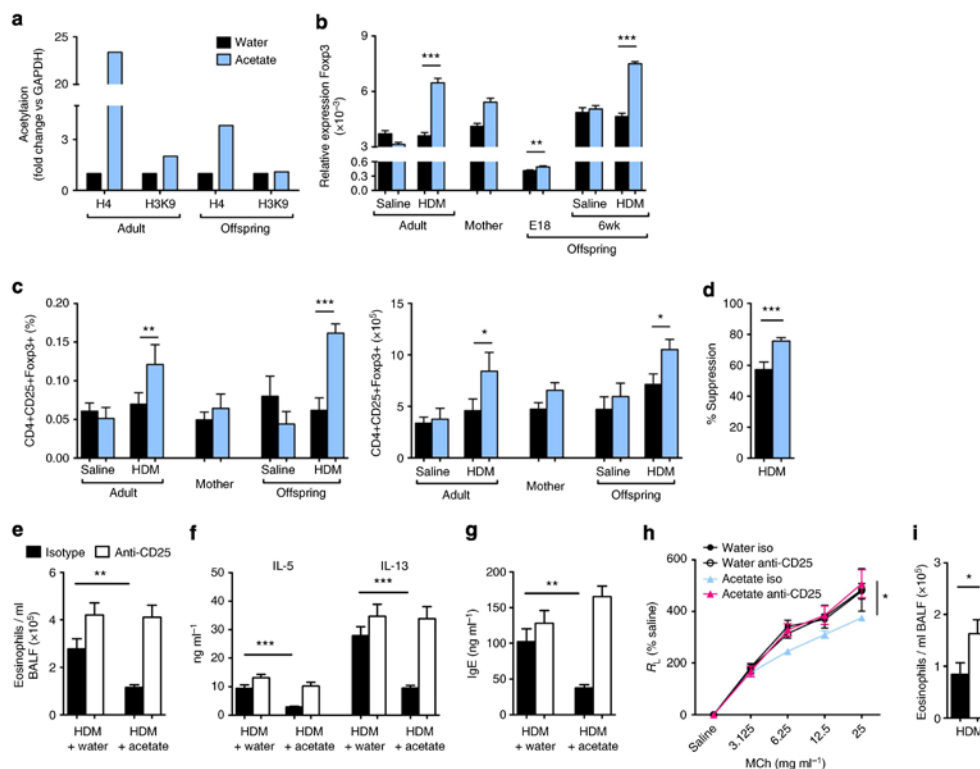


**Figure 7 | Priming of Foxp3, Foxp3 expression and Treg in acetate-mediated suppression of AAD.** (a) Acetylation of histones at the Foxp3 promoter (adult = acetate from day -21 to end of model, offspring = acetate by mother D12-lactation). (b) Foxp3 expression in the lung. (c) Percentage and number of Treg cells in the lung. (d) Effect of acetate on Treg suppressive capacity (Treg isolated from the spleen of mice receiving water or acetate). The effect of anti-CD25 mediated Treg depletion on acetate mediated suppression of AAD in terms of (e) eosinophil cell number in BALF, (f) IL-5 and IL-13 release from MLN T cells, (g) serum IgE and (h) airway hyperresponsiveness in terms of airway resistance ( $R_s$ ). (i) AAD and the effect of anti-CD25 mediated Treg depletion in 3-week-old female offspring from mothers (C57Bl/6) fed acetate, in terms of eosinophil cell number in BALF. Data represent mean  $\pm$  s.e.m.,  $n = 8$ . Significance is represented by \* $P < 0.05$ , \*\* $P < 0.01$ , \*\*\* $P < 0.001$ , Student's  $t$ -test. One representative experiment of three is shown.

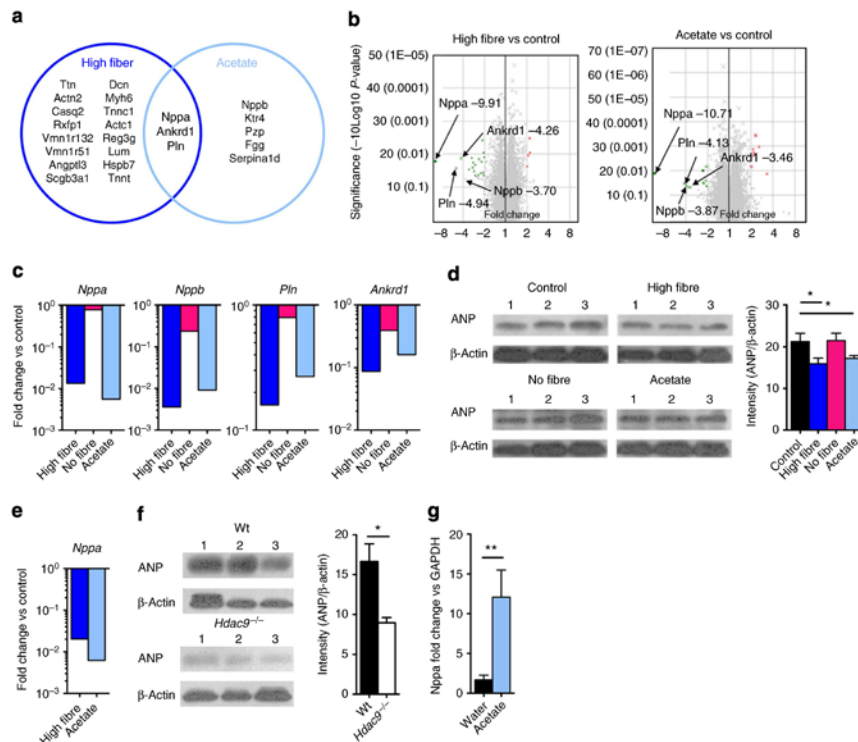


**Figure 8 | The effect of maternal diet and acetate on gene expression in the fetal lung.** (a) Venn diagram representation of gene expression in female fetal lung from mothers (C57Bl6) receiving high-fibre diet or acetate versus control,  $>2$ -fold change,  $P < 0.05$ ,  $n = 4$ . (b) Gene expression profile in fetal lungs by volcano plot of offspring from mother receiving high-fibre diet versus control and mother receiving acetate versus control. Fold change  $< 2$  (green dots) and  $> 2$  (red dots) where  $P < 0.05$  ( $P > 0.05$  grey dots),  $n = 4$ . (c) The effect of diets and acetate on (c) *Nppa*, *Nppb*, *Pln* and *Ankrd1* gene expression and (d) ANP in fetal lung, assessed by western blot. The effect of diets and acetate on (e) *Nppa* gene expression in adult lung, and (f) ANP levels in whole lungs of *Hdac9*<sup>-/-</sup> versus WT mice. (g) Foxp3 was immunoprecipitated from splenocytes and screened for *Nppa* gene expression versus GAPDH by RT-PCR. Data represent mean  $\pm$  s.e.m.,  $n = 3$ , \* $P < 0.05$ , Student's *t*-test. One representative experiment of three is shown. Throughout this figure, blue bars = high-fibre fed, red bars = no-fibre fed, and green bars = acetate-fed.

recorded the highest fold-changes (Fig. 8b, Supplementary Table 5). These genes (and *Nppb*) are co-regulated (Supplementary Fig. 16), and their downregulation was confirmed using RT-qPCR (Fig. 8c). *Nppa* encodes for atrial natriuretic peptide (ANP), a molecule mostly associated with heart function, but which also has immune-modifying effects<sup>36</sup>. We confirmed lower ANP protein in the lungs by western blot (Fig. 8d). Moreover, *Nppa* transcripts remained downregulated when the offspring were adults (Fig. 8e) suggestive of a sustained epigenetic modification. We then investigated whether HDAC9 was involved in regulation of ANP. Interestingly, network analysis predicted that HDAC9 was an inhibited upstream regulator (Supplementary Table 6), which reiterates our findings in *Hdac9*<sup>-/-</sup> mice (Fig. 6b–e). Indeed, the whole lung of *Hdac9*<sup>-/-</sup> mice expressed very low amounts of ANP compared with WT mice (Fig. 8f). Therefore, acetate-mediated inhibition of HDAC9 is likely to account for the downregulation of ANP. We then investigated whether Foxp3 was involved in the downregulation of *Nppa*. Indeed, *Nppa*-bound Foxp3 was detected at higher levels when the mice received acetate (Fig. 8g), thereby demonstrating that Foxp3 binds directly to

the *Nppa* promoter region, which contains six putative binding sites (Supplementary Fig. 17). Together these data demonstrate that acetate alters gene expression in the fetal lung, including downregulation of *Nppa*, which involves inhibition of HDACs (likely HDAC9) and Foxp3 binding upstream of *Nppa* to suppress ANP production.

## Discussion

This study highlights the importance of a high-fibre diet and acetate in priming Foxp3-mediated protection against the development of asthma. A general scheme for this model is summarized in Fig. 9. We showed that a high-fibre diet altered the composition of the microbiota, increased SCFA production (particularly acetate) and protected against the development of AAD in adult mice. One of the main cellular mechanisms related to acetate effects on Treg cells, particularly HDAC inhibition and epigenetic modification of the Foxp3 promoter. As acetate crosses the placenta, and previous studies had suggested a role for maternal influences on asthma development in offspring, we assessed effects of maternal diet during fetal development. These

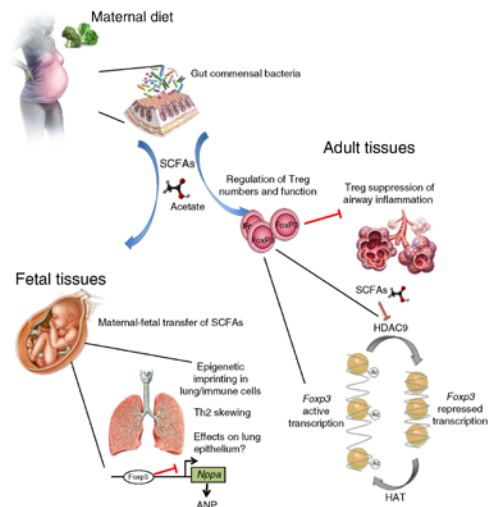


**Figure 9 | Schematic representation of mechanism underlying the effect of maternal fibre intake on the development of asthma, both in the adult, and in offspring.** Fibre consumption leads to changes in the microbiota and SCFA production. Acetate enters the bloodstream and inhibits HDACs, leading to transcription of Foxp3. Foxp3 promotes Treg numbers and function, which suppress airway inflammation. During pregnancy, SCFAs such as acetate are capable of crossing the placenta, and influencing gene expression in the fetal lung, such as *Nppa*, which encodes ANP, a molecule implicated in epithelial biology and immune regulation. It is also likely that maternally transferred acetate affects Treg biology in the fetus.

studies indicated an additional 'developmental origin' to asthma, whereby *in utero* effects of maternal diet shape immune responses in the airways of offspring later in life. This also involved Treg biology, but also likely involves Foxp3-regulated genes in other cell types such as epithelia.

Many studies now implicate an altered gut microbiota for the pathogenesis of various diseases. Gut microbiota composition relates to diet<sup>9,37</sup>; hence, a causative factor for asthma susceptibility may be insufficient consumption of dietary fibre, although antibiotic use could be an additional factor. A Western diet-shaped gut microbiota may produce lower amounts of SCFAs<sup>38</sup>. In our study, change in dietary fibre consumption led to clear variations in the microbiota, evidenced by distinct population clustering in principle component analysis. Further analysis revealed a small decrease in microbial diversity when mice were fed a no-fibre diet, which parallels associations between Western and low-fibre diets and reduced diversity in human population studies<sup>38,39</sup>. However, more marked changes were observed in phylogenetic specifications. Our data in mice showed that high-fibre diet increased Bacteroidetes and decreased Firmicutes, which parallels findings in humans<sup>38</sup>. No-fibre diet enriched Proteobacteria, which has been associated with Western diets and disease states<sup>38,40,41</sup>. On the family level, high-fibre diet supported the outgrowth of Bacteroidaceae, as reported elsewhere<sup>6</sup>. This family contains particularly high-SCFA-producing bacteria such as *Bacteroides acidifaciens*, of which similar species were detected in our analysis. Bacteroides have been associated with increases in Foxp3 expression among CD4<sup>+</sup> T cells<sup>28</sup>. Altogether our study shows that a high-fibre diet, which was effective at preventing robust AAD in mice,

supports a microbiota containing a high abundance of regulatory and non-pathogenic bacteria, which produce high levels of immunoregulatory products such as SCFAs.

We have shown previously that acetate feeding suppressed AAD, implicating a role for fibre. Recently, Trompette *et al.*<sup>6</sup> showed similar findings on the role of dietary fibre. However, we establish a distinct cellular and molecular mechanism: acetate effects on Treg biology. This fits with the established role of SCFAs in regulating HDAC activity, and the important role of Tregs in asthma pathogenesis<sup>21</sup>. A clear result from the present study was the important role of HDAC9 for development of AAD. We showed that *Hdac9*<sup>-/-</sup> mice were resistant to the development of AAD, suggesting that HDAC9 may in part be involved in acetate-mediated suppression of AAD. Indeed, *Hdac9*<sup>-/-</sup> mice have increased numbers of Tregs<sup>31</sup>, which are known to suppress the development of AAD<sup>42</sup>. Furthermore, higher levels of *Hdac9* have been reported in human asthmatics<sup>43</sup>. More specific analysis revealed that the Foxp3 promoter region was highly acetylated at H4 and H3K9. Foxp3 activity is regulated by reversible acetylation, and these acetylation patterns are an indicator of a primed transcriptional state<sup>44,45</sup>. Indeed, acetylation levels correlated with Foxp3 gene expression and Treg number, when AAD was induced, presumably because Tregs are required to prevent inflammation. We speculate that inadequate Treg immune regulation in individuals that consume insufficient quantities of fibre may lead to inappropriate immune responses to airborne and gut-encountered allergens. Such a defect may be additive to other pathways relating to diet or gut microbiota, and asthma pathogenesis.

A striking finding from this study was the ability of maternal diet to shape airway responses in offspring, later in life. On top of the influences that determine airway responses during adulthood, this adds another dimension to the aetiology of asthma. However, molecular and cellular pathways likely overlap. Acetate is the likely mediator of this developmental effect, as acetate in drinking water also yielded similar effects, and acetate is the predominant metabolite produced from fibre by gut bacteria. Acetate is also the main SCFA distributed throughout the body, including to the developing fetus. For instance the concentrations of acetate, butyrate and propionate in the lower colon range from 20 to 40 mM, yet in the blood butyrate and propionate are usually <5 μM, while acetate is 50–100 μM. There is a large body of evidence for epigenetic influences *in utero*, which manifest later in life<sup>46</sup> particularly with regard to obesity, diabetes and cardiovascular disease. The actions of HDACs are one of the main epigenetic mechanisms for the regulation of gene transcription. We also provided preliminary evidence that a developmental origin of asthma could be extended to humans. Our data showed a positive correlation between dietary fibre intake and acetate levels in serum. This finding supports other studies that show high-fibre diet correlates with high SCFA levels<sup>38</sup>. We found that high-acetate levels in pregnant individuals correlated with reduced GP visits for cough and wheeze per year and wheeze in the first 12 months for their offspring. These features are some of the most significant predictors for the subsequent development of asthma in later life<sup>47,48</sup>. Future analysis, when the children are older, will determine whether these children do indeed go on to develop asthma.

Another mechanism whereby bacterial metabolites may influence asthma susceptibility is through effects on cell types in the lung, other than Tregs. This fits with evidence for an epithelial cell contribution to asthma pathogenesis. High-fibre/acetate consumption during pregnancy led to marked down-regulation of *Nppa* transcripts in the lung. The *Nppa* gene in humans has known polymorphisms that are associated with asthma, with SNPs in the minor allele conferring protection<sup>49,50</sup>.



How these SNPs affect the transcription of *Nppa* and subsequent function and level of expression of ANP remains to be determined. ANP binding to its receptors in the airways has been implicated in causing persistent pro-inflammatory effects. In one study, isatin, an endogenous inhibitor of ANP receptor (NPRA) signalling and expression, inhibited airway inflammation in a mouse model of allergic asthma. Leukocyte infiltration to the airways, and airway hyper-reactivity were markedly suppressed by blocking ANP signalling<sup>51</sup>. Receptors for ANP are highly expressed in the lung tissue, including the lung epithelium. Mice deficient in NPRA are resistant to methacholine-induced bronchoconstriction<sup>52</sup>. Another report found that ANP polarizes human DCs towards a Th2-promoting phenotype<sup>53</sup>. Therefore, it is likely that inhibition of *Nppa* transcript expression and the subsequent effect on ANP protein levels is consistent with protection against AAD. Our finding that *Hdac9*<sup>-/-</sup> mice show very low expression of ANP strengthens this conclusion. Furthermore, we found that acetate increased *Nppa*-bound Foxp3, demonstrating that Foxp3 binds directly to the *Nppa* promoter region. Acetate-induced Foxp3 binding to *Nppa* implicates Foxp3 not only in Treg induction but also direct silencing of certain genes. Indeed, Foxp3 binding to promoter regions has been associated with gene silencing<sup>53</sup>. It will be important to determine the precise role of Foxp3 in gene regulation in various cell types other than Tregs, such as macrophages/DCs or epithelial cells. Deficiency of acetate/SCFAs and consequent higher ANP production by DCs or epithelial cells may be one mechanism responsible for skewing T-cell responses to Th2. The fact that acetate and dietary fibre had such a profound effect on gene expression in the fetal lung may relate to the developmental state of cells, and the fact they have yet to be 'locked in' to a gene expression programme<sup>54</sup>. Thus, environmental effects that influence epigenetic mechanisms may be particularly prominent in the developing fetus.

In summary, our findings show that high-fibre diet via the production of acetate primes Foxp3-mediated protection against the development of asthma. These findings align with the current understanding that Tregs are critical in maintaining immune regulation in asthma<sup>21</sup>. These findings potentially explain one aspect of the 'inheritance' of asthma, via diet and epigenetic effects. Furthermore, our data link known gene associations with the development of asthma. Our data may relate to other associations such as the low incidence of asthma in children growing up on a farm<sup>55</sup>, which we speculate may relate to dietary differences between rural and urban settings, or may relate to microbes encountered in the farm environment that are geared for high SCFA production (that is, faeces from livestock that mostly digest fibre). Other organs and disease processes may well be affected by maternal diet and epigenetic effects, such as cardiovascular disease<sup>56</sup> and may involve similar pathways—microbiota-mediated production of SCFAs, acetylation leading to Foxp3 expression and regulation of target genes within Treg cells, or other Foxp3-expressing cells.

## Methods

**Animals.** Female C57Bl6 and BALB/c mice were obtained from the Monash Animal Research Platform, Monash University. *Gpr43*<sup>-/-</sup> and *Hdac9*<sup>-/-</sup> mice were bred and maintained at the Monash Animal Research Platform. All mice were maintained under specific pathogen-free and controlled environmental conditions and randomly allocated to groups. All procedures were approved by the Animal Ethics Committee of Monash University.

**Diet and SCFAs.** Diets used were 'Control' (8720310), 'High fibre' (SF11-025) and 'No fibre' (SF09-028) (Specialty feeds, Perth, Australia; see Supplementary Table S1 for nutritional parameters) and were refreshed three times per week. Acetate or propionate (200 mM, except where indicated) was dissolved into the drinking water

and refreshed three times per week. SCFA levels were determined by <sup>1</sup>H-NMR spectroscopy<sup>57</sup>.

**Bacteria DNA sequencing and bioinformatics.** DNA was extracted in accordance with method of Yu and Morrison<sup>58</sup>. In brief, DNA was extracted and purified using QIAamp DNA stool mini kit (Qiagen) and amplified using primers selected to cover V1-V3 region of bacterial 16S rRNA gene. Sequencing of 16S rRNA gene amplicons was performed with Roche/454 FLX Genome Sequencer using Titanium chemistry and manufacturer's protocols and kits. Data analysis was done using PyroBayes<sup>59</sup>, Pintail<sup>60</sup> and Acacia<sup>61</sup> for pre-processing, and final analysis using Qiime v1.6.0 (ref. 62) with quality trimming settings: sequence lengths of 300–600 bases, no ambiguous sequences and a maximum of 6 homopolymer bases. Data have been deposited into the metagenomic database MG-RAST, ID 12662.

**Models of AAD.** Mice were sensitized to HDM (*Dermatophagoides pteronyssinus*) extract (i.n.; day 0, 1 and 2; 50 µg; Greer Labs, Lenoir, NC) in sterile saline (50 µl) and challenged with HDM (i.n.; day 14–17; 5 µg in 50 µl saline) under isoflurane anaesthesia. Where indicated mice were sensitized to OVA (i.p.; day 0 and 7; 50 µg; Sigma-Aldrich, St Louis, MO) with Rehydrol (1 mg; Reheis, Berkeley Heights, NJ) in sterile saline and challenged (i.n.; day 12–15; 10 µg in 50 µl saline). To recapitulate established disease, mice received HDM (i.n.; day 0, 1 and 2; 50 µg) followed by two sets of challenges (days 11–13 and 33–34)<sup>64</sup>. Where indicated, mice received an anti-CD25 antibody (i.p.; day -3; 100 µg, PC61).

**Assessment of AAD.** BALF and blood cell counts were performed<sup>64</sup>. Cytokine release from MLN and serum IgE was assessed by ELISA. Single-cell suspensions were prepared from MLNs by pushing through 70-µm sieves. A total of 1 × 10<sup>6</sup> cells per well in 96-well U-bottomed plates were cultured in RPMI media supplemented with 10% FCS, HEPES (20 mM), penicillin/streptomycin (10 µg ml<sup>-1</sup>), L-glutamine (2 mM), 2-mercaptoethanol (50 µM), sodium pyruvate (1 mM). Cells were stimulated with HDM (20 µg ml<sup>-1</sup>) and cultured for 96 h (37 °C, 5% CO<sub>2</sub>). Lungs were perfused, inflated, fixed, embedded, sectioned and stained to enumerate tissue eosinophils (H&E) and MSCs<sup>23</sup>. AHR was assessed as per the manufacturer's instructions<sup>63,64</sup>. The investigator was blinded to experimental groups.

**Serum acetate from mothers.** STUDY 1. Serum samples were collected from *n* = 40 pregnant women without asthma, who were participating in a prospective cohort study of viral infection in pregnancy at the John Hunter Hospital, Newcastle between 2007 and 2009 (ref. 65). Samples were collected at a median gestational age of 37.6 weeks (interquartile range: 36.6, 38.4 weeks). Infants of these mothers were prospectively followed to 12 months of age<sup>66</sup> and a validated parent completed questionnaire<sup>67</sup> on respiratory health, family medical history, immunizations and infant feeding was completed. STUDY 2. Serum samples were collected from *n* = 61 pregnant women who were participating in a prospective cohort study at the John Hunter Hospital, Newcastle between 2004 and 2006 (refs 65,68). Samples were collected at a median gestational age of 36 weeks. At this time, women also completed a 24 h food recall. Data were analysed using the Foodworks database (Xyris, Brisbane)<sup>68</sup>. All procedures were approved and patient consent was obtained.

**HDAC activity.** Nuclear extracts were isolated using an extraction kit (Abcam) and HDAC activity assays (BioVision) were performed as per the manufacturer's instructions.

**Chromatin immunoprecipitation.** ChIP was performed as per the manufacturer's instructions. In brief, CD4<sup>+</sup> Foxp3 cells were fixed in 0.6% paraformaldehyde, washed with PBS then lysed in NP-40 lysis buffer (0.5% NP-40, 10 mM Tris-HCl at pH 7.4, 10 mM NaCl, 10 mM MgCl<sub>2</sub> and protease inhibitors) followed by SDS lysis buffer (1% SDS, 10 mM EDTA, 50 mM Tris-HCl at pH 8.1 and protease inhibitors). Sonicated chromatin product was diluted in 1% Triton X-100, 20 mM Tris-HCl at pH 8.0, 150 mM NaCl, 2 mM EDTA and protease inhibitors then pre-cleared with Protein A/G-Sepharose and salmon sperm. ChIP was performed with Anti-acetyl-Histone H3 (Lys9) and Anti-hyperacetylated Histone H4 (Penta) Antibody (Millipore, USA). Chromatin was isolated with Protein A/G-Sepharose and washed with low-salt buffer (0.1% SDS, 1% Triton X-100, 20 mM Tris-HCl at pH 8.1, 150 mM NaCl and 2 mM EDTA), high-salt buffer (0.1% SDS, 1% Triton X-100, 20 mM Tris-HCl at pH 8.1, 500 mM NaCl and 2 mM EDTA) and diluted in LiCl buffer (0.5% NP-40, 0.5% Deoxycholate, 10 mM Tris-HCl at pH 8.1, 1 mM EDTA and 0.25 M LiCl). DNA was eluted in elution buffer (1% SDS and 100 mM NaHCO<sub>3</sub>), de-crosslinked by high-salt treatment (200 mM NaCl) at 65 °C and treated with proteinase K (40 µg ml<sup>-1</sup> proteinase K, 10 mM EDTA, 40 mM Tris-HCl at pH 8.1) at 50 °C. Isolated DNA was subject to qPCR using primers specific for GAPDH (F 5'-CTG CAG TAC TGT GGG GAG GT-3', R 5'-CAA AGG CGG AGT TAC CAG AG-3'), Foxp3 promoter (F 5'-CTG AGG TTT GGA GCA GAA GGA, R 5'-GAG GCA GGT AGA GAC AGC ATT G-3'). *Nppa* promoter



(F 5'-TCT TCT GCT GGC TCC TCA CT-3', R 5'-GCA CGA TCT GAT GTT TGC TG-3').

**Treg assessment.** A total of  $1 \times 10^6$  cells per well in 96-well U-bottomed plates were stained for CD4, CD25 and Foxp3 using the eBioscience perm kit as per manufacturer's instructions and analysed by flow cytometry. For suppression assays CD4+Foxp3GFP+ and CD4+Foxp3GFP cells were isolated by FACS (>95% pure). CD4+Foxp3GFP cells ( $5 \times 10^4$ ) and varying numbers of CD4+Foxp3GFP+ cells were cultured in RPMI (200  $\mu$ l, 10% fetal calf serum; 72 h, 37 °C) with anti-CD28 (1  $\mu$ g ml<sup>-1</sup>; BD Pharmingen) and plate bound anti-CD3 (1  $\mu$ g ml<sup>-1</sup>). Cells were pulsed for the final 18 h of culture with [<sup>3</sup>H] thymidine (Amersham International, UK) and enumerated using a microbeta counter.

**Gene array and RT-PCR.** Cells were lysed in Trizol and RNA extracted as per manufacturer's instructions (Sigma). Gene array was carried out using Affymetrix (Ramacott Centre, Sydney) including analysis by Affymetrix Transcription Analysis Console (TAC) 2.0 software. For RT-PCR, RNA was reverse transcribed into cDNA and gene expression determined by SYBR Green (Sigma) incorporation relative to the house keeping gene *rpl13* (F 5'-ATC CCT CCA CCC TAT GAC AA-3', R 5'-GCC CCA GGT AAG CAA ACT T-3'). *Foxp3* (F 5'-ACT CGC ATG TTC GCC TAC TT-3', R 5'-AGG GAT TGG AGC ACT TGT TG-3'), *Ankrd1* (F 5'-TGC GAT GAG TAT AAA CGG ACG-3', R 5'-GTG GAT TCA AGC ATA TCT CGG AA-3'), *Phi* (F 5'-AAA GTG CAA TAC CTC ACT CGC-3', R 5'-GGC ATT TCA ATA GTG GAG GCT C-3'), *Nppb* (F 5'-GAG GTC ACT CCT ATC CTC TGG-3', R 5'-CC ATT TCC TCC GAC TTT TCT C-3').

**Western blot.** Samples were lysed and protein extracted according to the established protocols (Abcam). BCA (Biorad) was used to determine protein concentrations for loading. Samples were run on 15% SDS-PAGE, transferred to nitrocellulose membranes and using the SNAP i.d. system (Millipore) probed with anti-ANP (Sigma, 1/500) or anti- $\beta$ -actin (Millipore, 1/500) and anti-rabbit secondary antibody (Abcam). Development was by West Pico chemiluminescent substrate (Thermo Scientific) with 10 s exposure to autoradiography film. Band intensity was determined by ImageJ 1.47. Images have been cropped for presentation. Full-size images are presented in Supplementary Figs 18 and 19.

**Statistical analysis.** Animal numbers were initially predetermined using Mead's resource equation. Data were analysed using GraphPad Prism (GraphPad Software, CA) and are represented as the mean  $\pm$  s.e.m. Unpaired Student's *t*-test was used to determine differences between two groups.  $P < 0.05$  was considered statistically significant. Outliers were determined and excluded using Grubb's test. For human data,  $\chi^2$ -test was used to determine the difference between proportions, and Spearman's rank correlation was used. To validate findings, each experiment was performed at least twice. Significance in microbiota comparisons was calculated with QIIME-based ANOVA, beta diversity significance was based on Anosim and  $10^6$  Monte Carlo permutations. Non-parametric two-sample *t*-test with 1000 Monte Carlo permutations was used in alpha diversity comparisons.

## References

- Strachan, D. P. Family size, infection and atopy: the first decade of the "hygiene hypothesis". *Thorax* 55(Suppl 1): S2–S10 (2000).
- Strachan, D. P. Hay fever, hygiene, and household size. *BMJ* 299, 1259–1260 (1989).
- Maslowski, K. M. & Mackay, C. R. Diet, gut microbiota and immune responses. *Nat. Immunol.* 12, 5–9 (2011).
- Thorburn, A. N., Macia, L. & Mackay, C. R. Diet, metabolites, and "Western-lifestyle" inflammatory diseases. *Immunity* 40, 833–842 (2014).
- Devereux, G. The increase in the prevalence of asthma and allergy: food for thought. *Nat. Rev. Immunol.* 6, 869–874 (2006).
- Trompette, A. *et al.* Gut microbiota metabolism of dietary fibre influences allergic airway disease and hematopoiesis. *Nat. Med.* 20, 159–166 (2014).
- Noverr, M. C. & Huffnagle, G. B. Does the microbiota regulate immune responses outside the gut? *Trends Microbiol.* 12, 562–568 (2004).
- Dorrestein, P. C., Mazmanian, S. K. & Knight, R. Finding the missing links among metabolites, microbes, and the host. *Immunity* 40, 824–832 (2014).
- Kau, A. L., Ahern, P. P., Griffin, N. W., Goodman, A. L. & Gordon, J. I. Human nutrition, the gut microbiome and the immune system. *Nature* 474, 327–336 (2011).
- Boulet, L. P. Asthma and obesity. *Clin. Exp. Allergy* 43, 8–21 (2013).
- Sin, D. D. & Sutherland, E. R. Obesity and the lung: 4. Obesity and asthma. *Thorax* 63, 1018–1023 (2008).
- Dixon, A. E. *et al.* An official American Thoracic Society Workshop report: obesity and asthma. *Proc. Am. Thorac. Soc.* 7, 325–335 (2010).
- Jensen, M. E., Wood, L. G. & Gibson, P. G. Obesity and childhood asthma - mechanisms and manifestations. *Curr. Opin. Allergy Clin. Immunol.* 12, 186–192 (2012).
- Wood, L. G., Garg, M. L. & Gibson, P. G. A high-fat challenge increases airway inflammation and impairs bronchodilator recovery in asthma. *J. Allergy Clin. Immunol.* 127, 1133–1140 (2011).
- Wood, L. G. *et al.* Manipulating antioxidant intake in asthma: a randomized controlled trial. *Am. J. Clin. Nutr.* 96, 534–543 (2012).
- Ellwood, P. *et al.* Do fast foods cause asthma, rhinoconjunctivitis and eczema? Global findings from the International Study of Asthma and Allergies in Childhood (ISAAC) phase three. *Thorax* 68, 351–360 (2013).
- Wickens, K. *et al.* Fast foods - are they a risk factor for asthma? *Allergy* 60, 1537–1541 (2005).
- Carey, O. J., Cookson, J. B., Britton, J. & Tattersfield, A. E. The effect of lifestyle on wheeze, atopy, and bronchial hyperreactivity in Asian and white children. *Am. J. Respir. Crit. Care Med.* 154, 537–540 (1996).
- Nagel, G., Weinmayr, G., Kleiner, A., Garcia-Marcos, L. & Strachan, D. P. Effect of diet on asthma and allergic sensitisation in the International Study on Allergies and Asthma in Childhood (ISAAC) Phase Two. *Thorax* 65, 516–522 (2010).
- Berthon, B. S., Macdonald-Wicks, L. K., Gibson, P. G. & Wood, L. G. Investigation of the association between dietary intake, disease severity and airway inflammation in asthma. *Respirology* 18, 447–454 (2013).
- Lloyd, C. M. & Hawrylowicz, C. M. Regulatory T cells in asthma. *Immunity* 31, 438–449 (2009).
- Holgate, S. T. The sentinel role of the airway epithelium in asthma pathogenesis. *Immunol. Rev.* 242, 205–219 (2011).
- Thorburn, A. N. *et al.* Pneumococcal conjugate vaccine-induced regulatory T cells suppress the development of allergic airways disease. *Thorax* 65, 1053–1060 (2010).
- Maslowski, K. M. *et al.* Regulation of inflammatory responses by gut microbiota and chemoattractant receptor GPR43. *Nature* 461, 1282–1286 (2009).
- Smith, P. M. *et al.* The microbial metabolites, short-chain fatty acids, regulate colonic Treg cell homeostasis. *Science* 341, 569–573 (2013).
- Arpaia, N. *et al.* Metabolites produced by commensal bacteria promote peripheral regulatory T-cell generation. *Nature* 504, 451–455 (2013).
- Furusawa, Y. *et al.* Commensal microbe-derived butyrate induces the differentiation of colonic regulatory T cells. *Nature* 504, 446–450 (2013).
- Faith, J. J., Ahern, P. P., Ridaura, V. K., Cheng, J. & Gordon, J. I. Identifying gut microbe-host phenotype relationships using combinatorial communities in gnotobiotic mice. *Sci. Transl. Med.* 6, 220ra211 (2014).
- Fukuda, S. *et al.* Bifidobacteria can protect from enteropathogenic infection through production of acetate. *Nature* 469, 543–547 (2011).
- Macia, L. *et al.* Metabolite-sensing receptors GPR43 and GPR109A facilitate dietary fibre-induced gut homeostasis through regulation of the inflammasome. *Nat. Commun.* 6, 6734 (2015).
- Tao, R. *et al.* Deacetylase inhibition promotes the generation and function of regulatory T cells. *Nat. Med.* 13, 1299–1307 (2007).
- Marson, A. *et al.* Foxp3 occupancy and regulation of key target genes during T-cell stimulation. *Nature* 445, 931–935 (2007).
- Chen, G. Y. *et al.* Cutting edge: Broad expression of the FoxP3 locus in epithelial cells: a caution against early interpretation of fatal inflammatory diseases following in vivo depletion of FoxP3-expressing cells. *J. Immunol.* 180, 5163–5166 (2008).
- Conrad, M. L. *et al.* Maternal TLR signaling is required for prenatal asthma protection by the nonpathogenic microbe *Acinetobacter lwoffii* F78. *J. Exp. Med.* 206, 2869–2877 (2009).
- Pomare, E. W., Branch, W. J. & Cummings, J. H. Carbohydrate fermentation in the human colon and its relation to acetate concentrations in venous blood. *J. Clin. Invest.* 75, 1448–1454 (1985).
- Morita, R., Ukyo, N., Furuya, M., Uchiyama, T. & Hori, T. Atrial natriuretic peptide polarizes human dendritic cells toward a Th2-promoting phenotype through its receptor guanylyl cyclase-coupled receptor A. *J. Immunol.* 170, 5869–5875 (2003).
- David, L. A. *et al.* Diet rapidly and reproducibly alters the human gut microbiome. *Nature* 505, 559–563 (2014).
- De Filippo, C. *et al.* Impact of diet in shaping gut microbiota revealed by a comparative study in children from Europe and rural Africa. *Proc. Natl Acad. Sci. USA* 107, 14691–14696 (2010).
- Yatsunenko, T. *et al.* Human gut microbiome viewed across age and geography. *Nature* 486, 222–227 (2012).
- Del Campo, R. *et al.* Improvement of digestive health and reduction in proteobacterial populations in the gut microbiota of cystic fibrosis patients using a *Lactobacillus reuteri* probiotic preparation: A double blind prospective study. *J. Cyst. Fibros.* 13, 716–722 (2014).
- De Cruz, P. *et al.* Specific mucosa-associated microbiota in Crohn's disease at the time of resection are associated with early disease recurrence: A Pilot Study. *J. Gastroenterol. Hepatol.* 30, 268–278 (2014).
- Kearley, J., Barker, J. E., Robinson, D. S. & Lloyd, C. M. Resolution of airway inflammation and hyperreactivity after *in vivo* transfer of CD4+CD25+ regulatory T cells is interleukin 10 dependent. *J. Exp. Med.* 202, 1539–1547 (2005).

43. Hou, X. X. *et al.* Characteristics of histone deacetylase 9 in peripheral blood of patients with bronchial asthma. *Zhonghua Jie He He Hu Xi Za Zhi* **35**, 340–344 (2012).
44. Kwon, D. H. *et al.* Steep left ventricle to aortic root angle and hypertrophic obstructive cardiomyopathy: study of a novel association using three-dimensional multimodality imaging. *Heart* **95**, 1784–1791 (2009).
45. Karmodiya, K., Krebs, A. R., Oulad-Abdelghani, M., Kimura, H. & Tora, L. H3K9 and H3K14 acetylation co-occur at many gene regulatory elements, while H3K14ac marks a subset of inactive inducible promoters in mouse embryonic stem cells. *BMC Genomics* **13**, 424 (2012).
46. Gluckman, P. D., Hanson, M. A., Cooper, C. & Thornburg, K. L. Effect of in utero and early-life conditions on adult health and disease. *N. Engl. J. Med.* **359**, 61–73 (2008).
47. Jackson, D. J. *et al.* Wheezing rhinovirus illnesses in early life predict asthma development in high-risk children. *Am. J. Respir. Crit. Care Med.* **178**, 667–672 (2008).
48. Dodge, R., Martinez, F. D., Cline, M. G., Lebowitz, M. D. & Burrows, B. Early childhood respiratory symptoms and the subsequent diagnosis of asthma. *J. Allergy Clin. Immunol.* **98**, 48–54 (1996).
49. Lima, J. J. *et al.* A polymorphism in the NPPA gene associates with asthma. *Clin. Exp. Allergy* **38**, 1117–1123 (2008).
50. Rogers, A. J. *et al.* Assessing the reproducibility of asthma candidate gene associations, using genome-wide data. *Am. J. Respir. Crit. Care Med.* **179**, 1084–1090 (2009).
51. Kandasamy, R. *et al.* Isatin down-regulates expression of atrial natriuretic peptide receptor A and inhibits airway inflammation in a mouse model of allergic asthma. *Int. Immunopharmacol.* **10**, 218–225 (2010).
52. Mohapatra, S. S., Lockey, R. F., Vesely, D. L. & Gower, Jr. W. R. Natriuretic peptides and genesis of asthma: an emerging paradigm? *J. Allergy Clin. Immunol.* **114**, 520–526 (2004).
53. Baine, I., Basu, S., Ames, R., Sellers, R. S. & Macian, F. Helios induces epigenetic silencing of IL2 gene expression in regulatory T cells. *J. Immunol.* **190**, 1008–1016 (2013).
54. Reik, W. Stability and flexibility of epigenetic gene regulation in mammalian development. *Nature* **447**, 425–432 (2007).
55. Eder, W., Ege, M. J. & von Mutius, E. The asthma epidemic. *N. Engl. J. Med.* **355**, 2226–2235 (2006).
56. Barker, D. J. *et al.* Fetal nutrition and cardiovascular disease in adult life. *Lancet* **341**, 938–941 (1993).
57. Sheedy, J. R., Ebeling, P. R., Gooley, P. R. & McConville, M. J. A sample preparation protocol for 1H nuclear magnetic resonance studies of water-soluble metabolites in blood and urine. *Anal. Biochem.* **398**, 263–265 (2010).
58. Yu, Z. & Morrison, M. Improved extraction of PCR-quality community DNA from digesta and fecal samples. *Biotechniques* **36**, 808–812 (2004).
59. Quinlan, A. R., Stewart, D. A., Stromberg, M. P. & Marth, G. T. PyroBayes: an improved base caller for SNP discovery in pyrosequences. *Nat. Methods* **5**, 179–181 (2008).
60. Ashelford, K. E., Chuzhanova, N. A., Fry, J. C., Jones, A. J. & Weightman, A. J. At least 1 in 20 16S rRNA sequence records currently held in public repositories is estimated to contain substantial anomalies. *Appl. Environ. Microbiol.* **71**, 7724–7736 (2005).
61. Bragg, L., Stone, G., Imelfort, M., Hugenholtz, P. & Tyson, G. W. Fast, accurate error-correction of amplicon pyrosequences using Acacia. *Nat. Methods* **9**, 425–426 (2012).
62. Caporaso, J. G. *et al.* QIIME allows analysis of high-throughput community sequencing data. *Nat. Methods* **7**, 335–336 (2010).
63. Thorburn, A. N., Foster, P. S., Gibson, P. G. & Hansbro, P. M. Components of *Streptococcus pneumoniae* suppress allergic airways disease and NK1 cells by inducing regulatory T cells. *J. Immunol.* **188**, 4611–4620 (2012).
64. Thorburn, A. N. *et al.* Pneumococcal components induce regulatory T cells that attenuate the development of allergic airways disease by deviating and suppressing the immune response to allergen. *J. Immunol.* **191**, 4112–4120 (2013).
65. Murphy, V. E., Powell, H., Wark, P. A. B. & Gibson, P. G. A prospective study of respiratory viral infection in pregnant women with and without asthma. *CHEST J.* **144**, 420–427 (2013).
66. Mattes, J., Murphy, V. E., Powell, H. & Gibson, P. G. Prenatal origins of bronchiolitis: protective effect of optimised asthma management during pregnancy. *Thorax* **69**, 383–384 (2013).
67. Powell, C. V. E., McNamara, P., Solis, A. & Shaw, N. J. A parent completed questionnaire to describe the patterns of wheezing and other respiratory symptoms in infants and preschool children. *Arch. Dis. Childhood* **87**, 376–379 (2002).
68. McLernon, P. C., Wood, L. G., Murphy, V. E., Hodyl, N. A. & Clifton, V. L. Circulating antioxidant profile of pregnant women with asthma. *Clin. Nutr.* **31**, 99–107 (2012).

## Acknowledgements

We thank Monash animal facilities, Histology Platform and FlowCore. We acknowledge Vicki Clifton, Philippa Talbot, Kelly Steel, Penelope McLernon and Karen McLaughlin for human sample and data collection, Phillippe Collas for assistance with ChIP, Andreas Subrier for IPA, Magdalena Hubalewska and Marcin Surmiak for qPCR and western blot, Ashlee Burt and Laurent Juglair for general assistance and Pat Holt for critically reviewing this manuscript. Jason Bell provided High Performance Computing support. This work was supported by NHMRC, CRC for Asthma and airways, The University of Newcastle, Asthma Foundation NSW, HMRI, Port Waratah Coal Services and Hunter Children's Research Foundation.

## Author contributions

A.N.T. conceived and initiated the project, planned and performed the experiments, analysed the data and wrote the manuscript. C.L.M. and S.S. planned and performed the experiments and analysed the data. D.S. performed the microbiota analysis. L.M. determined diets for use and provided general support. L.J.M. planned and performed experiments. L.E.R., C.H.Y.W., R.S., R.R., N.C. performed and/or assisted with experiments. J.K.T. and E.M. provided general support. R.J.M. contributed to microbiota analysis. L.W. performed/assisted with the ChIP experiments. M.J.M. and D.L.T. were involved in metabolite analysis. L.G.W. and V.E.M. were involved in clinical outcome data collection and analysis. J.M. and P.G.G. provided patient samples and clinical outcome data. C.R.M. established the overarching hypothesis for the study, supervised the study and wrote the manuscript.

## Additional information

**Accession codes:** Gene microarray data was deposited in GEO, accession number GSE69525.

**Supplementary Information** accompanies this paper at <http://www.nature.com/naturecommunications>

**Competing financial interests:** The authors declare no competing financial interests.

**Reprints and permission** information is available online at <http://npg.nature.com/reprintsandpermissions/>

**How to cite this article:** Thorburn, A. N. *et al.* Evidence that asthma is a developmental origin disease influenced by maternal diet and bacterial metabolites. *Nat. Commun.* 6:7320 doi: 10.1038/ncomms8320 (2015).

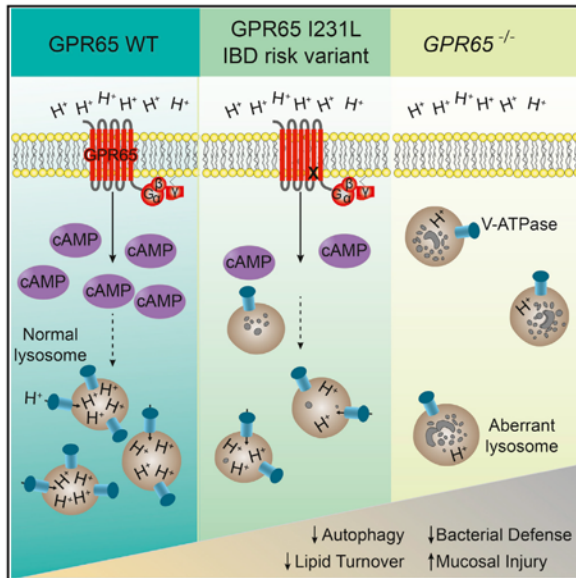
## Appendix 2

Kara G. Lassen, **Craig I McKenzie**, Muriel Mari, Tatsuro Murano, Jakob Begun, Leigh A. Baxt, Gautam Goel, Eduardo J. Villablanca, Szu-Yu Kuo, Hailiang Huang, Laurence Macia, Atul K. Bhan, Marcel Batten, Mark J. Daly, Fulvio Reggiori, Charles R. Mackay, Ramnik J. Xavier, Genetic coding variant in GPR65 alters lysosomal pH and links lysosomal dysfunction with colitis risk, *Immunity* (2016)

# Immunity

## Genetic Coding Variant in GPR65 Alters Lysosomal pH and Links Lysosomal Dysfunction with Colitis Risk

### Graphical Abstract



### Authors

Kara G. Lassen, Craig I. McKenzie, Muriel Mari, ..., Fulvio Reggiori, Charles R. Mackay, Ramnik J. Xavier

### Correspondence

klassen@broadinstitute.org (K.G.L.), xavier@molbio.mgh.harvard.edu (R.J.X.)

### In Brief

Gene mapping efforts have identified numerous disease-associated genes, but understanding how these genes influence disease has proved challenging. Xavier and colleagues identify a role for GPR65 in lysosomal homeostasis and demonstrate that the IBD-associated risk variant GPR65 I231L confers lysosomal dysfunction with effects on autophagy, pathogen clearance, and intestinal homeostasis.

### Highlights

- Genomic screen identifies role for nine genes in IBD susceptibility loci in autophagy
- *Gpr65*-deficient mice are more susceptible to bacteria-induced colitis
- Loss of GPR65 results in accumulation of aberrant phagosomes and lysosomes
- GPR65 IBD risk variant confers defects in lysosomal function and pathogen defense

### Accession Numbers

GSE69445



Lassen et al., 2016, *Immunity* 44, 1392–1405  
June 21, 2016 © 2016 Elsevier Inc.  
<http://dx.doi.org/10.1016/j.immuni.2016.05.007>

CellPress



# Genetic Coding Variant in GPR65 Alters Lysosomal pH and Links Lysosomal Dysfunction with Colitis Risk

Kara G. Lassen,<sup>1,2,\*</sup> Craig I. McKenzie,<sup>3</sup> Muriel Mari,<sup>4,5</sup> Tatsuro Murano,<sup>1,2</sup> Jakob Begun,<sup>2,6,7</sup> Leigh A. Baxt,<sup>2</sup> Gautam Goel,<sup>2</sup> Eduardo J. Villablanca,<sup>1,2,6</sup> Szu-Yu Kuo,<sup>1</sup> Hailiang Huang,<sup>1,8</sup> Laurence Macia,<sup>3</sup> Atul K. Bhan,<sup>9,10</sup> Marcel Batten,<sup>11</sup> Mark J. Daly,<sup>1,8,10</sup> Fulvio Reggiori,<sup>4,5</sup> Charles R. Mackay,<sup>3</sup> and Ramnik J. Xavier<sup>1,2,6,10,\*</sup>

<sup>1</sup>The Broad Institute of MIT and Harvard, Cambridge, MA 02142, USA

<sup>2</sup>Center for Computational and Integrative Biology, Massachusetts General Hospital, Boston, MA 02114, USA

<sup>3</sup>Monash Biomedicine Discovery Institute and Department of Biochemistry and Molecular Biology, Monash University, Melbourne, VIC 3800, Australia

<sup>4</sup>Department of Cell Biology, University of Groningen, University Medical Center Groningen, 3713 AV Groningen, the Netherlands

<sup>5</sup>Department of Cell Biology, University Medical Center Utrecht, 3564 CX Utrecht, the Netherlands

<sup>6</sup>Gastrointestinal Unit, Massachusetts General Hospital, Boston, MA 02114, USA

<sup>7</sup>Mater Research Institute and School of Medicine, University of Queensland, Brisbane, QLD 4101, Australia

<sup>8</sup>Analytic and Translational Genetics Unit, Massachusetts General Hospital, Harvard Medical School, Boston, MA 02114, USA

<sup>9</sup>Pathology Department, Massachusetts General Hospital and Harvard Medical School, Boston, MA 02114, USA

<sup>10</sup>Center for the Study of Inflammatory Bowel Disease, Massachusetts General Hospital, Boston, MA 02114, USA

<sup>11</sup>Garvan Institute of Medical Research and St. Vincent's Clinical School, University of New South Wales, Sydney, NSW 2010, Australia

\*Correspondence: [klassen@broadinstitute.org](mailto:klassen@broadinstitute.org) (K.G.L.), [xavier@molbio.mgh.harvard.edu](mailto:xavier@molbio.mgh.harvard.edu) (R.J.X.)

<http://dx.doi.org/10.1016/j.immuni.2016.05.007>

## SUMMARY

Although numerous polymorphisms have been associated with inflammatory bowel disease (IBD), identifying the function of these genetic factors has proved challenging. Here we identified a role for nine genes in IBD susceptibility loci in antibacterial autophagy and characterized a role for one of these genes, *GPR65*, in maintaining lysosome function. Mice lacking *Gpr65*, a proton-sensing G protein-coupled receptor, showed increased susceptibility to bacteria-induced colitis. Epithelial cells and macrophages lacking *GPR65* exhibited impaired clearance of intracellular bacteria and accumulation of aberrant lysosomes. Similarly, IBD patient cells and epithelial cells expressing an IBD-associated missense variant, *GPR65* I231L, displayed aberrant lysosomal pH resulting in lysosomal dysfunction, impaired bacterial restriction, and altered lipid droplet formation. The *GPR65* I231L polymorphism was sufficient to confer decreased *GPR65* signaling. Collectively, these data establish a role for *GPR65* in IBD susceptibility and identify lysosomal dysfunction as a potentially causative element in IBD pathogenesis with effects on cellular homeostasis and defense.

## INTRODUCTION

Gene mapping efforts have the potential to unlock profound insights into disease pathogenesis because each genetic association individually carries a biological link to disease. This approach is relevant to all genetic diseases as well as cancer (Reuter et al., 2015) and offers the potential to identify targets for development

of novel therapeutic interventions. However, the swift progress of genome-wide association studies (GWASs) in many disease areas has exposed limitations in translating genetic loci to pathogenic insights, and it is thus becoming clear that the primary challenge for human genetics is no longer discovering genetic associations, but in the identification of how the identified genes and corresponding alleles exert their influence on the biology of health and disease (Altshuler et al., 2008).

Inflammatory bowel disease (IBD), including Crohn's disease and ulcerative colitis, is a complex disease involving inflammation of the gastrointestinal tract. It is triggered by both genetic and environmental factors. There has been enormous progress in IBD genetics with the discovery of common genetic variants in more than 150 regions of the human genome that increase the risk and underlie the biology of IBD (Jostins et al., 2012). These common genetic variants have helped reveal key cell types controlling intestinal homeostasis and pathways such as antibacterial defense and autophagy as playing important roles in disease (Adolph et al., 2013; Cadwell et al., 2008; Cooney et al., 2010; Geremia et al., 2011; Lassen et al., 2014; Murthy et al., 2014). However, for the vast majority of these genetic associations, the specific implicated gene and causal variants have not been identified, limiting the near-term insights into pathogenesis and the longer-term ability to convert these associations into actionable therapeutic hypotheses.

The juxtaposition of the polymicrobial community with gut tissue creates an environment in which host and/or cell sensing of microbes is critical to homeostasis. Understanding how gut microbes, including potentially pathogenic microbes, are sensed by gut tissues to coordinate an appropriate inflammatory response is a critical question in IBD (Deretic et al., 2013). Recent work has characterized the role of microbes and their bacterial products in altering gut dynamics (Kishino et al., 2013; Macia et al., 2015; Maslowski et al., 2009; Venkatesh et al., 2014). In turn, host genetics impinging on host response pathways, including intracellular bacterial defense, autophagy, metabolite

receptor expression, and the ability to respond to cellular stresses, influences IBD susceptibility (Kaser et al., 2011; Knights et al., 2013). Autophagy (macroautophagy) is a prosurvival intracellular clearance system that directs cytoplasmic cargo to lysosomes for proteolytic degradation (Gomes and Dikic, 2014; Levine et al., 2011). Emerging data highlight the critical role of autophagy in host defense against a range of bacteria, viruses, and parasites (Deretic et al., 2015). Autophagy is critical for maintaining intestinal homeostasis in multiple cell types. To date, the IBD-associated genes *ATG16L1* and *IRGM* have each been implicated in antibacterial autophagy (Lassen et al., 2014; McCarroll et al., 2008; Murthy et al., 2014; Singh et al., 2006). It is currently unclear whether there are additional IBD-associated genes that function in autophagy or intracellular bacterial defense.

In this study, we used a functional genomic approach to identify 30 IBD-associated genes in host bacterial defense and pinpointed the role for GPR65 in IBD pathogenesis. In vivo, loss of GPR65 increased susceptibility to colitis. At the cellular level, we showed that GPR65 maintained lysosomal function, thus preserving autophagy and pathogen defense. Expression of an IBD-associated missense variant of GPR65 (rs3742704), which encodes an isoleucine-to-leucine substitution at amino acid 231 (I231L), in cell lines and in patient lymphoblasts resulted in impaired lysosomal acidification and disrupted lysosomal function. Genetic rescue of this aberrant lysosomal activity in GPR65 I231L-expressing cells restored intracellular bacterial defense. Together these data highlight a critical role for lysosomal function in intestinal homeostasis and suggest a framework for placing disease-associated genes into functional pathways.

## RESULTS

### Functional Genomics Identifies a Role for IBD Risk Genes in Pathogen Defense

To begin assigning function to genes in IBD risk loci, we selected two known IBD-relevant pathways: intracellular bacterial replication and antibacterial autophagy. We targeted genes in each IBD risk locus by using short interfering RNAs (siRNAs) and monitored changes in intracellular replication of a bioluminescent *Salmonella enterica* and serovar Typhimurium after infection of immortalized cervical HeLa cells via a high-throughput assay (Figure 1A; Shaw et al., 2013). A second siRNA screen was used to identify genes involved in antibacterial autophagy by monitoring changes in colocalization of *S. Typhimurium* and the autophagy marker LC3 (MAP1LC3A, microtubule-associated proteins 1 light chain 3A) in HeLa cells stably expressing green fluorescent protein-LC3 (GFP-LC3) (Figure 1A; Lassen et al., 2014; Murthy et al., 2014). siRNAs against *ATG16L1*, a core autophagy protein, served as a positive control for both screens (Figures S1A and S1B). The two screens were performed using siRNA pools containing three siRNAs targeting each gene and found that knockdown of 9.7% of the genes increased intracellular replication and knockdown of 10.5% of the genes reduced LC3 colocalization (Figure 1B and Tables S1 and S2). These data reinforce the functional importance of antibacterial autophagy in IBD susceptibility.

Genes that exhibited phenotypes in either primary assay screen were retested with three individual siRNAs per gene

and endogenous LC3 staining. Genes were then filtered based on performance of individual siRNAs in both high-throughput and manual assays, as well as mRNA expression level in HeLa cells and correlation of activity with knockdown efficiency (Tables S3 and S4). This filtering resulted in a list of 30 genes, 9 of which were confirmed to have positive effects on both bacterial replication and LC3-bacteria colocalization, including our positive control, *ATG16L1* (Figures 1C–1E and S1C). Most of the identified genes have not been previously suggested to alter pathogen defense or autophagy; however, some genes that scored in these screens were supported by published findings. *RUFY4* (RUN and FYVE domain containing 4) has recently been shown to positively regulate autophagy in response to the cytokine IL-4 (Terawaki et al., 2015). *SCAMP3* (secretory carrier membrane protein 3), a gene that scored only in the intracellular bacterial replication screen, has been shown to affect intracellular localization of *S. Typhimurium*, a phenotype that can have consequences for bacterial replication in host cells (Mota et al., 2009). Furthermore, the E3 ligase gene *SMURF1* and the peroxisomal biogenesis gene *PEX13* are implicated in selective autophagy of viruses and mitochondria, suggesting that these genes might function broadly in selective types of autophagy (Orvedahl et al., 2011).

Of the nine genes identified as positive regulators of pathogen defense in both screens, *GPR65* (G protein coupled receptor 65) was selected for follow-up analysis because the association of IBD to the *GPR65* locus implicates a set of 17 individual variants (Figure 1F and Table S5), including the missense mutation I231L (Jostins et al., 2012). The I231L variant has a frequency of 19.67% in the population. Additionally, protein expression and human transcriptome data indicate that GPR65 mRNA and protein expression is highest in immune cell compartments, including whole blood and spleen, as well as the intestinal tissue, suggesting that it plays a role in intestinal homeostasis (Kyaw et al., 1998; Melé et al., 2015). Although GPR65 is known to function as a  $H^+$ -sensing G protein-coupled receptor (GPCR) that responds to acidic pH, the role of GPR65 in intestinal inflammation is currently unknown (Wang et al., 2004). Nonetheless, luminal changes in pH have been associated with inflammation and IBD (Nugent et al., 2001). Taken together, these data suggest a molecular link between GPR65 function and disease.

### Loss of *Gpr65* Increases Bacteria-Induced Colitis Susceptibility

To determine whether GPR65 plays an important role in intestinal homeostasis in vivo and to test host defense against pathogenic bacteria, we used *Citrobacter rodentium*, a murine pathogen that results in colonic lesions similar to the clinical enteropathogenic *Escherichia coli* strains associated with Crohn's disease (Longman et al., 2014; Nell et al., 2010; Sasaki et al., 2007). Recent reports on *Atg16l1* hypomorphic mice suggest that impaired autophagy can protect against *C. rodentium* infection (Marchiando et al., 2013). To determine whether *Gpr65*<sup>−/−</sup> mice were resistant to infectious colitis, we infected wild-type (WT) and *Gpr65*<sup>−/−</sup> mice with *C. rodentium*. Untreated *Gpr65*<sup>−/−</sup> mice were healthy with no signs of spontaneous colitis or inflammation (Figure 2A). At 14 days after infection, *Gpr65*<sup>−/−</sup> mice infected with *C. rodentium* showed more severe inflammation by histopathology (Figures 2B and 2C). Moreover, *Gpr65*<sup>−/−</sup> mice had

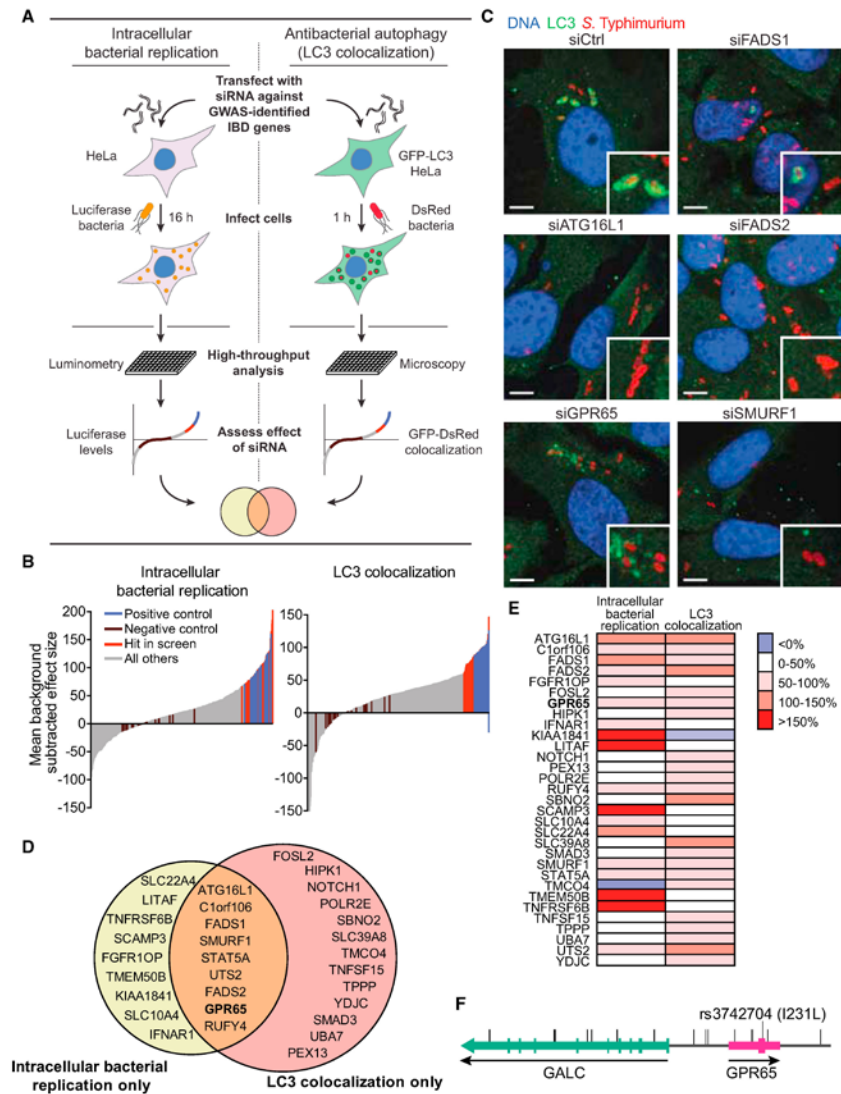


**Figure 1. Functional Genomic Analysis Identifies Genes Involved in Autophagy-Dependent Intracellular Pathogen Defense**  
 (A) Schematic of high-throughput genetic screens. HeLa or HeLa-GFP-LC3 cells were transfected with an siRNA library and infected with bioluminescent *S. Typhimurium* (intracellular bacterial replication) or DsRed-labeled *S. Typhimurium* (LC3 colocalization).  
 (B) Mean effect size of siRNAs in intracellular bacterial replication assay (left) and LC3 colocalization assay (right).  $n = 2$  independent experiments.  
 (C) Representative confocal micrographs of selected siRNA-treated HeLa cells infected for 1 hr with DsRed-labeled *S. Typhimurium*. Scale bars represent 7.5  $\mu\text{m}$ .  
 (D) Validated genes that scored in LC3 colocalization and intracellular bacterial replication assays using single siRNAs for a given gene.  
 (E) Heatmap illustration of effect size scores of confirmed hits.  
 (F) Schematic of *GPR65* locus with identified IBD risk SNPs from the IBD fine-mapping project.  
 See also Figure S1 and Tables S1, S2, and S3–S5.



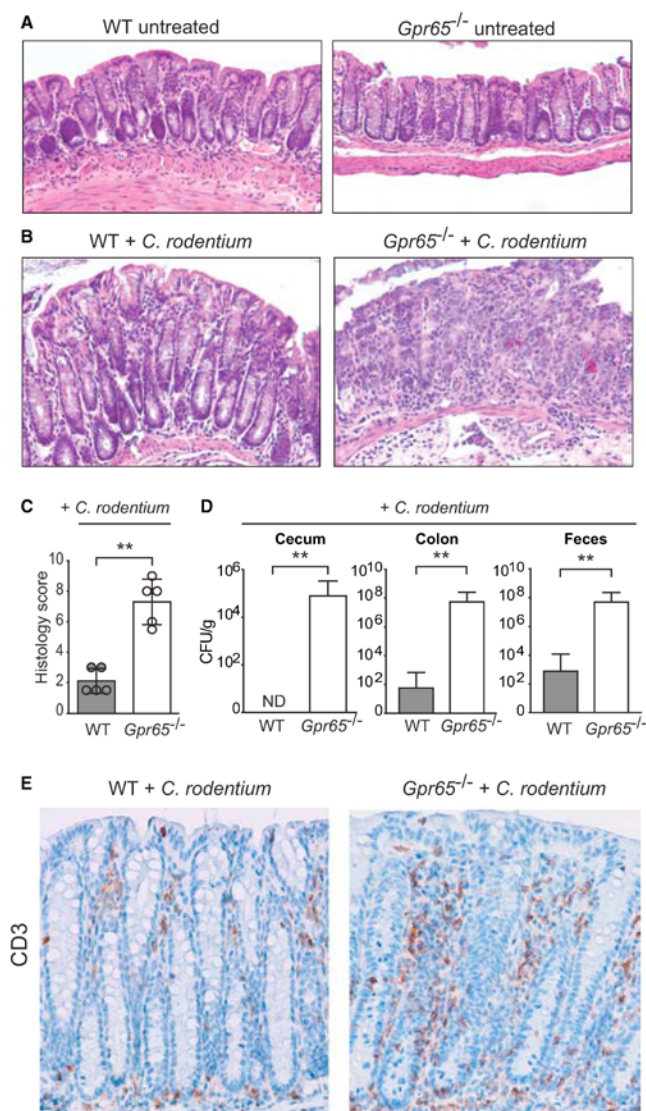


**Figure 2. *Gpr65*<sup>-/-</sup> Mice Are More Susceptible to Bacterial-Induced Colitis**

(A) Representative H&E-stained sections of distal colon tissue are shown from untreated WT and *Gpr65*<sup>-/-</sup> mice (20× magnification) (n = 4 mice per genotype).

(B) Representative H&E-stained sections of distal colon tissue are shown from infected WT and *Gpr65*<sup>-/-</sup> mice (20× magnification) (n = 8 mice per genotype).

(C) Histological score for inflammation in colon tissues 14 days after *C. rodentium* infection. Data shown as mean ± SD; n = 5/group. \*\*p < 0.01 (Mann-Whitney U test).

(D) WT and *Gpr65*<sup>-/-</sup> mice were orally infected with *C. rodentium* and bacterial numbers (CFU) were measured in the cecum, colon, and feces 14 days after infection. Data are means ± SEM (n = 10 [WT], 10 [*Gpr65*<sup>-/-</sup>]; 2 experiments). \*\*p < 0.01 (Mann-Whitney U test).

(E) Immunohistochemistry image of CD3 staining on WT and *Gpr65*<sup>-/-</sup> colon tissue 14 days after infection with *C. rodentium*.

See also Figure S2.

gested that GPR65 was required for effective pathogen clearance and modulated susceptibility to infectious colitis in vivo. Additionally, these results were consistent with GPR65 having functions beyond autophagy.

#### GPR65 Expression in Non-hematopoietic and Hematopoietic Cells Limits *C. rodentium* Infection

GPR65 is highly expressed in various immune cell types as well as intestinal tissue. Both non-hematopoietic and hematopoietic cells have been shown to contribute to defense against *C. rodentium* (Song-Zhao et al., 2014; Vallance et al., 2002). To determine which cellular compartment was responsible for *Gpr65*-mediated protection, bone marrow (BM) cells from WT and *Gpr65*<sup>-/-</sup> mice were transferred into lethally irradiated WT and *Gpr65*<sup>-/-</sup> mice, respectively. At 8 weeks after transfer, mice were infected with *C. rodentium* for 11 days to analyze the immune response closer to the peak of infection. Consistent with our results in Figure 2, *Gpr65*<sup>-/-</sup> mice that received *Gpr65*<sup>-/-</sup> BM (*Gpr65*<sup>-/-</sup> → *Gpr65*<sup>-/-</sup> BM chimeric mice) exhibited higher levels of

significantly higher levels of *C. rodentium* in the cecum, colon, and feces, a phenotype consistent with decreased pathogen clearance (Figure 2D). Immunohistochemistry of infected colon tissue revealed enhanced infiltration of T cells (detected as CD3<sup>+</sup>) in *Gpr65*<sup>-/-</sup> mice although no differences in macrophage infiltration were observed (Figures 2E and S2). These data sug-

*C. rodentium* in the colon compared to WT → WT BM chimeric mice as well as decreased colon length, a marker of colitis (Figures 3A and 3B). Restoration of *Gpr65* expression in the non-hematopoietic compartment (*Gpr65*<sup>-/-</sup> → WT) or in the hematopoietic compartment (WT → *Gpr65*<sup>-/-</sup>) alone was not sufficient to reduce *C. rodentium* bacterial loads to those of



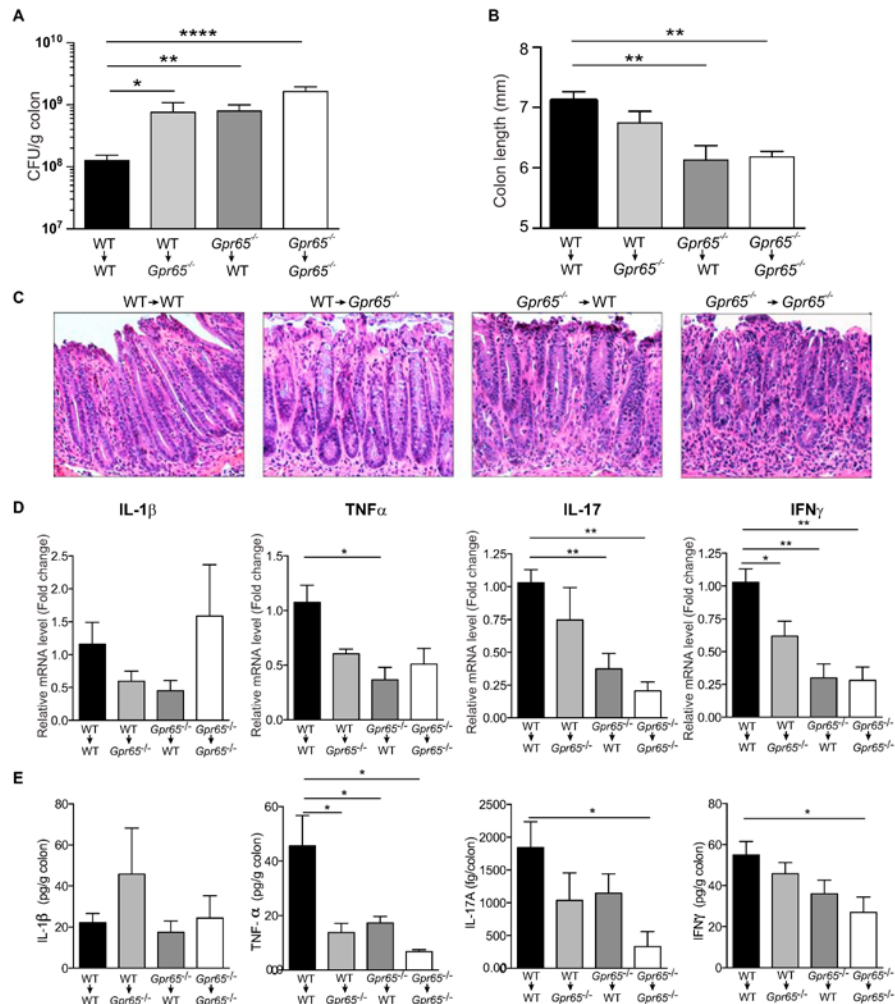


**Figure 3. *Gpr65* Expression in Non-hematopoietic and Hematopoietic Cells Limits *C. rodentium* Infection**

(A) Bone marrow chimeric mice were orally infected with *C. rodentium* and bacterial numbers (CFU) were measured in the colon at 11 days after infection. Data are means + SEM (n = 11 [WT → WT], n = 6 [WT → Gpr65<sup>-/-</sup>], n = 10 [Gpr65<sup>-/-</sup> → WT], n = 4 [Gpr65<sup>-/-</sup> → Gpr65<sup>-/-</sup>]). \*p < 0.05, \*\*p < 0.01, \*\*\*\*p < 0.0001 (unpaired t test).

(B) Colon length from bone marrow chimeric mice infected with *C. rodentium* for 11 days. Data are means + SEM. \*\*p < 0.01 (unpaired t test).

(C) Representative H&E-stained sections of distal colon tissue are shown from infected bone marrow chimeric mice at 11 days after infection (20× magnification).

(D) Cytokine expression in *C. rodentium*-infected mice, as quantified by qRT-PCR. Relative mRNA levels of the indicated cytokine are shown. \*p < 0.05; \*\*p < 0.01 (unpaired t test). Data are means + SEM.

(E) Secretion of cytokines from colon tissues 11 days after infection with *C. rodentium*. Data are means + SEM. \*p < 0.05 (unpaired t test).

See also Figure S3.

WT mice (Figure 3A). Data obtained using in vivo imaging of BM chimeric mice infected with a bioluminescent *C. rodentium* were consistent with bacterial CFU data (Figures S3A and S3B). Additionally, *Gpr65*<sup>-/-</sup> → WT BM chimeric mice displayed significantly shorter colon lengths (Figure 3B). Major differences in histopathology were not observed at this time point after infection (Figure 3C). Cytokine analysis demonstrated reduced expression of tumor necrosis factor  $\alpha$  (TNF- $\alpha$ ), interleukin 17 (IL-17), and interferon- $\gamma$  (IFN- $\gamma$ ) in infected colons associated with loss of *Gpr65* (Figures 3D and 3E). No difference was observed in IL-1 $\beta$  or IL-6 mRNA or protein expression in any BM chimeric mice (Figures 3D, 3E, S3C, and S3D). Additionally, levels of IL-23 mRNA were significantly reduced in mice lacking *Gpr65* in the hematopoietic compartment (Figure S3C). Taken together, these data are consistent with a role for epithelial GPR65 expression in limiting pathogen replication and a role for hematopoietic GPR65 expression in the inflammatory response to intestinal pathogens.

#### Loss of GPR65 Alters Pathogen Clearance and Confers Intracellular Degradative Defects

To investigate the role of GPR65 in intracellular pathogen defense, we generated *GPR65*-null HeLa cell lines using the CRISPR/Cas9 system. To confirm that *GPR65* ablation was specifically responsible for the observed phenotype and to control for any off-target effects of the CRISPR/Cas9 system, we stably re-expressed GPR65 or an empty vector control. We observed increased *S. Typhimurium* replication in *GPR65*-null cells compared to cells expressing GPR65, consistent with the knock-down results (Figure 4A). To determine whether GPR65 functions broadly in defense against other intracellular bacteria and in other cell types, we infected WT and *Gpr65*<sup>-/-</sup> primary bone-marrow-derived macrophages (BMDMs) with a strain of *Listeria monocytogenes* lacking the autophagy-evading protein ActA (*L. monocytogenes*  $\Delta$ actA) (Rich et al., 2003). In agreement with our *S. Typhimurium* infection results, *Gpr65*<sup>-/-</sup> BMDMs showed significantly increased CFUs of intracellular *L. monocytogenes*, indicative of increased survival of the bacteria (Figure 4B). These data suggest a broad role for GPR65 in controlling intracellular microbial clearance.

*GPR65* deficiency also resulted in decreased LC3-S. *Typhimurium* colocalization in HeLa cells (Figures 4C and 4D), and decreased LC3-*Listeria* colocalization was observed in *Gpr65*<sup>-/-</sup> BMDMs at 1 hr after infection, suggesting differences in intracellular bacterial targeting by autophagy in these cells (Figures S4A and S4B). Examination of LC3-S. *Typhimurium* autophagosomal structures by confocal microscopy revealed not only a decrease in LC3-containing membranes around *S. Typhimurium*, but also aberrant LC3 accumulation near *S. Typhimurium* within *GPR65*-null cells (arrowheads, Figure S4C). These LC3 accumulations presented as either empty circular structures or globular concentrations of LC3 adjacent to the bacteria without the characteristic engulfment observed during antibacterial autophagy (Figure S4D). This aberrant LC3 accumulation was reduced when GPR65 was re-expressed, showing that this phenotype was specific to GPR65 disruption (Figures 4E and S4D). Aberrant LC3 accumulation was also observed in *Lis-*

*teria*-infected *Gpr65*<sup>-/-</sup> BMDMs and in *S. Typhimurium*-infected HeLa cells treated with GPR65 siRNA, suggesting that GPR65 functions similarly in pathogen targeting in multiple cell types (Figures S4E–S4H). The impaired recruitment of LC3 to bacteria as well as aberrant LC3 accumulations around bacteria indicated a potential block in autophagic turnover in *GPR65*-null cells.

To investigate the observed phenotypes at the ultrastructural level, we performed electron microscopy (EM) analysis on primary WT and *Gpr65*<sup>-/-</sup> BMDMs as well as our *GPR65*-null HeLa cells. WT BMDMs exhibited classical morphology with numerous phagosomes distributed throughout the cytoplasm (Figure 4F). A significant proportion of the phagosomes in *Gpr65*<sup>-/-</sup> BMDMs lost their luminal homogeneity and accumulated membranous structures in their interiors, suggesting a defect in the hydrolytic processing of endocytosed material (Figures 4F and 4G). The observed defect in phagosome biogenesis did not affect phagocytic uptake of *Staphylococcus aureus*-coated bioparticles, indicating that this phenotype was restricted to intracellular pathways (Figure 4H).

Lysosomes from WT and *Gpr65*<sup>-/-</sup> BMDMs differed in their appearance; however, the number of total lysosomes in BMDMs was inadequate for quantitative analysis of these differences (data not shown). HeLa cells, on the other hand, contained numerous lysosomes, allowing quantitative analysis of the major ultrastructural differences between lysosomes of cells with or without GPR65. In WT HeLa cells, most of the lysosomes had a typical morphology with onion-like membranous conformations in their lumen (Figures 4I and 4J). Two minor subpopulations of these degradative organelles were also observed. The first included lysosomes that were partially filled with unprocessed subvacuolar material as well as onion-like membranes (middle panel, Figure 4I). The second subpopulation included aberrant lysosomes that displayed accumulated undigested material in their lumen (right panel, Figure 4I). In contrast to WT cells, *GPR65*-null cells contained significantly fewer typical lysosomes and an increase in lysosomes with a degradation defect (Figures 4I and 4J). Taken together, the accumulation of unprocessed endolysosomal content in *GPR65*-null cells supports a partial lysosomal degradative defect in these cells.

#### GPR65 Crohn's Disease Risk Variant Alters Lysosomal Activity

Consistent with our observation of aberrant lysosome accumulation in *GPR65*-null cells, an unbiased genome-wide analysis of gene expression differences between WT and *Gpr65*<sup>-/-</sup> BMDMs identified differential regulation of genes implicated in lysosomal function (*Atp6v1d* and *Atp6v1e1*) and vesicular transport (*Snx10*), suggesting potential dysregulation of these processes (Figure S5A; Efeyan et al., 2012; Qin et al., 2006). *Atp6v1d* and *Atp6v1e1*, two of the genes downregulated in *Gpr65*<sup>-/-</sup> cells, encode subunits of the H<sup>+</sup> transporting vacuolar ATPase (V-ATPase) that functions to acidify lysosomes as well as other intracellular compartments. Additionally, SNX10 is known to directly bind the V-ATPase complex, controlling the subcellular localization and function of the V-ATPase complex (Chen et al., 2012). To determine whether these genes were also downregulated in non-immune cell types, we performed quantitative RT-PCR on *GPR65*-null HeLa cells and cells expressing either GPR65 WT or the IBD risk variant GPR65 I231L (rs3742704).

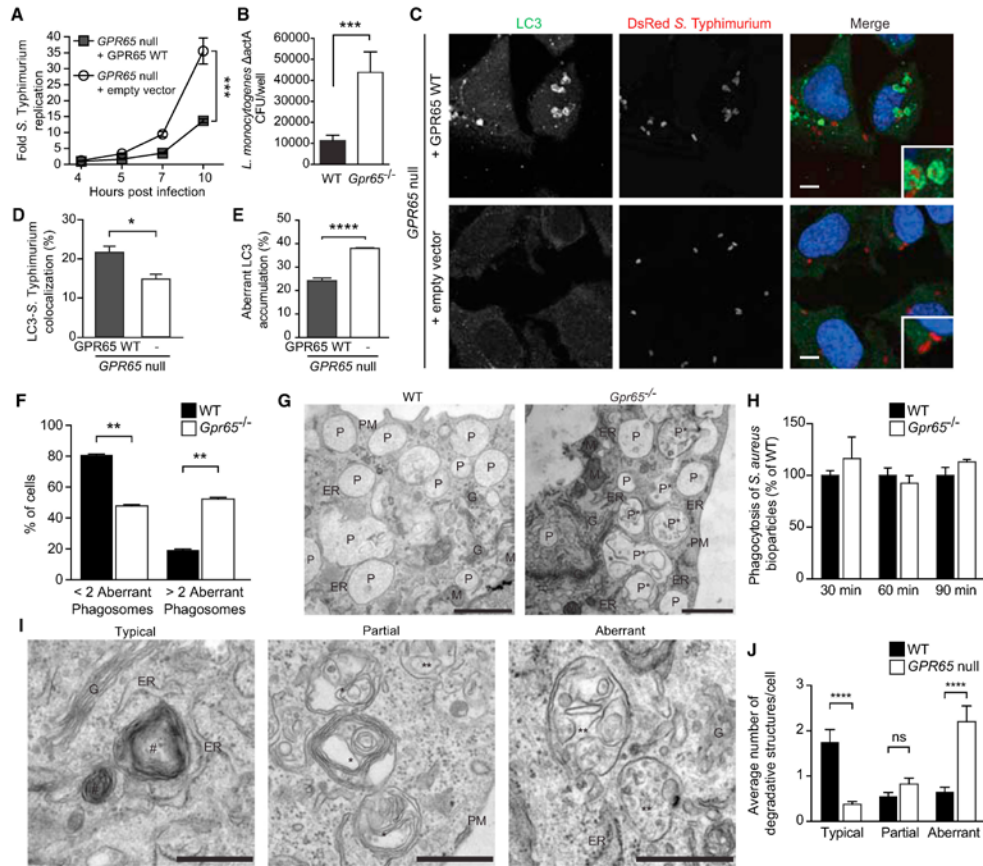


**Figure 4. Cells Lacking GPR65 Exhibit Impaired Antibacterial Autophagy and Accumulation of Aberrant Degradative Compartments**

(A) *S. Typhimurium* intracellular replication in GPR65-null HeLa cells stably expressing either an empty vector or GPR65 WT. Bars represent means  $\pm$  SD from  $n = 4$ . \*\*\*p < 0.001 (unpaired t test).

(B) CFU of intracellular *Listeria*  $\Delta$ actA recovered from WT or GPR65<sup>-/-</sup> BMDMs at 3 hr after infection. \*\*\*p < 0.001 (unpaired t test).

(C) Confocal micrographs of endogenous LC3-*S. Typhimurium* colocalization in GPR65-null HeLa cells stably expressing either an empty vector or GPR65 WT at 1 hr after infection. Scale bars represent 7.5  $\mu$ m.

(D) Quantification of colocalization of *S. Typhimurium* and endogenous LC3 in indicated cells 1 hr after infection. Data shown represent means  $\pm$  SEM from  $n = 3$  independent experiments. \*p < 0.05 (unpaired t test).

(E) Quantification of aberrant endogenous LC3 accumulation at sites of *S. Typhimurium*-LC3 colocalization in cells shown in Figure S4C. Data shown represent means  $\pm$  SEM of  $n = 3$  independent experiments. \*\*\*\*p < 0.0001 (unpaired t test).

(F) Quantification of the percentage of BMDMs displaying more than two aberrant phagosomes as shown in (B). Results are expressed as percent of cells with a defined type of phagosome in the cell population  $\pm$  SEM. \*\*p < 0.01 (t test).

(G) Representative EM micrographs of WT and GPR65<sup>-/-</sup> BMDMs showing phagosomal morphology. Abbreviations are as follows: ER, endoplasmic reticulum; G, Golgi; M, mitochondria; P, phagosomes; P\*, aberrant phagosomes; PM, plasma membrane. Scale bars represent 1  $\mu$ m.

(H) WT and GPR65<sup>-/-</sup> BMDMs were treated with *S. aureus*-coated bioparticles conjugated to the pH indicator dye for the indicated times. Number of puncta were normalized to WT levels at each time point.  $n = 3$  independent experiments.

(I) Representative EM micrographs of the lysosomal subpopulations observed in WT and GPR65-null HeLa cells. Abbreviations and symbols are as follows: #, typical lysosome; \*, lysosome with a partial degradation defect; \*\*, aberrant lysosome with a degradative defect; ER, endoplasmic reticulum; G, Golgi; PM, plasma membrane. Scale bars represent 500 nm.

(J) Quantification of each lysosome subpopulation shown in (I). Results are expressed as the number of lysosomes per cell  $\pm$  SEM. \*\*\*\*p < 0.0001 (t test). See also Figure S4.



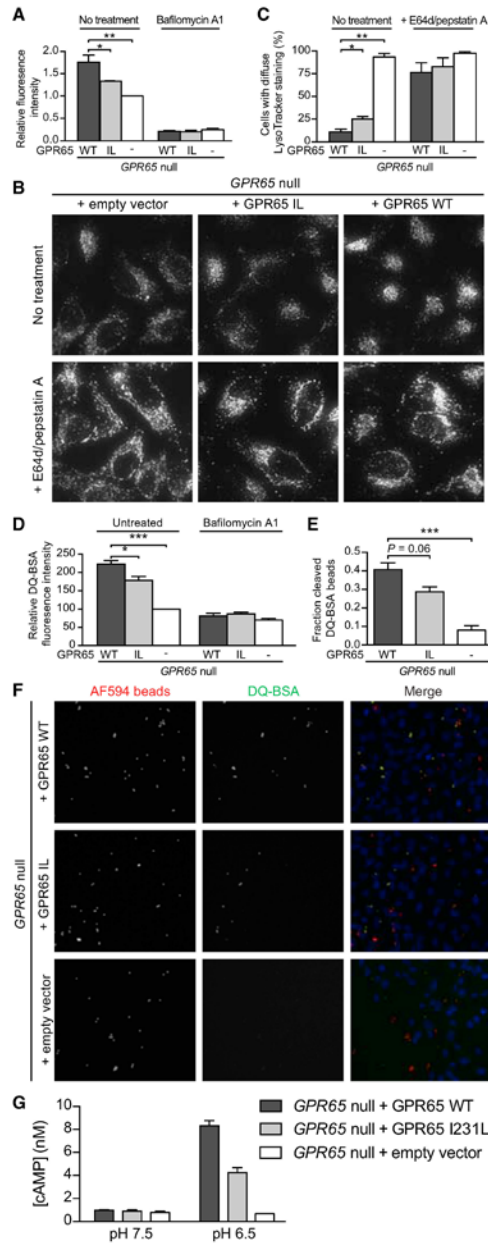


**Figure 5. GPR65 I231L-Expressing Cells Exhibit Aberrant Lysosomal Function and Increased Bacterial Replication**

(A) Relative LysoTracker fluorescence in GPR65-null HeLa cells stably expressing either an empty vector, GPR65 WT, or GPR65 I231L. Cells were left untreated or treated with 100 nM bafilomycin A1 for 2 hr. Data shown as mean  $\pm$  SEM of three independent experiments.

(B) Representative micrographs of GPR65-null HeLa cells stably expressing an empty vector, GPR65 WT, or GPR65 I231L stained with LysoTracker. Cells were left untreated or treated with 10  $\mu$ M E64d and pepstatin A for 3 hr prior to staining.

(C) Quantification of cells imaged in (B) with aberrant lysosomal localization. Data shown as mean  $\pm$  SEM of three independent experiments.

(D) Relative DQ-BSA fluorescence in GPR65-null, GPR65 WT, or GPR65 I231L HeLa cells. Cells were left untreated or treated with 100 nM bafilomycin A1 for 2 hr. Data shown as mean  $\pm$  SEM of three independent experiments.

(E) Fraction of DQ-BSA-positive fluorescent beads compared to total internalized beads in GPR65-null, GPR65 WT, or GPR65 I231L HeLa cells.

(F) HeLa cells treated with DQ BSA-conjugated beads. AF594 (red) was used to monitor total uptake of beads into cells. DQ-BSA (green) was used to monitor phagolysosomal activity.

(G) GPR65-null HeLa cells stably expressing an empty vector or GPR65-V5 WT were treated with buffers at the indicated pH for 30 min and cAMP levels were measured. Average of  $n = 3$  independent experiments. Error bars represent  $\pm$  SEM.

For all panels, \* $p < 0.05$ , \*\* $p < 0.01$ , \*\*\* $p < 0.001$ , one-way ANOVA with multiple comparisons. See also Figures S5 and S6.

Reduced mRNA expression of *ATP6V1D*, *ATP6V1E1*, and *SNX10* was also observed in GPR65-null HeLa cells and GPR65 I231L-expressing cells relative to WT cells, suggesting that this is a common feature of cells lacking GPR65 and not limited to specialized cell types (Figure S5B). Together, these data suggest that GPR65 signaling could alter V-ATPase complex trafficking and lysosomal function.

Expression of GPR65 WT and GPR65 I231L was equivalent in the generated cell lines and both proteins showed similar subcellular localization (Figures S6A and S6B). Knockout of *GPR65* or expression of GPR65 I231L each resulted in an accumulation of the autophagy protein LC3-I and the autophagy target p62, consistent with a late block in autophagy and impairment of autophagic turnover (Figure S6C). Consistent results were obtained with *Gpr65*<sup>-/-</sup> BMDMs (Figure S6D). Similar protein levels of LC3-I and p62 were observed in the presence of the autophagy inducer Torin 1, as well as the lysosomal protease inhibitors E64d and pepstatin A, and these data are consistent with impaired lysosomal processing in both GPR65-null and GPR65 I231L cells (Figures S6C and S6D).

Loss of GPR65 resulted in an increase in lysosomal pH compared to cells expressing GPR65 WT as measured by a decrease in the relative fluorescence intensity of the pH-sensitive LysoTracker Green probe in live cells, which marks acidic organelles (Figure 5A). Expression of GPR65 I231L also resulted in abnormal organelle pH (Figure 5A). Cells with or without GPR65 were similarly sensitive to treatment with the specific V-ATPase inhibitor bafilomycin A1, which increases lysosomal pH and thus abolishes LysoTracker fluorescence. Imaging of LysoTracker-stained cells also revealed peripheral localization and accumulation of lysosomes in GPR65-null cells (Figures 5B and 5C). This aberrant accumulation of lysosomes was also observed to a lesser extent in cells expressing GPR65 I231L compared to GPR65 WT (Figures 5B and 5C). To

determine whether this aberrant subcellular distribution of lysosomes was associated with defects in lysosomal function, cells were treated with the protease inhibitors pepstatin A and E64d to impair lysosomal proteolytic activity without perturbing lysosomal pH, thereby allowing tracking of lysosomal localization with pH-sensitive dyes. Treatment of cells with these inhibitors resulted in aberrant lysosome localization and accumulation in GPR65 I231L and GPR65 WT cells, but no change in the distribution of lysosomes in GPR65-null cells (Figures 5B and 5C). These findings align with a previous study demonstrating that lysosomal positioning is critical for lysosome function (Korolchuk et al., 2011).

To specifically test whether endolysosomal activity was disrupted in GPR65-null cells, we treated cells with DQ-BSA, a bovine serum albumin derivative that is conjugated to a self-quenched fluorophore that becomes fluorescent upon proteolysis in the lysosome (Reis et al., 1998). DQ-BSA fluorescence was higher in GPR65 WT-expressing cells compared to either GPR65-null or GPR65 I231L cells (Figure 5D). To measure phagolysosomal activity, we used 3- $\mu$ m diameter beads conjugated to DQ-BSA and a pH-insensitive fluorochrome to measure the fraction of internalized beads that underwent lysosomal proteolysis. Consistent with aberrant phagolysosomal function, GPR65-null and GPR65 I231L cells contained significantly lower levels of cleaved DQ-BSA beads than did GPR65 WT cells despite similar levels of total internalized beads (Figures 5E, 5F, and S6E). These results suggest that loss of GPR65 or expression of GPR65 I231L increases lysosomal pH and impairs lysosomal function.

Increases in intracellular cAMP (cyclic adenosine monophosphate) regulate V-ATPase trafficking and reduce both phagosomal and lysosomal pH; however, the source of cAMP that regulates these processes is currently undefined (Breton and Brown, 2013; Coffey et al., 2014; Di et al., 2006). We hypothesized that cAMP produced in response to GPR65 activation could stimulate lysosomal acidification. We confirmed that treatment of HeLa cells with forskolin, a cAMP inducer, was sufficient to reduce lysosomal pH (Figure S6F). We next tested whether cAMP production was impaired in GPR65-null cells in response to low pH, a known activator of GPR65 (Mogi et al., 2009). GPR65-null cells did not produce cAMP in response to low pH, and re-expression of GPR65 rescued this phenotype, consistent with previous reports (Figure 5G). cAMP production was reduced in response to low pH in GPR65 I231L-expressing cells, suggesting that this polymorphism confers reduced activity in response to its protons (Figure 5G). GPR65-null HeLa cells were similarly responsive to forskolin independent of GPR65 expression, demonstrating that these cells are capable of producing cAMP and that the defect in cAMP production in response to an acidic buffer is specific to GPR65-dependent signaling (Figure S6G). Given the known role of SNX10 in V-ATPase trafficking, we also tested whether SNX10-null cells exhibited increased organelle pH. The pH of organelles in SNX10-null cells was higher, suggesting that SNX10 is required to maintain organelle pH (Figure S6H). In sum, these data suggest a model in which impaired GPR65-dependent cAMP production in response to changes in extracellular pH results in alterations to V-ATPase dynamics, potentially through SNX10, and subsequent dysregulation of organelle pH.

### GPR65 I231L Alters Lipid Droplet Levels

Recent reports have suggested an important role for lysosomal degradation and autophagy in formation and turnover of intracellular lipid stores during nutrient deprivation (Rambold et al., 2015; Singh et al., 2009). Aberrant accumulation of lipid can result in cellular toxicity and inflammation, which could have important consequences for intestinal homeostasis. Expression data from *Gpr65*<sup>-/-</sup> BMDMs revealed differential regulation of genes involved in lipid uptake and/or metabolism (*Cd51*, *Pla2g7*, and *Fcrls*), suggesting that this pathway might be altered (Figure S5). Cells store neutral lipids in the form of lipid droplets (LDs), which are broken down into free fatty acids during starvation and transported to mitochondria, where they undergo fatty acid oxidation to generate energy for the cell (Hashemi and Goodman, 2015). GPR65-null or rescued cells were treated with complete medium or nutrient-depleted medium (HBSS) and stained for LDs using BODIPY, a dye that stains neutral lipids. At steady-state, GPR65-null and GPR65 I231L-expressing cells exhibited an accumulation of lipid droplets compared to GPR65 WT cells (Figures 6A and 6B). Under conditions of nutrient depletion, there was a strong increase in the number of LD puncta in GPR65 WT cells. This increase was inhibited by treatment with the lysosomal inhibitor bafilomycin A1, consistent with the reported role for autophagy and lysosomal function in LD growth during starvation (Figure 6C; Rambold et al., 2015). LD growth during starvation was dramatically impaired in GPR65-null cells and partially impaired in GPR65 I231L-expressing cells (Figures 6A and 6B). Taken together, these data suggest that GPR65 I231L confers changes to lipid droplet turnover, which could have important consequences for lipid metabolism and cellular energetics.

### GPR65 Risk Variant-Associated Lysosomal Dysfunction Disrupts Pathogen Clearance

To determine whether the observed lysosomal impairment in GPR65 I231L-expressing cells results in alterations in pathogen clearance, we performed an intracellular replication assay with *S. Typhimurium*. Expression of GPR65 I231L in GPR65-null cells resulted in an increase in intracellular bacterial replication compared to cells expressing GPR65 WT (Figure 7A). Expression of either of the V-ATPase subunits identified by RNA-seq, ATP6V1D or ATP6V1E1, was sufficient to restore lysosomal function and reduce bacterial replication in GPR65 I231L-expressing cells to WT levels, suggesting that lysosomal dysfunction contributes to the observed deficits in intracellular bacterial defense (Figures 7B and 7C).

We also performed bacterial replication assays in lymphoblasts derived from IBD patient peripheral blood mononuclear cells homozygous for the tagged GPR65 risk polymorphism and compared these results with age- and disease-matched controls. Enhanced *S. Typhimurium* replication was observed in lymphoblasts derived from individuals expressing the GPR65 risk polymorphism (Figure 7D). The enhanced intracellular bacterial replication observed with the IBD-associated coding variant in both engineered and patient-derived cells suggests that impaired lysosomal function decreases antimicrobial defense and that this could contribute to disease susceptibility.

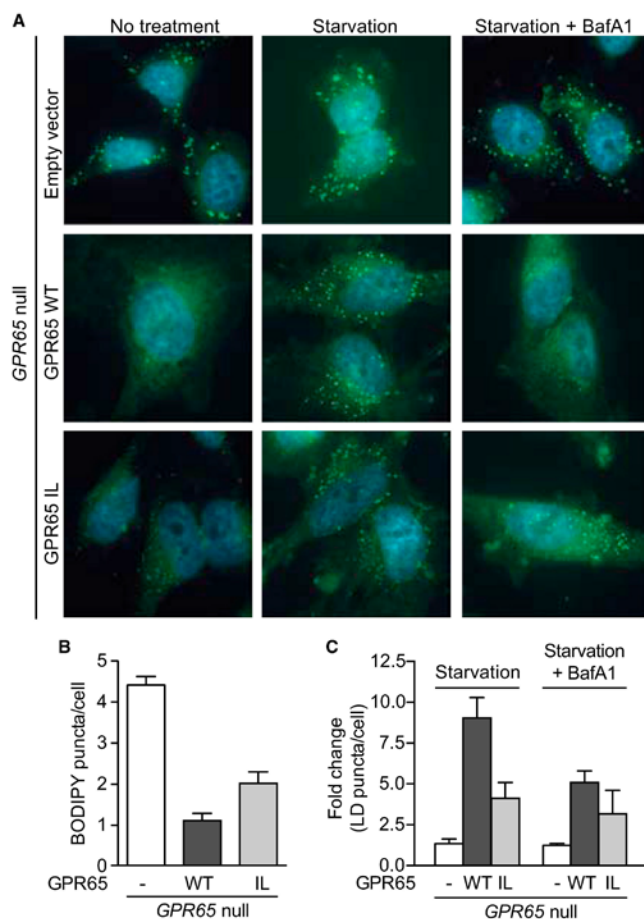


**Figure 6. GPR65 I231L Impairs Lipid Droplet Turnover**

(A) Representative micrographs of cells treated for 4 hr with complete medium, HBSS, or HBSS and 200 nM bafilomycin A1 and stained with BODIPY.  $n = 4$  independent experiments.

(B and C) Quantification of images as shown in (A). Results are representative of  $n = 4$  independent experiments. Bars show mean  $\pm$  SEM.

Our data suggest a model in which GPR65 signaling helps maintain appropriate organelle pH and that this signaling is impaired with the IBD-associated I231L polymorphism. This polymorphism in GPR65 is predicted to lie within one of the transmembrane regions of GPR65 (Kyaw et al., 1998). Experimental data suggest that changing an isoleucine to leucine alters the stability of alpha helices in the transmembrane region of proteins (Lyu et al., 1991). Thus, the I231L polymorphism could disrupt the transmembrane helix structure in GPR65, leading to the observed impaired signaling and cAMP induction. To date, the source of cAMP that regulates lysosomal pH is unclear (Rahman et al., 2013). Our data suggest a model in which GPR65 senses changes in pH, inducing cAMP production, which in turn regulates V-ATPase activity, potentially through SNX10. We show that loss of SNX10 is sufficient to alter lysosomal pH. Taken together, this study defines the role of GPR65 signaling in the maintenance of lysosomal pH and function and demonstrates that a single polymorphism could alter this process.

To date, little was known about the role of lysosomal function in IBD susceptibility. Our data suggest that the IBD-associated risk variant GPR65 I231L disrupts lysosomal function and impairs pathogen

defense, reinforcing the concept that decreases in bacterial clearance have important consequences for IBD pathogenesis (Lassen et al., 2014; Murthy et al., 2014). However, given the central role of lysosomal function in cellular homeostasis, our finding that GPR65 I231L alters lysosomal function has broad implications for tissue homeostasis beyond autophagy and pathogen clearance. We demonstrate that *Gpr65*<sup>-/-</sup> mice are highly susceptible to infection with *C. rodentium*, in contrast to reports using *Atg16l1* hypomorphic mice, which have a reduction in autophagy but no effect on lysosome function (Marchiando et al., 2013). Additionally, WT and *Gpr65*<sup>-/-</sup> mice infected with *C. rodentium* produced similar levels of IL-1 $\beta$  to WT whereas an impairment of autophagy is known to increase IL-1 $\beta$  production from macrophages (Saitoh et al., 2008). Finally, our data in BM chimeric mice demonstrate an important role for GPR65 in

## DISCUSSION

Functional genetic approaches offer the potential to identify genes of interest and provide key functional clues into pathways involved in pathogenesis. Our findings provide an experimental framework for pinpointing potentially relevant genetic targets from disease-associated risk loci identified through GWASs, an approach that could lead to the identification of relevant therapeutic targets. Using this approach, we identified a number of genes that alter antibacterial autophagy and pathogen defense; however, the majority of these genes are probably not directly altering autophagy, as is the case for *ATG16L1*. Further assessment of relevant hits will be required to understand the individual contributions of these genes and their associated polymorphisms.



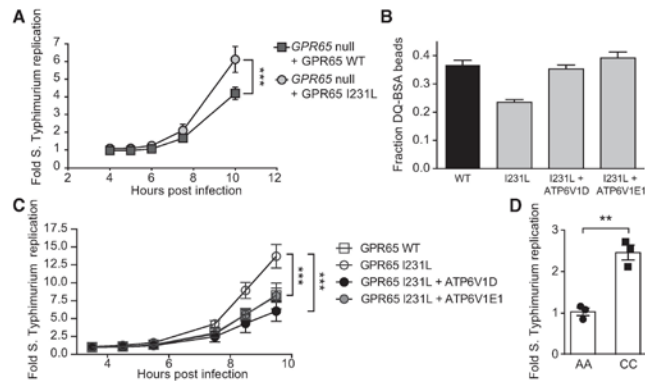


**Figure 7. Impaired Lysosomal Function in GPR65 I231L-Expressing Cells Results in Increased Bacterial Replication**

(A) *S. Typhimurium* intracellular replication in GPR65-null HeLa cells stably expressing either GPR65 WT or GPR65 I231L. Bars represent means  $\pm$  SD from  $n = 4$ .

(B) Fraction of DQ-BSA-positive fluorescent beads compared to total internalized beads in GPR65 WT cells or GPR65 I231L cells stably expressing either ATP6V1D or ATP6V1E1. Data shown as mean  $\pm$  SEM of three independent experiments.

(C) *S. Typhimurium* intracellular replication in GPR65 WT cells or GPR65 I231L cells stably expressing either ATP6V1D or ATP6V1E1. Bars represent means  $\pm$  SD from  $n = 3$  independent experiments.

(D) Intracellular *S. Typhimurium* replication in IBD patient-derived lymphoblasts expressing the ancestral SNP (AA) or the risk allele (CC). Data shown as mean  $\pm$  SEM.

For all panels, \*\* $p < 0.01$ , \*\*\* $p < 0.001$  (unpaired  $t$  test in A and D, one-way ANOVA with multiple comparisons in C).

both the hematopoietic and non-hematopoietic compartments, consistent with the broad role of lysosomes in cellular physiology.

It is likely that GPR65 is playing a critical role in phagocytic cells that require high levels of V-ATPase activity to maintain phagosomal and lysosomal pH, and this activity aids in the direct clearance of enteric pathogens. Recent studies have shed light on the critical role that lysosomes play in the immune response, signaling, tissue repair, and cellular energetics, and it is likely that disruptions in these responses contribute to IBD susceptibility (Ferguson, 2015; Settembre et al., 2013).

Parallels can be drawn between our findings and other diseases known to alter lysosomal function. Hermansky-Pudlak syndrome (HPS) is a rare autosomal-recessive disorder resulting from mutations in genes involved in the formation and trafficking of lysosome-related organelles. Interestingly, a subset of HPS patients develop Crohn's disease-like colitis, suggesting that genetic alterations to lysosomal function can result in Crohn's-like pathologies (Hazzan et al., 2006). Although inherited lysosomal disorders are known to cause severe disease, our data suggest that subtle changes to lysosomal function through genetic polymorphisms can alter susceptibility to microbes, particularly in the gut at the host-commensal interface (Ferguson, 2015).

We demonstrated that lysosomal dysfunction in GPR65-null cells and GPR65 I231L-expressing cells disrupted lipid droplet formation during acute starvation. Aberrant lipid turnover and metabolism might also directly contribute to IBD pathogenesis. Of note, the fatty acid desaturases *FADS1* and *FADS2* each scored in both the bacterial replication and LC3-bacteria colocalization assays. *FADS1* and *FADS2* are rate-limiting enzymes that regulate the unsaturation of  $\omega$ -3 and  $\omega$ -6 long-chain polyunsaturated fatty acids. Another gene that scored in our screen, *PEX13*, underlies the peroxisomal disorder Zellweger syndrome (Shimozawa et al., 1999). Loss of *PEX13* in humans or mice is characterized by impaired peroxisomal  $\beta$ -oxidation of very long chain fatty acids and an accumulation of lipid droplets (Maxwell et al., 2003). Recent studies have explored the role of lipid meta-

bolism and lipid signaling in immune activation and pathogen defense (O'Neill and Pearce, 2016; York et al., 2015). For example, fatty acid synthesis and turnover are critical for the Treg/Th17 cell signaling axis as well as M1/M2 macrophage activation (Berod et al., 2014; Huang et al., 2014). Potentially, lipid metabolism in immunity could be a common pathway contributing to IBD pathogenesis.

In conclusion, our investigation used an unbiased screening approach to identify GPR65 as a previously uncharacterized key gene controlling susceptibility to colitis. Defects in lysosomal activity associated with GPR65 I231L will negatively impact autophagy, a known IBD-associated pathway; however, therapeutic approaches aimed to boost overall levels of autophagy in these cells could exacerbate disease in these individuals. By increasing the flux of materials to the lysosome, autophagy modulators could stress lysosomes that are functioning at capacity and further disrupt cellular homeostasis. Potentially, a GPR65 agonist could help restore lysosomal function in individuals who harbor GPR65 risk polymorphisms. For this reason, development of personalized therapeutic strategies will require an understanding of not only the pathogenic contributions of disease-associated genes, but also the function of specific polymorphisms.

#### EXPERIMENTAL PROCEDURES

##### siRNA Screens

HeLa cells (parental strain or stably transduced with GFP-LC3) were reverse transfected with 5 pmol pooled siRNA (three siRNAs targeting one specific human gene per well) against selected genes within IBD susceptibility loci from the Silencer Select Human Druggable Genome siRNA Library (Ambion) available in 96-well glass-bottomed plates at a density of  $6 \times 10^5$  cells per well for imaging analysis. *S. Typhimurium* overnight cultures were subcultured 1:33 for 3 hr and then infected at MOI 100:1 for DsRed *S. Typhimurium* and bioluminescent *S. Typhimurium* (Perkin Elmer). See the Supplemental Experimental Procedures for further details.

##### Antibacterial Autophagy Assays

*S. Typhimurium* infection of HeLa cells and LC3 quantification were performed as previously described (Lassen et al., 2014). In brief,  $1 \times 10^5$  HeLa cells were

plated on glass coverslips in 12-well plates. Cells were infected with SL1344 DsRed-*Salmonella enterica* serovar Typhimurium for 1 hr, fixed in ice-cold methanol, and stained with rabbit anti-LC3 (Sigma), goat anti-CSA (S. Typhimurium), and Hoechst. See the [Supplemental Experimental Procedures](#) for further details.

#### Lysosomal Function Assays

To measure the pH of acidic intracellular compartments, cells were loaded with 75 nM LysoTracker Green DND-26 (Invitrogen) for 5 min. Cells were analyzed on a BD FACSVerser instrument and mean fluorescence intensity (MFI) was calculated via FlowJo software. MFI was normalized to *GPR65*-null cells. For DQ-BSA assays, 10,000 cells/well were plated in 96-well plates. The next day, cells were starved for 1 hr with HBSS and then treated with 10  $\mu$ g/mL DQ-BSA Green dye (Life Technologies) in complete media to increase endocytosis. Cells were incubated for 1 hr and then washed. Cells were stained with Hoechst 33342 (Molecular Probes) for 5 min to visualize nuclei and imaged with the ImageXpress Micro Widefield High-Content Screening System with a 20 $\times$  lens. Fluorescence intensity of internalized DQ-BSA was quantified with MetaExpress software. See the [Supplemental Experimental Procedures](#) for further details.

#### Lipid Droplet Analysis

Cells were plated in 96-well plates as described above. For starvation experiments, cells were starved for 3 hr in HBSS. Cells were washed in PBS and fixed in 4% PFA with Hoechst for 15 min. Cells were washed and stained for 15 min with BODIPY 493/503 in PBS at a final concentration of 1  $\mu$ g/mL. For each well, 6–9 fields were imaged and analyzed to obtain an average number of LDs/cell for each well. For each experiment, 3–6 replicate wells were analyzed. See the [Supplemental Experimental Procedures](#) for further details.

#### Mouse Experiments

All experiments involving mice were carried out according to protocols approved by the relevant animal ethics committees. *Gpr65*<sup>−/−</sup> mice, in which exon 2 coding sequences are replaced by promoterless IRES-EGFP sequences, were obtained from Jax laboratories and backcrossed on a C57BL/6 background to 13 generations. All experiments were performed on age- and gender-matched animals. *C. rodentium* infections were performed as described previously. *C. rodentium* were grown overnight at 37°C in 10 mL LB with 100  $\mu$ g/mL nalidixic acid or in LB with ampicillin for bioluminescent *C. rodentium*. Overnight *C. rodentium* cultures were harvested by centrifugation and resuspended in PBS. Mice were orally gavaged with 1–4  $\times$  10<sup>9</sup> colony-forming units (CFUs) of the bacterial suspension. CFUs from the indicated organs were determined by plating on LB agar containing nalidixic acid. Histological slides of colon were scored blinded for *C. rodentium* infection, with a maximum possible score of 10. See the [Supplemental Experimental Procedures](#) for further details.

#### ACCESSION NUMBERS

The RNA-seq data reported in this paper are archived at GEO under accession number GSE69445.

#### SUPPLEMENTAL INFORMATION

Supplemental Information includes six figures, five tables, and Supplemental Experimental Procedures and can be found with this article online at <http://dx.doi.org/10.1016/j.immuni.2016.05.007>.

#### AUTHOR CONTRIBUTIONS

K.G.L., J.B., M.M., C.I.M., T.M., L.A.B., E.J.V., and S.-Y.K. performed experiments. K.G.L., J.B., M.M., C.I.M., T.M., L.A.B., E.J.V., G.G., S.-Y.K., H.H., L.M., and A.K.B. analyzed data. M.B. provided reagents. K.G.L., J.B., C.I.M., L.A.B., G.G., H.H., M.J.D., F.R., C.R.M., and R.J.X. designed research. K.G.L., J.B., E.J.V., L.M., A.K.B., M.B., M.J.D., F.R., C.R.M., and R.J.X. provided intellectual contributions throughout the project. K.G.L. and R.J.X. wrote the paper.

#### ACKNOWLEDGMENTS

We thank Natalia Nedelsky for editorial assistance, Jenny Tam for help with the generation of DQ-BSA-conjugated beads, and Rushika C. Wirasinha for support with *Gpr65*<sup>−/−</sup> mice. We thank Skip Virgin and Beth Levine for comments. This work was supported by funding from The Leona M. and Harry B. Helmsley Charitable Trust, Crohn's and Colitis Foundation of America, and NIH grants DK097485 and AI109725 to R.J.X. F.R. is supported by ALW Open Program (B22.02.014), DFG-NWO cooperation (DN82-303), SNF (CRSII3\_154421), and ZonMW VICI (016.130.606) grants.

Received: November 16, 2015

Revised: February 19, 2016

Accepted: March 21, 2016

Published: June 7, 2016

#### REFERENCES

- Adolph, T.E., Tomczak, M.F., Niederreiter, L., Ko, H.J., Böck, J., Martinez-Naves, E., Glickman, J.N., Tschurtschenthaler, M., Hartwig, J., Hosomi, S., et al. (2013). Paneth cells as a site of origin for intestinal inflammation. *Nature* 503, 272–276.
- Altshuler, D., Daly, M.J., and Lander, E.S. (2008). Genetic mapping in human disease. *Science* 322, 881–888.
- Berod, L., Friedrich, C., Nandan, A., Freitag, J., Hagemann, S., Harmrolfs, K., Sandouk, A., Hesse, C., Castro, C.N., Bähr, H., et al. (2014). De novo fatty acid synthesis controls the fate between regulatory T and T helper 17 cells. *Nat. Med.* 20, 1327–1333.
- Breton, S., and Brown, D. (2013). Regulation of luminal acidification by the V-ATPase. *Physiology (Bethesda)* 28, 318–329.
- Cadwell, K., Liu, J.Y., Brown, S.L., Miyoshi, H., Loh, J., Lennerz, J.K., Kishi, C., Kc, W., Carrero, J.A., Hunt, S., et al. (2008). A key role for autophagy and the autophagy gene Atg16l1 in mouse and human intestinal Paneth cells. *Nature* 456, 259–263.
- Chen, Y., Wu, B., Xu, L., Li, H., Xia, J., Yin, W., Li, Z., Shi, D., Li, S., Lin, S., et al. (2012). A SNX10/V-ATPase pathway regulates ciliogenesis in vitro and in vivo. *Cell Res.* 22, 333–345.
- Coffey, E.E., Beckel, J.M., Laties, A.M., and Mitchell, C.H. (2014). Lysosomal alkalization and dysfunction in human fibroblasts with the Alzheimer's disease-linked presenilin 1 A246E mutation can be reversed with cAMP. *Neuroscience* 263, 111–124.
- Cooney, R., Baker, J., Brain, O., Danis, B., Pichulik, T., Allan, P., Ferguson, D.J., Campbell, B.J., Jewell, D., and Simmons, A. (2010). NOD2 stimulation induces autophagy in dendritic cells influencing bacterial handling and antigen presentation. *Nat. Med.* 16, 90–97.
- Deretic, V., Saitoh, T., and Akira, S. (2013). Autophagy in infection, inflammation and immunity. *Nat. Rev. Immunol.* 13, 722–737.
- Deretic, V., Kimura, T., Timmins, G., Moseley, P., Chauhan, S., and Mandell, M. (2015). Immunologic manifestations of autophagy. *J. Clin. Invest.* 125, 75–84.
- Di, A., Brown, M.E., Deriy, L.V., Li, C., Szeto, F.L., Chen, Y., Huang, P., Tong, J., Naren, A.P., Bindokas, V., et al. (2006). CFTR regulates phagosome acidification in macrophages and alters bactericidal activity. *Nat. Cell Biol.* 8, 933–944.
- Efeyan, A., Zoncu, R., and Sabatini, D.M. (2012). Amino acids and mTORC1: from lysosomes to disease. *Trends Mol. Med.* 18, 524–533.
- Ferguson, S.M. (2015). Beyond indigestion: emerging roles for lysosome-based signaling in human disease. *Curr. Opin. Cell Biol.* 35, 59–68.
- Geremia, A., Arancibia-Carcamo, C.V., Fleming, M.P., Rust, N., Singh, B., Mortensen, N.J., Travis, S.P., and Powrie, F. (2011). IL-23-responsive innate lymphoid cells are increased in inflammatory bowel disease. *J. Exp. Med.* 208, 1127–1133.
- Gomes, L.C., and Dikic, I. (2014). Autophagy in antimicrobial immunity. *Mol. Cell* 54, 224–233.
- Hashemi, H.F., and Goodman, J.M. (2015). The life cycle of lipid droplets. *Curr. Opin. Cell Biol.* 33, 119–124.



- Hazzan, D., Seward, S., Stock, H., Zisman, S., Gabriel, K., Harpaz, N., and Bauer, J.J. (2006). Crohn's-like colitis, enterocolitis and perianal disease in Hermansky-Pudlak syndrome. *Colorectal Dis.* 8, 539–543.
- Huang, S.C., Everts, B., Ivanova, Y., O'Sullivan, D., Nascimento, M., Smith, A.M., Beatty, W., Love-Gregory, L., Lam, W.Y., O'Neill, C.M., et al. (2014). Cell-intrinsic lysosomal lipolysis is essential for alternative activation of macrophages. *Nat. Immunol.* 15, 846–855.
- Jostins, L., Ripke, S., Weersma, R.K., Duerr, R.H., McGovern, D.P., Hui, K.Y., Lee, J.C., Schumm, L.P., Sharma, Y., Anderson, C.A., et al.; International IBD Genetics Consortium (IIBDGC) (2012). Host-microbe interactions have shaped the genetic architecture of inflammatory bowel disease. *Nature* 491, 119–124.
- Kaser, A., Niederreiter, L., and Blumberg, R.S. (2011). Genetically determined epithelial dysfunction and its consequences for microflora-host interactions. *Cell. Mol. Life Sci.* 68, 3643–3649.
- Kishino, S., Takeuchi, M., Park, S.B., Hirata, A., Kitamura, N., Kunisawa, J., Kiyono, H., Iwamoto, R., Isobe, Y., Arita, M., et al. (2013). Polyunsaturated fatty acid saturation by gut lactic acid bacteria affecting host lipid composition. *Proc. Natl. Acad. Sci. USA* 110, 17808–17813.
- Knights, D., Lassen, K.G., and Xavier, R.J. (2013). Advances in inflammatory bowel disease pathogenesis: linking host genetics and the microbiome. *Gut* 62, 1505–1510.
- Korolchuk, V.I., Saiki, S., Lichtenberg, M., Siddiqi, F.H., Roberts, E.A., Imarisio, S., Jahreis, L., Sarkar, S., Futter, M., Menzies, F.M., et al. (2011). Lysosomal positioning coordinates cellular nutrient responses. *Nat. Cell Biol.* 13, 453–460.
- Kyaw, H., Zeng, Z., Su, K., Fan, P., Shell, B.K., Carter, K.C., and Li, Y. (1998). Cloning, characterization, and mapping of human homolog of mouse T-cell death-associated gene. *DNA Cell Biol.* 17, 493–500.
- Lassen, K.G., Kuballa, P., Conway, K.L., Patel, K.K., Becker, C.E., Pelloquin, J.M., Villablanca, E.J., Norman, J.M., Liu, T.C., Heath, R.J., et al. (2014). Atg16L1 T300A variant decreases selective autophagy resulting in altered cytokine signaling and decreased antibacterial defense. *Proc. Natl. Acad. Sci. USA* 111, 7741–7746.
- Levine, B., Mizushima, N., and Virgin, H.W. (2011). Autophagy in immunity and inflammation. *Nature* 469, 323–335.
- Longman, R.S., Diehl, G.E., Victorio, D.A., Huh, J.R., Galan, C., Miraldi, E.R., Swaminath, A., Bonneau, R., Scherl, E.J., and Littman, D.R. (2014). CX<sub>3</sub>CR1<sup>+</sup> mononuclear phagocytes support colitis-associated innate lymphoid cell production of IL-22. *J. Exp. Med.* 211, 1571–1583.
- Lyu, P.C., Sherman, J.C., Chen, A., and Kallenbach, N.R. (1991). Alpha-helix stabilization by natural and unnatural amino acids with alkyl side chains. *Proc. Natl. Acad. Sci. USA* 88, 5317–5320.
- Macia, L., Tan, J., Vieira, A.T., Leach, K., Stanley, D., Luong, S., Maruya, M., Ian McKenzie, C., Hijikata, A., Wong, C., et al. (2015). Metabolite-sensing receptors GPR43 and GPR109A facilitate dietary fibre-induced gut homeostasis through regulation of the inflammasome. *Nat. Commun.* 6, 6734.
- Marchiando, A.M., Ramanan, D., Ding, Y., Gomez, L.E., Hubbard-Lucey, V.M., Maurer, K., Wang, C., Ziel, J.W., van Rooijen, N., Nuñez, G., et al. (2013). A deficiency in the autophagy gene Atg16L1 enhances resistance to enteric bacterial infection. *Cell Host Microbe* 14, 216–224.
- Maslowski, K.M., Vieira, A.T., Ng, A., Kranich, J., Sierro, F., Yu, D., Schilter, H.C., Rolph, M.S., Mackay, F., Artis, D., et al. (2009). Regulation of inflammatory responses by gut microbiota and chemoattractant receptor GPR43. *Nature* 461, 1282–1286.
- Maxwell, M., Bjorkman, J., Nguyen, T., Sharp, P., Finn, J., Paterson, C., Tonks, I., Paton, B.C., Kay, G.F., and Crane, D.I. (2003). Pex13 inactivation in the mouse disrupts peroxisome biogenesis and leads to a Zellweger syndrome phenotype. *Mol. Cell Biol.* 23, 5947–5957.
- McCarroll, S.A., Huett, A., Kuballa, P., Chileski, S.D., Landry, A., Goyette, P., Zody, M.C., Hall, J.L., Brant, S.R., Cho, J.H., et al. (2008). Deletion polymorphism upstream of IRGM associated with altered IRGM expression and Crohn's disease. *Nat. Genet.* 40, 1107–1112.
- Melé, M., Ferreira, P.G., Reverter, F., DeLuca, D.S., Monlong, J., Sammeth, M., Young, T.R., Goldmann, J.M., Pervouchine, D.D., Sullivan, T.J., et al.; GTEx Consortium (2015). Human genomics. The human transcriptome across tissues and individuals. *Science* 348, 660–665.
- Mogi, C., Tobo, M., Tomura, H., Murata, N., He, X.D., Sato, K., Kimura, T., Ishizuka, T., Sasaki, T., Sato, T., et al. (2009). Involvement of proton-sensing TDAG8 in extracellular acidification-induced inhibition of proinflammatory cytokine production in peritoneal macrophages. *J. Immunol.* 182, 3243–3251.
- Mota, L.J., Ramsden, A.E., Liu, M., Castle, J.D., and Holden, D.W. (2009). SCAMP3 is a component of the Salmonella-induced tubular network and reveals an interaction between bacterial effectors and post-Golgi trafficking. *Cell. Microbiol.* 11, 1236–1253.
- Murthy, A., Li, Y., Peng, I., Reichelt, M., Katakam, A.K., Noubade, R., Roose-Girma, M., DeVoss, J., Diehl, L., Graham, R.R., and van Lookeren Campagne, M. (2014). A Crohn's disease variant in Atg16L1 enhances its degradation by caspase 3. *Nature* 506, 456–462.
- Nell, S., Suerbaum, S., and Josenhans, C. (2010). The impact of the microbiota on the pathogenesis of IBD: lessons from mouse infection models. *Nat. Rev. Microbiol.* 8, 564–577.
- Nugent, S.G., Kumar, D., Rampton, D.S., and Evans, D.F. (2001). Intestinal luminal pH in inflammatory bowel disease: possible determinants and implications for therapy with aminosaccharides and other drugs. *Gut* 48, 571–577.
- O'Neill, L.A., and Pearce, E.J. (2016). Immunometabolism governs dendritic cell and macrophage function. *J. Exp. Med.* 213, 15–23.
- Orvedahl, A., Sumpter, R., Jr., Xiao, G., Ng, A., Zou, Z., Tang, Y., Narimatsu, M., Gilpin, C., Sun, Q., Roth, M., et al. (2011). Image-based genome-wide siRNA screen identifies selective autophagy factors. *Nature* 480, 113–117.
- Qin, B., He, M., Chen, X., and Pei, D. (2006). Sorting nexin 10 induces giant vacuoles in mammalian cells. *J. Biol. Chem.* 281, 36891–36896.
- Rahman, N., Buck, J., and Levin, L.R. (2013). pH sensing via bicarbonate-regulated "soluble" adenylyl cyclase (sAC). *Front. Physiol.* 4, 343.
- Rambold, A.S., Cohen, S., and Lippincott-Schwartz, J. (2015). Fatty acid trafficking in starved cells: regulation by lipid droplet lipolysis, autophagy, and mitochondrial fusion dynamics. *Dev. Cell* 32, 678–692.
- Reis, R.C., Sorgine, M.H., and Coelho-Sampaio, T. (1998). A novel methodology for the investigation of intracellular proteolytic processing in intact cells. *Eur. J. Cell Biol.* 75, 192–197.
- Reuter, J.A., Spacek, D.V., and Snyder, M.P. (2015). High-throughput sequencing technologies. *Mol. Cell* 58, 586–597.
- Rich, K.A., Burkett, C., and Webster, P. (2003). Cytoplasmic bacteria can be targets for autophagy. *Cell. Microbiol.* 5, 455–468.
- Saitoh, T., Fujita, N., Jang, M.H., Uematsu, S., Yang, B.G., Satoh, T., Omori, H., Noda, T., Yamamoto, N., Komatsu, M., et al. (2008). Loss of the autophagy protein Atg16L1 enhances endotoxin-induced IL-1 $\beta$  production. *Nature* 456, 264–268.
- Sasaki, M., Sitaraman, S.V., Babbitt, B.A., Gerner-Smidt, P., Ribot, E.M., Garrett, N., Alpern, J.A., Akyildiz, A., Theiss, A.L., Nusrat, A., and Klapproth, J.M. (2007). Invasive *Escherichia coli* are a feature of Crohn's disease. *Lab. Invest.* 87, 1042–1054.
- Settembre, C., Fraldi, A., Medina, D.L., and Ballabio, A. (2013). Signals from the lysosome: a control centre for cellular clearance and energy metabolism. *Nat. Rev. Mol. Cell Biol.* 14, 283–296.
- Shaw, S.Y., Tran, K., Castoreno, A.B., Pelloquin, J.M., Lassen, K.G., Khor, B., Aldrich, L.N., Tan, P.H., Graham, D.B., Kuballa, P., et al. (2013). Selective modulation of autophagy, innate immunity, and adaptive immunity by small molecules. *ACS Chem. Biol.* 8, 2724–2733.
- Shimozawa, N., Suzuki, Y., Zhang, Z., Imamura, A., Toyama, R., Mukai, S., Fujiki, Y., Tsukamoto, T., Osumi, T., Orii, T., et al. (1999). Nonsense and temperature-sensitive mutations in PEX13 are the cause of complementation group H of peroxisome biogenesis disorders. *Hum. Mol. Genet.* 8, 1077–1083.
- Singh, S.B., Davis, A.S., Taylor, G.A., and Deretic, V. (2006). Human IRGM induces autophagy to eliminate intracellular mycobacteria. *Science* 313, 1438–1441.

- Singh, R., Kaushik, S., Wang, Y., Xiang, Y., Novak, I., Komatsu, M., Tanaka, K., Cuervo, A.M., and Czaja, M.J. (2009). Autophagy regulates lipid metabolism. *Nature* 458, 1131–1135.
- Song-Zhao, G.X., Srinivasan, N., Pott, J., Baban, D., Frankel, G., and Maloy, K.J. (2014). Nlrp3 activation in the intestinal epithelium protects against a mucosal pathogen. *Mucosal Immunol.* 7, 763–774.
- Terawaki, S., Camosseto, V., Prete, F., Wenger, T., Papadopoulos, A., Rondeau, C., Combes, A., Rodriguez Rodriguez, C., Vu Manh, T.P., Fallet, M., et al. (2015). RUN and FYVE domain-containing protein 4 enhances autophagy and lysosome tethering in response to Interleukin-4. *J. Cell Biol.* 210, 1133–1152.
- Vallance, B.A., Deng, W., Knodler, L.A., and Finlay, B.B. (2002). Mice lacking T and B lymphocytes develop transient colitis and crypt hyperplasia yet suffer impaired bacterial clearance during *Citrobacter rodentium* infection. *Infect. Immun.* 70, 2070–2081.
- Venkatesh, M., Mukherjee, S., Wang, H., Li, H., Sun, K., Benechet, A.P., Qiu, Z., Maher, L., Redinbo, M.R., Phillips, R.S., et al. (2014). Symbiotic bacterial metabolites regulate gastrointestinal barrier function via the xenobiotic sensor PXR and Toll-like receptor 4. *Immunity* 41, 296–310.
- Wang, J.Q., Kon, J., Mogi, C., Tobo, M., Damin, A., Sato, K., Komachi, M., Malchinkhuu, E., Murata, N., Kimura, T., et al. (2004). TDAG8 is a proton-sensing and psychosine-sensitive G-protein-coupled receptor. *J. Biol. Chem.* 279, 45626–45633.
- York, A.G., Williams, K.J., Argus, J.P., Zhou, Q.D., Brar, G., Vergnes, L., Gray, E.E., Zhen, A., Wu, N.C., Yamada, D.H., et al. (2015). Limiting cholesterol biosynthetic flux spontaneously engages type I IFN signaling. *Cell* 163, 1716–1729.